On the imidazole-2-thione-based route to tricyclic 1,4-diphosphinines: synthesis, structures and reactions

Dissertation

zur

Erlangung des Doktorgrades (Dr. rer. nat.)

der

Mathematisch-Naturwissenschaftlichen Fakultät

der

Rheinischen Friedrich-Wilhelms-Universität Bonn

vorgelegt von

Abhishek Koner

aus

West Bengal, India

Bonn, 2017

Angefertigt mit Genehmigung der Mathematisch-Naturwissenschaftlichen Fakultät der
Rheinischen Friedrich-Wilhelms-Universität Bonn

1. Gutachter: Prof. Dr. R. Streubel

2. Gutachter: Prof. Dr. J. Beck

Tag der Promotion: 13.12.2017

Erscheinungsjahr: 2018

"Education is the manifestation of the perfection already in man"

- Swami Vivekananda

Some of the results of this Thesis were previously published

1. **A. Koner**, G. Pfeifer, Z. Kelemen, G. Schnakenburg, L. Nyulászi, T. Sasamori, R. Streubel, 1,4-Diphosphinines from Imidazole-2-thiones, *Angew. Chem. Int. Ed.* **2017**, *56*, 9231-9235.
2. **A. Koner**, S. C. Serin, G. Schnakenburg, B. O. Patrick, D. P. Gates, R. Streubel, Exploring the chemistry of backbone amino(chloro)phosphanyl-substituted imidazole-2-thiones, *Dalton Trans.* **2017**, *46*, 10504-10514.
3. P. K. Majhi, **A. Koner**, G. Schnakenburg, Z. Kelemen, L. Nyulászi, R. Streubel, Application of Imidazole-2-thione Substituents in Low-Coordinate Phosphorus Chemistry – Probing the Scope, *Eur. J. Inorg. Chem.* **2016**, 3559-3573.

Conference/colloquia contributions

1. I. Begum, **A. Koner**, R. Streubel, 11th European Workshop on Phosphorus Chemistry, Sofia/ Bulgaria, March 24-26, 2014: "Synthesis, structure and reactivity of novel backbone P-functionalized NHC-precursors" (Poster contribution).
2. **A Koner**, G. Pfeifer, R. Streubel, 9th International Conference on Inorganic Chemistry (AGICHEM), Edinburgh/ Scotland, July 30 – Aug 1, 2014. "Synthesis of Novel Tricyclic Imidazole-2-thiones" (poster contribution).
3. **A. Koner**, G. Pfeifer, R. Streubel, 1st European Conference on Smart Inorganic Polymers, Maribor/ Slovenia, September 21-23, 2014: "P-functional tricyclic imidazole-2-thione based ligands"(poster contribution).
4. **A. Koner**, G. Pfeifer, R. Streubel, 12th European Workshop on Phosphorus Chemistry, Kassel/Germany, March 16-18, 2015: "Synthesis and reactions of tricyclic1,4-diphosphinines – en route to coordination polymers "(poster contribution)
5. **A. Koner**, R. Streubel, Anorganisch Chemisches Kolloquium, January 28th , 2016, Universität Bonn, "Backbone P-functionalization of Imidazole-2-thione; en route to Imidazole-2-thione based tricycles" (oral contribution).
6. **A. Koner**, G. Pfeifer, R. Streubel, 13th European Workshop on Phosphorus Chemistry, 7 th -9 th March, 2016: Berlin-Germany, "Synthesis and reactivities of novel tricyclic imidazole-2- thiones and related 1,4-diphosphinines" (poster Contribution).
7. **A. Koner**, G. Pfeiffer, R. Streubel, 21st International Conference on Phosphorus Chemistry, June 5 th -10th , 2016: Kazan, Russia, "Imidazole-2-thione-based tricyclic

1,4-dihydro-1,4-diphosphinines: synthesis, structure and reactivity" (poster contribution).

8. **A. Koner**, R. Streubel, European workshop on Phosphorus Chemistry, Cluj-Napoca, Romania, March 20th – 22 nd 2017: "Imidazole-2-thione based electron rich 1,4-diphosphinines" (oral contribution).

Die vorliegende Arbeit wurde im Zeitraum von Oktober 2013 bis April 2017 im Arbeitskreis von Prof. Dr. R. Streubel am Institut für Anorganische Chemie der Rheinischen Friedrich-Wilhelms-Universität in Bonn angefertigt.

Hiermit versichere ich, dass ich diese Arbeit selbst verfasst und keine anderen als die angegebenen Quellen und Hilfsmittel verwendet habe.

Bonn, den 05.09.2017

Acknowledgements

First and foremost I would like to express my gratitude to my supervisor Prof. Dr. Rainer Streubel for the immense support and comprehensive guidance during last four years of my work. I thank him also for the valuable inputs during the challenging situations that I will cherish in my life.

I am also thankful to Prof. Dr. Johannes Beck, Prof. Dr. Arne Lützen and Prof. Dr. Uwe Deppenmeier for refereeing my thesis.

I earnestly convey my regards to Prof. Dr. Derek Gates for giving the chance to work in his group as a visiting research student for four months at the Department of Chemistry, The University of British Columbia, Vancouver, Canada. I also appreciate the friendly working conditions in his working group.

I sincerely acknowledge Prof. Dr. Laszlo Nyulaszi and Dr. Zsolt Kelemen, Department of Inorganic and Analytical Chemistry, Budapest university of Technology and Economy, Budapest, Hungary for the fruitful theoretical calculations.

I also humbly thank Prof. Dr. Antonio Frontera and Dr. Antonio Bauzá, Department of Chemistry-Universitat de les Illes Balears, Palma de Mallorca (Baleares), Spain for being involved in the collaboration for theoretical investigations.

I thank Dr. Gregor Schnakenburg, Ms. Charlotte Rödde, Mr. Brian Patrick and Dr. Spencer Serin for the single crystal X-ray diffraction measurements.

At this point of my life I am still grateful to Prof. Dr. Raja Angamuthu, Indian Institute of Chemistry, Kanpur, India for nurturing my background knowledge and giving me a carefully guided entry point into research life.

Without the timely and careful service of our Analytical department it would be impossible to carry out the work properly. Therefore I thank Dr. Claud Schmidt, Ms. Karen Procknicki and Ms. Hannelore Spitz (NMR spectroscopy), Dr. Marianne Engeser and her colleagues (Mass spectrometry), Dr. Sabine Rings and Ms. Anna Martens (Elemental Analyses) and all members in Chemical Store, Glass Blowing section, Mechanical and Electrical workshops.

This acknowledgement would never be complete without thanking Dr. Paresh Kumar Majhi and Dr. Vitaly Nesterov for the watchful introductory guidance into the inert atmosphere techniques and lab culture. I am also thankful to Andreas Kyri for all those valuable late evening discussions. Besides, I also thank the rest of my lab colleagues (especially Tobias Heurich, Dr. Jose Manuel Villalba Franco, Imtiaz Begum) for the friendly atmosphere and for being as a team during the highs and lows of my working time. I acknowledge my bachelor student, Michael Kunz, for the memorable time and experiences during his Bachelor Thesis.

I warmly forward my gratefulness to the University of Bonn and DAAD for the financial support during my stay in Bonn, Germany and Vancouver, Canada. I also thank them for giving the opportunity to enrich myself with the experiences gained during my stay in Germany and Canada.

And finally I am obliged to my parents and family members for the endless moral support and guidance throughout my life.

Contents

Abbreviations

Xa,a' = a mixture of two isomers (*cis*, *trans*); where **X**= compound number and **a,a'** are two isomers

Å	Ångström ($1 \cdot 10^{-10}$ m)	eV	electron volt
°	angle in degree	FWHM	full width at half maximum
Ar	aromatic substituent	g	gram
ATR	Attenual Total Reflexion	h	height or hour
au	Atomic unit	HMDS	hexamethyldisilazide
br	broad signal	KHMDS	Potassium hexamethyldisilazide
calc.	calculated	HMQC	Heteronuclear Multiple Quantum Correlation
°C	degree Celsius	Hz	Hertz
C_6D_6	deuerated benzene	^{i}Pr	*iso*-propyl
$CDCl_3$	deuterated chloroform	IR	infrared
cm	centimeter	$^{n}J_{X,Y}$	coupling constant (between the elements X,Y over n bonds) in Hz
CSD	Cambridge Structural Database	K	Kelvin
^{n}Bu	*n*-butyl	Et	ethyl
d	days	ø	diameter
δ	chemical shift in ppm	Δδ	chemical shift difference
T	temperature	DBU	1,8-diazabicyclo[5.4.0]undec-7-ene
tert	tertiary	dec.	decomposition

ESI	electrospray ionization	DEPT	Distortionless Enhancement by Polarization
Et_2O	diethyl ether	M	metal or molar weight in g/mol
EA	elemental analysis	LDA	Lithium diisopropylamide
EI	electron impact ionization	Me	methyl (CH_3)
eq.	equivalent	mg	milligram
ML_n	transition metal fragment bearing n ligands	min	minutes
mmol	millimol	mL	millilitre
MS	mass spectrometry	THF	tetrahydrofuran
m/z	mass to charge ratio	TfOH	trifluoromethanesulfonic acid
n	normal	THF-d_8	deuterated tetrahydrofuran
^{n}Bu	*n*-butyl	TMEDA	Tetramethylethylenediamine
nm	nanometre	toluene-d_8	deuterated toluene
NMR	nuclear magnetic resonance	$\tilde{\nu}$	wave number
%	percent	vs	very strong
PE	petroleum ether (40/60)	VT-NMR	Variable Temperature NMR
Ph	phenyl (C_6H_5)	w	weak
ppm	parts per million	X	halogen or leaving group
q	quartet	quin	quintet
L	ligand	R, R´, R´´	organic substituent
m	medium	r.t.	room temperature
m	multiplett	s	singlet

Chapter 1

1. Introduction

1.1 Imidazole-2-thiones and their applications

Imidazole-2-thiones **I**, the cyclic analogues of thiourea, despite being known over a century, hold a significant importance in chemistry till date due to their ample use in both chemical and pharmaceutical industries. Much of the research on applications of imidazole-2-thiones is driven by their coordination properties. For example, the bacteriostatic activities[1] of imidazole-2-thiones have been related to their metal binding abilities and this is the same reason why they are also used in gravimetric[2] and spectrophotometric titration[3] for a wide series of metals. Barring these, medical implications of imidazole-2-thiones include thyrotoxic activity[4], central nervous system depressant and anti-convulsant activity.[5] Furthermore it is also used in metal finishing, electroplating industries where it helps to stop metal corrosion.[6]

Due to this sustained utility, the synthetic protocol for the imidazole-2-thiones have also gone through a significant evolution.[7, 8] Nowadays they are readily obtained by a single-pot reaction protocol where the corresponding imidazolium salts are treated with a base to generate the imidazole-2-ylidene, which is then *in situ* trapped as the imidazole-2-thione by reacting with elemental sulfur (Scheme 1).[9, 10]

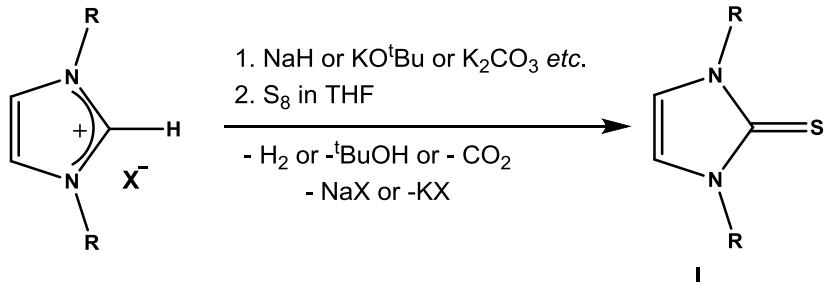

Scheme 1: Synthesis of imidazole-2-thiones

Apart from all the industrial and medicinal applications, in synthetic chemistry imidazole-2-thiones also act as a potent source for the corresponding imidazole-2-ylidenes **II** (via reductive desulfurization) and imidazolium salts **III** (via oxidative desulfurization) (Figure 1). In the reductive desulfurization process,[11] under thermal conditions and in presence of a metal as reducing agent, sulfur is transformed into a metal sulfide. On the other hand, *i.e.* during the oxidative desulfurization,[12] H_2O_2 is used as the oxidant to remove sulfur and form the bisulfate (hydrogensulfate) anion. The imidazolium salts obtained by the oxidative desulfurization can also be converted into the corresponding imidazole-2-ylidene by means of deprotonation by a base.[10]

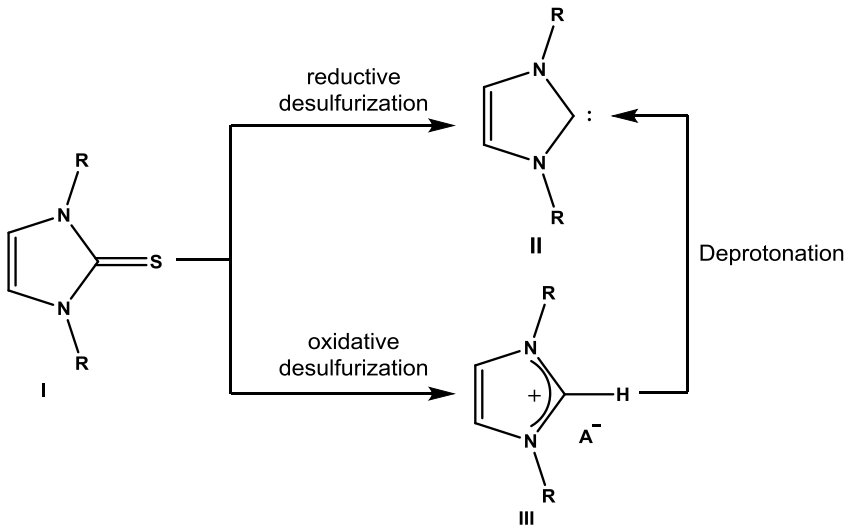

Figure 1: Examples for the use of imidazole-2-thiones in synthetic chemistry.

Imidazolium salts **III** can become ionic liquids [8, 13] given that suitable substituents and counter anions are employed. This also offers the opportunity to access halogen-free and functionalized ionic liquids, which are also sometimes called as task-specific ionic liquids (introduced by Davis).[14]

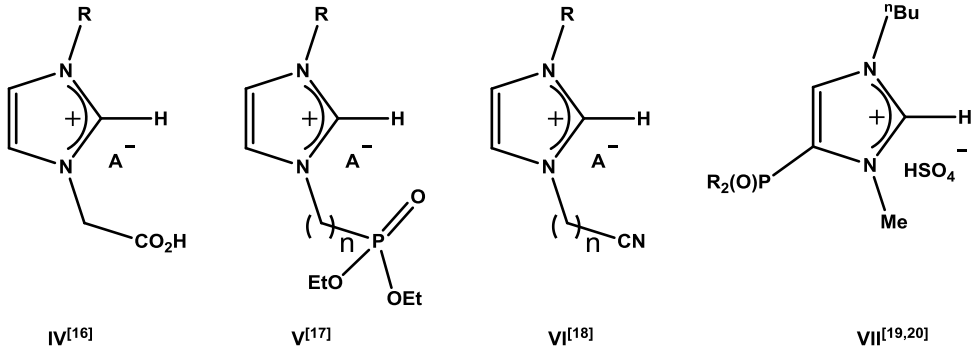

Figure 2: Selected examples of functionalized ionic liquids.

Some selected examples of functionalized ionic liquids are listed in Figure 2.

These task-specific ionic liquids (TSILs), also known as "designer solvents",[15] provide a diverse combination of cations and anions, which enables to design ionic liquids suitable for catalyzing a wide spectrum of chemical reactions. Those ionic liquids containing carboxylic acid (**IV**) are supreme for catalyzing acetalization of aldehydes.[16] Ionic liquids **V** fall into a special class of ionic liquids which contains a phosphorus-containing alkyl chain on the ring N-atom and are useful as lubricants for an aluminium-on-steal system.[17] Presence of a nitrile group on the side chain enables ionic liquids **VI** to act as catalysts in Heck, Suzuki and Stille coupling along with charge transfer complexes formation.[18] Compound class **VII**, which were recently developed by the Streubel group,[19, 20] fall into a unique category of ionic liquids containing a phosphinoyl functionality in the backbone and are completely halogen free. The catalytic utilities of **VII** are yet to be explored.

1.2 Backbone functionalization of imidazole-2-ylidenes

The first ever example of backbone functionalization of an imidazole-2-ylidene without touching the C^2-center, was published by Arduengo in 1999,[21] where he showed the backbone chlorination (and bromination)[22] using CCl_4 (and CBr_4) as the chlorinating (and brominating) agents (Figure 3).

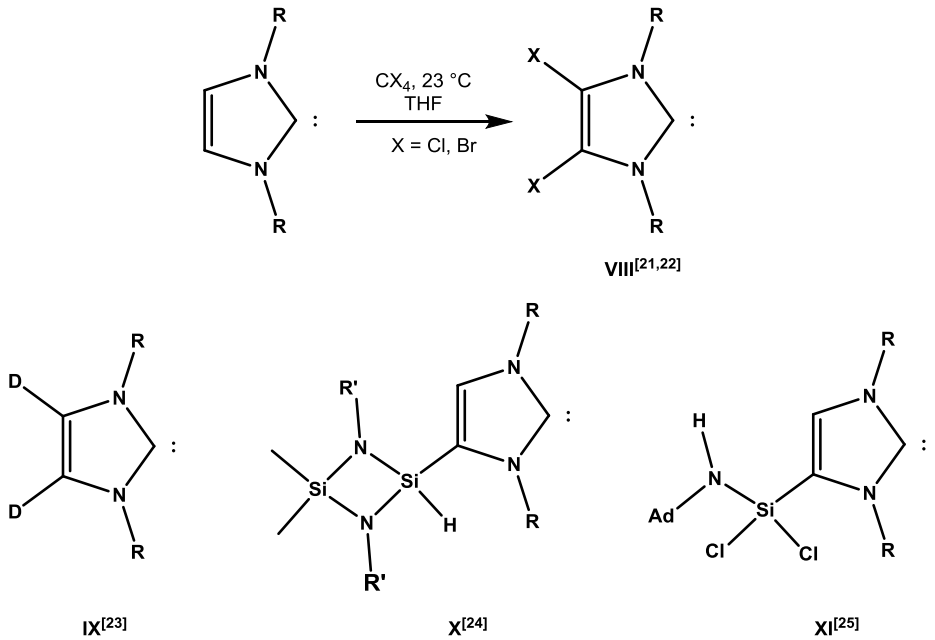

Figure 3: Backbone substitution of imidazole-2-ylidenes.

Introduction of two strongly electron withdrawing halogen atoms in the backbone diminishes the air and moisture sensitivity of **VIII** to an significant extent.[21, 22] Following this report, the chemistry of backbone substitution of imidazole-2-thione kick-started and examples of backbone-deuteration **IX**,[23] -silylation **X**[24]**-XI**[25] were published. These compounds created a quest for obtaining the versatility in the backbone substitution, especially for the inclusion of phosphorus containing functional groups.

The first breakthrough came with the work of Gates in 2009, in which a sterically demanding NHC **XII** reacted with a phosphaalkene to access the backbone phosphanyl substituted imidazole-2-ylidene **XIII** (Scheme 2).[26] During the course of the reaction, an abnormal form of the NHC (**IMes**) is believed to be formed, which then attacks the electrophilic P-center in the phosphaalkene to give a zwitterionic structure.

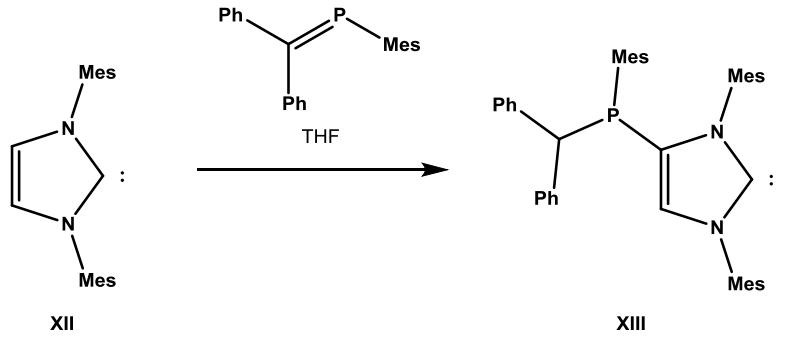

Scheme 2: First reported example of backbone substitution of imidazole-2-ylidene.[26]

This zwitterionic form in the next step converts to **XIII** via an intramolecular proton transfer. One year later, Bertrand[27] reported a more versatile and flexible route for a backbone phosphanylation of an imidazole-2-ylidene. They could show that the imidazolium salt **XV**, obtained by reacting the sterically protected NHC **XIV** with an electrophile (**E-X**), undergoes an intramolecular transfer of the

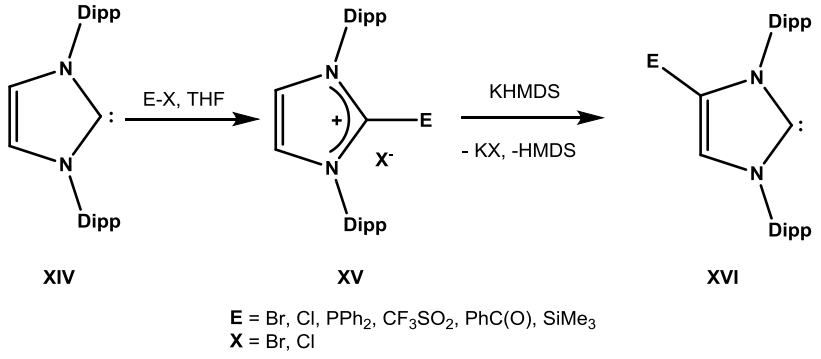

Scheme 3: Examples of backbone phosphanylation of imidazole-2-ylidene.[27]

electrophile from the C^2 to the C^4 position in the presence of a bulky and non-nucleophilic base e.g. KHMDS (Scheme 3). The treatment of **XV** with the base creates again an intermediate, abnormal NHC,[28] which thereafter undergoes intramolecular shift of the electrophile to isomerize to the more stable analogue **XVI**. This protocol also provides access to the disubstituted imidazole-2-ylidene, and therefore can be used to fine-tune the σ-donating and π-accepting properties of the backbone functionalized NHCs.

In the same manner compound **XVIII**, which represents a less sterically demanding version of **XIII** and **XVI**, was recently reported by the group of Ruiz.[29] This synthetic protocol proves that sterically demanding group on the N-center is not necessary to achieve backbone phosphanylation. Furthermore, they also garnered evidences for the utilization of this backbone phosphanylated imidazole-2-ylidene **XVIII** as a bidentate ligand (Scheme 4).[30]

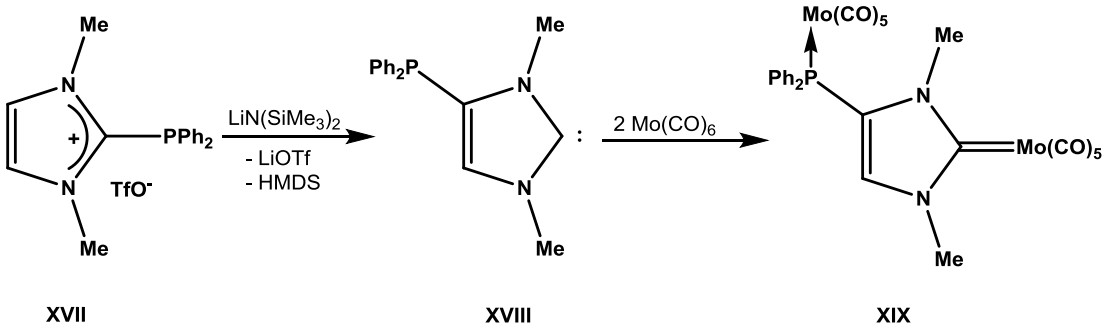

XVII XVIII XIX

Scheme 4: Synthesis of backbone phosphanylated bidentate imidazole-2-ylidene **XIX**.[29, 30]

The borane adduct of imidazole-2-ylidenes were also recently employed by Curran and co-workers for the purpose of backbone P-substitution. They could use the borane adduct **XX** in a salt with a wide range of electrophiles to get access to the backbone functionalized borane adducts **XXI** (Scheme 5).[31]

Moreover, it was also possible to achieve the backbone bis-substitution along this synthetic protocol. They also reported the way to remove the protection at the C^2-center of the NHC, so that the NHC can again be regenerated, if necessary. Compound **XXI**, upon treatment with methyltriflate or I_2 gets converted into the corresponding imidazolium salt which can be used for the generation of the NHC again at a later stage. This synthetic pathway also works very well with most of the substitution patterns at the backbone carbon center but has some inbuilt drawbacks when the backbone phosphanylation is concerned. The protocol is limited to the use of P^V-centers only as electrophiles and not so "functional group tolerant" in the context of phosphanylation. Against this

background, the use of imidazole-2-thiones for the purpose of backbone phosphanylation of imidazole-2-ylidenes becomes very promising.

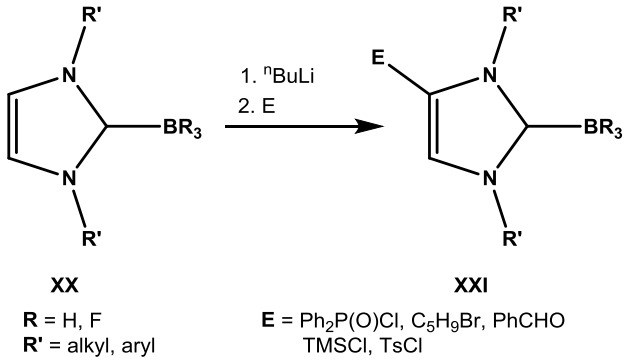

Scheme 5: Use of borane adducts of imidazole-2-ylidenes for backbone functionalization.[31]

1.3 Imidazole-2-thiones and backbone phosphanylation

The backbone phosphanylation of imidazole-2-thiones were reported first by Streubel and co-workers in 2012.[10] The final compound **XXIII** was obtained by treating the imidazole-2-thione **XXII** first with ^{n}BuLi to generate the lithiated intermediate which reacted *in situ* with a chloro-(diorgano)phosphane (Scheme 6). This particular approach to backbone phosphanylation is extremely selective, functional group tolerant, high yielding and a single-pot reaction. Therefore, it could be explored to create a wider spectrum of substitution patterns, using different chlorophosphanes and different alkyl/aryl groups on the N-center of the imidazole-2-thione. Later on, further reactions of these backbone phosphanylated imidazole-2-thiones were also studied in detail and reported by the Streubel group.

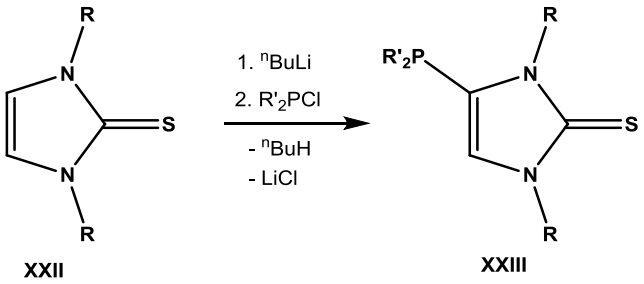

Scheme 6: Backbone phosphanylation of imidazole-2-thiones.[10]

Compound **XXIII** can further be phosphanylated in the backbone, but the conversion of the backbone P^{III}-center into a P^{V}-center is required prior to that (Scheme 7).[32] The oxidation of the backbone P^{III}-center makes the remaining vinylic proton (in compound **XXIV**) acidic enough which enables the second phosphanylation. Compounds **XXV** have been further oxidized to get access to the backbone P^{V}/P^{V}-substituted imidazole-2-thione, and, hereafter, coordination properties of **XXIII**-**XXV** were investigated.

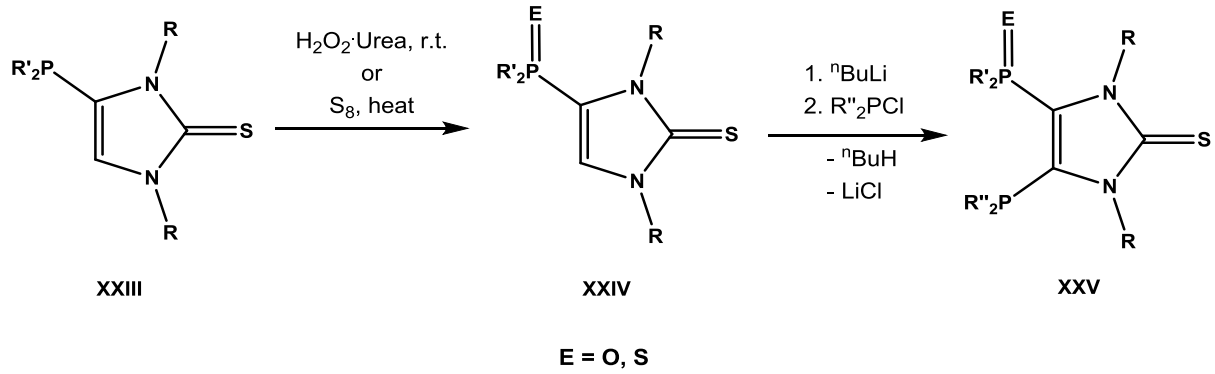

Scheme 7: Introduction of a second phosphanyl group in the backbone of imidazole-2-thiones.[32]

The main reason why these studies stand out in the chemistry of backbone phosphanylation of imidazole-2-ylidenes is the likelihood of these backbone phosphanylated imidazole-2-thiones to act as starting materials for the generation of corresponding NHCs. Both the reductive and oxidative pathways of desulfurizing the C^{2}-center of the thione were explored in the Streubel group in recent years. In case of reductive desulfurization in the presence of an alkali metal, these backbone phosphanylated imidazole-2-thiones gave access to first examples of imidazolium phosphanide zwitterions **XXVI** (Scheme 8).[33] Under these harsh reductive conditions the backbone P-C bond was also cleaved along with the C=S bond to produce these zwitterions. But in the case of oxidative desulfurization the scenario is different, *i.e.*, compounds **XXVI,** upon treatment with aq. solution of hydrogen peroxide, gives an easy access to backbone phosphinoyl substituted imidazolium salts **XXVII** (Scheme 8).[19, 20, 34] These imidazolium salts were also successfully employed to synthesize the corresponding backbone P-substituted imidazole-2-ylidenes **XXVIII**.[20, 34] This new pathway enables also to fine-tune the σ-donating and π-accepting properties of NHCs by means of careful choice of suitable P-containing substituents in the imidazole backbone.

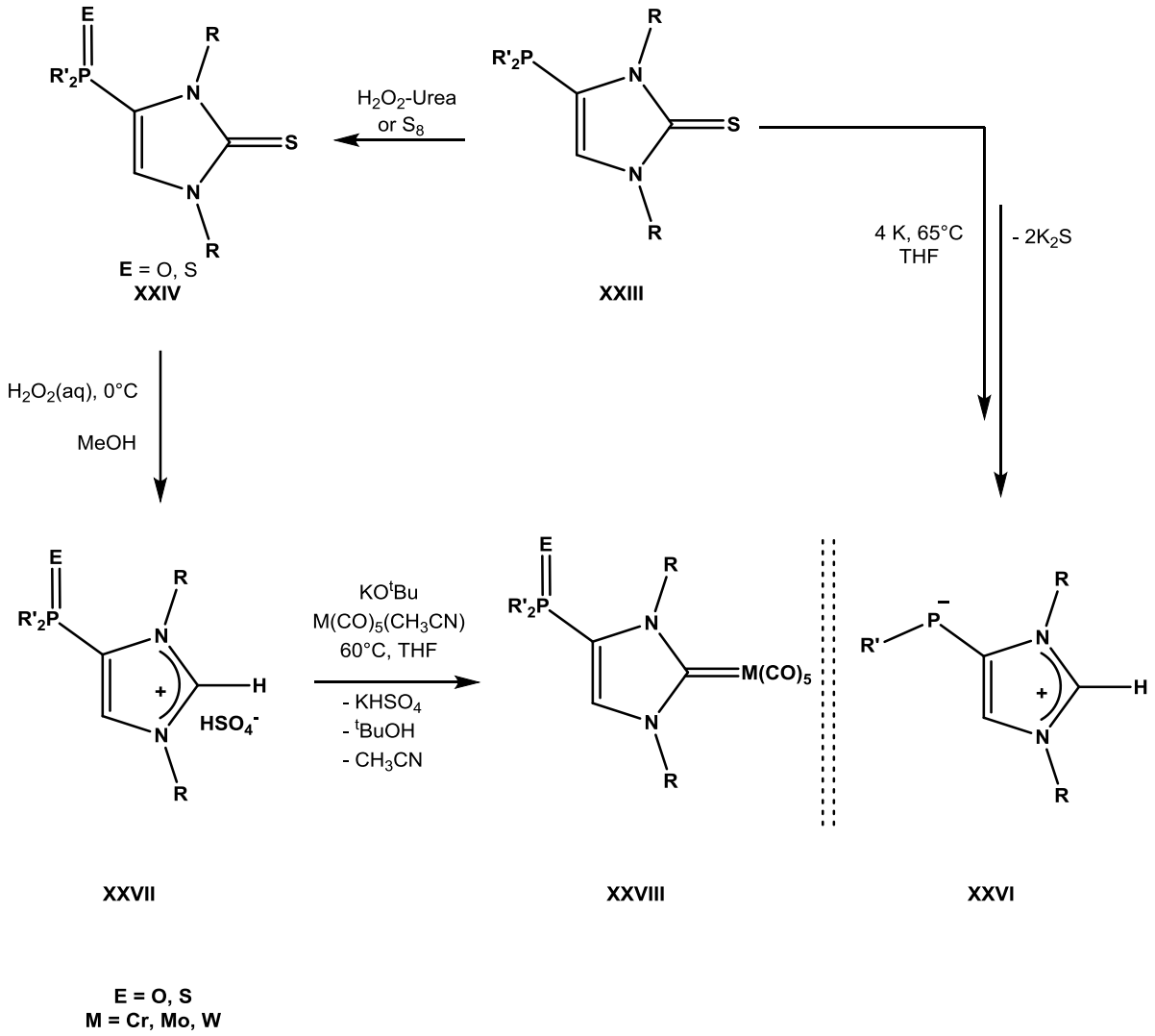

Scheme 8: Synthesis of backbone P-substituted imidazole-2-ylidene complexes and an imidazolium phosphanide zwitterion.[19, 33]

Having such a prudent protocol also helped to explore the possibilities of introducing more than one imidazole-2-thione moiety in the backbone phosphorus center. Use of a dichlorophosphane permits the synthesis of the bis(imidazole-2-thione-4-yl)phosphanes **XXIX** (Scheme 9).[35] Compounds **XXIX** were later subjected to oxidation, complexation, acid-induced P-N bond cleavage[35, 36] and oxidative desulfurization,[34] respectively. The bis-imidazolium salts obtained from the oxidative desulfurization reactions of **XXIX** gave access to first examples of phosphanyl bridged bis-imidazole-2-ylidenes and their metal complexes.[34] These bis(imidazole-2-thione-4-yl)-phosphanes **XXIX** were also successfully employed recently in the chemistry of low-coordinated phosphorus chemistry.[36] With such a wide spread reactivity spectrum and applicability of these bis(imidazole-2-thione-4-yl)phosphanes are bound to draw more attentions in synthesis.

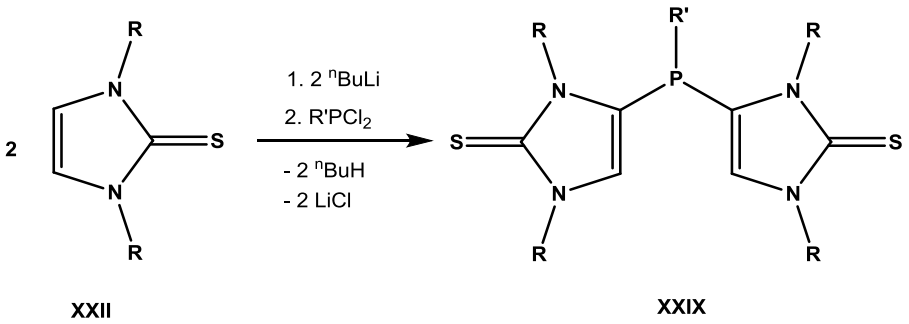

Scheme 9: Synthesis of bis(imidazole-2-thione-4-yl)phosphanes **XXIX**.[35]

1.4 An imidazole-2-thione based tricyclic 1,4-dihydro-1,4-diphosphinine by-product

Taking a closer look at the synthetic protocols for compounds **XXIX**, one can see that the reaction outcome is not always straightforward as in the case of **XIII**, and the outcome is related to the nature of R and R'. Backbone phosphanylation of 1,3-dimethylimidazole-2-thione using dimethyl-amino-dichlorophosphane as the electrophile produces the tricyclic compound **XXX**[37] (Scheme 10) as minor product along with **XXIX**. The limited solubility of compound **XXX** helped in its first isolation as it precipitates out of the reaction mixture as white powder during the course of the reaction. It is formed as a mixture of two stereoisomers (*cis* and *trans*), the latter is due to a substantial inversion barrier at the two P-centers. As compound **XXX** was formed in the reaction mixture only as the minor product (yield: up to 4%), and together with the limited solubility, studies on the chemistry of compound **XXX** were hold back substantially. In particular, the pathway of formation of compound **XXX** was not understood, and its chemistry was not investigated, too. Compound **XXX** contains the

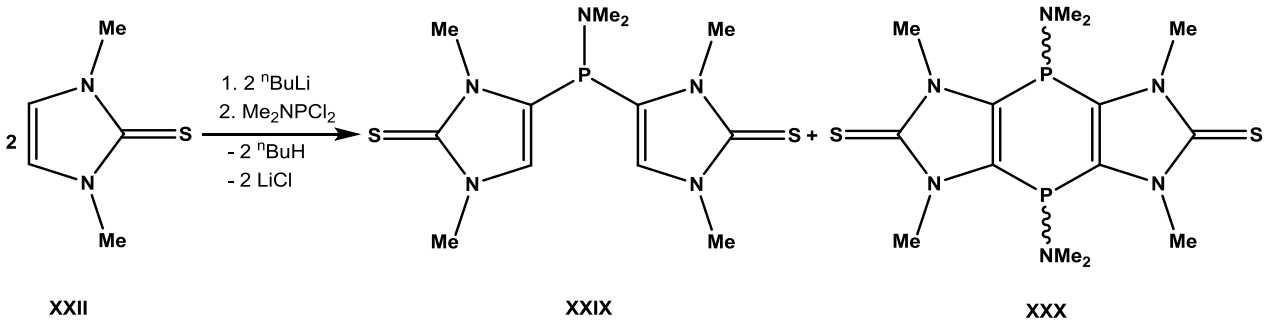

Scheme 10: Synthesis of imidazole-2-thione based tricyclic 1,4-dihydro-1,4-diphosphinine **XXX.**[37]

1,4-dihydro-1,4-diphosphinine motif, a six-membered heterocyclic compound with two $\sigma^3\lambda^3$-phosphorus centers; σ represents the coordination number of P and λ the number of valence electrons involved in bonding.

The first derivative related to **XXX** was reported in 1964 by Mann and co-workers.[38] They showed that the 1,4-dihydro-1,4-diphosphinine **XXXI** (Figure 4) (R = Et, Ph), condensed to two benzene rings, could easily be obtained via a stepwise ring closure using dichlorophosphane as the source of phosphorus. Later on, Uchida[39] added a further simplification to the synthetic protocol of **XXXI**. The synthesis of the monocyclic compound **XXXII** was reported by Märkl [40] where the six-membered ring was constructed by reacting di(ethinyl)phosphane with a primary phosphane. This synthetic protocol proved to be really convenient and leads to wide combination of substituents on the phosphorus. The idea of a formal replacement of the benzene rings in compound **XXXI** by other structural motifs has been established for the following units: tetrafluorobenzene,[41] thiophene,[42] xylene[43] and tetrathiafulvalene[44] systems have already been reported. Compound **XXXIII** (X = O, S), reported by Becher,[45] presents an unique synthetic pathway to the 1,4-dihydro-1,4-diphosphinine ring where elimination of volatile trimethylchlorosilane drives the cyclization. In this context, compound **XXXIV** was synthesized via thermal fusion of the corresponding backbone dichlorophosphanyl substituted 1-methyl-2-(alkyl)-imidazole and PCl_3 using pyridine as base.

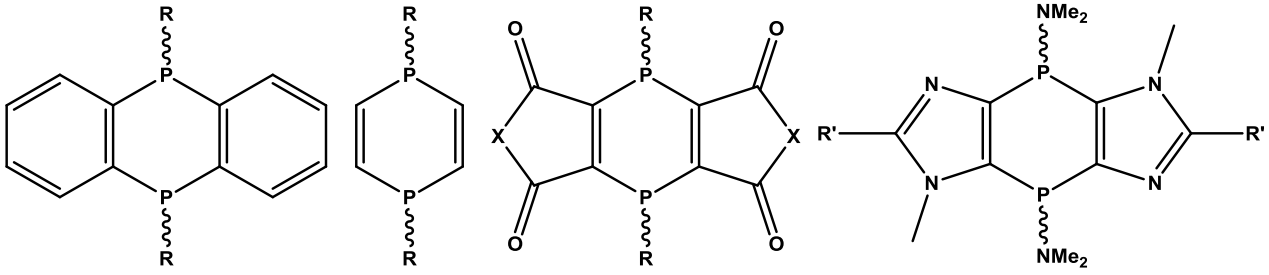

XXXI[39,40] **XXXII**[41] **XXXIII**[46] **XXXIV**[47]

Figure 4: Some literature known examples of 1,4-dihydro-1,4-diphosphinines.

XXXIV also includes another different heterocyclic structural motif.[46] Furthermore, Märkl had also envisaged the 1,4-dihydro-1,4-diphosphinines as the probable starting for obtaining the 1,4-diphosphinines under thermal elimination condition. But this remained to be experimentally established till today.[40]

1.5 Phosphinines and diphosphinines

Phosphinines, also previously termed phosphabenzenes, are P-analogues of benzene and their synthesis in 1966 by Märkl[47] has been a real landmark in the chemistry of low-coordinated P-chemistry. They possess planar, six-membered, aromatic heterocyclic ring with a $\sigma^2\lambda^3$-phosphorus atom in the ring. Due to the incorporation of the P-atom in the benzene ring the π-conjugation within the ring is perturbed and, therefore, the aromaticity is diminished. The aromaticity of phosphinine is ~ 88 % of the aromaticity[48] of benzene, but this slight reduction does not fully

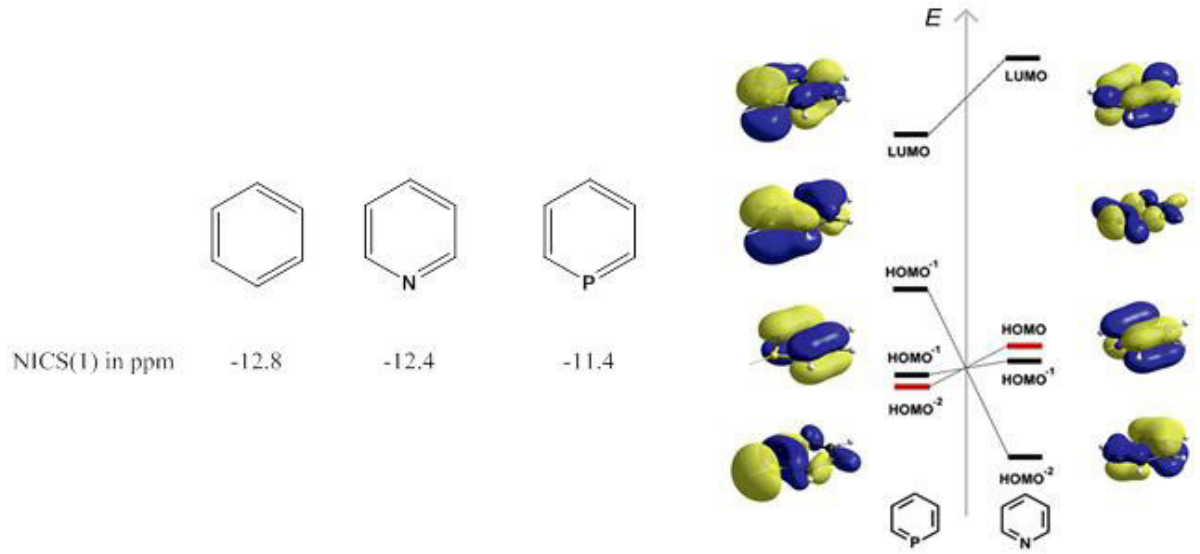

Figure 5: Benzene and its hetero-analogues.[49]

reflect the effect of the inclusion of the P-atom in the ring. When the molecular orbitals of phosphinine are compared to pyridine, the first substantial difference is the change in the nature of lone pair. The lone pair in phosphinine has little to no nucleophilic character left due to its occupation in a less directional and more diffused HOMO-2 orbital (Figure 5).[49] In fact the LUMO in phosphinine has a large coefficient on the phosphorus atom and is much lower in energy compared to that of pyridine. And this is why phosphinine is a much weaker σ-donor and much stronger π-acceptor ligand compared to pyridine.

The first synthesis of phosphinines was the thermal reaction between a formal PH_3 source and a pyrylium salt, as described by Märkl,[50] and compound **XXXV** (Figure 6) remained the most easily accessible derivative for long time. The most important illustrative example of this series though is the synthesis of the parent compound **XXXVI** which used a base-induced dehydrohalogenation

reaction starting from 1-bromo-phospha-cyclohexadiene.[51] In contrast, a [4+2]-cycloaddition reaction between 1,3-cyclopentadiene and ^{t}BuCP[52] was used for synthesis of compound **XXXVII**. Phosphinines can also be derived via thermal elimination of a small molecule which leads to aromatization, *e.g.*, 1-benzyl-1,2-dihydro-phospha-naphthalene loses a molecule of toluene upon heating at 260-300°C to produce compound **XXXVIII**.[53] Another illustrative synthetic route is the reaction between ethyldiazoacetate with a phosphole sulfide as addition of the carbene at the C^2-C^3 bond of the phosphole creates a bicyclic derivative in the first step which, under thermal conditions, subsequently rearranges to compound **XXXIX**.[54] Finally, compound **XL** was synthesized via a [4+2]-cycloaddition reaction between an 1,3-azaphosphinine and an alkyne, followed by elimination of a nitrile unit.[55] There are several more synthetic routes available to phosphinines as their chemistry has seen an enormous development since the first report by Märkl, and is still developing.

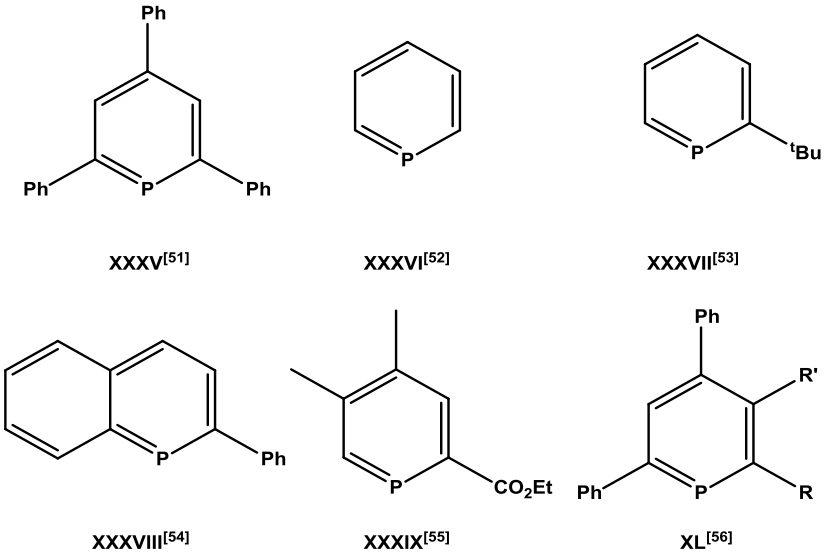

Figure 6: Some selected examples of $\sigma^2\lambda^3$-phosphinines **XXXV-XL**, derived from different synthetic protocols.

In case of diphosphinines, three possible regioisomers can be envisaged, *i.e.* 1,2-diphosphinine, 1,3-diphosphinine and 1,4-diphosphinine (Figure 7). The chemistry of these diphosphinines is still largely underdeveloped mainly due to their high reactivity and instability.

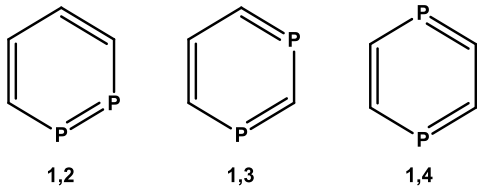

Figure 7: Regioisomers of $\sigma^3\lambda^3$-diphosphinines.

In the case of 1,2-diphosphinines, a single report came from Bickelhaupt and co-workers.[56] Upon treatment of compound **XLI** with hydrogen chloride a cyclic intermediate **XLII** was formed, instead of the originally targeted bis-dichlorophosphane derivative. This cyclic intermediate could be converted to the $1\lambda^5,2\lambda^3$-diphosphinine **XLIII** (Scheme 11) upon reduction with Mg. The final compound though could not be isolated and purified, and was exclusively evidenced via ^{31}P NMR spectroscopy, *i.e.*, compound **XLIII** shows two doublets at 94.5 and -129 ppm, respectively, with a large $^1J_{P,P}$ coupling constant of 469 Hz.

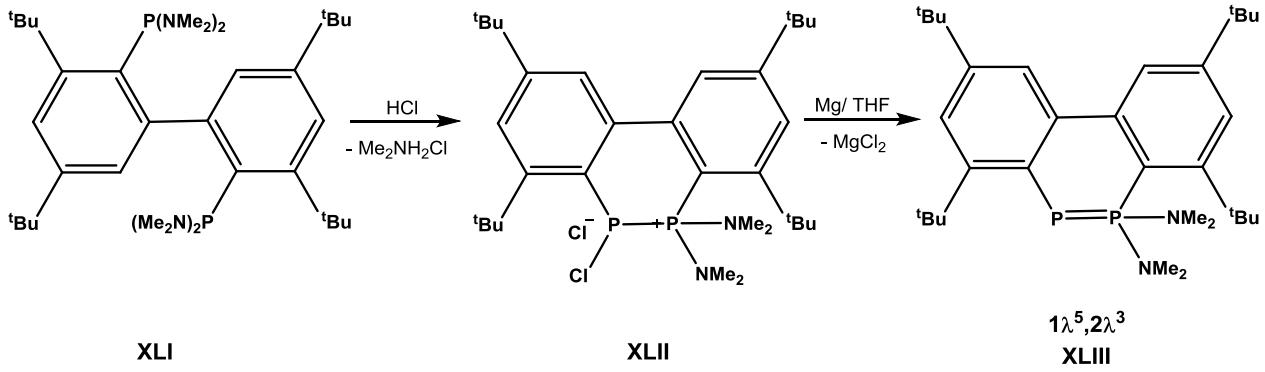

XLI **XLII** $1\lambda^5,2\lambda^3$ **XLIII**

Scheme 11: Synthesis of the only known example of 1,2-diphosphinine **XLIII**.[56]

Comparatively well-known are $1\lambda^3,3\lambda^3$-diphosphinines and the first example was reported by Zenneck and co-workers in 1995.[57] Compound **XLIV** was synthesized via an iron(0)-catalyzed regiospecific [2+2+2]-cycloaddition of two molecules of *tert*-butyl-phosphaethyne with an alkyne under mild reaction conditions. The final product was formed as an iron complex, from which the free 1,3-diphosphinine ligand was released via oxidation with CCl_4 at elevated temperature (Figure 8). Compound **XLV**[58] represents a phosphonium-substituted 1,3-diphosphinine and could be synthesized by means of dechlorination of the corresponding 1,3-diphosphatetraline derivative, using $GaCl_3$ as the halide-abstracting reagent. A wide range of $1\lambda^5,3\lambda^5$-diphosphinines are also known in the literature. Fluck and co-workers obtained compound **XLVI** [59] as the final product of the attempted synthesis of 1,1,3,3,-tetrakis(dimethylamino)-$1\lambda^5,3\lambda^5$-diphosphete. Here, the diphosphinine was formed in a Diels-Alder reaction of the targeted compound (1,1,3,3,-tetrakis(dimethylamino)-$1\lambda^5,3\lambda^5$-diphosphete) with an alkyne derivative. Finally, compound **XLVII** represents a highly stable version of a $1\lambda^5,3\lambda^5$-diphosphinine reported by Märkl in 1963 that was easily obtained by stepwise deprotonation of 1,1,3,3,-tetraphenyl-1,3-diphosphoniocyclohex-4-ene.[60]

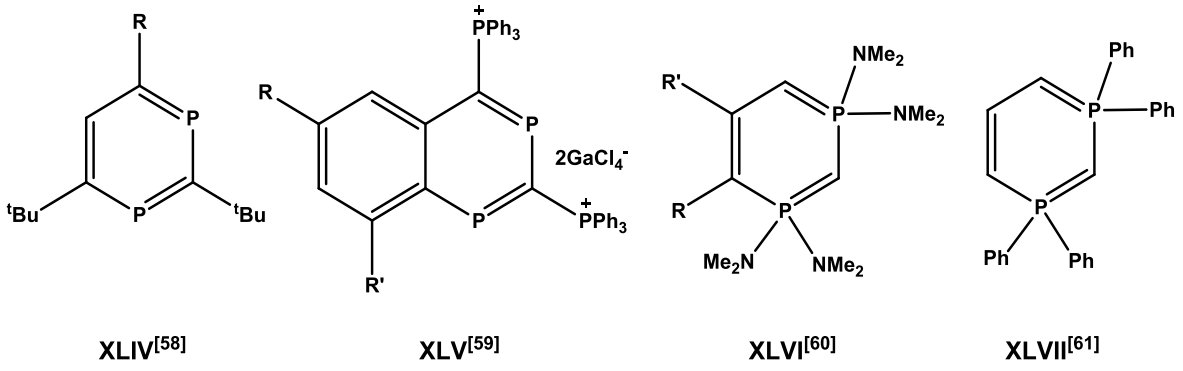

Figure 8: Selected examples of 1,3-diphosphinines.

In case of 1,4-diphosphinines, **L** is the only known example, and it possesses four trifluoromethyl substituents (Scheme 12).[61] **L** was obtained from a two-step synthetic protocol in which the perfluormethylated-1,4-phosphabarrelene **XLVIII** undergoes a Rh^{III}-catalyzed addition of methanol to form compound **XLIX** which, finally, eliminates the alkene fragment **LI** to produce the final compound **L** under prolonged reflux condition. Due to its extreme air and moisture sensitivity, compound **L** has never been isolated and fully characterized, and no structural information of a 1,4-diphosphinine is known till date. In the ^{31}P NMR spectrum the resonance signal of **L** appears in the downfield region at 287 ppm which might be due to the presence of four strongly electron-withdrawing groups.[62] Compound **L** could be handled as *n*-hexane solution and used in a few reactions, described in scheme 13.

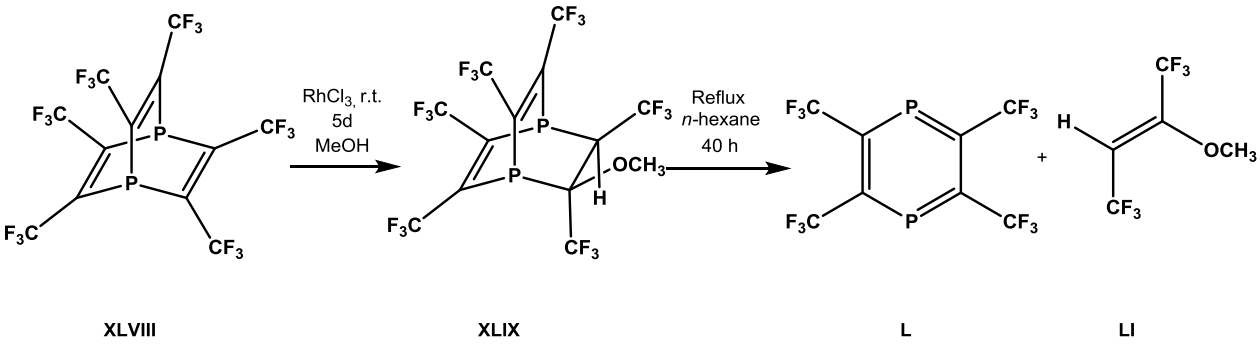

Scheme 12: Synthesis of the solely known 1,4-diphosphinine.[62]

Kobayashi and co-workers carried out some reactivity studies of compound **L**. For example, heating compound **L** with carbon tetrachloride in a sealed tube at 130°C causes formation of diphosphanorbornadiene derivative **LII**[62] by a pathway, possibly analogous to the reaction between PPh_3

and CCl_4.[63] Compound **L** was also used as a diene in several thermal [4+2]-cycloaddition reaction to get access to the diphosphabarrelenes **LIII**.[62]

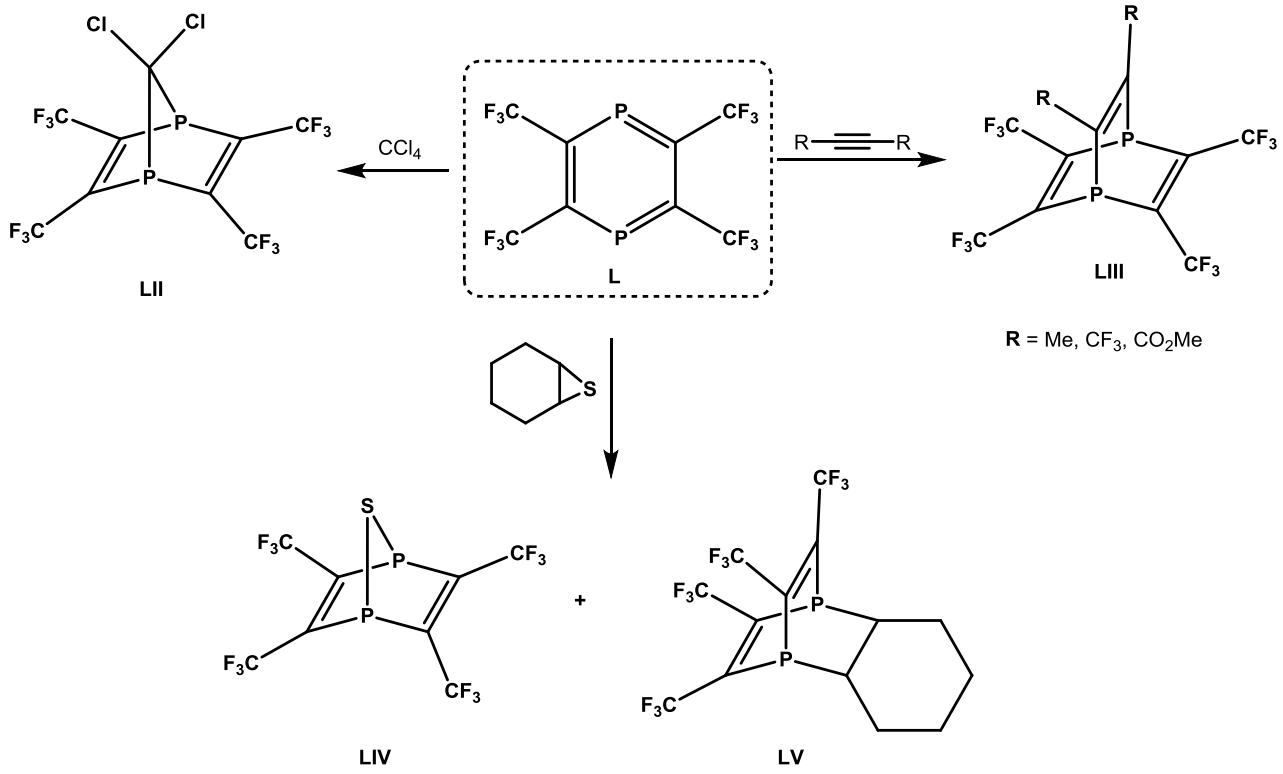

Scheme 13: Literature reported reactivities of 1,4-diphosphinine **L**.[62]

In the same manner, when heated with an episulfide, compound **L** produces 2,3,5,6-tetrakis(trifluoromethyl)-7-thia-1,4-diphosphanorbornadiene **LV** via a formal [4+1]-cycloaddition reaction. Formation of compound **LV** was further confirmed via desulfurization with PPh_3 thus producing the starting material **L**, again.[64]

Chapter 2

2. Objectives of this PhD thesis

As compound **XXX** showed the structural and chemical potential to act as starting point to access imidazole-2-thione-based tricyclic 1,4-diphosphinines, the main goals and objectives of this PhD thesis were:

- to investigate the formation of tricyclic 1,4-dihydro-1,4-diphosphinines
- to develop an alternative reaction protocol for tricyclic 1,4-dihydro-1,4-diphosphinines
- to study reactions of tricyclic 1,4-dihydro-1,4-diphosphinines
- to develop a P-functionality that enables substitution reactions
- to establish pathways towards 1,4-diphosphinine derivatives and develop their chemistry.

Chapter 3

3. Investigations on the formation of tricyclic1,4-dihydro-1,4-diphosphinines

As briefly mentioned beforehand (*cf.* Scheme 10), compound **XXX** was initially isolated in low yield from the attempted backbone phosphanylation of 1,3-dimethylimidazole-2-thione while using dimethylamino(dichloro)phosphane as the electrophile, and the pathway remained unclear. Assuming a large synthetic potential of such compounds, especially in further stabilization of the targeted 1,4-diphosphinines by virtue of extended electronic delocalization due to the planar structure of the thione, it was decided to investigate the effect of N- and P-substituents and the stoichiometry on the reaction outcome.

3.1 Effect of N- and P-substituents

To start this study, the reaction stoichiometry was followed as described in scheme 13 and applied to derivatives with a wide range of *P*- and *N*-substituents (R' and R respectively) (Table 1). The presence of the *P*-NMe_2 group led to 1,4-dihydro-1,4-diphosphinines in low yields (4% for **4a**, 16%

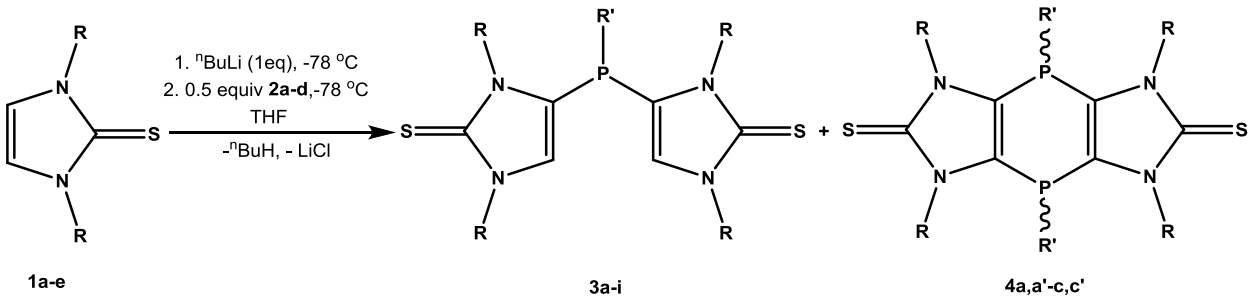

Scheme 14: Synthesis of bis-(imidazole-2-thione)substituted phosphanes **3a-i** and tricyclic 1,4-dihydro-1,4-diphosphinines **4a-c**.

for **4b**), but only for primary alkyl groups (**4a,b**) at the thione *N*-centers. Both **4a** and **4b** were isolated and completely characterized. Interestingly, **4a,b** showed two resonance signals in the $^{31}P\{^{1}H\}$ NMR spectra, which could be assigned to the pair of stereoisomers originated due to the hindered inversion of the dimethylamino group at the P-center at room temperature (Figure 9). In case of **4a,a'**, the *trans* isomer could be separated using the solubility differences of the isomers by repeated washing of the *cis/trans* isomeric mixture of **4a,a'** with THF at room temperature. The *trans* isomer was left in the residue due to its lower solubility.

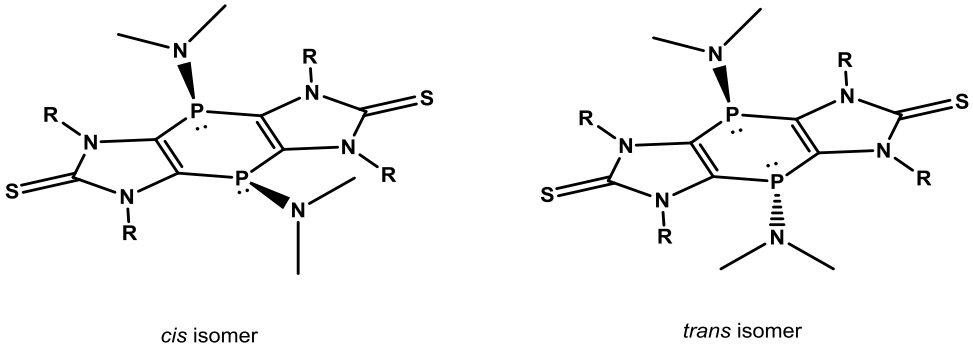

Figure 9: *cis* and *trans* isomers of tricyclic 1,4-dihydro-1,4-diphosphinines **4**.

In contrast, compound **4b,b',** could only be isolated as a mixture of two isomers by means of column chromatography using diethyl ether /petrol ether (40/60) mixtures as eluents, due to the increased solubility of **4b,b'** stemming from longer alkyl chains. This pure *cis/trans* isomeric mixture was used as such for the full characterization of compound **4b,b'**. The ^{31}P NMR spectrum (in $CDCl_3$) of the reaction solution of **4b,b'** showed chemical shifts of 8.7 and 9.2 ppm for the two isomers (ratio 3:1). These values for **4** were in good agreement with literature reported values for 1,4-dihydro-1,4-diphosphinine **XXXIV** bearing a *P*-NR_2 (R = Me) fragment (15.6 ppm).[46] Furthermore, the ^{1}H NMR spectrum of **4b** revealed the absence of any backbone proton resonance, which in turn confirmed the occurrence of cyclization. The yield improved marginally in case of **4b** (16%) compared to **4a** (only 4%). The main products of these two reaction mixture, *i.e.,* **3a** and **3b** were also isolated in moderate to good yields (Table 1) and completely characterized. Compound **3b** showed exactly similar trends in case of physical and chemical properties as the previously reported *N*-Me analogue **3a**.[35]

Single crystals of **4a,b** suitable for X-ray crystallographic measurements could be easily grown from its saturated dichloromethane solution at –20 °C, **4a** after separation as described beforehand; crystals of **4b** were obtained from the isomer mixture. The solid state structures of *trans* **4a** and of

Table 1: $^{31}P\{^{1}H\}$ NMR spectroscopic data and yields of products **3** and **4** .

P-substituents (R') in $R'PCl_2$ (**2a-d**)	N-substituents (R) in thiones (**1a-e**)	δ_P (from reaction mixture, THF)		Isolated yield (%)	
		3	**4**	**3**	**4**
NMe_2 (**2a**)	Me (**1a**)	14.7[35] (**3a**)	9.8 , 10.2 (**4a,a'**)	60	4
	Et (**1b**)	11.9 (**3b**)	8.7 , 9.2 (**4b,b'**)	32	16
	Ph (**1c**)	16.7[35] (**3c**)	-	75	-
	^{i}Pr (**1d**)	15.6[36] (**3d**)	-	81	-
$N^{i}Pr_2$ (**2b**)	Me (**1a**)	10.7 (**3e**)	-12.9 , -13.2 (**4c,c'**)	-	-
OEt (**2c**)	Me (**1a**)	68.4 (**3f**)	-	-	
	^{i}Pr (**1d**)	70.2 (**3g**)	-	75	-
Ph (**2d**)	Me (**1a**)	-56.2 (**3h**)	-	-	-
	^{n}Bu (**1e**)	-59.2 (**3i**)	-	60	-

cis **4b** are shown in figure 10. In both isomers the metrical parameters for the middle six-membered ring are invariant, with the exception of the quest for "planarity" of the middle ring. In *cis* **4b**, the two P atoms are slightly out of plane by 0.13 Å and the folding angle between P(1)-C(1)-C(2)-P(2) and P(1)-C(4)-C(3)-P(2) planes is 14.1° whereas in *trans* **4a** the 6 atoms are within one plane.

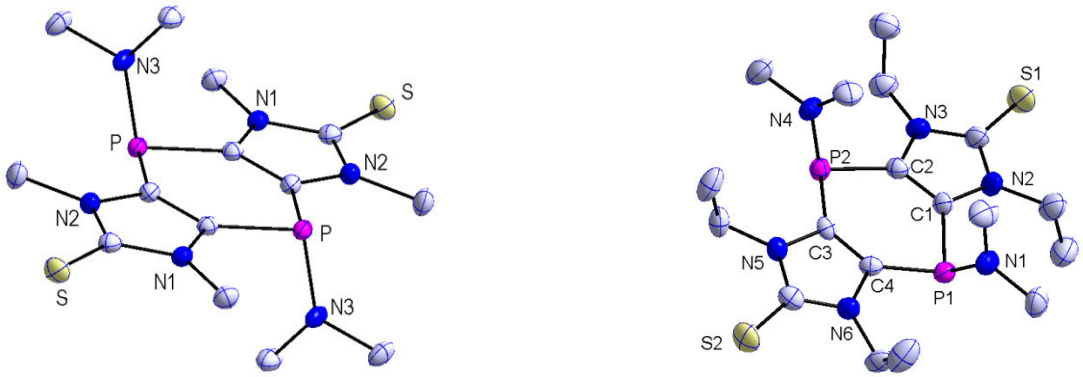

Figure 10: Molecular structure of *trans* **4a** and *cis* **4b**; hydrogen atoms are omitted for clarity (50% probability level). Selected bond distances (Å) and angles (°) for trans **4a**: P-C(3) 1.8104(4), P-N(3) 1.6631(3), C(3)-C(4) 1.3670(2); C(3)-P-C(4) 94.894(8), C(3)-P-N(3) 103.8. For cis-**4b**: P(1)-C(1) 1.8143(1), P(1)-N(1) 1.6641(0), C(1)-C(2) 1.3689(0); C(1)-P(1)-C(4) 95.220(1), N(1)-P(1)-C(1) 107.307(1).

On the other hand, when the N-substituent was changed to aryl (Ph, **1c**) or secondary alkyl (^{i}Pr, **1d**) group, the formation of 1,4-dihydro-1,4-diphosphinines was no longer detected, and the acyclic

phosphanes **3c-d** were obtained as sole products. Compound **3c** was reported earlier,[35] and compound **3d** was isolated and completely characterized. Both **3b** and **3c** were isolated in high yields as white powders and the ^{31}P NMR spectra of them revealed same trends in chemical shifts as seen for **3a,b** (16.8 ppm for **3c**, 15.5 ppm for **3d**).

If a sterically more demanding dichlorophosphane was used, having N^{i}Pr$_2$ group at the *P*-center (**2b**), the formation of two isomers of the tricyclic 1,4-dihydro-1,4-diphosphinine (**4c**) were observed, along with the acyclic compound (**3e**). The ^{31}P{1H} NMR spectrum of the reaction mixture showed two resonance signals at -12.9 and -13.2 ppm, respectively, which were tentatively assigned to the two isomers of **4c**. While the resonance signal at 10.7 ppm could be assigned to the corresponding acyclic compound **3e**. Unfortunately, it was not achieved to get **3e** and **4c** in pure form. Though the isolation of **4c** was not achieved, the NMR spectroscopic investigation of the reaction mixture lend some support to its formation.

After the examined the case of aminodichlorophosphanes, we became interested to exploit the scope of this synthetic protocol by employing *P*-alkoxy derivatives. As a case In point, the dichloro-(ethoxy)phosphane (**2c**) was employed but no formation of a tricyclic 1,4-dihydro-1,4-diphos-phinine was observed, regardless of the thione used (Table 1). In case of thione **1a**, formation of the tris(imidazole-2-thione-4-yl)phosphane was observed in the ^{31}P{^{1}H} NMR spectrum of the reaction mixture (singlet at -78.2 ppm). Apart from that, the reaction mixture was not informative due to an unselective reaction. But in the case of thione **1d**, having the ^{i}Pr group on the N-centers, the reaction was selective and the only product formed in this case was the acyclic compound **3g**. Compound **3g** could be easily isolated from the reaction mixture in excellent yield as a white powder and was completely characterized by means of all standard analytical methods. The ^{31}P NMR spectrum of compound **3g** showed a triplet resonance signal at 70.3 ppm ($^{3}J_{P,H}$ = 10.1 Hz), which proves the bond of the ethoxy group to the P-center. Apart from the analytical confirmation, formation of compound **3g** was also established by X-ray crystallographic measurements. Single crystals of compound **3g**, were grown carefully from its saturated dichloromethane solution at –20°C. Compound **3g** crystallizes in the monoclinic crystal system with the P2$_1$/n space group. The sum of bond angles at the P-center is 292.6°, which reflects the non-planar geometry around the P-center. The P-C(1) bond length is 1.8134(1) Å, which falls in accordance with previously reported compounds [*cf.* PhP(IMS^{iPr,Me})$_2$ 1.817(2), Ph$_2$P-IMS^{Me,Me} 1.8185(18), Ph$_2$P-IMS^{Ph,Ph} 1.8190(5) etc.; where IMS^{R,R} = 1,3-dialkylimidazole-2-thione-4-yl].

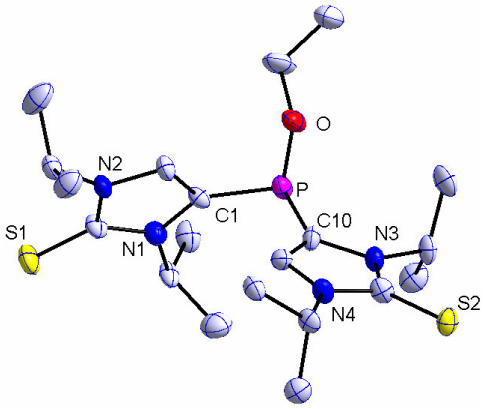

Figure 11: Molecular structure of **3g**; hydrogen atoms are omitted for clarity (50% probability *level*). Selected bond distances (Å) and angles (°): P-C(1) 1.8134(1), P-O 1.6380(1), P-C(10) 1.8010(1); C(1)-P-C(10) 97.162(2), C(1)-P-O 98.913(2).

After this unsuccessful attempt, the dichloro(phenyl)phosphane was employed to see the effect of a *P*-aryl substituent on the reaction outcome, but also here the result was negative as no tricyclic 1,4-dihydro-1,4-diphosphinines could be detected, even for derivatives having primary alkyl groups at the N-centers of the thione such as Me (**1a**) or ^{n}Bu (**1e**) (Table 1). In both cases the acyclic bis(imidazole-2-thione-4-yl)phosphanes were the main products. Although compound **3h** could not be isolated from the reaction mixture owing to the limited selectivity, compound **3i** was isolated as light yellow powder. The ^{31}P NMR spectrum of pure **3i** shows a triplet resonance signal at -59.2 ppm ($^{3}J_{P,H}$ = 8.5 Hz). The molecular structure of **3i** was confirmed by X-ray crystallographic measurements using single crystals grown from saturated diethylether solution at room temperature. Compound **3i** crystallizes in the monoclinic crystal system with the C2/c space group. The metrical parameters are in agreement with previously reported analogous phosphorus compounds.

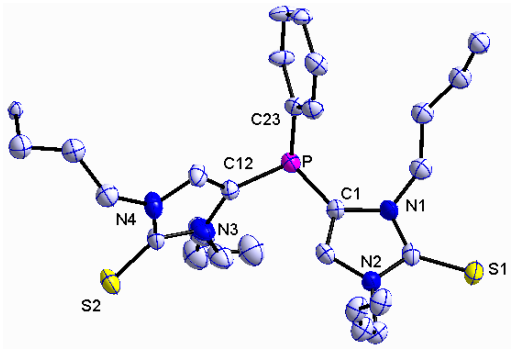

Figure 12: Molecular structure of **3i**; hydrogen atoms are omitted for clarity (50% probability level). Selected bond distances (Å) and angles (°): P-C(1) 1.8183(1), P-C(23) 1.8291(1), P-C(12) 1.8078(1); C(1)-P-C(12) 99.043(3), C(12)-P-C(23) 98.966(3).

3.2 Effect of the reaction stoichiometry

After the exploration of N and P-substituents (R and R') effects on the reaction outcome, the next aspect of interest was the effect of the stoichiometry on the product formation according to scheme 13. To investigate this, the reaction of **1a** and **2a** was used for this study. Firstly, the amount of ^{n}BuLi and **2a** were changed, keeping the thione amount constant and when 1 eq. of **1a** was treated with 1 eq. of ^{n}BuLi and 0.5 eq. of **2a**, a minimal yield of only 4% **4a,a'** was formed. If the amount of **2a** was doubled keeping the amount of thione and ^{n}BuLi constant, there was no change in the yield of **4a**. If both the amounts of **2a** and ^{n}BuLi were doubled then a slight increase of **4a,a'** was observed (from 4% to 10%) (Table 2).

Table 2: Changes in the reaction outcome as effect of a changed reaction stoichiometry.

1a (eq.)	**^{n}BuLi** (eq.)	**2a** (eq.)	Yield (%) of **4a,a'**
1	1	0.5	4
1	1	1	5
1	2	1	10

This study showed the possibility to increase the yield of **3a,** but only at the expense of a significantly reduced reaction selectivity. Although some new insight were gained from these results, one basic question remained: how do tricyclic 1,4-dihydro-1,4-diphosphinines form, and/or how do different solubility of tricyclic 1,4-dihydro-1,4-diphosphinines play an important role?

Therefore, the ^{31}P NMR spectra of the reaction mixtures of **1c,d** and **2a** (R = Ph, ^{i}Pr and R' = NMe_2) were again carefully inspected. They showed resonance signals in low intensities at 108.4 ppm (R = ^{i}Pr; 6%) and 109.2 ppm (R = Ph, 9%) which were tentatively assigned to reactive intermediates, *i.e.*, the mono-substituted compounds, namely the amino(chloro)phosphanyl imidazole-2-thiones **5c,d**. Based on this assignment as starting hypothesis, two possible routes I,II (Scheme 15) of cyclization could be imagined: (i) a stepwise deprotonation at the backbone of the acyclic bis(imidazole-2-thione-4-yl)phosphane **3** and a cyclizing phosphanylation, or (ii) the amino(chloro)phosphanyl imidazole-2-thione **5** is deprotonated first, followed by dimerization via double salt metathesis.

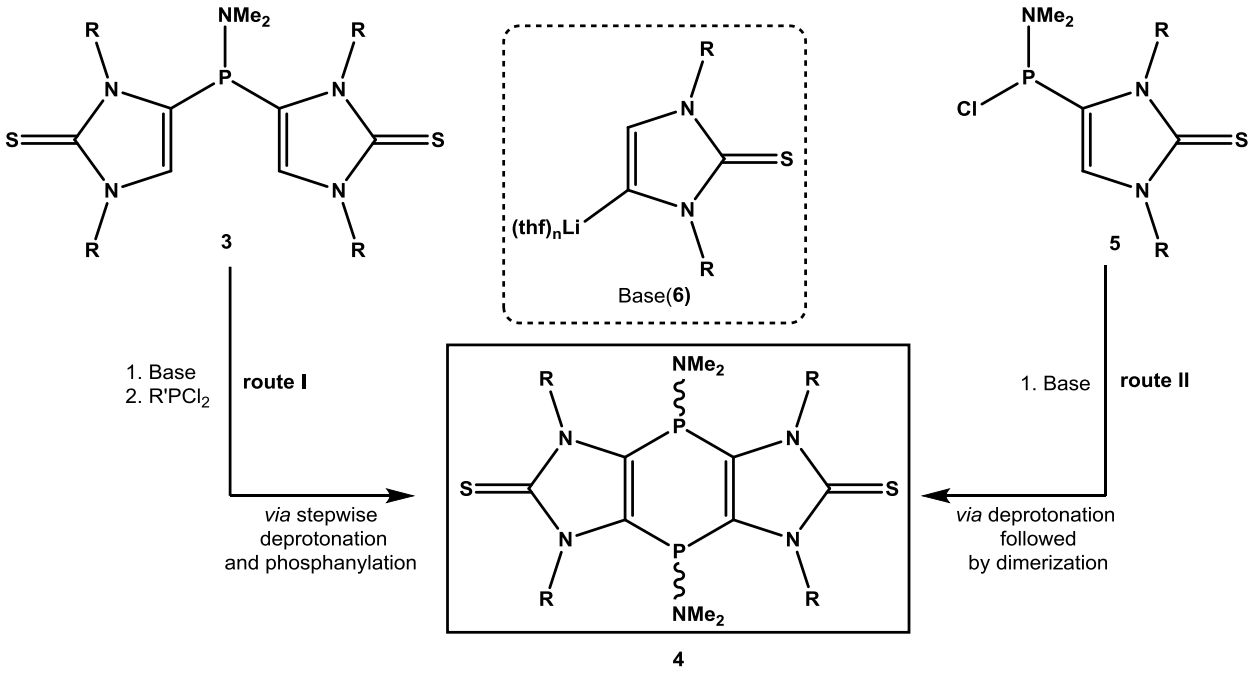

Scheme 15: Hypothetical pathways of cyclization.

In both cases the base involved could be the backbone-lithiated 1,3-dialkyl-imidazole-2-thione **6** as the ^{n}BuLi solution was added first in the reaction mixture which slowly gets consumed via reaction with either **2** and/or **3** and/or **5**.

Therefore, the backbone-lithiated 1,3-dimethyl-imidazole-2-thione **6** was synthesized by reacting the corresponding thione with ^{n}BuLi at –78 °C (Scheme 16), and could be isolated as white solid via evaporation of all volatiles at room temperature and trituration with *n*-pentane, hence, obtained only as crude product.

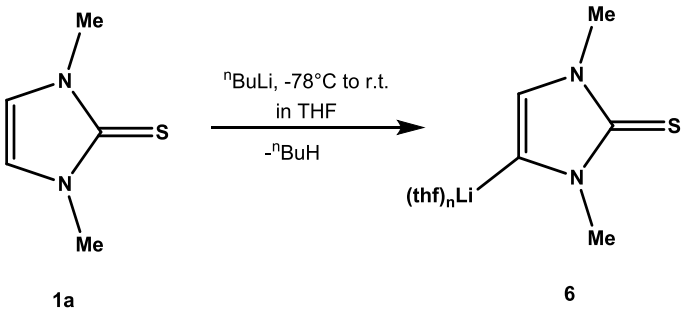

Scheme 16: Synthesis of backbone-lithiated imidazole-2-thione **6**.

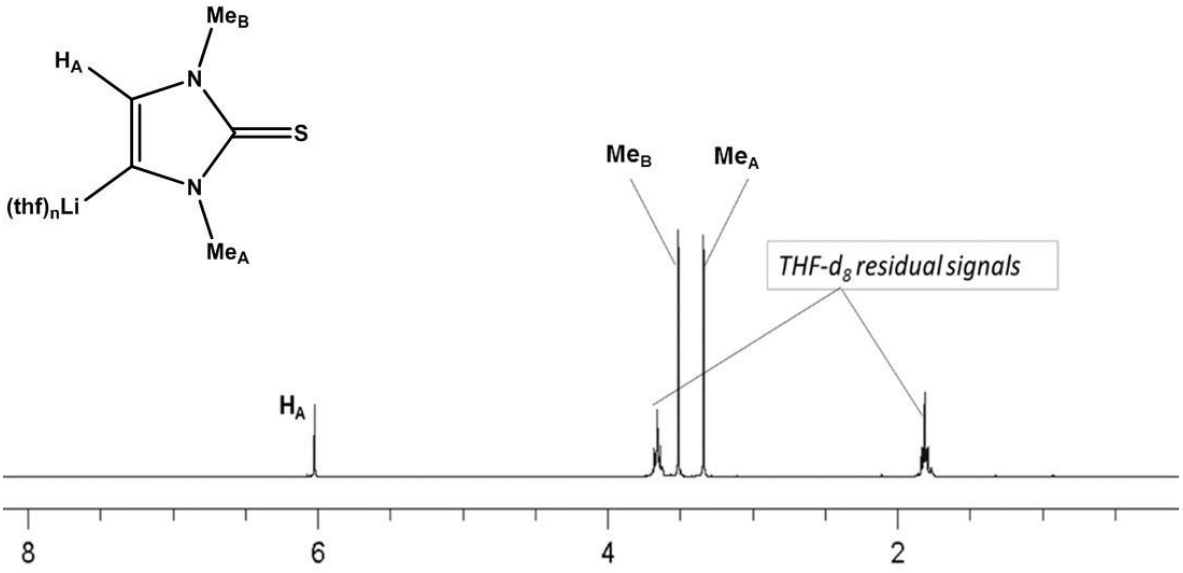

Figure 13: ^{1}H NMR spectrum of compound **6** in THF-d_8.

This white solid after trituration with *n*-pentane gave pure compound **6** as a fine white powder in excellent yield. The ^{1}H NMR spectra (Figure 13) of compound **6** shows loss of symmetry of the *N*-CH_3 protons upon deprotonation along with further shielding of the backbone proton (6.0 ppm) compared 1,3-dimethylimidazole-2-thione (6.7 ppm). Further proof of the formation of **6** was given by the ^{7}Li NMR spectroscopy where it shows a singlet resonance at 0.9 ppm, which was found to be slightly highfield shifted compared to PhLi (1.55 ppm),[65] indicating at higher electron donating ability of the imidazole-2-thione-4-yl substituent in **6**. With compound **6** in hand, the viability of the first route was checked in detail using compound **6**, ^{n}BuLi, ^{t}BuLi or MeLi as the base and **2a** as the electrophile. Unfortunately, none of these reactions led to the desired tricyclic 1,4-dihydro-1,4-diphosphinines which underlined that the amino(chloro)phosphanyl-imidazole-2-thione (**5**) seems to be responsible for the cyclization. Therefore synthesis, isolation and characterization of compound **5** along with its utilization in the synthesis of tricyclic 1,4-dihydro-1,4-diphosphinines is discussed in the next chapter.

Chapter 4

4. Synthesis and use of amino(chloro)phosphanyl-substituted imidazole-2-thiones in the chemistry tricyclic 1,4-dihydro-1,4-diphosphinine

4.1 Synthesis of backbone amino(chloro)phosphanyl-substituted imidazole-2-thiones

The synthesis of the backbone amino(chloro)phosphanyl-substituted imidazole-2-thiones **5** started from previously reported $(R'_2N)_2P$-substituted imidazole-2-thiones **7**, which was chosen due to the facile synthesis of $(Et_2N)_2PCl$ and the more laborious and costly synthesis of $(Me_2N)_2PCl$.

To synthesize compounds **5a-f** the reaction of **7a-f** with PCl_3 was examined using a wide range of solvents and conditions (Scheme 17). Independent of the reaction conditions, when dichloromethane was the solvent, a mixture of the amino(chloro)phosphane (ca. 85 % by $^{31}P\{^1H\}$ NMR spectroscopy) and the diorganoamino(dichloro)phosphane (ca. 15 %) were obtained. But if

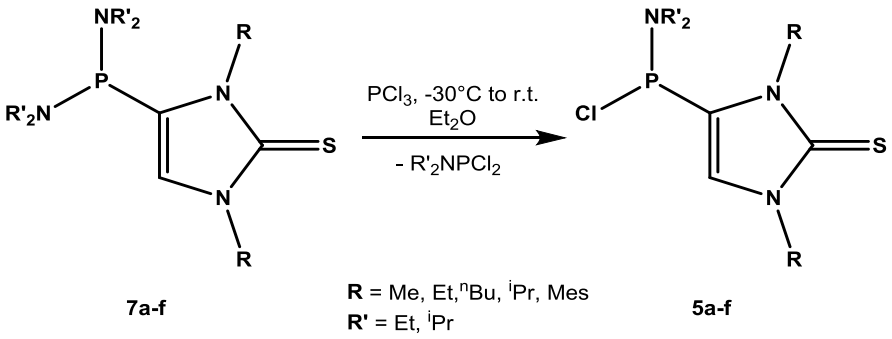

Scheme 17: Synthesis of the backbone amino(chloro)phosphanyl substituted imidazole-2-thiones **5a-f**.

the solvent was changed to diethyl ether and the reactions were carried out at lower temperatures (–20 to –40 °C), the amino(chloro)phosphanes **5a-f** were observed as sole products.

Compounds **5a-f** were isolated as white powders in good to excellent yields via precipitation from *n*-pentane solutions at –40 °C. The $^{31}P\{^{1}H\}$ NMR spectra of **5a-f** showed singlet resonance signals around 98.9-108.4 ppm being significantly downfield-shifted compared to **7a-f** (Table 3). Apart from full NMR spectroscopic characterization of **5**, **5f** was also confirmed by X-ray crystallography using single crystals obtained by slow evaporation of its saturated dichloromethane solution at –20°C. Compound **5f** crystallizes in the monoclinic crystal system with the space group $P2_1/c$.

Table 3: $^{31}P\{^{1}H\}$ NMR chemical shifts ($CDCl_3$) and yields for compounds **5a-f**.

	R	R'	δ_P	Yields (%)
5a	Me	Et	106.1	87
5b	Et	Et	106.5	78
5c	^{n}Bu	Et	106.4	83
5d	^{i}Pr	Et	108.4	92
5e	Mes	Et	102.9	88
5f	Me	^{i}Pr	98.9	85

Interestingly, the molecular structure of **5f** (Figure 14) reveals that the dihedral angle between the thione plane and the plane consisting of C1-P-Cl is only 1.7°. In other words, the P-Cl bond is almost coplanar with the imidazole-2-thione ring. Closer inspection of the metrical parameters revealed the

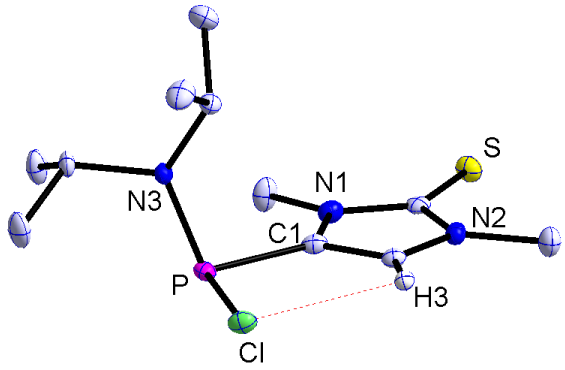

Figure 14: Molecular structure of compound **5f**; hydrogen atoms are omitted for clarity (50% probability level). Selected bond distances (Å) and angles (°): P-Cl 2.1274(9), P-C(1) 1.812(3), P-N(3) 1.654(2); Cl-P-N(3) 105.90(8), Cl-P-C(1) 101.69(11).

presence of an intramolecular hydrogen bond [$d_{Cl\text{-}H3}$ = 2.7557(7) Å] between the backbone H atom and the Cl atom. This H-bonding interaction is accompanied by a P-Cl bond (2.1274(9) Å) that is slightly elongated compared to any "normal" covalent P-Cl [*cf.* 2.061(1) Å in $(2,4\text{-}(CF_3)_2C_6H_4)_2PCl$][66] but significantly shorter than P-Cl bonds with some ionic character [*cf.* 2.759(2) Å for the chlorodiazaphospholene [(^{t}BuN-CH=CH-N^{t}Bu)P]Cl[67] and 2.3136(7) Å for the chlorodiazaphosphole [(^{t}BuN-CH_2CH_2-N^{t}Bu)P-Cl][67]] Presumably, this H-bonding interaction causes the co-planarity of the P-Cl bond and the imidazole-2-thione ring plane.

4.2 Optimization of the ring formation reaction

4.2.1 Reaction of amino(chloro) compound 5 with backbone lithiated imidazole-2-thione

Having the amino(chloro)phosphanyl-substituted imidazole-2-thiones **5a-f** and backbone-lithiated 1,3-dimethylimidazole-2-thione **6** in hand, the reactions were monitored by $^{31}P\{^1H\}$ NMR spectroscopy under different reaction conditions to check the viability of route **II** to tricyclic 1,4-dihydro-1,4-diphosphinines.

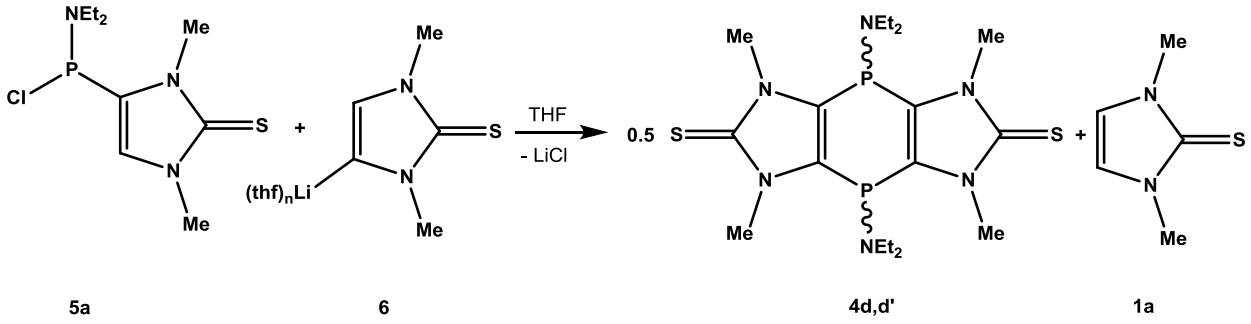

Scheme 18: Reaction of the amino(chloro)compound **5a** with the organolithium derivative **6**.

In all cases, a THF solution of **5a** was treated with a THF solution of **6** (Scheme 18), changing only the minimum temperature. When the reaction was started at –78 °C, compound **6** acted only as a nucleophile and gave rise to the bis(imidazole-2-thione-4-yl)phosphane **3j** appearing at 10.4 ppm in the $^{31}P\{^1H\}$ NMR spectra of the reaction mixture (Figure 15).

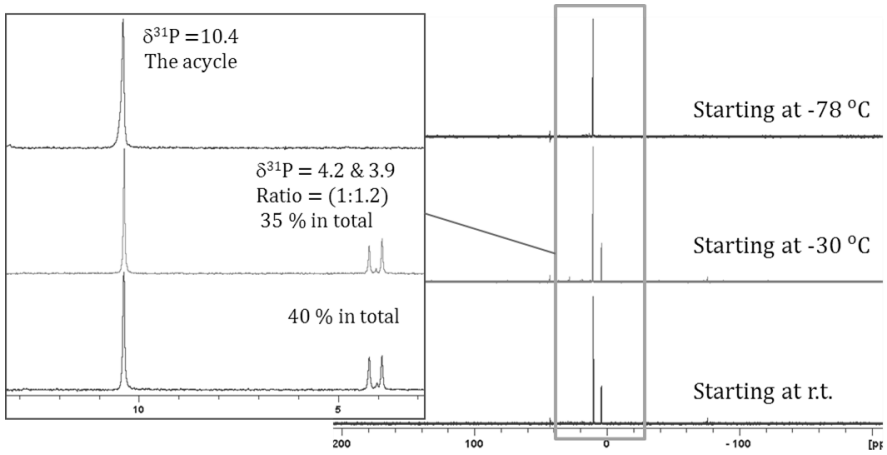

Figure 15: ^{31}P NMR spectroscopic monitoring of the reaction between **4d** and **6**.

If the reaction was started at a higher temperature, e.g., at –40 °C; then a pair of singlet resonance signals at 3.9 and 4.2 ppm appeared, and if the reaction was performed at room temperature, then a further increase of these two signals were observed. The chemical shifts of these new compounds (**4d,d'**) were found to be very close to those of **4a,b**. Apart from that, further evidence came from the EI-MS data of the reaction mixture which revealed a peak at m/z 458.2. Unfortunately, isolation of **4d,d'** from this reaction mixture was not achieved, but using a more appropriate base it could be accomplished (shown later in this chapter).

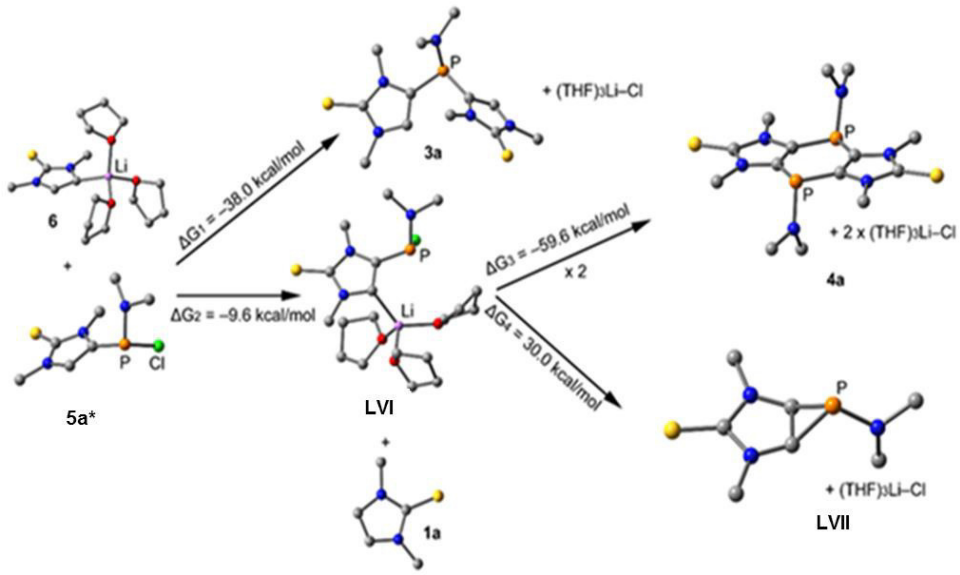

Figure 16: Optimized intermediates and final products (H-atoms omitted for clarity) along with the reaction energies of the different steps.

Theoretical insight[68] into this reaction was provided by Frontera on a slightly less bulky model compound **5a*** (Me instead of Et) (Figure 16). For the calculations three discrete THF molecules were used to solvate the lithium cation, and THF was used as continuum model to further simulate the experimental conditions. In this theoretical reaction, two possible paths were calculated: the acid-base reaction (i) and the nucleophilic substitution (ii). The formation of **3a** (the substitution product) was found to be thermodynamically favored (ΔG_1 = –38 kcal/mol) compared to the acid-base reaction, which is also an exergonic process (–9.6 kcal/mol) and produces the intermediate **LVI**. This intermediate is able to yield directly compound **4a** (self-complementary double S_N2 reaction) via a highly exergonic process. The possibility of generation of a bicyclic three-membered ring compound **LVII**, the product of a possible intramolecular substitution reaction, was also studied. But this pathway was highly disfavored from thermodynamic point of view (ΔG_4 = +30.0 kcal/mol). Thus theoretical investigations provided further evidence that the use of a suitable base could lead to the tricyclic 1,4-dihydro-1,4-diphosphinines **4** starting from **5**.

4.2.2 Searching for the most suitable base

In order to identify the best base and reaction conditions under which the 1,4-dihydro-1,4-diphosphinines can be prepared with an optimized yield, potassium hexamethyldisilazide (KHMDS) was employed as it is known to act as sterically demanding and weakly nucleophilic base (Scheme 19). When THF solutions of compounds **5a** and **5d** were treated with a THF solution of 1 eq. of KHMDS at –78 °C, surprisingly no tricyclic 1,4-dihydro-1,4-diphosphane was observed in the $^{31}P\{^1H\}$ NMR spectrum of the reaction mixture.

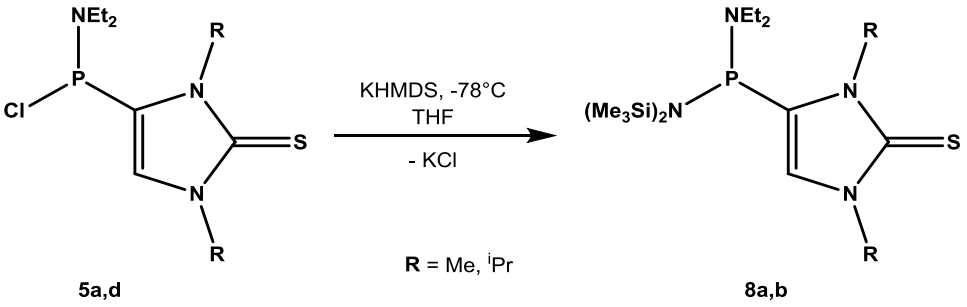

Scheme 19: Formation of the substitution products **8a,b** via reaction with KMHDS.

Instead, singlet resonance signals were observed at 74.9 (**8a**) and 74.6 ppm (**8b**) being very close to the corresponding backbone $(R'_2N)_2$-substituted imidazole-2-thiones **7a** and **7d**. The presence of the resonance signal of the C^5-H hydrogen in the ^{1}H NMR spectra of **8a,b** also supported the formation of substitution products. This was confirmed by the appearance of a doublet resonance signal with a $^2J_{P,Si}$ coupling constant in the ^{29}Si dept-20 spectra of **8a,b** (Table 4). Compounds **8a,b** could be easily extracted with toluene from the residue obtained after drying the reaction mixture, and isolated in moderate to good yields.

On the other hand, when LDA was employed (Scheme 20) as base under the same reaction conditions the tricyclic 1,4-dihydro-1,4-diphosphinines **4d,d'-f,f'** were formed as the sole products in very clean reactions.

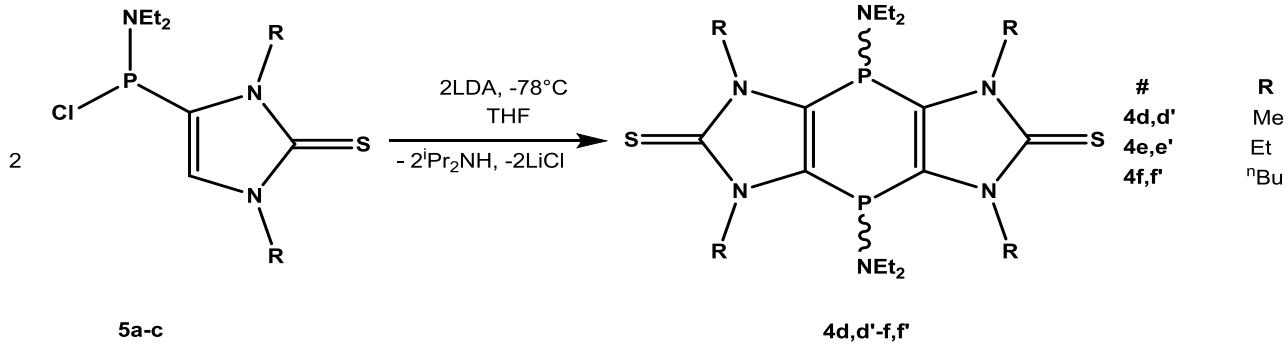

Scheme 20: Formation of the tricyclic 1,4-dihydro-1,4-diphosphinines **4d-f** via reaction with LDA.

The ^{31}P{^{1}H} NMR spectra of the reaction mixtures showed a pair of singlet resonance signals as depicted in Table 5.

Table 4: ^{31}P and ^{1}H NMR data for **8a,b**.

	δ_P	$^2J_{Si,P}$(Hz)	$\delta_{H\ of}$ C^5-H	yield (%)
8a	74.9	7.0	6.5	75
8b	74.6	7.2	6.6	81

Table 5: ^{31}P NMR data for **4d,d'-f,f'**.

	δ_P*	Isomeric ratio	yield (%)
4d,d'	3.3 & 3.9	1:1	84
4e,e'	0.4 & 2.9	1.5:1	62
4f,f'	0.2 & 3.6	1:1.2	50

*From reaction mixture in THF

Compounds **4d,d'-f,f'** were easily isolated from the reaction mixture simply by a flash column chromatography using dichloromethane as the eluent followed by washing with an diethyl-ether/*n*-

pentane mixture. The ^{31}P NMR spectra of **4d,d'-f,f'** (as they are mixture of two isomers) showed a similar trend as depicted in Figure 17. Only difference between the alkyl analogues is the $\Delta\delta_P$ value between the two isomers. As we go from the *N*-Me derivative **4d** to the *N*-^{n}Bu derivative **4f**, the $\Delta\delta_P$ value of two isomers gradually increased (Figure 17). Besides the good yields of these three derivatives, a profoundly improved solubility was observed. Whereas the Me derivative showed limited solubility in standard laboratory solvents, the Et analogue could be dissolved in solvents like tetrahydrofuran and dichloromethane with great ease, and the ^{n}Bu derivative could be even dissolved in *n*-pentane to some extent (up to ~10 g/L). It was also noticed that this reaction protocol led to isomeric ratios of **4d,d'-f,f'** that were almost unchanged, thus ruling out any priority for an isomer.

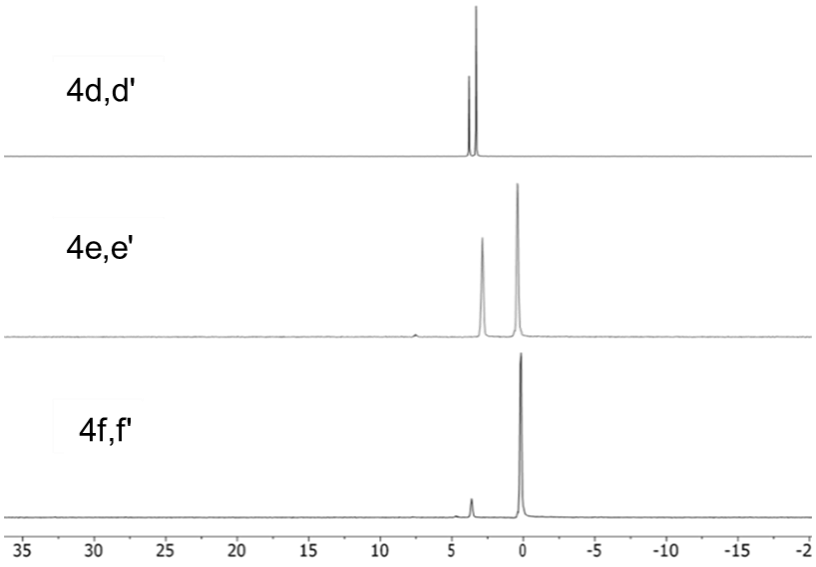

Figure 17: Comparison of the ^{31}P NMR spectra (in $CDCl_3$) of **4d,d'-f,f'**.

4.2.3 X-ray crystal structures and isomer assignment

Single crystals for compound **4d** could be grown from the mixture of two isomers by slow evaporation of a saturated dichloromethane solution at –20 °C (Figure 18). In this case the *cis* isomer crystallized preferably. *Cis* **4d** crystallized in the triclinic crystal system with the $P\bar{1}$ space group. The metrical parameters were in complete alignment with values of *cis* **4b**, but the six-membered ring was not completely planar (atoms P1 and P2 deviate by 0.09 Å from the ring), in

contrast to *trans* **4a**.

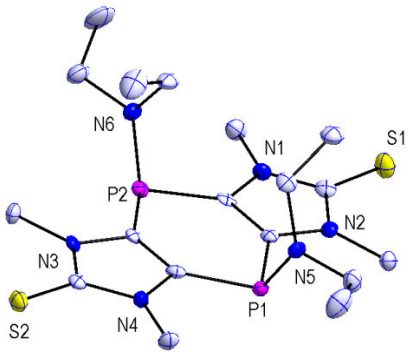

Figure 18: Molecular structure of compound **4d**; hydrogen atoms are omitted for clarity (50% probability level). Selected bond distances (Å) and angles (°):P1-N5 1.685(4), P1–C1 1.819(5), C1-C2 1.367(7), C1-P1-C6 94.9(2), C1-P1-N5 105.9(2).

In case of **4f,** the high solubility difference between the two isomers enabled separation by repeated washing with *n*-pentane at –40 °C, thus separate the *trans* isomer in 98 % purity. This 98:2 isomeric mixture was then subjected to crystallization from *n*-pentane solution –20 °C, thus providing suitable single crystals for X-ray measurements which confirmed the structure for the *trans* isomer of **4f** (Figure 19).

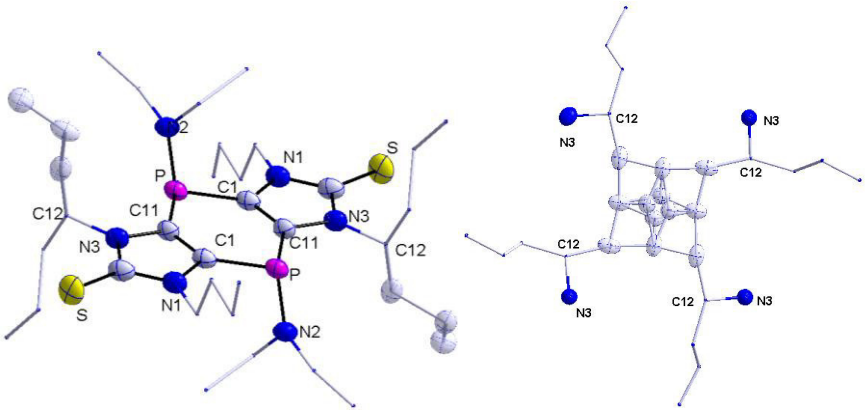

Figure 19: Molecular structure (left) of *trans* **4f** with dispersive interaction (right) between the *n*-butyl chains shown; hydrogen atoms are omitted for clarity (50% probability level). Selected bond distances (Å) and angles (°):P-N2 1.673(3), P–C1 1.818(3), C1-C11 1.358(4), C1-P-C11 94.59(14), C1-P-N2 105.89(14).

The $^{31}P\{^{1}H\}$ NMR spectrum of a solution of this crystalline material showed a resonance signal at 3.6 ppm which clearly revealed that the peak at lower field has to be assigned to the *trans* isomer. The compound *trans* **4f** crystallized in the tetragonal crystal system with the $I4_1/a$ space group, and as in the case of *trans* **4a**, the six-membered ring was entirely planar. Closer inspection of the crystal

packing in *trans* **4f** revealed that the *n*-butyl chains attached to N(3) have two possible orientations (split layers with the ratio of 43:57) (shown with transparent ellipsoids in Figure 19). One of these two orientations of *n*-butyl groups interact with three more molecules to form a square aggregate of carbon atoms (twelve of them, three from each *n*-butyl groups), held together by dispersive interactions.

4.2.4 Effect of the P-substitution on the outcome using the optimized protocol

The cyclization reaction was repeated for compounds **5d-f** using LDA. Unfortunately, for **5d,e** (**d**: R = ^{i}Pr, R' = Et; **e**: R = Mes, R' = Et) the selectivity of the reaction mixtures were very low and formation of tricyclic 1,4-dihydro-1,4-diphosphinines was not observed in the $^{31}P\{^{1}H\}$ NMR spectra of the reaction mixtures. But in the reaction of **5f** (R = Me, R' = ^{i}Pr) and LDA at –78 °C, the formation of a *P*-N^{i}Pr$_2$ 1,4-dihydro-1,4-diphosphinine derivative was observed in the $^{31}P\{^{1}H\}$ NMR spectrum (Figure 20), *i.e.*, the spectrum showed two resonance signals at -12.5 and -13.1 ppm (ratio 1:2), but also those of several other by-products of unknown identity. But these two peaks can be tentatively assigned to the two isomers of the *P*-N^{i}Pr$_2$ derivative although it could not be isolated from the reaction mixture. This study clearly demonstrated, again, the clear need of a sterically less demanding primary alkyl substituent at the thione N-center for the cyclization process to occur in a clean manner.

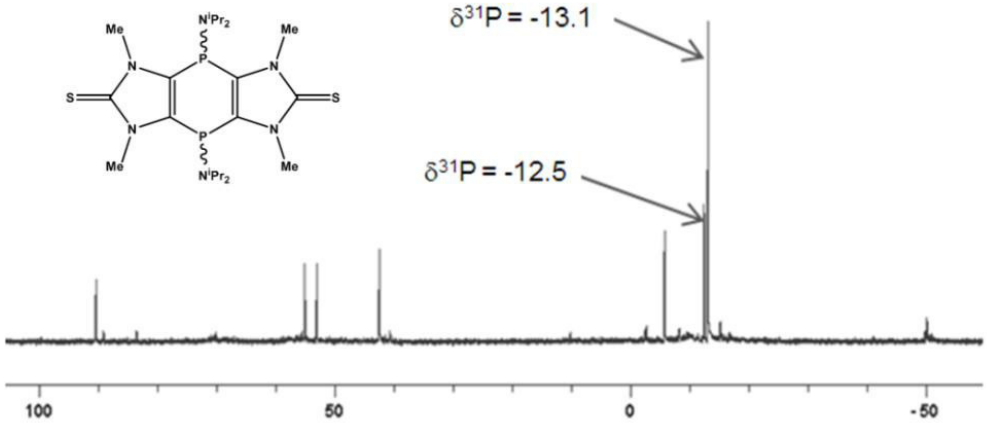

Figure 20: The $^{31}P\{^{1}H\}$ NMR spectrum of the reaction solution of **5f** and LDA.

4.3 Further reactivity studies on amino(chloro)phosphanyl-substituted imidazole-2-thiones

Apart from their usefulness in the synthesis of tricyclic 1,4-dihydro-1,4-diphosphinines, the amino-(chloro)phosphanyl-substituted **5a-f** were also tested with respect to their potential as gateway towards phosphaalkenyl-substituted imidazole-2-thiones or NHCs. For this purpose **5d** and **5e** were selected as they provide more steric protection, compared to **5a-c**, which can be anticipated to be very important in the stabilization of a low-coordinate P-center. To start this study of their reactivity towards sterically demanding organolithium derivatives, *i.e.* fluorenyl- and diphenylmethyllithium were investigated. In both cases, nucleophilic substitution led to products **9a-c** in excellent selectivity (Scheme 21). Importantly, no spectroscopic evidence for a competing backbone deprotonation was obtained. The $^{31}P\{^{1}H\}$ NMR spectra of **9a-c** revealed singlets at 34.9 (broad), 30.6

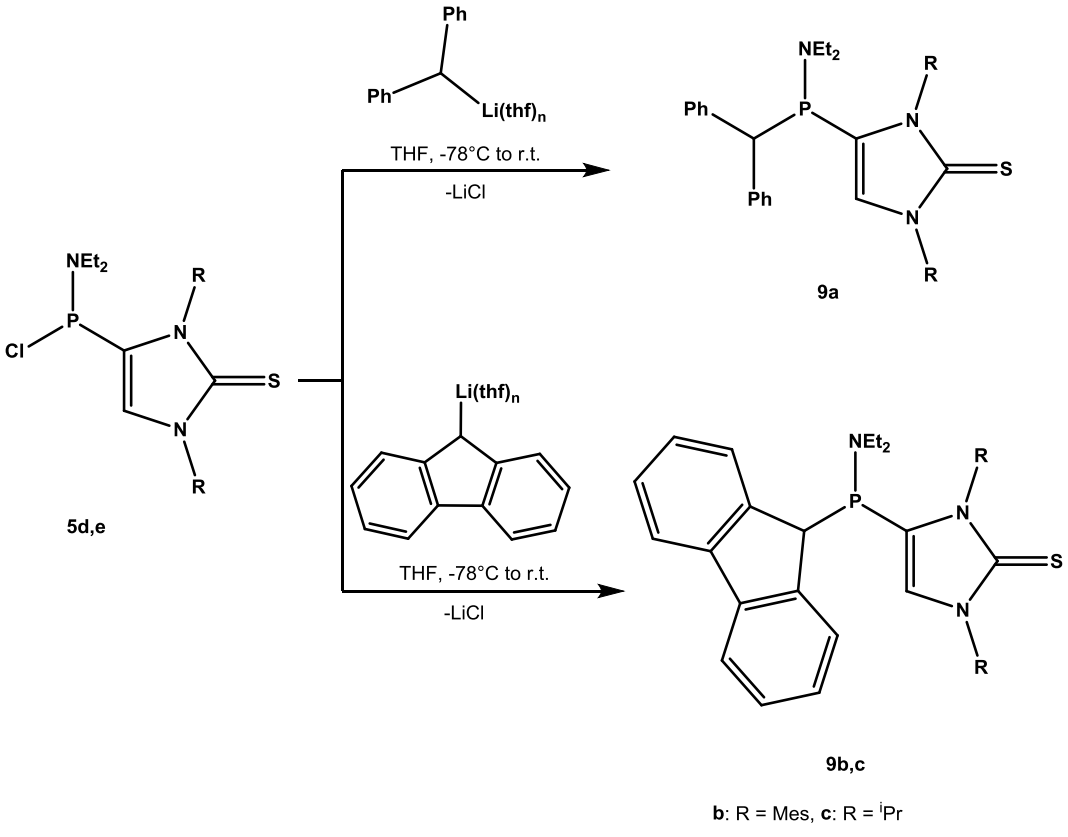

Scheme 21: Nucleophilic substitution to introduce sterically demanding groups at the P-center in **9**.

(sharp) and 28.9 (broad), respectively, which are significantly upfield-shifted compared to **8d,e** (108.4 and 102.9 ppm). Firm evidence for the successful formation of **9a-c** was provided by the $^{13}C\{^1H\}$ NMR spectra where doublet resonances were observed that were consistent with the successful formation of the new P-C bond (Table 6). For comparison, the chemical shifts are typical of P–*C*HPh$_2$ and P–*C*^{Fluorenyl} carbon atoms in related compounds [cf. Ph$_2$PCHPh$_2$: 46.19 ppm (24 Hz)[69]; Mes(^{n}Bu)PCHPh$_2$: 51.6 ppm (16 Hz)[70]; FluP^{t}Bu(NH^{t}Bu): 47.3 ppm (39.2 Hz)[71]]. Compounds **9a-c** could be easily isolated in excellent yields from the reaction mixture by flash column chromatography at room temperature using dichloromethane as the eluent.

Table 6: ^{31}P and ^1H NMR data of **9a-c**.

	δ_P	δ_P of P-C	$^1J_{P,C}$(Hz)	δ_H of P-CH	$^1J_{P,H}$(Hz)	yield (%)
9a	34.9	51.6	13.0	4.7	3.4	60
9b	30.6	46.5	21.7	4.5	-	60
9c	28.9	47.6	22.7	4.8	-	74

Single crystals of **9a** and **9b**, suitable for X-ray measurements grown from dichloromethane solution, were examined by X-ray crystallography. The compound **9a** (Figure 21) crystallizes in the triclinic crystal system with the space group $P\bar{1}$. In case of **9b** the crystal system was monoclinic and the space group C2/c. The unit cell of compound **9a** contains two independent molecules (70:30) which have similar metrical parameters, thus only one molecule is displayed in Figure 21. The molecular structure reveals the effects of a sterically demanding group at the phosphorus center.

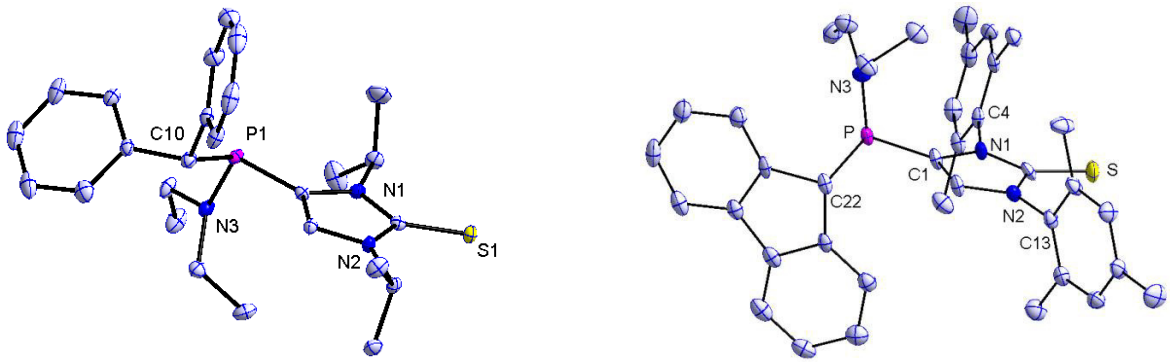

Figure 21: Molecular structures of compound **9a** (left) and **9b** (right): hydrogen atoms are omitted for clarity (50% probability level). Selected bond distances (Å) and angles (°): P(1)-C(2) 1.8260(18), P(1)-N(3) 1.6877(18), P(1)-C(10) 1.8905(16); C(2)-P(1)-N(3) 101.995(73), C(10)-P(1)-C(2) 100.198(72). For compound **9b** P-C(1) 1.8253(1), P-N(3) 1.6683(1), P-C(22) 1.8813(1); C(1)-P-N(3) 87.991(4), C(22)-P-C(1) 98.362(5).

Although the P(1)-C(2) [**9a**: 1.8260(18) Å] and analogous P-C(1) [**9b**: 1.8253(1) Å] bond length falls in accordance with previously reported analogous P-imidazole-2-thione compounds [cf. $PhP(IMS^{iPr,Me})_2$ 1.817(2)[35], Ph_2P-$IMS^{Me,Me}$ 1.8185(18)[10], Ph_2P-$IMS^{Ph,Ph}$ 1.8190(5)[10] etc.], the P(1)-C(10) [**9a**:1.8905(16) Å] and analogous P-C(22) bond [**9b**: 1.8813(1) Å] are significantly elongated compared to P-C bonds in related type of compounds with other substituents on the P-center [cf. $Ph_2P(O)$-$(IMS^{iPr,Me})$-PPh_2 1.8360(18)[32], Ph_2P-$IMS^{Me,Me}$ 1.8368(18),[10] etc.]. Likely, this elongation of the P-C bond reflects the increased steric demand at the P-center caused by the introduction of diphenylmethyl (**9a**) and fluorenyl (**9b**) moiety.

To examine whether **9** may serve as a gateway for the broader exploration of phosphorus chemistry, we focused first on the possibility of phosphaalkene formation. To provide protection against dimerization and/or oxidation of the desired P=C bond, the borane adduct **10** was prepared. The reaction of **9c** with BH_3-SMe_2 in dichloromethane was monitored by $^{31}P\{^1H\}$ NMR spectroscopy to reveal a singlet resonance at 58.1 ppm assigned to **10** that was significantly downfield shifted compared to **9c** (δ = 28.9) (Scheme 22). Compound **10** was crystallized from a saturated dichlorom-

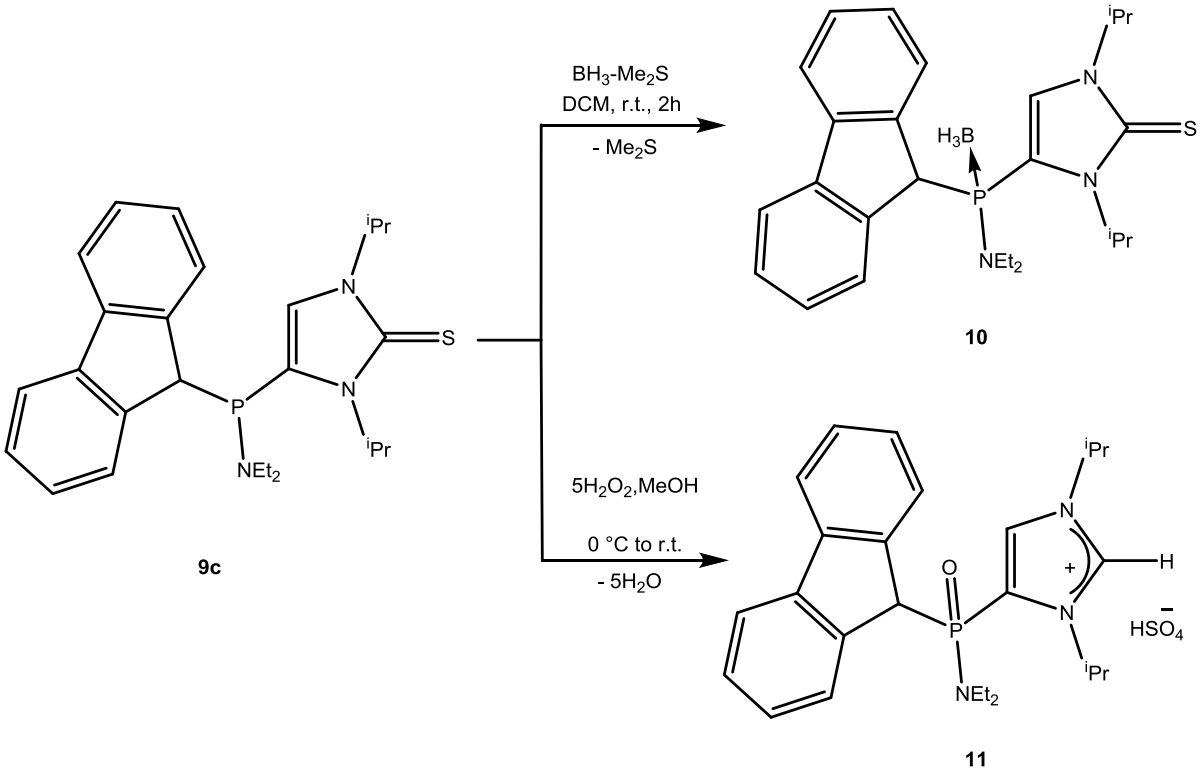

Scheme 22: Synthesis of BH_3 complex **5** and imidazolium salt **6**.

ethane solution at –20 °C. The borane-adduct **10** crystallized in monoclinic crystal system with the space group $P2_1/c$ (Figure 22). The molecular structure revealed a slightly shortened P(1)-N(3) bond distance [1.6519(13) Å] compared to a P-N bond in **9a** [1.6877(18) Å], upon complexation to borane. The fluorenyl group and the imidazole-2-thione are arranged in an almost perpendicular fashion (dihedral angle 85.24°) which is possibly due to intramolecular steric effects. To check whether compound **9** can act as a precursor for an imidazolium salt and, hence, a precursor to an NHC, compound **9c** was reacted with 5.5 eq. of H_2O_2 in methanol at 0 °C (Scheme 22).

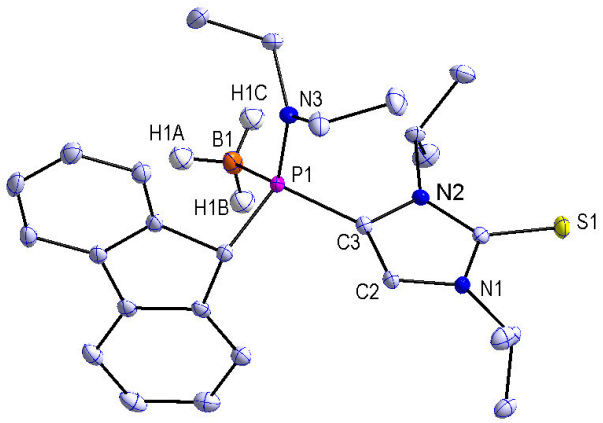

Figure 22: Molecular structure of compound **10**; hydrogen atoms are omitted for clarity (50% probability level). Selected bond distances (Å) and angles (°): P(1)-B(1) 1.9277(17), P(1)-N(3) 1.6519(13), P(1)-C(10) 1.8568(13), P(1)-C(3) 1.8099(12); N(3)-P(1)-C(10) 109.793(59), C(3)-P(1)-C(10) 101.389(59), B(1)-P(1)-C(10) 109.067(65), B(1)-P(1)-N(3) 114.678(65), B(1)-P(1)-C(3) 117.085(66).

Surprisingly, the $^{31}P\{^1H\}$ NMR spectrum of the reaction mixture revealed only a minor change in the chemical shift of **11** (29.5 ppm) compared to **9c** (28.9 ppm). For this reason successful formation of **11** had to be confirmed from the ^1H and $^{13}C\{^1H\}$ NMR spectra of the isolated product. Importantly, the ^1H NMR spectrum showed a new resonance at 9.89 ppm assigned to the C^2-H of imidazolium derivative **11**. Further evidence for the formation of **11** was collected from the $^{13}C\{^1H\}$ NMR spectrum as the resonance signal for the C=S carbon nucleus was not present (162.4 ppm) and was replaced by a doublet at 142.5 ppm ($^3J_{P,C}$ = 5.4 Hz). The latter is characteristic of an imidazolium salt having a C^4–bound P-substituent (cf. $[Ph(O)P(IMH^{tBu,Me})_2]Cl_2$: 141.5 ppm; $^3J_{P,C}$ = 5.8 Hz).[19, 34, 72] Conclusive evidence for the assignment of the product as imidazolium **11** was revealed by the ESI-MS spectrum which showed an ion peak at m/z 436.3 corresponding to a cation of $C_{29}H_{36}N_4OP$.

To have a broader scope of future investigations on P-substitution reactions, the amino group in **9a,b** was exchanged for a P-Cl group using 1 molar eq. of PCl_3 in dichloromethane at –20 °C (Scheme 23). The reaction mixture was monitored by $^{31}P\{^1H\}$ NMR spectroscopy to reveal that the signal for **9a,b** (34.9 and 30.6 ppm) had been completely replaced by a new, singlet at 53.4 tentatively assigned to **12a** (64.7 ppm for **12b**) together with (Et_2NPCl_2 (163.3 ppm) as the other phosphorus-containing product. Compounds **12a,b** were isolated in excellent yields as white powders from the reaction mixture via precipitation from *n*-pentane at –40 °C. The ^1H NMR spectrum of **12a,b** confirmed that the signals for the ethyl moieties of the (replaced) NEt_2 group were no longer present.

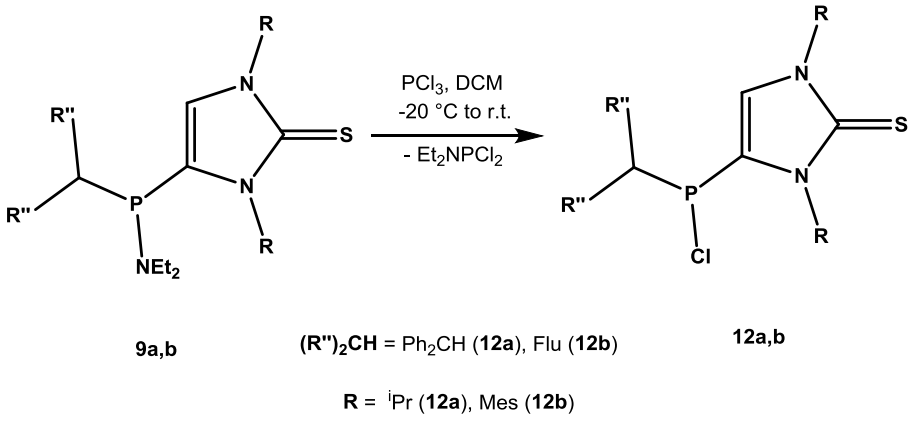

Scheme 23: Synthesis of *P*-Cl derivatives **12** by PCl_3 mediated P-N bond cleavage.

To examine the reactivity of the *P*-chloro function in **12** towards a strong donor (and neutral base), reaction of **12a** with 1,3,4,5-tetramethylimidazole-2-ylidene[11] in THF at –40 °C was carried out. This showed a clean conversion of compound **12a** into the NHC-stabilized phosphenium salt **13** (Scheme 24). Compound **13**, due to its ionic character precipitated from the reaction mixture. The crude product was filtered and washed with THF to purify compound **13**. This resulted in its isolation in good yields (60 %) and purity. Compound **13** was fully characterized by means of all standard analytical methods. The $^{31}P\{^1H\}$ NMR spectrum of NHC-phosphenium adduct **13** in $CDCl_3$ showed singlet resonance –47.4 ppm in which is shifted upfield compared to **14** (Figure 23, δ_P = –27.3 ppm).[73] Nevertheless, the value is in good agreement with the related phosphenium cation **15** (δ_P = –68.6 ppm)[36] (Figure 23), reported recently. Further evidence for the assigned structure of **13** was obtained from an ESI-MS experiment which exhibited an ion peak at m/z 505.6, assigned to a cation of $C_{29}H_{36}N_4PS$, which is the m/z value of the cation in **13**.

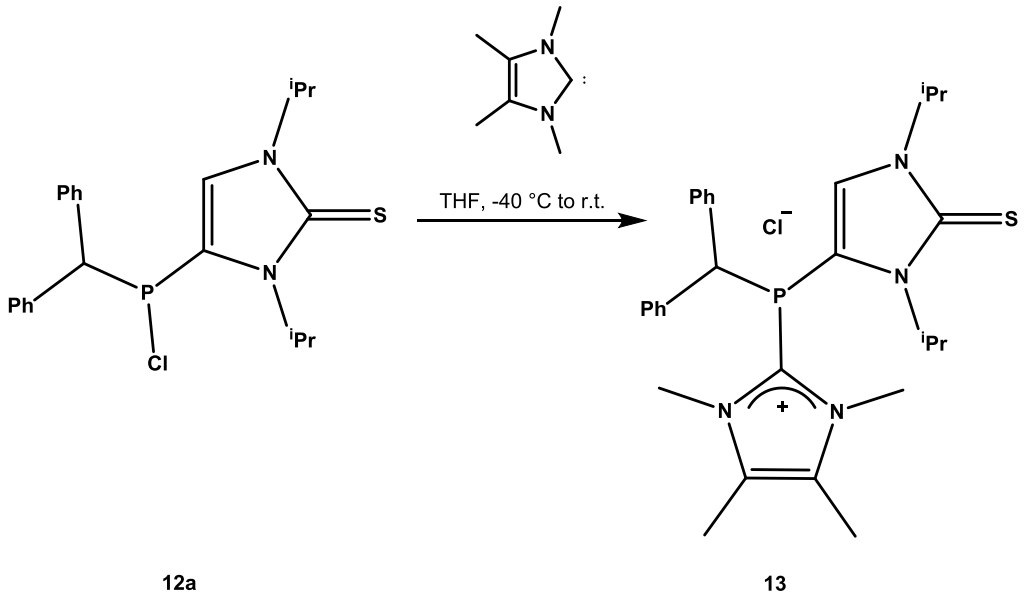

Scheme 24: Reaction of **12a** with IME4 to form NHC-stabilized phosphenium salt **13**.

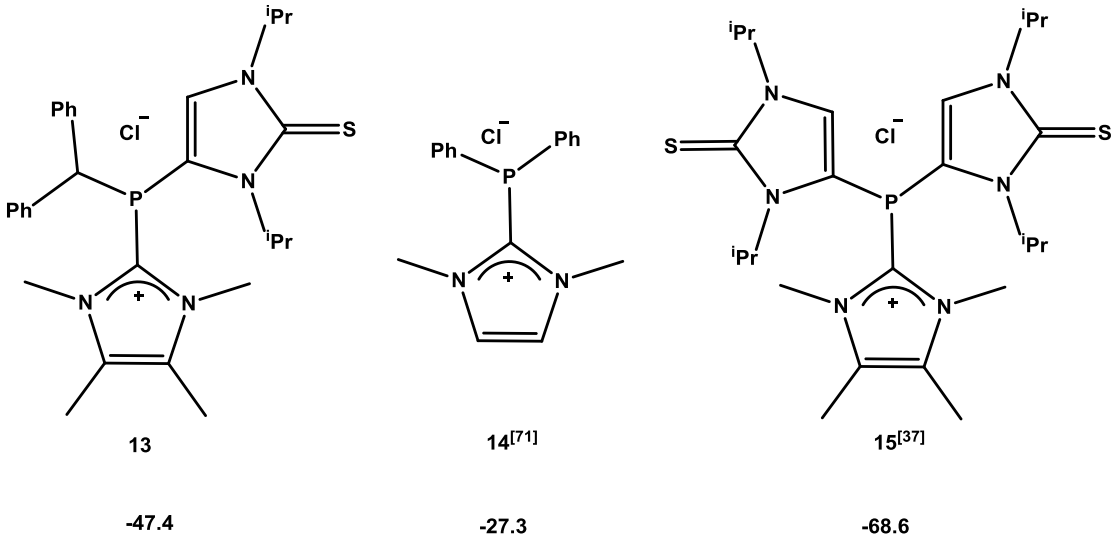

Figure 23: Chemical shifts of known NHC-stabilized phosphenium derivatives **13-15**.

The interesting perspective to examine was the viability of *P*-chloro phosphane **12a** as precursor to a novel backbone substituted phosphaalkenyl imidazole-2-thione. Thus, THF solutions of **12a** were treated with different bases to achieve the desired dehydrohalogenation. Unfortunately, these efforts were met with limited success as inseparable product mixtures were obtained, irrespective

of the reaction conditions. For example, treatment of a colorless solution of compound **12a** with ^{n}BuLi (1 eq.) at –78 °C in THF yielded instantly a dark purple solution, which slowly turned yellow over a period of 30 min. The $^{31}P\{^{1}H\}$ NMR spectrum of this reaction mixture showed a broad resonance for the major product at –33.9 ppm which was tentatively assigned as **17** (Scheme 25). For comparison, a similar chemical shift was observed for the related lithium-ate complex Li[MesP(^{n}Bu)-CPh$_2$] (δ_P = –31.1 ppm).[70] Interestingly, this compound, which was obtained from the reaction of MesP=CPh$_2$ and ^{n}BuLi under similar reaction conditions, is also purple in solution. Thus, it was assumed that the target molecule (**16**) might be formed transiently but reacted with the nucleophile ^{n}BuLi to give **17** due to its high reactivity. At this point, it was concluded that an increased steric protection of the P-center might be required.

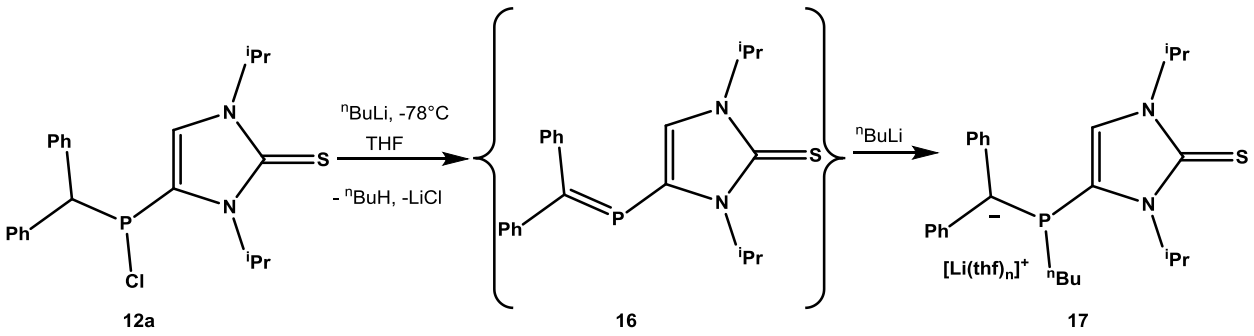

Scheme 25: Attempted dehydrohalogenation of compound **12a** using ^{n}BuLi.

With this result in hand, the reaction was repeated using the sterically more hindered **12b** in an effort to stabilize a transiently formed phosphaalkene. Thus **12b** was treated first with ^{n}BuLi (1 eq.) under same reaction conditions as in the case of **12a**. The $^{31}P\{^{1}H\}$ NMR spectrum of the reaction mixture showed a resonance signal at –30.6 ppm for the major product along with a signal for a minor product at –60.7 ppm. Interestingly, when **12b** was treated with ^{n}BuLi (2 eq.) the same species became the major product. Addition of HCl (1 eq. in diethyl ether solution) to this intermediate species resulted in complete conversion to the product having the resonance at –30.6 ppm. This final product was isolated and fully characterized as compound **18** (Scheme 26). The ^{31}P NMR spectrum of compound **18** in $CDCl_3$ shows a triplet at –31.3 ppm ($^{3}J_{P,H}$ = 7.9 Hz) indicative of the presence of the *P*-^{n}Bu moiety. Furthermore, the appearance of a doublet at 27.6 ppm ($^{1}J_{P,C}$ = 17.8 Hz) in the $^{13}C\{^{1}H\}$ NMR spectrum provides evidence for the P-C bond of the *P*-^{n}Bu moiety in **18**.

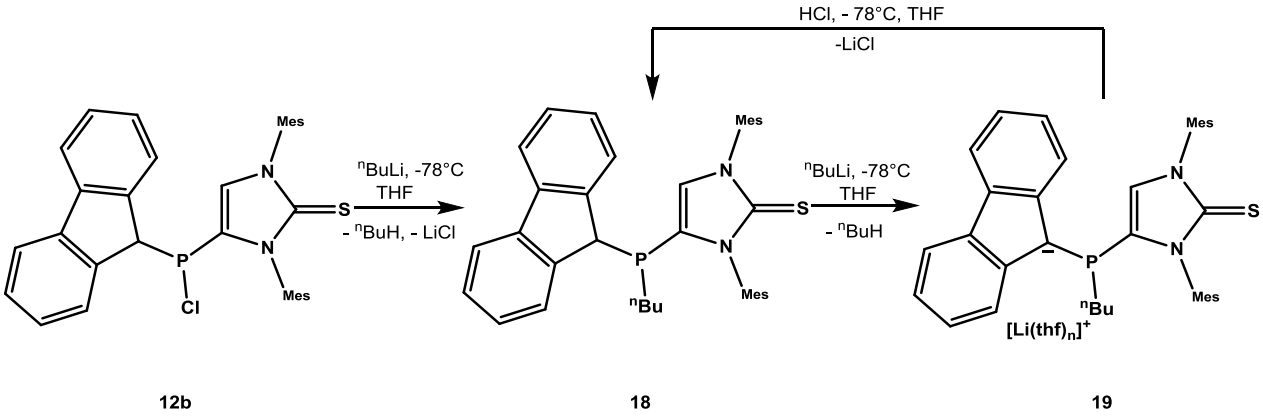

Scheme 26: Attempted dehydrohalogenation of compound **12b** using ^{n}BuLi.

This result is remarkable as it suggests that compounds **12a,b**, in the presence of ^{n}BuLi, have a clear preference for nucleophilic substitution to give **18** over dehydrohalogenation to give the phospha-alkene. In the presence of an excess ^{n}BuLi, compound **18** undergoes deprotonation to afford lithium–ate complex **19** which on protonation gives **18**. In a final attempt to obtain evidence for a phosphaalkene intermediate, **12b** was treated with ^{t}BuLi (1 eq.). In stark contrast to reactions involving ^{n}BuLi, the ^{31}P NMR spectrum of this reaction mixture showed a doublet at –117.1 ppm ($^{1}J_{P,H}$ = 217.4 Hz) for the major product. The latter data clearly do not correspond to the desired phosphaalkene and the large P-H coupling constant suggests a compound with a direct P–H bond.[36] Unfortunately, attempts to isolate this P-H derivative failed due to decomposition during isolation. In closing, none of the aforementioned reactions of **12** with RLi provided confirmation for the involvement of a phosphaalkene.

Chapter 5

5. Investigations on the synthesis of P-Ph and P-alkyl substituted tricyclic 1,4-dihydro-1,4-diphosphinines

As described in chapter **3**, the previous route to tricyclic 1,4-dihydro-1,4-diphosphinines, described in Scheme 13, gave access only to P-amino derivatives of compound **4**, but other derivatives differing in the nature of the P-substituents failed. Therefore, the synthesis of *P*-phenyl-substituted derivatives could be promising if the new LDA-based protocol would be employed.

5.1 Synthesis of *P*-phenyl-substituted 1,4-dihydro-1,4-diphosphinines

5.1.1 Synthesis of the required precursors

The plan to synthesizing *P*-Ph derivatives of compounds **4** had to start with the diethylamino-(phenyl)phosphanyl-substituted imidazole-2-thiones **20a-c**. Here, we initially focused on the synthesis of compounds with only primary alkyl groups on the thione N-centers, as they had allowed to access tricyclic 1,4-dihydro-1,4-diphosphinines when treated with LDA. Compounds **20a-c** were easily synthesized via phosphanylation of the corresponding 1,3-dialkyl-imidazole-2-thiones following the literature reported methodology[10, 32, 35, 74] using $Et_2N(Ph)PCl$ as the electrophile. These reactions were monitored by ^{31}P NMR spectroscopy, where broad singlet resonance signals were observed at 35.2 ppm (**20a**), 33.5 ppm (**20b**), and 32.7 ppm (**20c**), respectively. Compounds **20a-c** were isolated from the reaction mixture in 90-95 % purity in all cases, and were used as such for the next step. The ultimate purification was not done as it was known that this type of reaction is not sensitive towards the presence of slight amount of impurities. Compounds **20a-c** reacted with 1molar eq. of PCl_3 at r.t. in dichloromethane solution to convert the P-NEt_2 into the P-Cl functionality selectively (Scheme 27) which was further confirmed by ^1H and ^{31}P NMR spectroscopy. In the ^1H NMR spectra of **21a-c** the resonance signals for the NEt_2 protons

were absent and the ^{31}P NMR spectra showed significantly downfield-shifted triplet resonances when compared to **20a-c** (Table 7).

Both compounds **21a** and **21b** were isolated as white powders after trituration of the crude residue obtained after drying the reaction mixture and removal of all volatiles. But in case of **21c**, the crude mixture could be purified by washing with *n*-pentane due to its solubility in *n*-pentane along with that of the impurities. For this reason the side product, *i.e.*, $Et_2N\,PCl_2$ distilled out (60 °C and 5×10^{-3} mbar) from the crude product mixture. The effect of the replacement of the dialkylamino group with a phenyl group in **21a-c** was apparent from the $^{31}P\{^1H\}$ NMR spectra as a significant upfield-shift, compared to compound **5a-f,** was observed (Table 7).

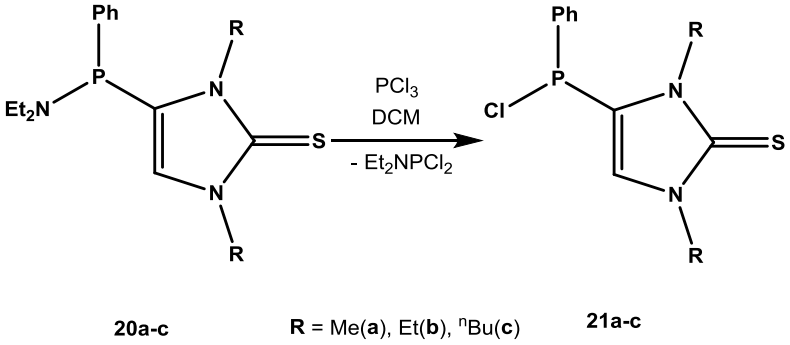

Scheme 27: Synthesis of chloro(phenyl)phosphanyl-substituted imidazole-2-thiones **21**.

Table 7: $^{31}P\{^1H\}$ NMR data ($CDCl_3$) and yields for **21a-c**.

	δ_P	δ_P comparision	$^3J_{P,H}$ (Hz)	Yield (%)
21a	50.5	35.2 (**20a**)	8.5	85
21b	50.2	33.5 (**20b**)	8.9	74
21c	49.9	32.7 (**20c**)	8.9	80

Single crystal of compound **21a** suitable for X-ray crystallographic measurements was grown from its saturated dichloromethane solution at –20 °C (Figure 24). It crystallized in the triclinic crystal system with the $P\bar{1}$ space group. The P-Cl bond in this case is out of the imidazole-2-thione ring plane (dihedral angle between C3-C1-P and Cl-P-C1 planes is 55.204°) unlike in the case of its diisopropylamino analogue where it was almost coplanar with the thione plane. Still the P-Cl bond length is in the same range of previously discussed **5f**.

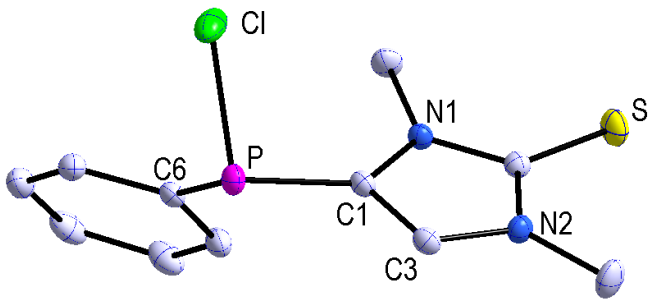

Figure 24: Molecular structure of compound **21a**; hydrogen atoms are omitted for clarity (50% probability level). Selected bond distances (Å) and angles (°): P-C(1) 1.7879(1), P-C(6) 1.8270(1), P-Cl 2.1056(1) ; C(6)-P-C(1) 103.853(3), C(1)-P-Cl 101.480(2).

5.1.2 Application of the new protocol with compounds 21a-c

In order to examine the newly developed protocol to form tricyclic 1,4-dihydro-1,4-diphosphinine, the compounds **21a-c** were treated with a THF solution of LDA at –78 °C , leading to a clean conversion into two products in each case.

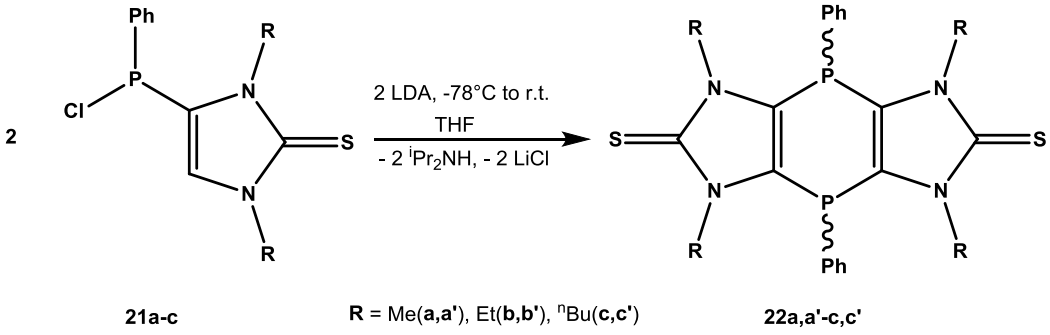

Scheme 28: Synthesis of P-Ph tricyclic derivatives **22**.

According to significantly highfield-shifted singlet resonances in the ^{31}P NMR spectra they were tentatively assigned to the two isomers of 1,4-dihydro-1,4-diphosphinines **22a-c** (Scheme 28 and Table 8); **21c** and **22c,c'** (two isomers) are shown as examples in figure 25. In case of **21a** a white precipitate was formed that could be filtered and characterized as the tricyclic 1,4-dihydro-1,4-diphosphinines **22a,a'**. For **21b,c** the reactions resulted in clear solutions due to the longer N-bound alkyl chains of the tricyclic 1,4-dihydro-1,4-diphosphinine **22b,b'-c,c'.** The latter two were isolated as white powders in moderate to good yields via flash chromatography through a silica bed at room temperature using dichloromethane as the eluent.

Table 8: $^{31}P\{^{1}H\}$ NMR chemical shifts, isomer ratio and yields of **22a,a'-c,c'**.

	δ_P	Isomer ratio	Yield (%)
22a,a'	-55.9 , -57.1	6:1	80
22b,b'	-54.9 , -56.6	1.2:1	51
22c,c'	-54.9 , -56.2	1:1.9	48

In case of all three tricyclic 1,4-dihydro-1,4-diphosphinine **22a-c** two stereoisomers were present in the reaction mixture (Table 8), but with different ratios. For example, for compounds **22a,a'** the ratio of 6:1 was determined by ^{31}P NMR integration revealing the preference for the formation of the *cis* isomer.

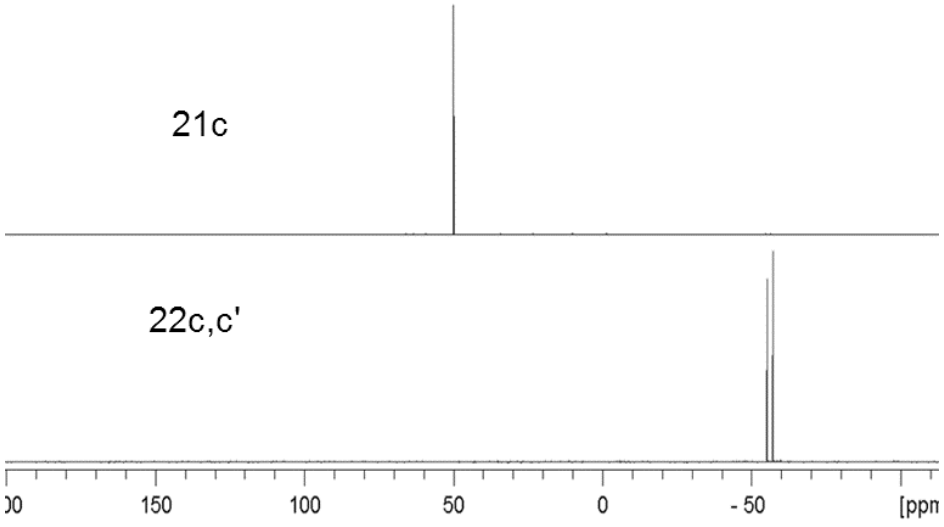

Figure 25: Comparison of $^{31}P\{^{1}H\}$ NMR spectra of compounds **21c** and **22c,c'**.

Interestingly, the solubility difference between the isomers was pronounced, *i.e.*, the *trans* isomer was always much less soluble. Furthermore, it was observed that during flash chromatography through a silica bed using dichloromethane as the eluent) the isomeric ratio changed to 17:1 due to a significant loss of the *trans* isomer on the solid phase of the column.

The mixture mentioned beforehand and being rich in the *cis* isomer, was used for the crystallization of **22a** and single crystal X-ray diffraction measurements confirmed the stereochemistry of *cis* **22a** (see below). The $^{31}P\{^{1}H\}$ NMR spectrum of crystals, dissolved in dichloromethane, showed a signal at -55.9 ppm thus leading to the assignments of the other signal at -57.1 ppm to the *trans* isomer.

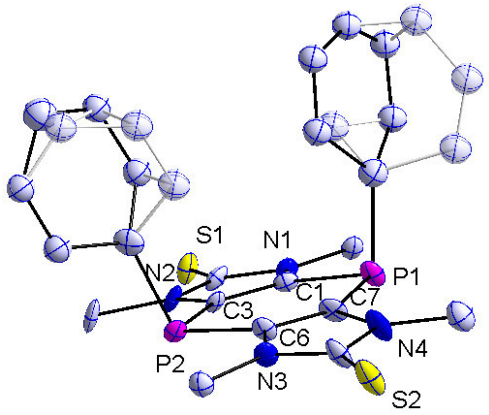

Figure 26: Molecular structure of compound **22a**; hydrogen atoms are omitted for clarity (50% probability level). Selected bond distances (Å) and angles (°): P(1)-C(1) 1.8149(8), P(1)-C(7) 1.8084(9), C(1)-C(3) 1.3493(6); C(1)-P(1)-C(7) 94.580(22).

Single crystals of *cis* **22a** suitable for X-ray crystallographic analysis were grown by slow evaporation of a dichloromethane solution at room temperature. **22a** crystallized in the monoclinic crystal system with the $P2_1/c$ space group (Figure 26). Although the phenyl rings were found to be significantly distorted, the structure confirmed the constitution of **22a**. Unfortunately, single crystals for **22b** could not be grown in good quality, but for **22c** crystals were grown from a dichlor-

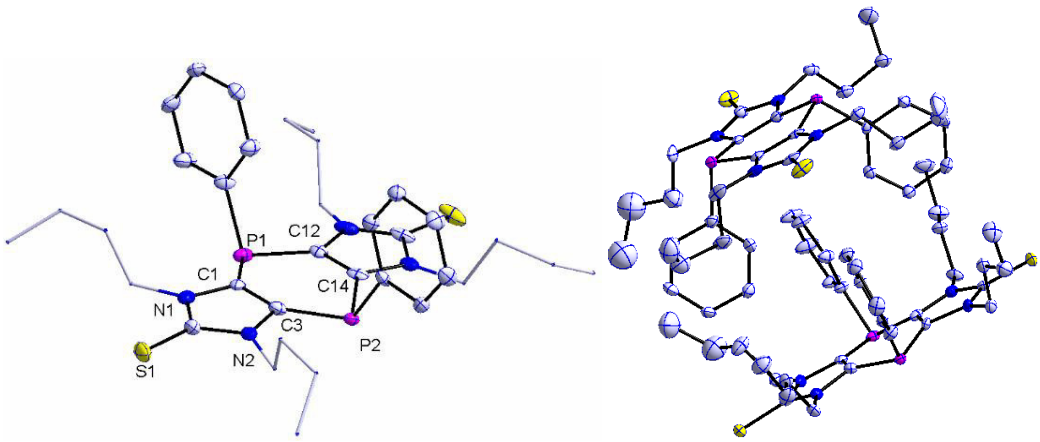

Figure 27: Molecular structure of *cis* **22c** (left) and its solid state arrangement (right); hydrogen atoms are omitted for clarity (50% probability level). Selected bond distances (Å) and angles (°): P(1)-C(1) 1.8149(8), P(1)-C(7) 1.8084(9), C(1)-C(3) 1.3493(6); C(1)-P(1)-C(7) 94.580(22).

omethane solution at –20 °C. X-ray crystallographic measurements revealed that **22c** crystallized in the triclinic crystal system with the $P\bar{1}$ space group (Figure 27). The six-membered ring was slightly

ring was slightly bent showing dihedral angle between the planes C(1)-C(3)-C(12)-C(14) and C(1)-P(1)-C(12) of 10.85°. The packing pattern in compound *cis* **22c** revealed that two neighboring layers juxtaposed on each other in a crisscross fashion with all the *n*-butyl chains and phenyl ring directed to the inwards direction. This particular orientation is probably due to the presence of dispersion interaction between the alkyl chains of two layers.

5.1.3 Reaction with KHMDS

As in the case of **5**, compounds **21a-c** were subjected to treatment with KHMDS in THF solution at –78 °C (Scheme 29) but the same substitution reaction occurred under this condition to give two products With singlet resonances at 27.1 ppm (**23a**) and 24.5 ppm (**23b**) in the $^{31}P\{^{1}H\}$ NMR spectrum. Compounds **23a** and **23b** were isolated by a flash chromatography using a silica bed and toluene as the eluent. Further proof for the substitution was then obtained from the ^{1}H NMR spectra of **23a** and **23b** showing doublet resonances for the backbone C^{5}-H at 6.5 ppm (for **23a**, $^{3}J_{P,H}$ = 1.6 Hz) and 6.3 ppm(for **23b**, $^{3}J_{P,H}$ = 1.5 Hz), respectively.

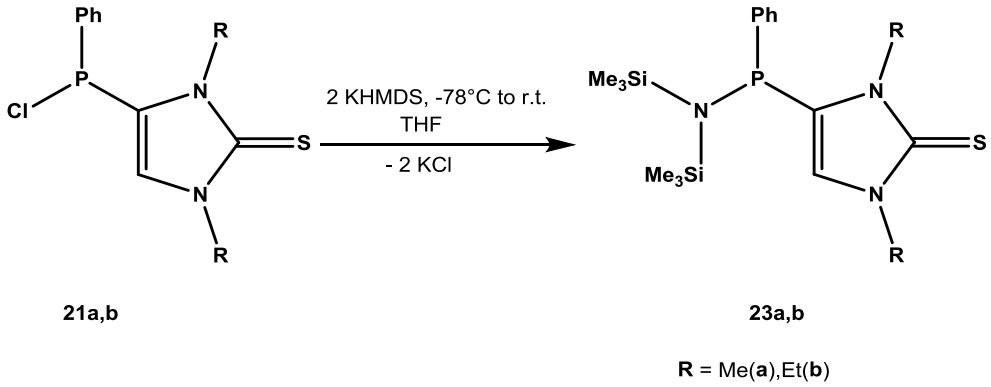

Scheme 29: Reaction of compounds **21a,b** with KHMDS.

The substitution product was finally confirmed by X-ray crystallographic measurements of compound **23b** using single crystals grown from a saturated solution in diethylether at –20 °C. Compound **23b** crystallized in the orthorhombic crystal system with the $P2_12_12_1$ space group (Figure 28).

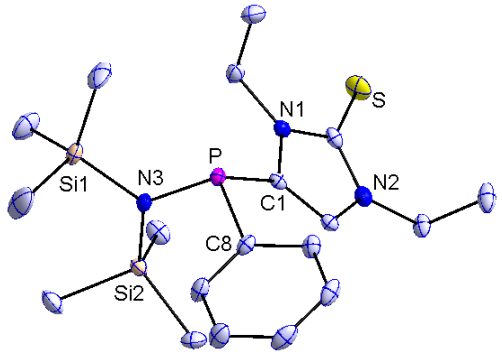

Figure 28: Molecular structure of compound **23b**; hydrogen atoms are omitted for clarity (50% probability level). Selected bond distances (Å) and angles (°):P-C(1) 1.8267(1), P(1)-C(8) 1.8327(1), P-N(3) 1.7177(1), N(3)-Si(1) 1.7736(1) ; C(1)-P-C(8) 101.459(3), C(1)-P-N(3) 105.288(3).

5.2 Synthesis of tricyclic 1,4-dihydro-1,4-diphosphinines with *P-alkyl* substituents

5.2.1 Synthesis of 1,4-dihydro-1,4-dichloro-1,4-diphosphinines

In order to enable broader investigations, a study on the synthesis of tricyclic 1,4-dichloro-1,4-dihydro-1,4-diphosphinines, starting from their *P*-amino analogues, was initiated. Therefore, the with *P*-diethylamino-substituted 1,4-dihydro-1,4-diphosphines **4d,d' and 4f,f'** were preferentially used to ensure a high solubility of the products. Treatment of colorless solutions of compounds **4d,f** in dichloromethane with 2 eq. of PCl_3 at room temperature (Scheme 30) resulted in an immediate color change to yellow-orange which, in case of **4d,d'**, was accompanied by the formation of a yellow-orange precipitate.

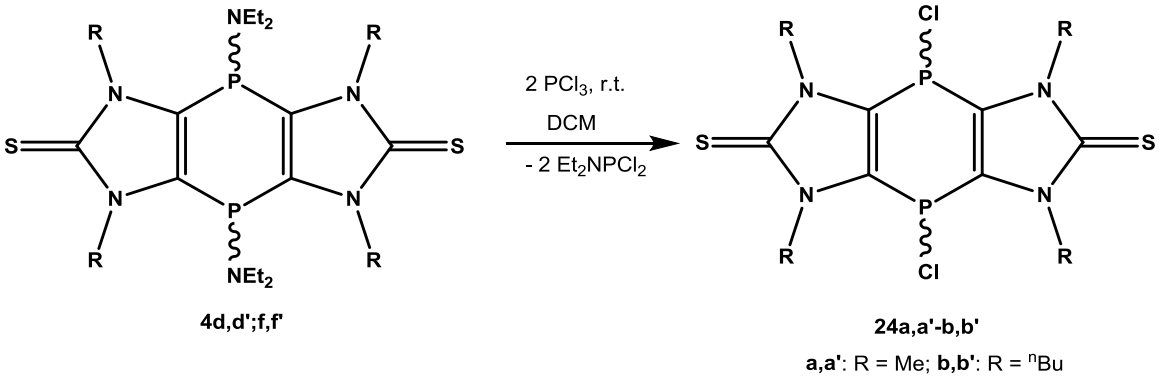

Scheme 30: Synthesis of *P*-Cl functional tricyclic compounds **24a,a'-b,b'**.

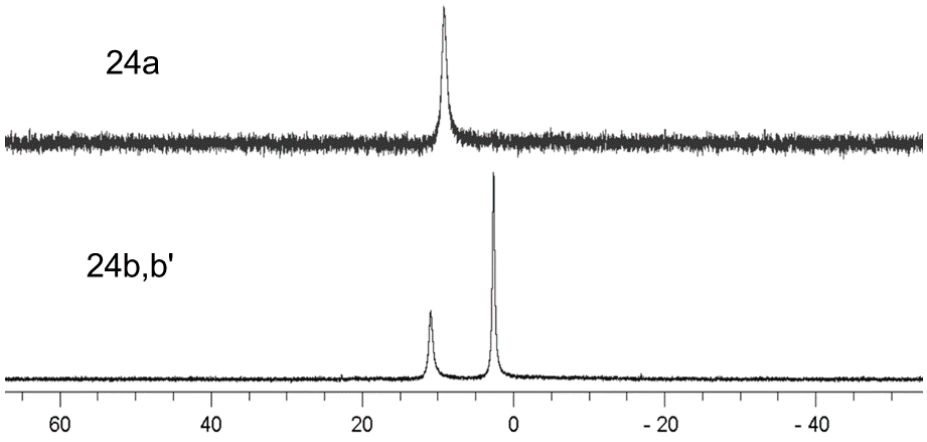

Figure 29: $^{31}P\{^{1}H\}$ NMR spectra of **24a,b** in CD_2Cl_2, room temperature.

Surprisingly, the $^{31}P\{^{1}H\}$ NMR spectrum of the reaction mixtures did not show any change of the chemical shift values but a broadening of the resonance signals, *e.g.,* the FWHM for **4d** was 2.7 Hz compared to 93.5 Hz for **24a** (in CD_2Cl_2). After separation of the yellow precipitate, the $^{31}P\{^{1}H\}$ NMR spectrum of this solid, dissolved in dichloromethane, showed two singlet resonance signals at 5.7 and 10.5 ppm, respectively (ratio 1:1.5) which were different from the starting material **4d**; a similar observation was made for **4f** and **24b** (2.6 and 10.9 ppm respectively for two isomers with a ratio of 1.8:1) (Figure 29). Further analytical studies (EI-MS, EA analysis and HRMS data) confirmed the nature as to be the 1,4-dichloro-1,4-dihydro-1,4-diphosphinines **24a,a'** (two isomers). The δ_P value of **24a** appeared to be highfield-shifted compared to the literature reported 1,4-dichloro-1,4-dihydro-1,4-diphosphinine (25.8 ppm), reported by Huryeva *et al*. in 2010;[46] this is certainly due to their different backbone natures. Both 1,4-dihydro-1,4-dichloro-1,4-diphosphinines **24a,a'-b,b'** were isolated in good yields (90 % for **24a**; 82 % for **24b**), and a complete analytical data set was obtained for both of them.

5.2.2 Nucleophilic substitution of *P*-chloro compounds

Having the *P*-chloro derivatives **24a,b** in hand, the first reactivity feature was to study substitution reactions, in general, and reactions of carbon-based nucleophiles, in particular. To get access to *P*-alkyl 1,4-dihydro-1,4-diphosphinines, firstly ^{n}BuLi was chosen and the reaction with compounds **24a,a-b,b'** studied at –78 °C in THF (Scheme 31). Due to its limited solubility in THF under the reaction conditions, compound **24a,a'** formed an orange suspension but, upon addition of ^{n}BuLi, the

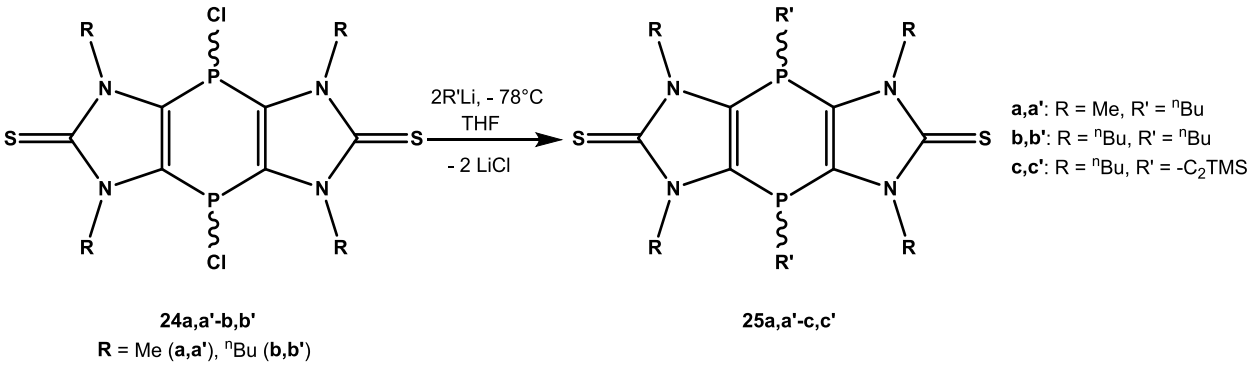

Scheme 31: P-substitution reactions on **24a,b** using carbon-based nucleophiles.

color of the reaction mixture turned dark brown and became a clear solution after some minutes.

The $^{31}P\{^{1}H\}$ NMR spectrum of an aliquot showed two singlets at –56.5 and –63.5 ppm (ratio 1:2.9), respectively, (Figure 30). As the reaction was very selective, compound **25a,a'** was isolated easily by flash column chromatography; the ratio of the *cis* and *trans* isomer was 1:2.3. In a similar vein, compound **25b,b'** (mixture of two isomers) was easily obtained as a mixture of *cis* (-66.3 ppm) and *trans* (-58.5 ppm) isomers (ratio 1:12) (Figure 30) via treatment of **24b,b'** with ^{n}BuLi. Compound **25b** was fully characterized using crystalline samples of the *trans* isomer, confirmed by X-ray crystallography, and standard analytical methods.

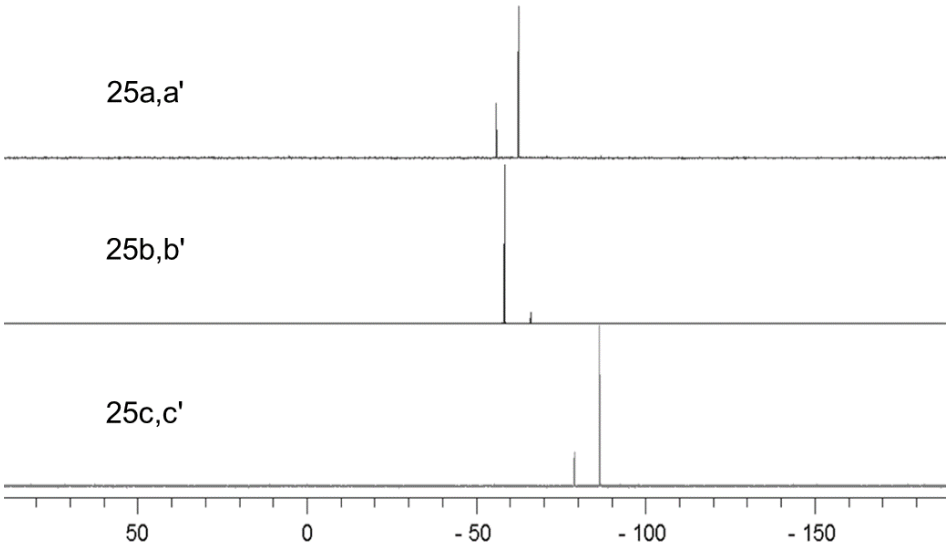

Figure 30: $^{31}P\{^{1}H\}$ NMR spectra of **25a,a'-c,c'** in $CDCl_3$, room temperature.

The presence of six hydrophobic *n*-butyl chains in compound **25b** made it highly soluble in solvents like diethyl ether or even in *n*-pentane to some extent, which is a rare observation in this tricyclic 1,4-dihydro-1,4-diphosphinine chemistry. The molecular structure of *trans* **25b** was confirmed by X-ray diffraction measurements using single crystals grown from a saturated diethylether solution at –20 °C. The compound **25b** crystallizes in the monoclinic crystal system with the $P2_1/c$ space group (Figure 31). The molecular structure reveals planarity of the tricyclic ring and an intermolecular dispersive interaction between the *n*-butyl chains, thus leading to an alkyl chain pairing that was described previously in compound **4e**.

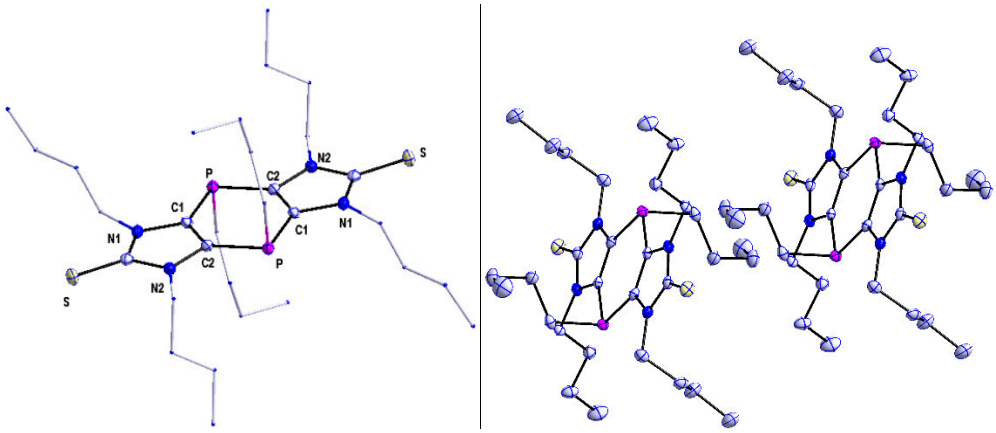

Figure 31: Molecular structure of *trans* **25b** (left) and alkyl chain pairing (right) in the solid state; hydrogen atoms are omitted for clarity (50% probability level). Selected bond distances (Å) and angles (°): P-C(1) 1.8108(2), P-C(2) 1.8175(2), P-C(12) 1.8602(2); C(1)-P-C(2) 95.998(7), P-C(1)-C(2) 131.740(12).

To obtain a P-substituent that would allow further functionalization/modification, lithium trimethylsilylacetylide was chosen as the nucleophile, obtained by reacting trimethylsilylacetylene and ^{n}BuLi at –78 °C in THF solution, and used *in situ* in the reaction with **24b,b'** to yield a clean outcome. The ^{31}P NMR spectrum consisted only of two isomers of **25c** (Scheme 30) with resonance signals at –79.9 and –88.1 ppm (Figure 30), respectively, (ratio of 1:2). Compound **25c,c'** was isolated as beige powder in moderate yield (45%) via flash column chromatography over a solid phase of silica using toluene as the eluent.

Chapter 6

6. Reactivity studies on P- and S-centers of tricyclic 1,4-dihydro-1,4-diphosphinines

Though 1,4-dihydro-1,4-diphosphinines are known for over five decades, their reactivity studies lack diversity beyond coordination chemistry which concerns mostly the chemistry of the P-centers. All previously known derivatives, except compound **XXXIV**, possessed only P-C bonds, thus clearly restricting further functionalization. But even for compound **XXXIV**, no further reactivity studies were described, except preliminary oxidative studies.[38, 40, 46] Therefore, the exploration of this novel class of tricyclic imidazole-2-thione-based 1,4-dihydro-1,4-diphosphinines **4a-f** and **22a-c** was a great opportunity. The reactivity studies focused on examples of fundamental reactions of the P-centers such as oxidation/sulfurization and coordination. In addition, reactivity towards hard electrophiles were of interest.

6.1 Oxidation of the P-centers in tricyclic 1,4-dihydro-1,4-diphosphinines

For the purpose of oxidizing the P-centers without touching the C=S units, compounds **4d,d'-f,f'**, **22a,a'-c,c'** were treated with hydrogen peroxide-urea adduct. From the *P*-NR_2 derivatives of these tricyclic 1,4-dihydro-1,4-diphosphinines compounds **4d-f** were chosen for this oxidation studies, mainly because of their superior solubility compared to **4a-b**. When dichloromethane solutions of compounds **4d,d'-f,f'** were treated with 2 molar eq. of hydrogen peroxide-urea adduct at ambient temperature, the $^{31}P\{^{1}H\}$ NMR spectra of the reaction mixtures revealed complete consumption of the starting materials after 24h for **4d,d',** 36 h for **4e,e'** and almost 2 days for **4f,f'** (Scheme 32).

For example, the $^{31}P\{^{1}H\}$ NMR spectrum of the reaction mixture of **26a,a'** (mixture of two isomers) showed two singlets at -4.3 and -5.1 ppm, respectively, (ratio 1.9:1) (Figure 32), and the isomeric

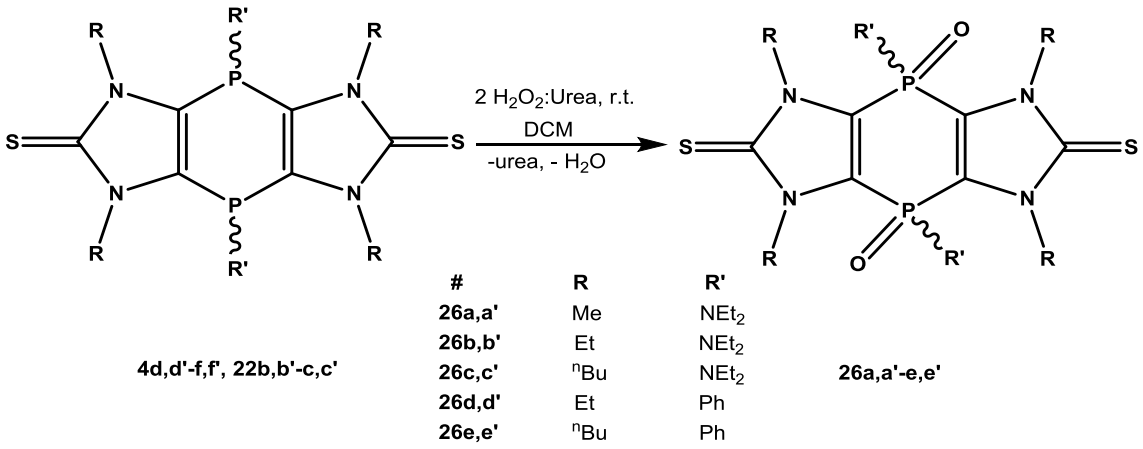

Scheme 32: Oxidation of compounds **4d,d'-f,f'; 22b,b'-c,c'** using the hydrogen peroxide-urea adduct.

ratio did not change during the reaction course. Due to lack of any reported δ_P values for the bis-oxides of 1,4-dihydro-1,4-diphosphinines, a comparison of δ_P values is not possible. Compound **26a** was isolated easily in moderate yields by a two-step protocol which includes filtration at the first step to remove the urea and drying over $MgSO_4$ in the next step (Table 9). In all these three cases of **26a,a'-c,c'**, the solubility of the products were not largely altered due to oxidation of the P-centers. But for both **26a,a'** and **26b,b'** the melting points went up markedly, compared to their parent compounds **4d,d'-f,f'**. For example, upon P-oxidation the $^3J_{P,H}$ coupling constant value between theP-center and the methylene protons of the NEt_2 group increased significantly, e.g., from 6.6 Hz in **4d,d'** to 12.5 Hz in **26a,a'**, thus also enabling the splitting pattern (quintet) of the resonance signals in the ^{31}P NMR spectrum distinguishable. In the same manner compound **26b,b'** was also isolated easily

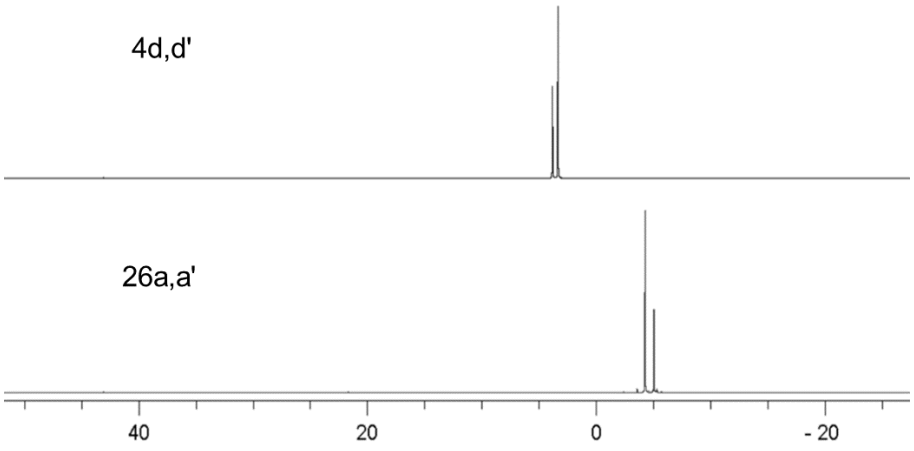

Figure 32: Comparison of the $^{31}P\{^1H\}$ NMR spectra ($CDCl_3$) of compounds **4d,d'** and **26a,a'**.

and the chemical shifts (with isomeric ratio) are listed in tabular form in Table 9. For compound **26c,c'** unfortunately the selectivity of the reaction mixture went down significantly which prevented the successful isolation of compound **26c,c'** in proper purity.

Table 9: $^{31}P\{^{1}H\}$ NMR chemical shifts, isomer ratio and yields of **26a,a'-e,e'**.

	R	R'	δ_P ($CDCl_3$)	Isomer ratio	Yield (%)
26a,a'	Me	NEt_2	-4.3 , -5.1	1.9 : 1	56
26b,b'	Et	NEt_2	-4.6 , -5.2	1.5 : 1	65
26c,c'*	^{n}Bu	NEt_2	-4.8 , -5.4	5.3 : 1	-
26d,d'	Et	Ph	-5.9 , -7.4	1 : 1.3	68
26e,e'	^{n}Bu	Ph	-6.7 , -8.4	1.3 : 1	75

* data from the reaction mixture in dichloromethane

But closer inspection of the $^{31}P\{^{1}H\}$ NMR spectrum of the reaction mixture showed two singlet resonance signals at -4.8 and -5.4 ppm respectively revealing the formation of compound **26c,c'** in the reaction mixture. Single crystals of compound **26a**, suitable for X-ray crystallographic measurements could be grown by slow evaporation of its saturated dichloromethane solution at room temperature (Figure 33). The result of this measurement revealed the solid state molecular structure for the *trans* isomer of compound **26a** which crystallized in the triclinic crystal system with the $P\bar{1}$ space group. The six-membered ring was in plane with the other two five-membered rings.

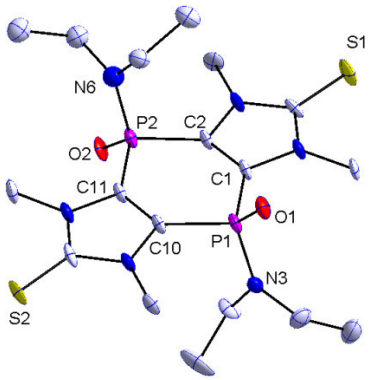

Figure 33: Molecular structure of trans **26a**; hydrogen atoms are omitted for clarity (50% probability level). Selected bond distances (Å) and angles (°): P(1)-C(1) 1.7779(1), P(2)-C(2) 1.7784(1), P(1)-O(1) 1.4851(1), P(1)-N(3) 1.6256(1) ;C(1)-P(1)-C(10) 99.446(4), N(3)-P(1)-O(1) 113.239(5).

It seemed to be an obvious next step, to compare the reactivity of *P*-Ph derivatives in this oxidation study using the *N*-Et (**22b,b'**) and *N*-^{n}Bu (**22c,c'**) compounds, but not the *N*-Me derivative (**22a,a'**) due to its comparatively lower solubility. The reaction mixtures containing **22b,b'-c,c'** and hydrogen peroxide-urea adduct showed again two singlet resonance signals in their $^{31}P\{^{1}H\}$ NMR spectra. The P-dioxides **26d,d'-e,e'** showed a much more pronounced change in the δ_P value from their starting materials **22b,b'-c,c'** (Table 9). This huge change in the δ_P value reflects the drastic change that occurs in the electronic environment of the P-centers upon oxidation (Figure 34). Again the isomeric ratio didn't change during the process of oxidation but the relative position of the isomers did change. Upon oxidation, the $^{3}J_{P,H}$ between the P-centers and the two *ortho*-protons of the phenyl rings increased notably, which changed the signal splitting pattern from **22b,b'** (broad signal) to **26d,d'** (triplet). Compounds **26d,d'-e,e'** could easily be isolated as white powders and the melting point of the *P,P'*-dioxides **26d,d'-e,e'** were again much more raised than those of compounds **22b,b'-c,c'** like in the cases of compounds *P*-NR_2 derivatives.

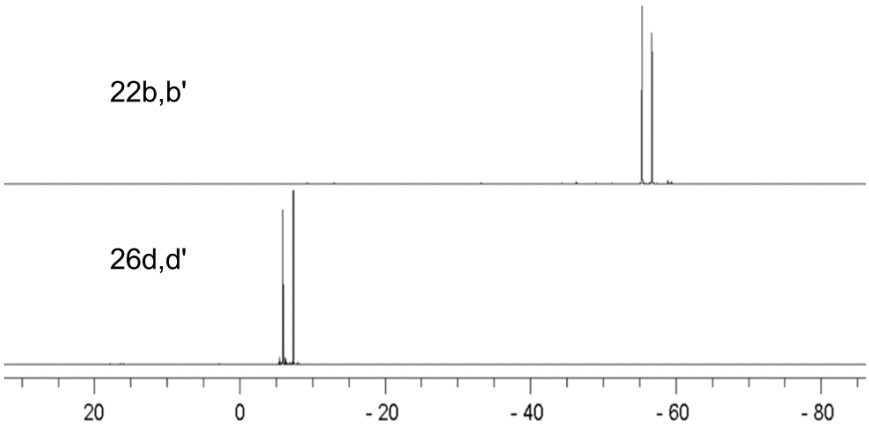

Figure 34: Comparison of $^{31}P\{^{1}H\}$ NMR spectra of compounds **22b,b'** and **26d,d'**.

Single crystals of compound **26d** (Figure 35) could be grown from the *cis/trans* isomer mixture and were subjected to X-ray crystallographic measurement revealing the solid state structure for the *cis*-**26d**; it crystallized in the monoclinic crystal system with the $P2_1/n$ space group. Although the resulting quality of this crystal structure was not very good, it could be still used to confirm the molecular constitution. The low quality resulted from distorted imidazole-2-thione (C16-N4-C15' fragment) rings which showed unusually short C16-N4 bond and long C15'-N4 bond.

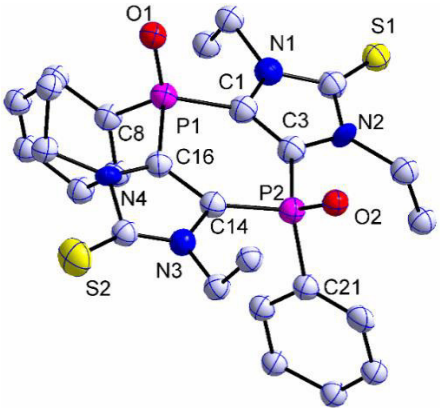

Figure 35: Molecular structure of *cis* **26d**; hydrogen atoms are omitted for clarity (50% probability level).

6.2 Oxidation using elemental sulfur

The sulfurization of the 1,4-dihydro-1,4-diphosphinines were performed following the same protocol which was reported previously for the sulfurization of backbone phosphanyl-substituted imidazole-2-thiones[32] and bis(imidazole-2-thione-4-yl)phosphanes.[35] In all these reactions **4d,d'-f,f'** and **22b,b'-c,c'** were employed as starting materials and 2.2 molar eq. of elemental sulfur in each case and heated in toluene solution at 110°C (Scheme 33). All reaction mixtures were monitored with $^{31}P\{^{1}H\}$ NMR spectroscopy and consumption was observed after largely varying time spans of 1 day to 1 week.

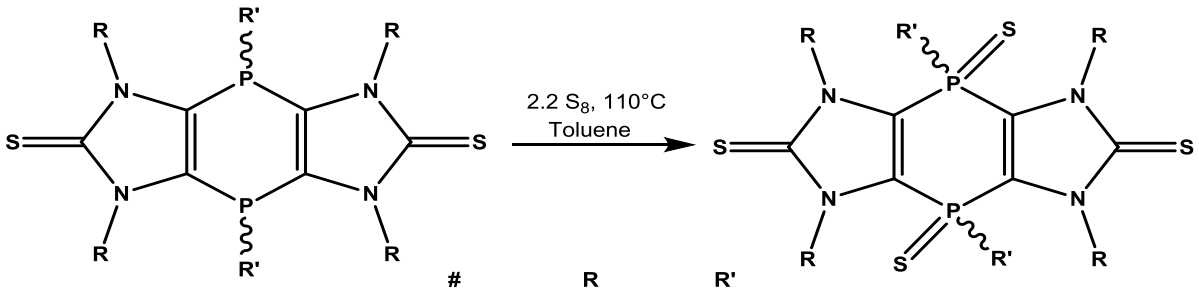

#	R	R'
27a,a'	Me	NEt_2
27b,b'	Et	NEt_2
27c,c'	^{n}Bu	NEt_2
27d,d'	Et	Ph
27e,e'	^{n}Bu	Ph

Scheme 33: Synthesis of the *P*-sulfides **27a,a'-e,e'**.

The isomeric ratio, revealed from the $^{31}P\{^{1}H\}$ NMR spectra of the reaction mixtures, in this case did not change during the course of sulfurization, but the relative position of the isomers did change (Figure 36). After completion, the products **27a,a'-c,c'** were easily isolated by removing the solvent and washing with *n*-pentane in good yields as white powder. The solubility of these products were not largely altered due to oxidation of the P-centers. Two new singlet resonance signals appeared in the downfield region (around 20 ppm) (Table 10), corresponding to two isomers (*cis*/*trans*) of the products. For example, in case of compound **27a,a'** the $^{31}P\{^{1}H\}$ NMR spectrum shows two peaks at 19.3 and 20.7 ppm (ratio 1:1.5) respectively for two isomers (Figure 37), which fell in the range of δ_P value for the *P,P'*-disulfides of compound **XXXIV** (31.9 ppm).[46] The $^{3}J_{P,H}$ coupling constant for the methylene protons of the NEt_2 groups increased, again, significantly (from 6.6 Hz in **4c** to 13.6 Hz in **27a**, quintet). This incremental increase of the coupling constant seems to be typical for the increased oxidation state of the P-center (**III** to **V**). The reaction times, the yields, the ratio of the isomers and the $^{31}P\{^{1}H\}$ NMR chemical shifts are listed in Table 10.

Table 10: $^{31}P\{^{1}H\}$ NMR chemical shifts, isomer ratio and yields of **27a,a'-e,e'**.

	R	R'	δ_P	Isomeric ratio	Reaction time	Yield (%)
27a,a'	Me	NEt_2	19.7 , 20.3	1: 1.5	1 day	65
27b,b'	Et	NEt_2	20.1 , 20.5	1:1.2	1 day	72
27c,c'	^{n}Bu	NEt_2	19.9 , 20.2	15 : 1	1.5 day	55
27d,d'	Et	Ph	1.5 , 3.0	1.3 : 1	1 week	80
27e,e'	^{n}Bu	Ph	1.4 , 3.1	10 : 1	1 week	75

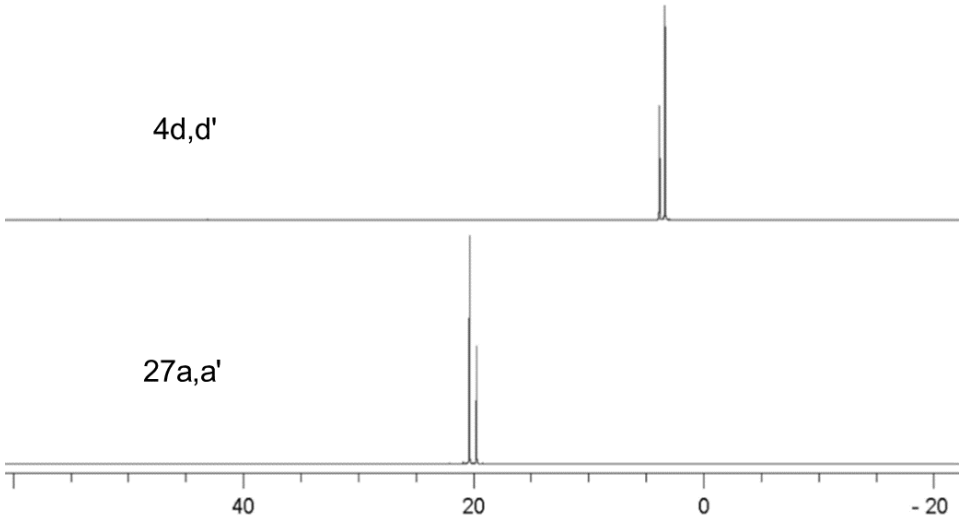

Figure 36: $^{31}P\{^{1}H\}$ NMR spectra of the isomer mixtures of compounds **4d,d'** and **27a,a'**.

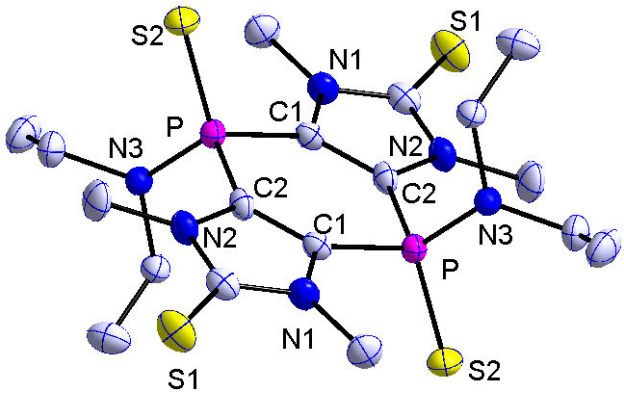

Figure 37: Molecular structure of *trans* **27a**; hydrogen atoms are omitted for clarity (50% probability level). Selected bond distances (Å) and angles (°):P-C(1) 1.7942(1), P-C(2) 1.7946(1), P-S(2) 1.9376(1), P-N(3) 1.6451(1) ;C(1)-P-C(2) 99.687(5), N(3)-P-S(2) 114.107(4).

Single crystals, suitable for X-ray crystallographic measurements, of compound **27a** could be grown by slow evaporation of its saturated dichloromethane solution at room temperature (Figure 37). The X-ray crystallographic analysis revealed solid state structure for the *trans* isomer of compound **27a**. It crystallized in the triclinic crystal system with the $P\bar{1}$ space group. Closer inspection of the metrical parameters revealed that crystal structure of compound **27a** showed close similarities with that of literature reported P-disulfide of compound **XXXIV**.[46]

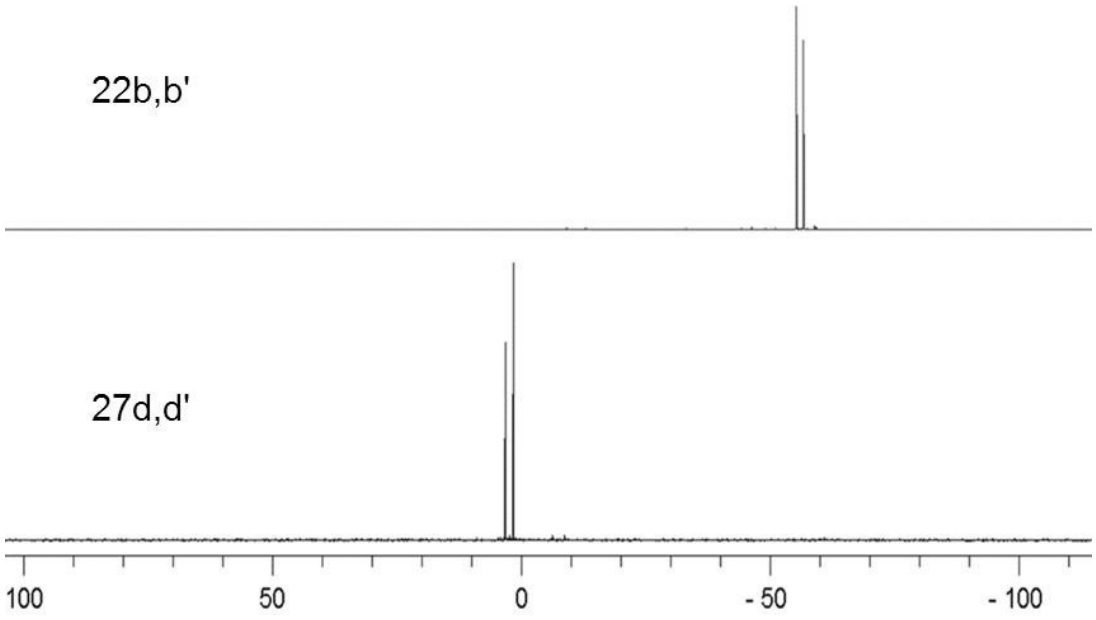

Figure 38: Comparison of $^{31}P\{^{1}H\}$ NMR spectra of compounds **22b,b'** and **27d,d'**.

In case of the *P*-Ph derivatives **22b,b'-c,c'**, the reactions proceeded extremely slow even at this high temperature (110 °C). The $^{31}P\{^{1}H\}$ NMR spectra of the reaction mixtures revealed only ~20 % (max.) conversion of the starting materials after a day of heating and completion was achieved after one week at high temperature. The $^{31}P\{^{1}H\}$ NMR spectra of the reaction mixtures showed two singlets in the downfield region, again, compared to the starting material. For example, compound **27d,d'** showed two singlets at 1.5 and 3.0 ppm, respectively, (ratio 1.3:1) for its two isomers, shifted almost 50 ppm towards the downfield region.

The isomeric ratio in this case was found to be changing slightly from that of the starting material **22b,b'** (1:1.5). This could be due to inversion of the $-NR_2$ at the P-center at higher temperature. Compounds **27d,d'-e,e'** could easily be isolated as white powders from the reaction mixture in excellent yields (Table 10). The increment in the oxidation state of the P-center showed its clear reflection on the δ_P value of the *P,P'*-disulfide **27d,d'**. (Figure 38). Upon sulfurization, the $^{3}J_{P,H}$ between the P-centers and the two *ortho*-protons of the phenyl rings increased notably, which changed the signal splitting pattern from **22b,b'** (broad signal) to **27d,d'** (triplet).

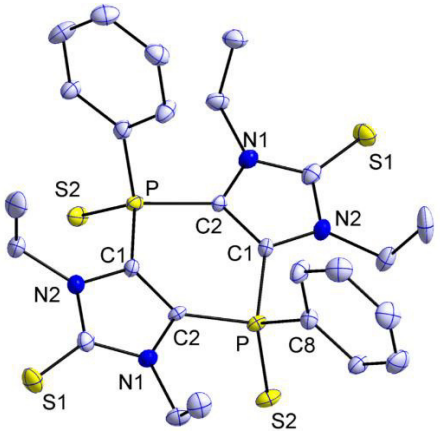

Figure 39: Molecular structure of *cis* isomer of compound **27d**; hydrogen atoms are omitted for clarity (50% probability level). Selected bond distances (Å) and angles (°): P-C(1) 1.8037(0), P-C(2) 1.7967(1), P-S(2) 1.9731(1), P-C(8) 1.8016(1) ;C(1)-P-C(2) 100.332(2), C(8)-P-S(2) 115.633(1).

X-ray crystallographic analysis of compound **27d** revealed the solid state structure of the *trans* isomer, which crystallized in the trigonal crystal system with the $P3_121$ space group. The metrical parameters were found to be similar to the *P*-NR_2 derivative **27a**, with the exception of a slightly elongated P-S(2) bond [1.9731(1) Å] compared to **27a** [1.9376(1) Å].

6.3 Oxidation using *ortho*-chloranil

Having seen a clear preference for a *P*-oxidation and *P*-sulfurization, the 1,4-dihydro-1,4-diphosphinines **4d,d'-f,f'** and **22b,b'-c,c'** were used to investigate reactions with *o*-chloranil. Here, the idea was to access first examples of spirocyclic phosphorane derivatives having a tricyclic array. Treatment of **4d,d'-f,f'** and **22b,b'-c,c'** with two eq. of *o*-chloranil in dichloromethane at ambient temperature, resulted in clean reaction only in case of **4d,d'-f,f'**. In the case of 1,4-dihydro-1,4-diphosphinines **22b,b'-c,c'** the reactions were unfortunately very unselective and nothing could be concluded or isolated from the reaction mixtures.

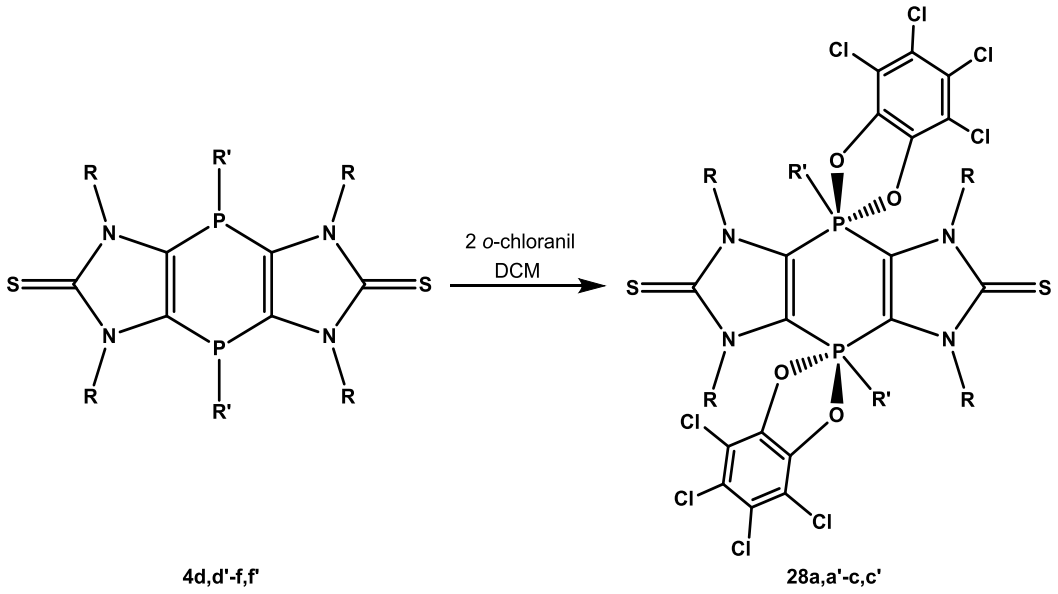

Scheme 34: Oxidation reactions of tricyclic 1,4-dihydro-1,4-diphosphinines **4d,d'-f,f'** using *o*-chloranil.

In case of the *P*-dialkylamino derivatives **4d,d'-f,f'** (Scheme 34), the $^{31}P\{^{1}H\}$ NMR spectra revealed a selective formation of **28a,a'-c,c'**. The time needed to complete the reaction in these cases was found to have a direct dependence on the N-substituents on the thione fragments of the tricyclic 1,4-dihydro-1,4-diphosphinines **4d,d'-f,f'**. The *N*-Me derivative reacted much faster (6h to reach completion) compared to the bulkier *N*-^{n}Bu analogue (it took 16h, despite the better solubility of the latter). Compound **28a,a'** could be easily isolated from the reaction mixture just by successive washing with dichloromethane (with minimum amount of solvent at 0 °C to minimize compound loss) and diethyl ether in excellent yield (Table 11). In the same manner, compound **28b,b'-c,c'** could also be isolated in great yield as a mixture of two isomers. The $^{31}P\{^{1}H\}$ NMR spectrum of

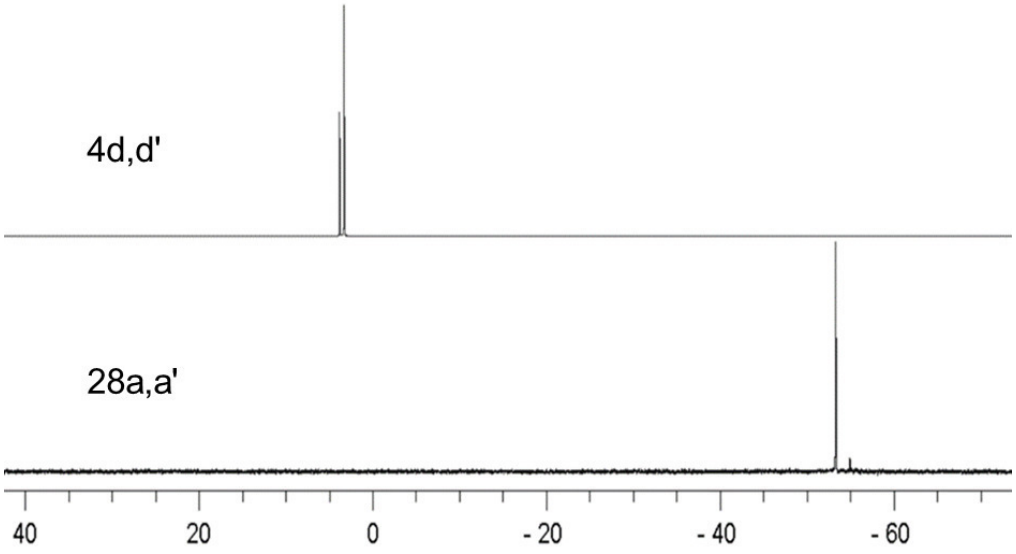

Figure 40: Comparison of $^{31}P\{^{1}H\}$ NMR spectra of compounds **4d,d'** and **28a,a'**.

compound **28a,a'** showed two singlets at -53.2 and -54.9 ppm respectively, for two isomers, with a huge upfield shift of about 50 ppm with respect to the starting material (**4d,d'**) (Figure 40).

The drastic change in the δ_P value could be attributed to the reshaped geometry and change in the co-ordination number for the P-centers in these spirocyclic phosphorane.[75] One more notable aspects that stands out of the comparison between compound **4d,d'** and **28a,a'** is the dramatic change in the isomeric ratio. This change is due to remarkable difference in the solubility between two isomers. One of the isomers precipitated out of the reaction mixture during the course of the reaction as beige powder, due to its limited solubility; hence causing these visible change in the isomeric ratio in the $^{31}P\{^{1}H\}$ NMR spectrum (from 1:1 in **4d,d'** to 12:1 in **28a,a'**). For **28b,b'-c,c'** also the isomeric ratio remained unaltered. The analytical details for **28a,a'-c,c'** are listed in table 11.

Table 11: $^{31}P\{^{1}H\}$ NMR chemical shifts, isomer ratio and yields of **28a,a'-c,c'**.

	R	R'	δ_{P*}	Isomer ratio	Reaction time	yield (%)
28a,a'	Me	NEt_2	-53.2 , -54.9	12:1	6h	82
28b,b'	Et	NEt_2	-46.7 , -52.2	1:2.5	10h	80
28c,c'	^{n}Bu	NEt_2	-43.6 , -52.2	1:1	16h	88

6.4 Reaction with electrophiles: Competition between the P- and the S-centers

Among the most important reactivity aspects of these tricyclic 1,4-dihydro-1,4-diphosphinines was their behavior towards different electrophiles as this may indicate future possible exploitations. Firstly, theoretical calculations were performed by Frontera[68] to allow for a closer inspection of the relative nucleophilicities of the P- and S-centers. Therefore, molecular electrostatic potential (MEP) isosurfaces of compound **4d** (*P*-NEt_2) and **22a** (*P*-Ph) were calculated which showed that the MEP value at the S-centers are more negative than that of the P-centers (Figure 41 a,c).

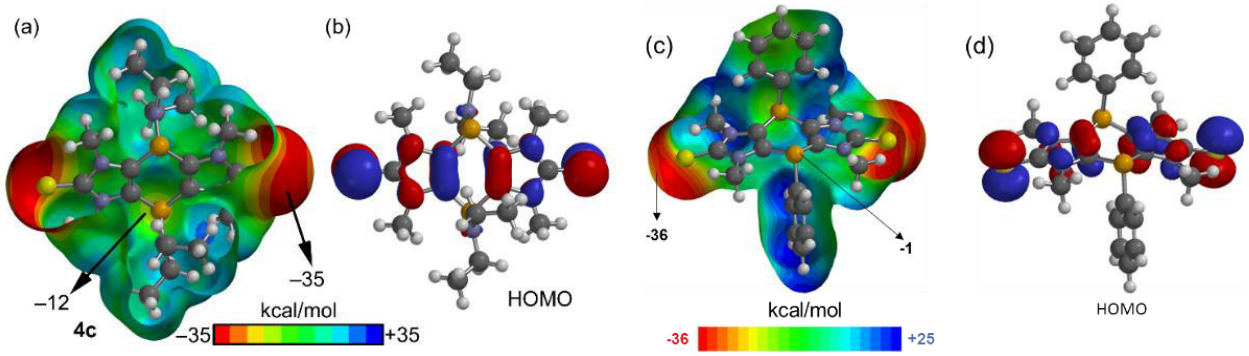

Figure 41: (a) MEP isosurface (0.002 a.u.) of compound **4d**; selected points of the surface are indicated. (b) HOMO plot of compound **4d**. (c) MEP isosurface of compound **22a**. (d) HOMO plot of **22a**.

Furthermore, the orbital coefficients for the HOMO of the molecules were found to be more located at the S- than at the P-centers (Figure 41 b,d). These two data provided strong evidence for a largely pronounced nucleophilicity of the S-centers.

6.4.1 Reaction with methyl trifluoromethanesulfonate

To start with the examination of the relative reactivity of the P- and S-centers towards soft and hard carbon-based electrophiles, the methylation reaction was chosen as case study. Firstly, methyl iodide was used as the reagent in dichloromethane, but no reaction was observed for either the *P*-NR_2 derivatives **4d,d'-f,f'** or the *P*-Ph derivatives **22b,b'-c,c'** at ambient temperature Therefore, methyl trifluoromethanesulfonate (methyl triflate) was chosen as a hard electrophile and stronger methylating reagent and the derivatives **4d,d'-f,f'** and **22b,b'-c,c'** were treated with under the same conditions (Scheme 35). In case of **4d,d'** upon addition of the methylating agent there was no change of color in the reaction mixture, but it slowly turned turbid due to formation of a white

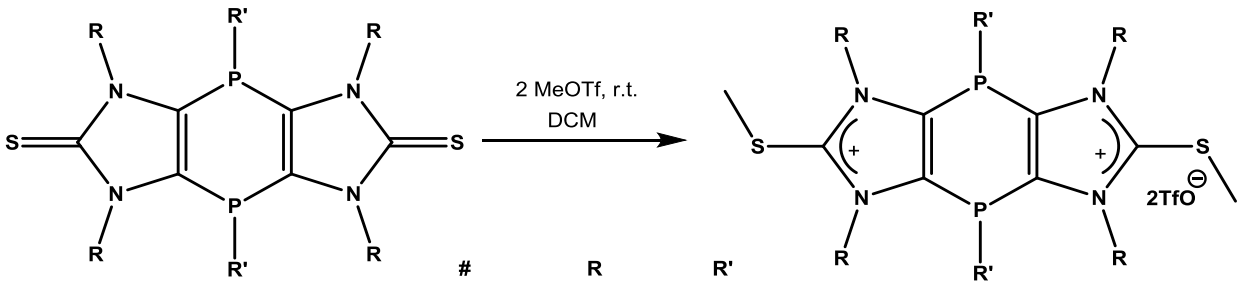

#	R	R'
29a,a'	Me	NEt_2
29b,b'	^{n}Bu	NEt_2
29c,c'	Et	Ph
29d,d'	^{n}Bu	Ph

Scheme 35: *S*-methylation of the tricyclic 1,4-dihydro-1,4-diphosphinines using methyl triflate.

precipitate. The reaction was monitored by $^{31}P\{^{1}H\}$ NMR spectroscopy. After 2h of stirring at room temperature the starting material was seemed to be completely consumed.

This white precipitate was filtered out and used for further analysis. The $^{31}P\{^{1}H\}$ NMR spectrum of the white precipitate in DMSO-d_6 didn't show much of change as per the δ_P value is concerned apart from slightly increased $\Delta\delta$ values between the two isomers compared to the starting material (**4d,d'**). But the $^{13}C\{^{1}H\}$ NMR spectrum of it showed the disappearance of the C=S carbon atom resonance and the appearance of a new singlet at 149.7 ppm, characteristic of a C^2-carbon nucleus of an imidazolium salt. This NMR data provided strong evidence for the *S*-methylation, meaning the formation of **29a,a'** as the final compound. Further support came from the ESI-MS experiment which exhibited an ion peak at m/z 244.1, assigned to the cation $C_{20}H_{38}NP_2S_2^{2+}$ in **29a,a'**. After having had confirmation for S-methylation, the question arose if sterics and electronics (a different P-substituent) might alter the reaction course. But when **4f,f';22b,b'-c,c'** were employed, compound **29b,b'-d,d'** was formed in the same vein. All of this bis(imidazolium) salts **29b,b'-d,d'** were isolated and fully characterized. The analytical data of these compounds are listed in Table 12.

Finally, the *S*-methylation in **29d,d'** was confirmed by the X-ray crystallographic measurement using single crystals grown from a saturated dichloromethane solution at –20 °C. The result

Table 12: $^{31}P\{^{1}H\}$ NMR chemical shifts, isomer ratio and yields of S-methylated bis(imidazolium salts) **29a,a'-d,d'**.

	R	R'	δ_P	Isomeric ratio	Appearance	yield (%)
29a,a'	Me	NEt_2	3.7 , 5.9	1:11	White solid	45
29b,b'	^{n}Bu	NEt_2	2.2 , 3.2	2.4:1	Orange liquid	89
29c,c'	Et	Ph	-49.5 , -55.8	1:1.3	White solid	85
29d,d'	^{n}Bu	Ph	-50.1 , -53.7	1.1:1	White solid	89

revealed that the *trans* isomer of compound **29d** (Figure 42) crystallized in the triclinic crystal system with the space group $P\bar{1}$. Close inspection of the packing pattern revealed that the two *S*-Me groups are anti-periplanar oriented with respect to each other and the plane of the tricycle. The plane of the Ph groups on the P-centers were found to be almost perpendicular (89.974°) to the planar six-membered ring. The triflate anions are located in between two planes of the cationic fragments in such a manner that it stays in vicinity of the S-Me protons. This could be a consequence of a moderate H-bonding interaction[76] (distance: 2.2698(3) Å) between the O atom of the OTf anion and the H atom of SMe, because the SO_3 fragment of the triflate anion sits on the imidazole-2-thione ring of the tricycle.

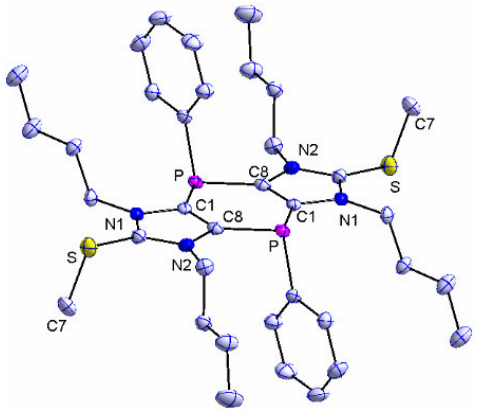

Figure 42: Molecular structure for the cationic part of *trans* **29d**; hydrogen atoms except the borane ones are omitted for clarity (50% probability level). Selected bond distances (Å) and angles (°): P-C(1) 1.8173(2), C(1)-C(8) 1.3688(2), P-C(13) 1.8291(2), S-C(7) 1.8114(1);C(1)-P-C(8) 95.223(10), C(1)-P-C(13) 101.210(11).

The reaction outcome of S-methylation was according to the prediction using the MEP analysis, *i.e.*, the S-centers were predicted to be more nucleophilic. Nevertheless, further theoretical investigations were performed by Frontera using **22c** to calculate the relative energies of the *S*-methylated (= **22c-SMe**) and the *P*-methylated (= **22c-PMe**) product and, surprisingly, the energetic

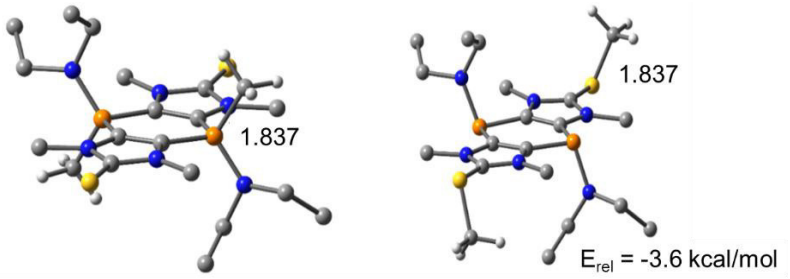

Figure 43: Relative energy difference between the *P*-methylated (left) and *S*-methylated (right) product; bond lengths are given in Å.

difference between the products is very small (3.6 kcal/mol) (Figure 43). Interestingly, it is the thermodynamically more stable product *trans* **29d** that was observed experimentally (S-methylated), but it might also play a role that this attack should be kinetically favored to a sterically less congested center.

6.4.2 Formation of P-borane adducts via reaction with borane-dimethyl sulfide

Equally important for future synthetic exploitations was to gather information on co-ordination properties of these tricyclic 1,4-dihydro-1,4-diphosphinines, and to examine if the results of the MEP calculations could also render useful predictions in this regard. To start this, compounds **4d,d'-f,f'** and **22b,b'-c,c'** were subjected to reactions with transition-metal complexes *e.g.* $[Cr(CO)_5(CH_3CN)]$, $[W(CO)_5(CH_3CN)]$ etc., representing examples of soft Lewis acids. But none of the metal complexes showed any reactivity; at least none at the P-centers.

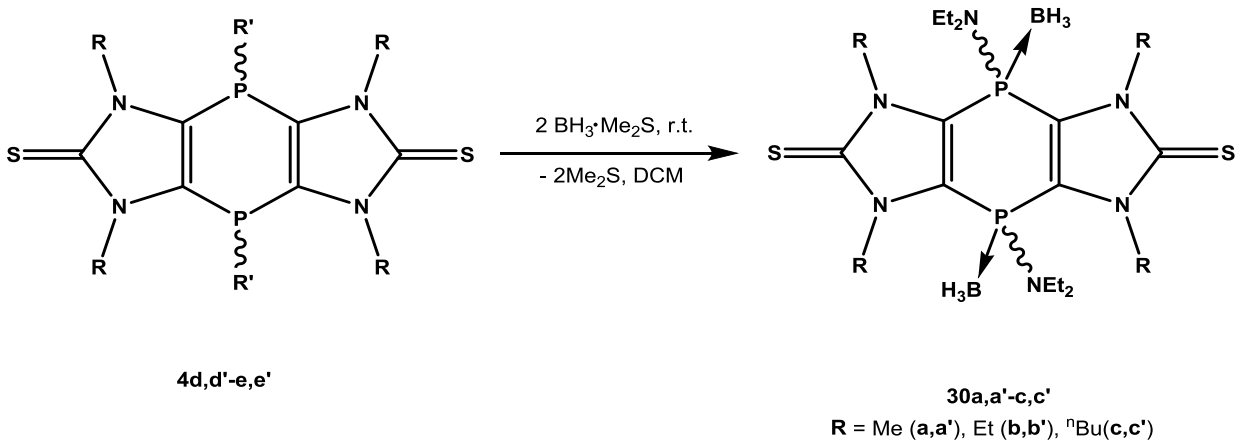

4d,d'-e,e'

30a,a'-c,c'
R = Me (**a,a'**), Et (**b,b'**), ^{n}Bu(**c,c'**)

Scheme 36: Synthesis of *P*-borane complexes **30a,a'-c,c'**.

To investigate if stronger Lewis acidic reagents might result in a complex formation, we decided to use the borane-dimethyl sulfide adduct. Compounds **4d,d'-f,f'** were treated first with borane-dimethyl sulfide in dichloromethane at room temperature, and the reaction progress monitored by $^{31}P\{^{1}H\}$ NMR spectroscopy (Scheme 36). The $^{31}P\{^{1}H\}$ NMR spectra of the reaction mixtures showed complete consumption of the starting materials after 2h. Compounds **30a-c** could be isolated from the reaction mixture by simply concentrating the reaction mixture and washing the residues with *n*-pentane to obtain white powders in excellent yield (Table 13).

The $^{31}P\{^{1}H\}$ NMR spectrum of **30a,a'** showed a significantly downfield-shifted and broad (FWHM 82.5 Hz) resonance signal at 34.4 ppm (Figure 44). The appearance of a broad resonance signal could be attributed to the direct connectivity of P-atom to a quadrupolar boron center, thus

confirming the occurrence of P- instead of S-borylation. The apparent disappearance of the isomers, depicted in Figure **44**, could be due to the close vicinity of the two isomeric signals in the ^{31}P-NMR spectrum leading to superimposed signals, thus only one broad peak is visible in the ^{31}P{^{1}H} NMR spectrum. In case of **30c** there were no isomers observed as the pure trans-**4f** was used as the starting material.

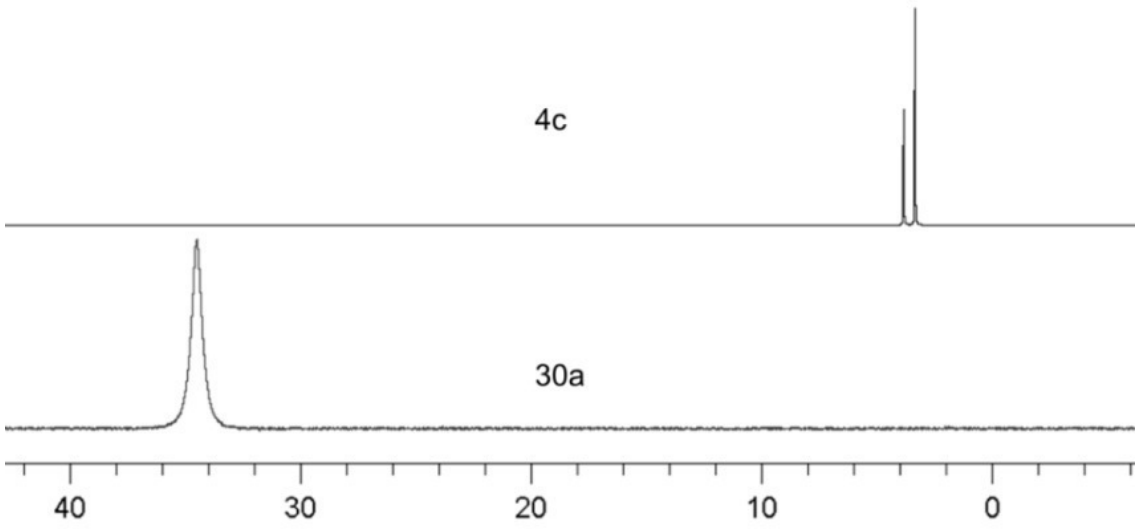

Figure 44: Comparison of ^{31}P{^{1}H} NMR spectra ($CDCl_3$) of compounds **4d,d'** and **30a**.

Table 13: ^{31}P{^{1}H} NMR chemical shifts, isomer ratio and yields of the P-borane complexes **30a-c**.

	R	R'	δ_{P*}	Isomer ratio	FWHM (Hz)	yield (%)
30a,a'	Me	NEt_2	34.4	-*	82.5	85
30b,b'	Et	NEt_2	33.7 , 34.3	1.3:1	86.6	82
30c,c'	^{n}Bu	NEt_2	33.3	-*	81.7	60

* the isomeric ratio could not be determined due to broad signals

The *P*-borane adduct formation in case of the P-NR_2 derivatives of tricyclic 1,4-dihydro-1,4-diphosphinines could also be confirmed by means of X-ray crystallographic measurement. Single crystals for compound **30a**, obtained by slow evaporation of its saturated dichloromethane solution, were analysed by X-ray crystallography and the results showed the solid state structure for its *trans*-isomer (Figure 45). It crystallized in the monoclinic crystal system with the $P2_1/c$ space group. The molecular structure confirmed that the tricyclic array is planar and P-N(3) bond (1.6376(1) Å) is shortened significantly upon borane coordination (compared to compound **4d** (1.685(4) Å)).

After having studied the P-borane complex formation using *P*-NR_2 derivatives of **4d,d'-f,f'**, the same reaction conditions were also exerted on the *P*-Ph derivative of the tricyclic 1,4-dihydro-1,4-diphosphinine **22b,b'**. Surprisingly, in case of **22b,b'** the ^{31}P{^{1}H} NMR spectrum of the reaction

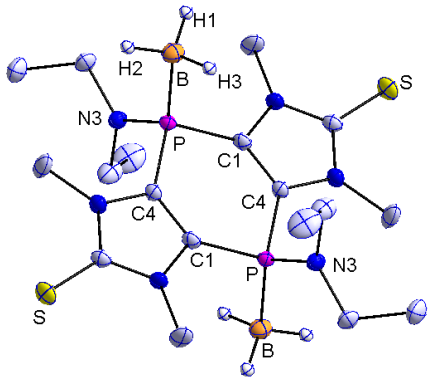

Figure 45: Molecular structure of *trans* **30a**; hydrogen atoms except the borane ones are omitted for clarity (50% probability level). Selected bond distances (Å) and angles (°):P-C(1) 1.8083(1), P-C(4) 1.7999(1), P-B 1.9157(1), P-N(3) 1.6376(1), B-H(1) 1.1170(1);C(1)-P-C(4) 98.569(3), B-P-N(3) 117.562(3).

mixtures showed a competing S-borylation (Figure 47) as two sets of resonances appeared, *i.e.*, a set of two broad resonance signals at -3.8 ppm and 4.5 ppm, that might be assigned to the isomers of the P-borane adducts. But there were also two pairs of two singlets at -60.5 ppm and -60.6 ppm; assignable to the mono S-borane adduct isomers, whereas the singlets at -55.1 ppm and -55.2 ppm could be attributed to the isomers of the bis(S-borane adduct). The higher Δδ value between the isomers of the mono and bis(S-borane adduct) supported this tentative assignment. Unfortunately, this product mixture could not be successfully worked-up to get the products separated.

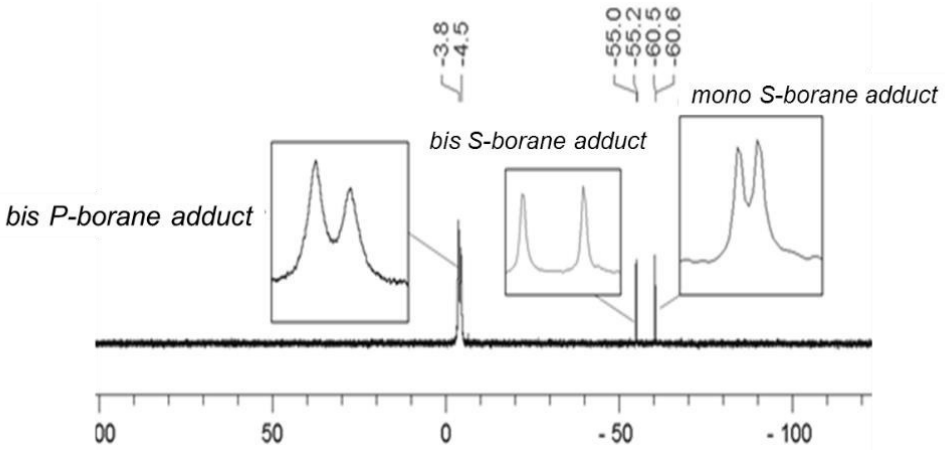

Figure 46: The $^{31}P\{^{1}H\}$ NMR spectra for the reaction of **22b,b'** with borane-dimethyl sulfide in dichloromethane.

As the MEP analysis did not enable to explain the formation of compounds **30a,a'-c,c'** when BH_3 was used as an electrophile, since the S-centers were supposed to be more nucleophilic. In order to shed some light on this issue, the structures were calculated by Frontera for compound **30a** (= **30a-*P*-**

BH_3) and its hypothetical S-borane analogue (= **30a-*S*-BH_3**) (Figure 47). The optimized structure of compound **30a** was found to be almost identical to the X-ray structure, as exemplified by the P–B distance [1.915 vs exp: 1.9157(1)]. This adduct is 30.2 kcal/mol more stable than the S-borane adduct, in agreement with the experimental result. It should also be mentioned that the S···B distance (2.051) in the S-borane adduct is longer than the sum of the covalent radii of S and B (1.89 Å). This makes the S···B bond in the S-borane adduct only partially covalent, and this weak bond also explains the energetic difference between the *P*- and *S*-boranation and, hence, explains the formation of the P-borane product as the preferred final product. In case of the *P*-Ph derivatives the reduced basicity of the P-centers could attribute to the formation of the S-borane adducts in competing reactions.

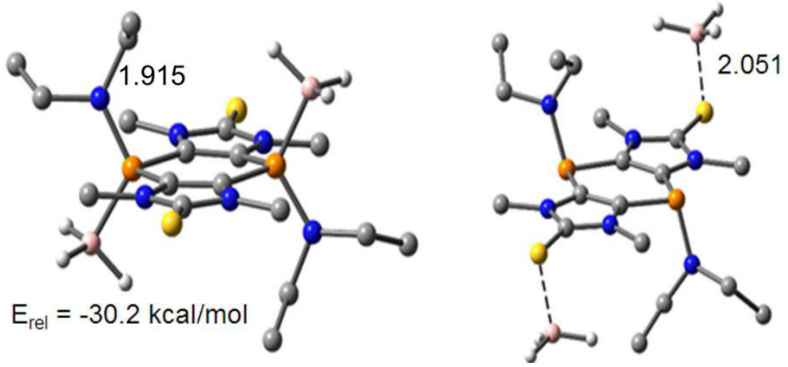

Figure 47: Optimized structures of **30a** (left) and the *S*-borane adduct (right); distances are given in Å.

6.5 Study on the formation of dianionic tricyclic 1,4-dihydro-1,4-diphosphinines

In addition to the electrophilic *P*-chloro derivatives, interest arose to complement this with anionic and/or dianionic derivatives of tricyclic 1,4-dihydro-1,4-diphosphinines. Having the *P*-Ph derivatives**22** in hand, the alkali metal-mediated P-C bond cleavage of the P-Ph bond was envisaged as key step towards the synthesis of the diphosphanido derivatives **31**. Compound **22c** was selected for these studies because of its higher solubility compared to **22a,b** in common organic solvents. Firstly compound **22c** was treated with Lithium metal at r.t. in THF with the goal of a reductive cleavage of the two *P*-Ph bonds,[77] following the literature reported methodology.[78] Surprisingly, compound**22c,c'** didn't react with lithium metal even under refluxing condition in THF, and also use of sodium metal didn't led to success. Finally, potassium metal was used successfully in THF (Scheme 37). Upon adding the THF solution of **22c,c'** to the suspension of potassium metal at ambient temperature the color of the solution changed from colorless to light orange, and the color

got more intense with an orange precipitate forming with time, indicative of formation of an ionic compound that has limited solubility in THF. The progress of the reaction was monitored by $^{31}P\{^{1}H\}$ NMR spectroscopy, which revealed complete consumption of the starting material after 12h. It also

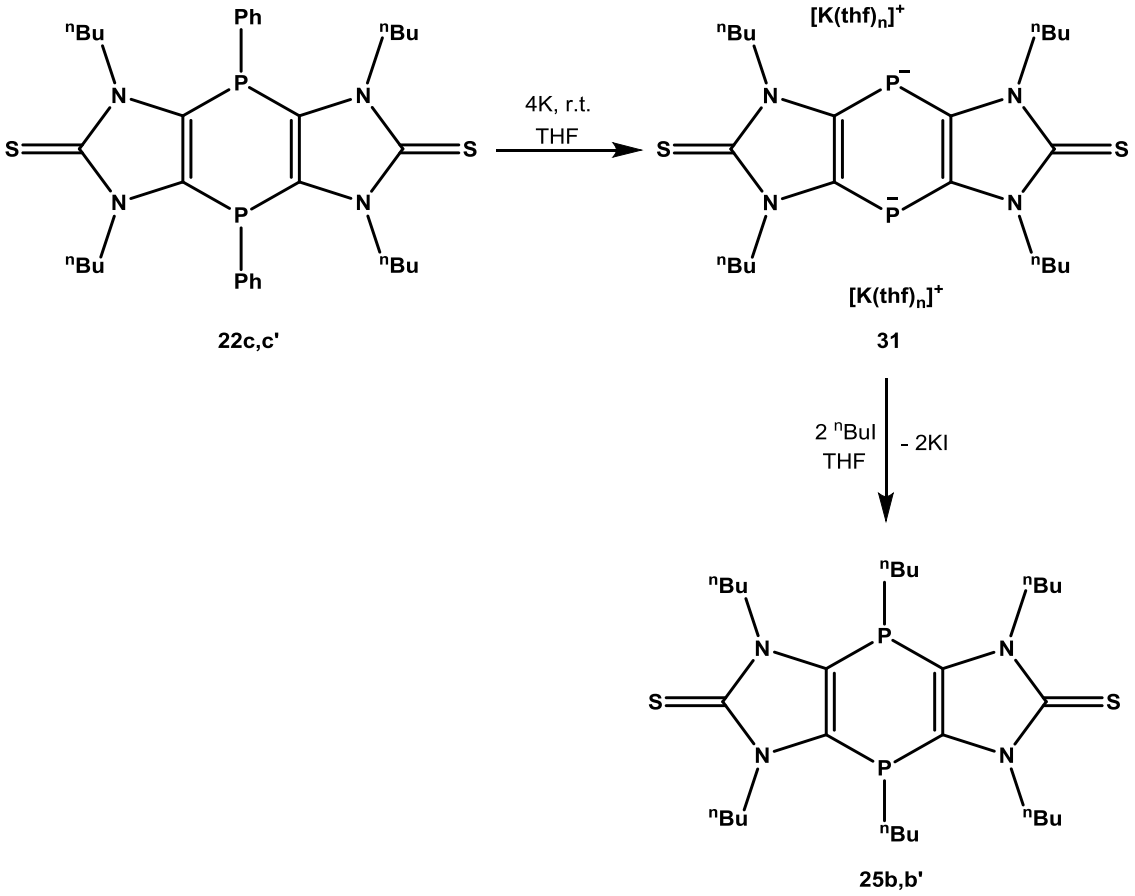

Scheme 37: Formation and reaction of intermediate bis-phosphanido derivative **31**.

showed complete disappearance of the two singlet resonances for the two isomers of compound **22c** and a new singlet resonance at –73.9 ppm had appeared; it was presumed to be the dianionic derivative **31** due to a symmetrical structure (Scheme 36). Unfortunately, **31** could not be isolated due to a slow decomposition in solution; the presence of phenyl potassium might also play a role.Therefore to prove the formation (and intermediacy) of **31**, it was generated and reacted *in situ* with *n*-butyl iodide at –78 °C. Upon addition of *n*-butyl iodide, the orange turbid reaction mixture immediately turned clear and became light yellow. The ^{31}P NMR spectrum (Figure 49) of this reaction mixture showed two singlet resonance signals at –58.5 and –66.3 ppm (ratio 12:1) , respectively, which was identical with the values of compound **25b,b'.** Compound **25b** was isolated as white powder in 45 % yield.

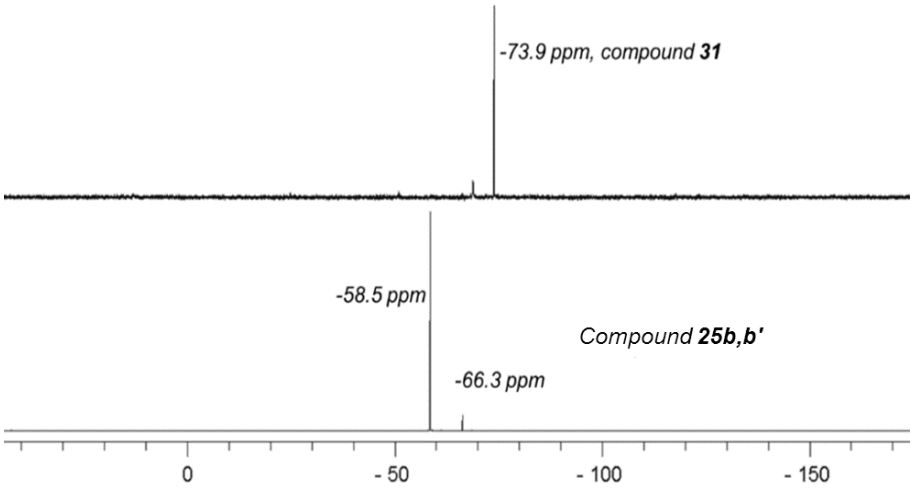

Figure 48: Quenching of the dianion **31** by *n*-butyl iodide to produce **25b**.

The δ_P value of this intermediate dianion **31**, was found to be significantly highfield-shifted compared to literature reported aromatic phospholides **LVIII-LIX**[79] and **LX**[80] (Figure 49); but on the other hand it appeared relatively downfield-shifted compared to the acyclic mono anion analogue **LXI** (δ_P = - 110.2).[36]

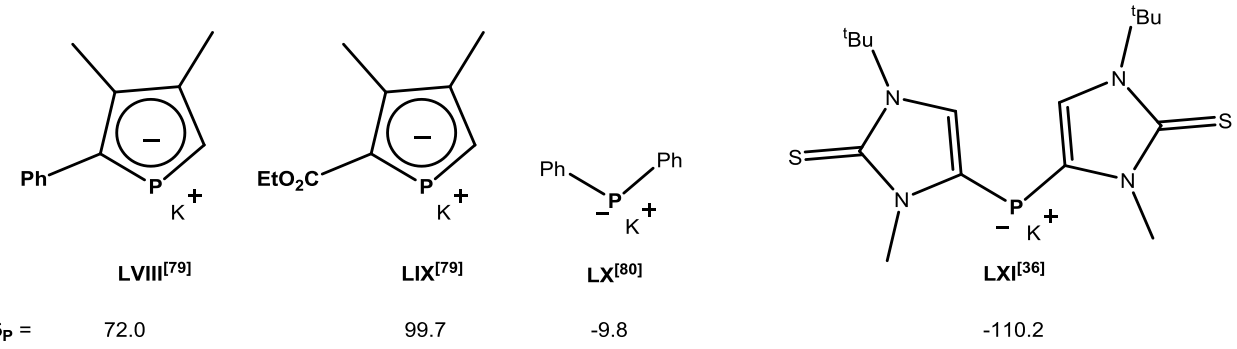

Figure 49: Selected examples of literature reported phospholides and acyclic phosphanides.

6.6 Oxidative desulfurization of the tricyclic 1,4-dihydro-1,4-diphosphinines

As described in the introductory chapter, imidazole-2-thiones can be easily subjected to oxidative desulfurization [34] to get access to imidazolium salts, which in turn can act as a starting material for imidazole-2-ylidenes.[34] Thus, presence of two such imidazole-2-thione moieties in these tricyclic 1,4-dihydro-1,4-diphosphinines makes them plausible precursors corresponding bis-imidazolium salts and, subsequently, bis-imidazole-2-ylidenes. With this objective, the *P*-NR_2 and *P*-Ph derivativ-

es **4d,d'** (*N*-Me)**, 22b,b'** (*N*-Et) were treated with 10 molar eq. of aqueous hydrogen peroxide in dichloromethane at 0 °C. The reactions were monitored by $^{31}P\{^{1}H\}$ NMR spectroscopy which revealed a clean conversion to give products with only slightly highfield-shifted resonance signals (Figure 50). For compound **4d,d'**, the$^{31}P\{^{1}H\}$ NMR spectrum showed a complete

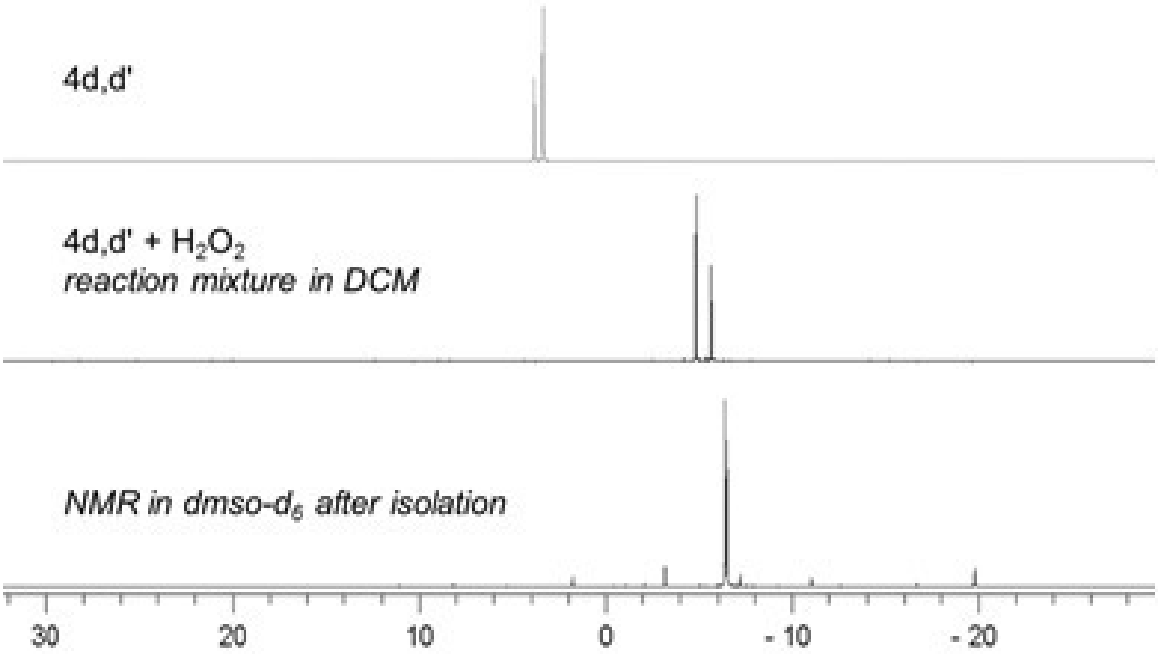

Figure 50: Oxidative desulfurization of compound **4d,d'**.

consumption of the starting material and showed two singlets at -4.8 and -5.6 ppm for two isomers respectively. But unfortunately, during the workup, *i.e.*, evaporation of solvent and washing with ether followed by *n*-pentane, the compound showed limited stability. The partial decomposition restricted the complete purification and characterization of these targeted bis-imidazolium salts with *P*-NR_2 fragments. The latter is somewhat surprising as related acyclic derivatives have been described formerly.[19, 34]

After this partial failure to get hands on the bis-imidazolium salts having the P-NR_2 substituents, the *P*-Ph derivative **22b,b'** (*N*-Et) was considered for this study. When compound **22b** was treated with hydrogen peroxide in dichloromethane solution at 0 °C (Scheme 38), the $^{31}P\{^{1}H\}$ NMR spectrum of the reaction mixture showed a clean conversion into the product **32,32'**. It also revealed a significant downfield shift of the product resonances after oxidative desulfurization but the $\Delta\delta_P$ value between the two isomers, formed in a 1:1.1 ratio, (0.3 ppm) was a bit smaller compared to that of **22b,b'** (1.4 ppm). The product could be isolated as white powder in excellent yield via

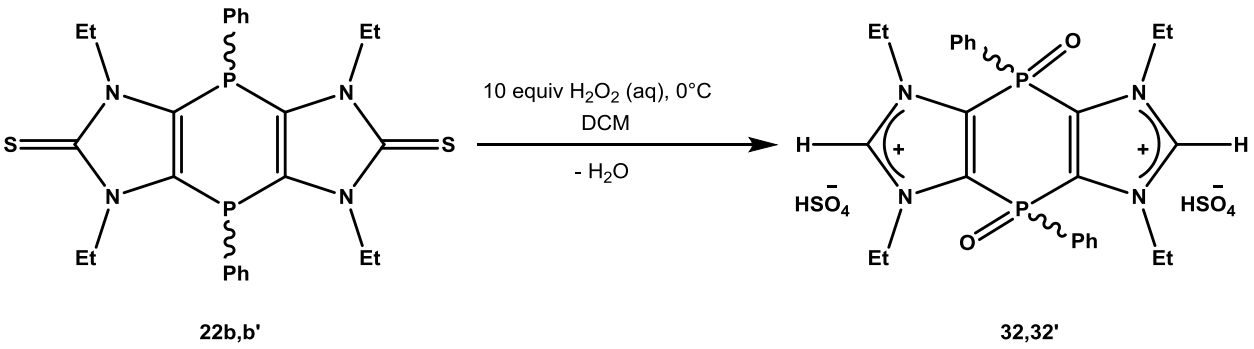

Scheme 38: Oxidative desulfurization of **22b,b'** to the bis-imidazolium salt **32,32'**.

removal of solvent and thereafter washing with diethylether.

Characterization of **32,32'** (mixture of two isomers) using ^{1}H, $^{13}C\{^{1}H\}$ NMR spectroscopy and ESI-MS provide proof for the constitution of the tricyclic bis-imidazolium salt. For example, the ^{1}H NMR spectrum of compound **32** showed a slight downfield shift of the signals for the Ph protons indicating a reduced electron density at the P-centers (supporting the P-oxidation), and it showed a pair of new triplet resonance signals ($^{4}J_{P,H}$ = 2.3 Hz)[72] in the downfield region (9.96 and 9.99 ppm, respectively, ratio 1.2:1) which is characteristic of imidazolium C^{2}-H protons. The $^{13}C\{^{1}H\}$ NMR spectra of compound **32** showed absence of typical C=S resonances but a new, broad signal at 146 ppm had appeared which indicates the presence of a imidazolium C^{2}-center.[34, 72] And finally the ESI-MS spectra showed a molecular ion peak at m/z 247.1 assigned to $[C_{26}H_{34}N_4P_2O_2]^{2+}$ (z = 2) which lends further support to the formation of the bis-imidazolium salt **32**. The δ_P values for this bis-imidazolium salt were found to be notably highfield-shifted compared to the acyclic backbone bis(diphenyl)phosphinoyl-substituted imidazolium salt (δ_P = 23.7 ppm)[20] and even the more closely related acyclic analogue ($[Ph(O)P(IMH^{tBu,Me})_2]Cl_2$, where $IMH^{R,R}$ = 1,3-dialkyl-imidazolium-4-yl) (δ_P = 7.4 ppm);[34] thus reflecting the different electronic nature of the imidazolium moiety compared to the phenyl groups.

Chapter 7

7. Entry to imidazole-2-thione-based tricyclic 1,4-diphosphinines

Compounds **4** and P,P'-dioxides **26**, having the tricyclic 1,4-dihydro-1,4-diphosphinine motif, represent an important extension of the known series of 1,4-dihydro-1,4-diphosphinines because the NHC chemistry seems within reach and, secondly, the six-membered ring might offer access to stable 1,4-diphosphinines. The chemistry of the latter is still largely underdeveloped due to the instability and problematic access of the only known derivative. Ideally, the two C=S fragments present in compound **4** offers an ideal situation to explore the possibility of getting hands on P-containing backbone annulated bis-carbenes **LXIII** and/or **LXIV** (containing a 1,4-diphosphinine motif) which would represent a unique variation of Bielawski-type bis-NHCs **LXII**.[81, 82]

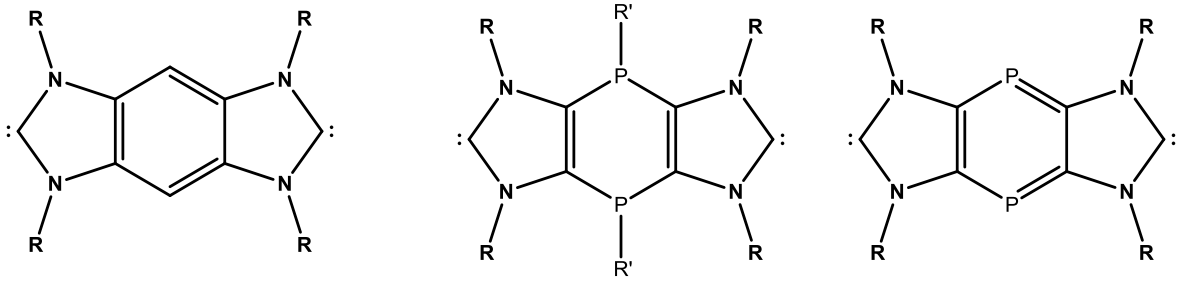

Figure 51: Bielawski-type annulated bis-NHCs **LXII** and new targeted P-analogues **LXIII** and **LXIV**.[82]

7.1 Study on the thermal decomposition of compounds 4

In the EI-MS spectrometric study of compounds **4** it was recognized that in each case the base peak accounted for an m/z value corresponding to the fragment cation $[M-2NR_2+H]^+$. For example in case

of compound **4e** (NR = NEt), the EI-MS spectrum showed a base peak with m/z value 371.0 that can be attributed to a cation with the formal composition of $[M\text{-}2NEt_2+H]^+$. This indicated that the P-N bonds in compound **4e** are labile under the EI-MS conditions and tend to be cleaved. To check the viability of a hypothesis concerning a thermal P-N bond cleavage, the neat white compound **4e** was exposed to high temperature (165 °C) *in vacuo* for prolonged time spans (8 h), and all volatile compounds were trapped. The progress was monitored by $^{31}P\{^1H\}$ NMR spectroscopy and small portion of the red solid remain were taken, and dissolved in THF. Initially compound **4e** had two isomers with a relative ratio of 28:72, but after heating for 3h, the color of the solid had turned bright red and the $^{31}P\{^1H\}$ NMR spectrum showed a small amount (~ 2 %) of a product appearing at 78.7 ppm (Figure 52). The heating was continued for 5 more hours and up to 18% of this product was formed in the product mixture. More importantly, only one of the two isomers showed this thermal decomposition and the amount of the other isomer remained unaltered during the course of heating. No further conversion, apart from some unknown decomposition, was observed if heating was continued (up to 8 h).

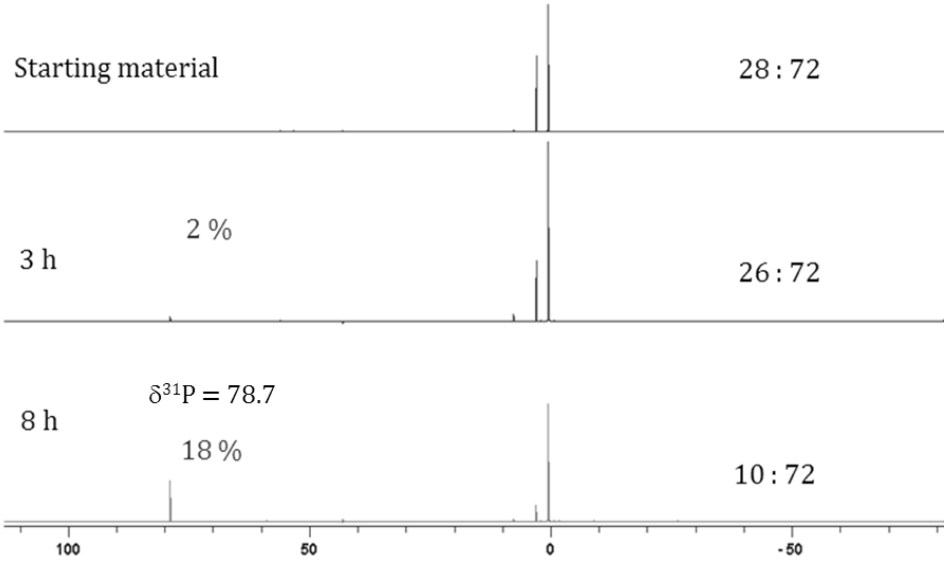

Figure 52: $^{31}P\{^1H\}$ NMR spectrum (THF) of the residue after thermal decomposition of compound **4e**.

After a total of 8 h at 165 °C, the trapped liquid, colorless compounds, were studied by ^1H NMR spectroscopy. The ^1H NMR spectrum (C_6D_6) showed a pair of triplet and quartet resonance signals, and the chemical shifts of which exactly fitted with that of diethylamine.[83] After this study on thermal decomposition of **4e**, alternative ways were investigated to get a more facile access to this product, observed in the $^{31}P\{^1H\}$ NMR spectrum, which might be red in color and relatively robust in

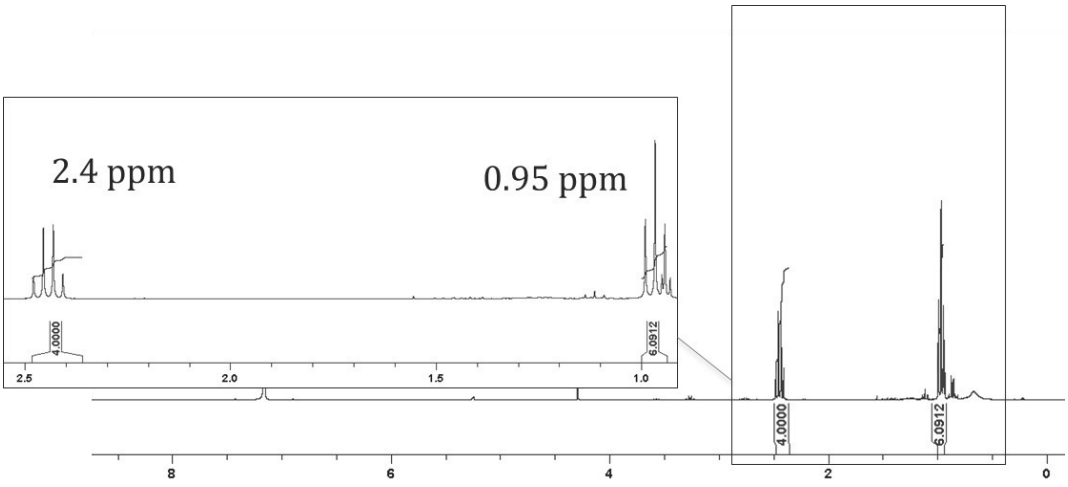

Figure 53: ^{1}H NMR spectrum of the liquid fraction collected in a cooling trap (taken in C_6D_6).

terms of thermal stability. As the most likely precursor the focus was on the 1,4-dihydro-1,4-dichloro-1,-diphosphinines **24a,a'-b,b'**.

7.2 Reduction of 1,4-dihydro-1,4-dichloro-1,4-diphosphinines: access to the first tricyclic 1,4-diphosphinines

As first step for the planned aromatization of the six-membered ring reduction of the 1,4-dihydro-1,4-dichloro-1,4-diphosphinines **24a,b** was chosen to target P-H compounds which might further be aromatized by means of dehydrogenation. Compounds **24a,a'-b,b'** where treated with common reagents such as $^{n}Bu_3SnH$ or $LiAlH_4$ in THF at –78°C and the color of the reaction mixture turned

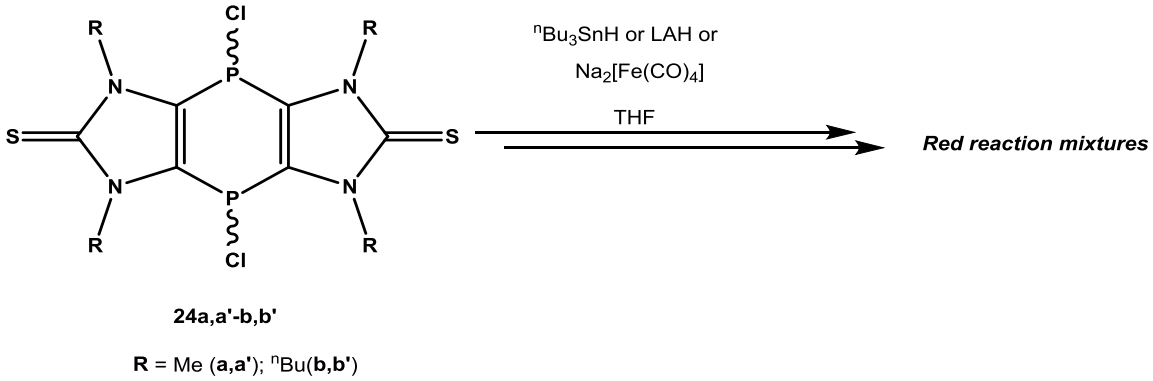

Scheme 39: Various reactions of compounds **24a,a'-b,b'** leading to red solutions.

dark red from orange, which was surprising as a red color for a targeted secondary phosphane-type heterocycle would be very rare (Scheme 39). The ^{31}P NMR spectra of the reaction mixtures not only

didn't show any signal with a $^{1}J_{P,H}$ coupling constant, indicative of the formation of a direct P-H bond, but the major products showed resonance signals at low field (76.2 for **24a** and 78.1 ppm for **24b**) which is also very unlikely for a secondary phosphane-type derivative. A very similar outcome was obtained if $Na_2[Fe(CO)_4]$ was used, but no compound possessing a P-Fe bond was detected.

Importantly, the selectivity of the reaction with $Na_2[Fe(CO)_4]$ was much better compared to those with $^{n}Bu_3SnH$ or $LiAlH_4$ which is illustrated by the clean conversion of the two isomers of **24b** yielding one product with a singlet resonance at 78.1 ppm in the $^{31}P\{^{1}H\}$ NMR spectrum of the reaction mixture (Figure 54).

First of all, the δ_P value of the new product indicated a significant change in the bonding environment of the P-center, and the disappearance of isomers provided a first hint to a low-coordinate P-center in the product. To examine if the reaction course is similar for the reduction of **24a**,**a'** $Na_2[Fe(CO)_4]$ was added to a slurry of the starting material in THF at -78 °C. Upon warming up, the reaction mixture gradually changed color from yellow-orange to red, but the product was not well soluble in THF, thus creating a red slurry. This red precipitate was filtered from the

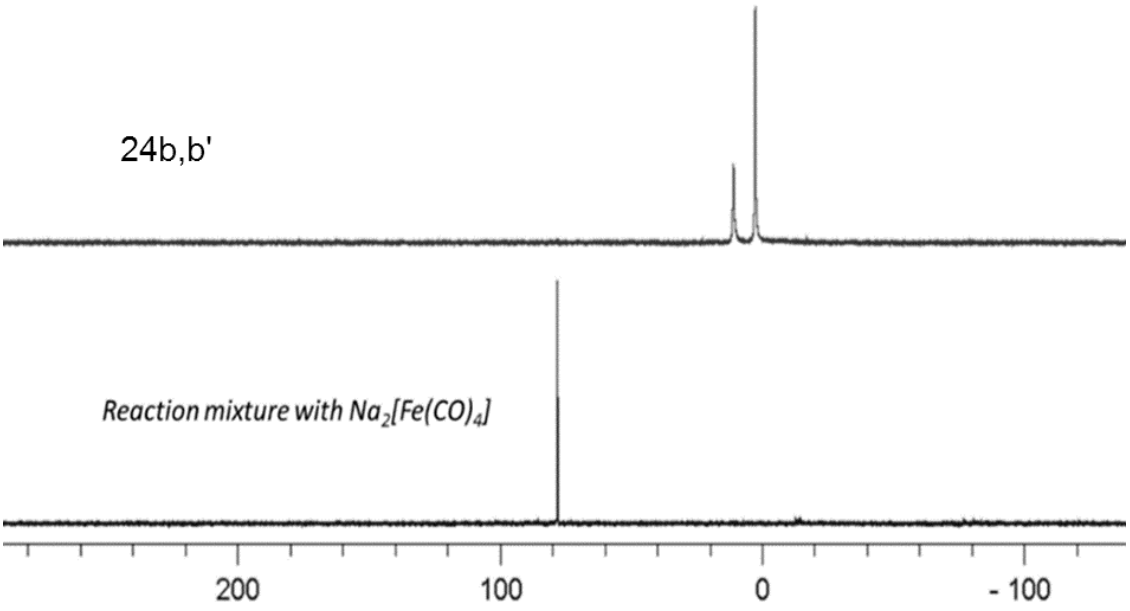

Figure 54: Reduction of compound **24b,b'** using $Na_2[Fe(CO)_4]$.

reaction mixture and washed several times with THF, to remove any impurities. On the other hand in case of reduction of **24b,b'** the reaction resulted in a clean red solution. The presence of *N*-butyl groups enabled the isolation of a red solid by means of filtration (through a silica bed) with *n*-pentane (in ~ 25 % yield, the low yield was due to the problem in separation of the red compound from metal components) which allowed for the full characterization applying all standard analytical methods.

In the ^{1}H NMR spectrum ($CDCl_3$) the solution of the red precipitate showed only a singlet resonance signal at 4.0 ppm indicating a highly symmetrical structure, excluding any P-substituent. The EI-MS spectrum showed a base peak at m/z 313.9 which can be attributed to a cation with the composition of $C_{10}H_{12}N_4P_2S_2$. The HRMS experiment showed an experimental exact mass of 313.9976 (cal. 313.9979) which also does match with the aforementioned chemical composition.

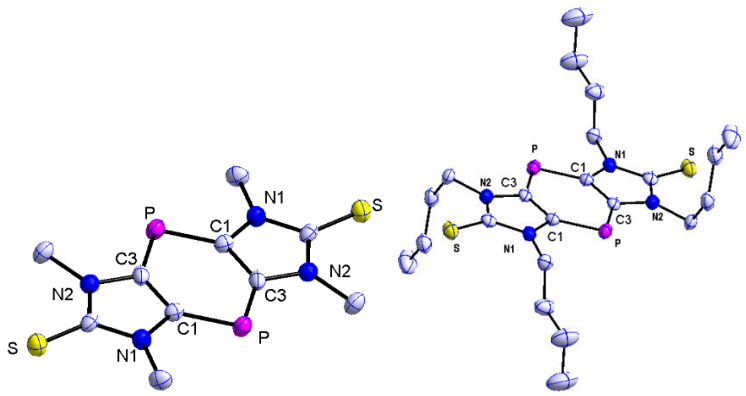

Figure 55: Diamond plot of the molecular structure of compound **33a,b**. (atomic displacement parameters set at 50% probability level); hydrogen atoms are omitted for clarity. Selected bond distances (Å) and angles (°): for **33a**:P-C(1) = 1.755(5), P-C(3) = 1.731(6), C(1)-C(3) = 1.409(7), C(1)-P-C(3) = 97.6(2); for **33b**: P-C1 1.741(3), P–C3 1.741(3), C1-C3 1.400(4), C1-P-C3 97.14(15).

Combining all these experimental data the red powder was tentatively assigned to the tricyclic 1,4-diphosphinine **33a** which was then finally confirmed by the results of an X-ray crystallographic measurement using single crystals grown from a saturated dichloromethane solution at 8 °C. Compound **33a** crystallized in the monoclinic crystal system with the $P2_1/c$ space group (Figure 55). Similarly, single crystal of compound **33b** could be grown by slow evaporation of saturated *n*-pentane solution at 8 °C (Figure 55 right). **33b** crystallized in the monoclinic crystal system with the $P2_1/n$ space group. Investigation of the metrical molecular parameters revealed similar bond lengths and angles for the six-membered ring compared to literature reported phosphinines. For example, the P-C(1) bond distance for compound **33a** was found to be 1.755(5) Å, which is close to

that of 2,4,6-triphenylphosphinine[47, 84] (1.758 Å) (Figure 57). The C(1)-C(3) bond distance in compound **33a** (1.409 Å) is also in good accordance with that in benzene (1.397 Å).[85] This coherence in the bonding parameters indicated a significant extent of aromaticity in the 1,4-diphosphinine. Further aspects of the solid state structure of **33a** is discussed later in this chapter (see Figures 58,59).

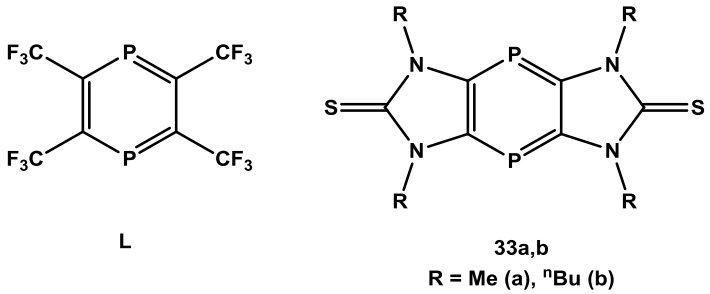

Figure 56: Literature known 1,4-diphosphinine **L** and imidazole-2-thione-based new 1,4-diphosphinines **33a,b**.

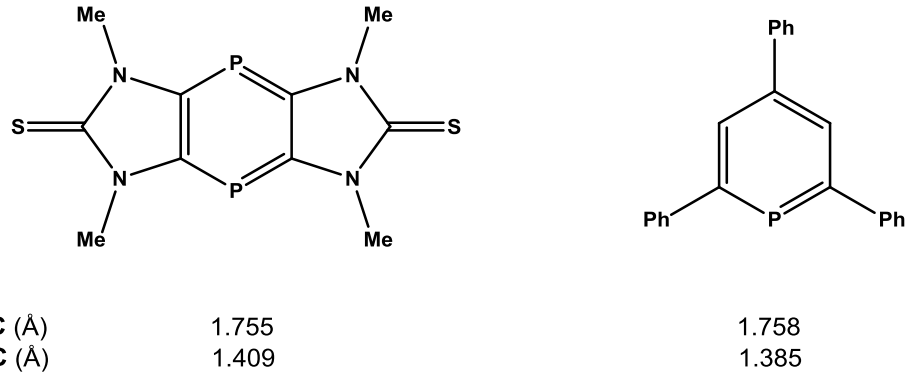

Figure 57: Comparison of endocyclic metrical parameters of **33a** and 2,4,6-triphenylphosphinine .

A special structural feature of compound **33b** was that the *n*-butyl groups of a given imidazole-2-thione unit are pairwise *trans* oriented due to dispersive interactions with the next molecules which indicate the presence of effective dispersive interactions between the alkyl chains.[86] The structures of both 1,4-diphosphinines **34a,b** showed planar tricyclic arrays with a center of inversion in the mid-point of the central ring. Their packing structures exhibited a laminar arrangement with interplanar distances of 3.56 Å (**33a**, from centroid of ring-**3** of plane-**A** to centroid of ring-**2** of plane-**B**) and 3.53 Å (**33b,** same as before) indicating effective π–π interaction (Figure 58).

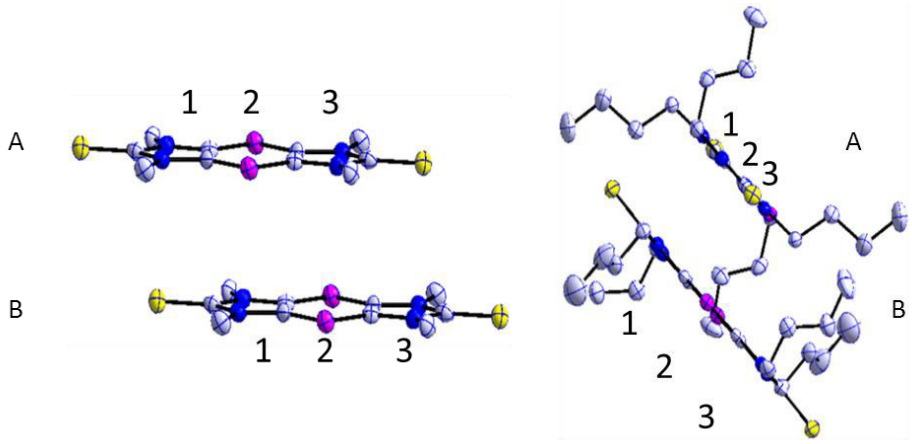

Figure 58: Packing diagrams of compounds **33a** (left) and **33b** (right). Solvent molecules and hydrogen atoms are omitted for clarity.

7.3 Optimization of the synthesis of tricyclic 1,4-diphosphinines 33

The synthetic route to the tricyclic 1,4-diphosphinines via reduction of the corresponding *P,P'*-dichloro compounds **24a,a'-b,b'** with $Na_2[Fe(CO)_4]$ furnished access to **33**, but only in low yields as the major problem to separate the metal-containing product(s) from **33** could not be solved satisfactorily. This problem was even more prominent in the case of the *N*-^{n}Bu derivative (**33b**) and resulted in low yield. As the low yield synthesis of compound **33b** was a serious hurdle for the development of the 1,4-diphosphinine chemistry, a new, improved synthetic protocol was needed.

An important observation was garnered from the $^{31}P\{^{1}H\}$ NMR spectrum of compound **24b,b'** in $CDCl_3$, where it showed two singlet resonance signals at 2.6 and 10.9 ppm respectively for its two stereoisomers and it did not show any color change, at least within the time needed for characterization. But when the compound **24b,b'** was dissolved in THF and a $^{31}P\{^{1}H\}$ NMR spectrum measured, it revealed a slow decomposition at room temperature which came together with a change in color of the solution from yellow-orange to red. If the spectrum was recorded immediately after dissolving **24b** in THF, there was no visible decomposition and no change of color (Figure 59 A). But keeping the solution at room temperature for 1h caused the color of the solution to turn dark red and the $^{31}P\{^{1}H\}$ NMR spectrum showed a new resonance signal at 78.1 ppm (11%) for the tricyclic 1,4-diphosphinine **33b**. The amount of **33b** in the mixture increased with heating to 65 °C (Figure 59 C and D). This spectroscopically monitored decomposition also revealed that one of

the isomers is being preferably converted to the 1,4-diphosphinine **33b**. The first conclusion was that the dichloro derivative **24b,b'** is losing two Cl atoms in an unknown pathway and got converted

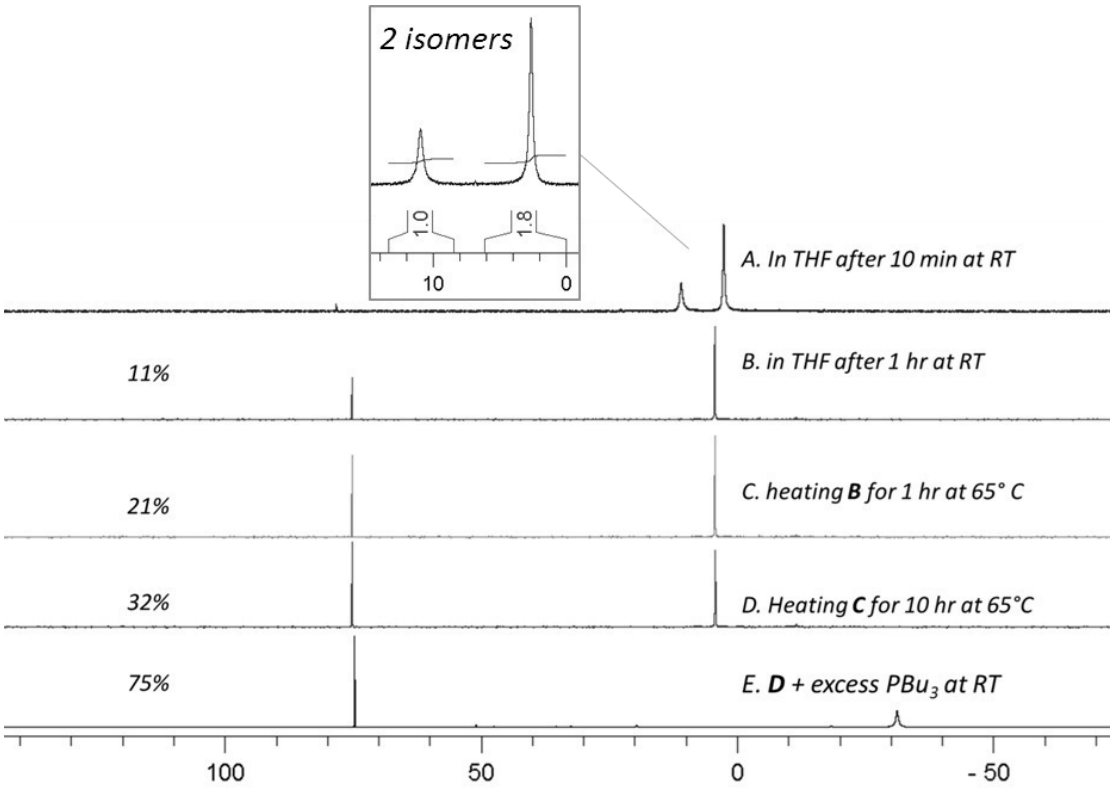

Figure 59: $^{31}P\{^{1}H\}$ NMR monitoring of compound **24b,b'** in THF.

into the 1,4-diphosphinine. In order to achieve a selective reduction the idea of using an electron-rich trialkyl phosphane was considered, as it is well known that oxidation with elemental halogens

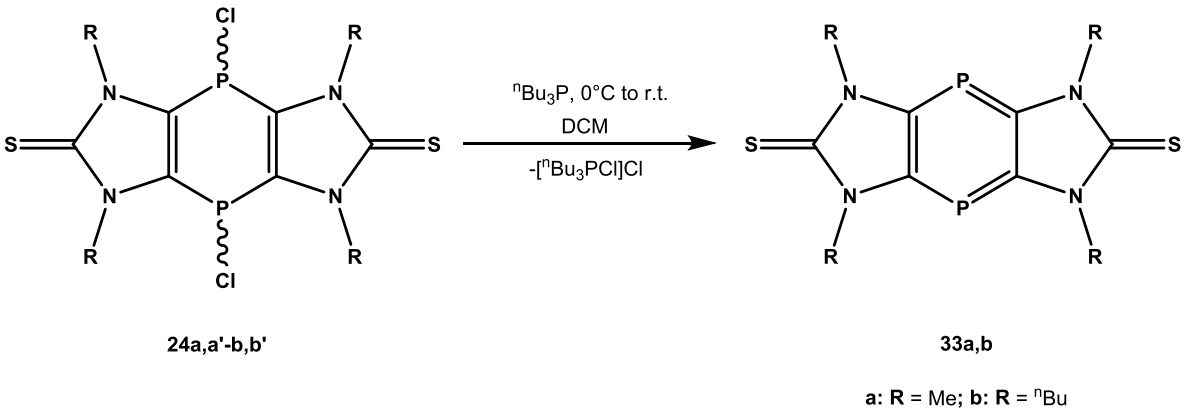

Scheme 40: Optimized protocol for the synthesis of tricyclic 1,4-diphosphinines **34a,b**.

such as chlorine occurs easily and produces the corresponding chlorophosphonium chloride salts. A first attempt of using a THF solution of **24b,b'** and $^{n}Bu_3P$ at room temperature was only partly successful. Immediately after the addition of the phosphane, the color of the solution turned blood-red but no chlorophosphonium chloride was observed in the $^{31}P\{^{1}H\}$ NMR spectrum of the reaction mixture besides the 1,4-diphosphinine **33b** (Figure 59 E).

The synthesis of the 1,4-diphosphinines could be optimized, if the reduction with $^{n}Bu_3P$ was performed in dichloromethane at 0 °C (Scheme 40). The $^{31}P\{^{1}H\}$ NMR spectrum not only showed a clean conversion, but also a resonance signal at 104.6 ppm that was assigned to the known chloro-phosphonium chloride $[Bu_3PCl]Cl$[87]. The final product **33b** was easily isolated in good yields (58 %) by a simple filtration of the reaction mixture through a silica bed using diethyl ether as solvent. The chlorophosphonium salt stayed on top of the silica column due to its high polarity and limited solubility in diethylether.

Taking advantage of this new protocol, the synthesis of the N-Me derivative **33a** was achieved taking a dichloromethane suspension (yellow-orange) of the *P,P'*-dichloro compound **24a,a'** and adding $^{n}Bu_3P$ at 0 °C. Here, also the color of the suspension changed to red and got darker with time but due to the limited solubility of the starting material **24a,a'** the progress of the reaction was much slower and the reaction took 12 hours to reach completion. With progress of the reaction a red precipitate of the final product (**33a**) formed which was in agreement with since later findings as **33a** was found to be almost insoluble in most organic solvents such as THF, dichloromethane, diethyl ether etc. After filtration, the precipitate was washed a few times with dichloromethane, and compound **33a** was isolated in 65 % yield.

7.4 Further insight into the properties of the tricyclic 1,4-diphosphinines

After having the tricyclic 1,4-diphosphinines **33a,b** isolated in good yield, both compounds were investigated by UV/vis spectroscopy and cyclic voltammetry and, additionally, by theoretical calculations of the aromaticity and the bonding situation including frontier orbitals

7.4.1 Theoretical investigations on the aromaticity of tricyclic 1,4-diphosphinines

Detailed theoretical studies on these 1,4-diphosphinines were carried out by Nyulaszi and co-workers using the Gaussian 09 suite of programs.[88] Geometry optimization was carried out at the

M06-2X/6-31+G* level of theory,[89] followed by subsequent calculations of the second derivatives at the optimized structures, which turned out to be real minima on the potential energy surface. This level of theory was also used for the GIAO calculations to obtain NICS values, and for calculation of the reference molecules of the isodesmic reactions, and also for cationic and anionic states, which were also geometry optimized. All the theoretical investigations were carried out on the *N*-Me derivative or compound **33a**, simply for the sake of faster calculations.

The HOMO of compound **33a** was fund to be rather high in energy (-5.80 eV), and as the antibonding combination of the HOMOs of the two imidazole-2-thione fragments (Figure 60). Furthermore, this orbital combination also matched with the HOMO-2 orbital of the parent (unsubstituted) 1,4-diphosphinine. As the imidazole-2-thione HOMO, responsible for the ylidic character of the C=S bond, is of rather high energy, the significant increase of the energy level of the HOMO in **33a** was quite reasonable.

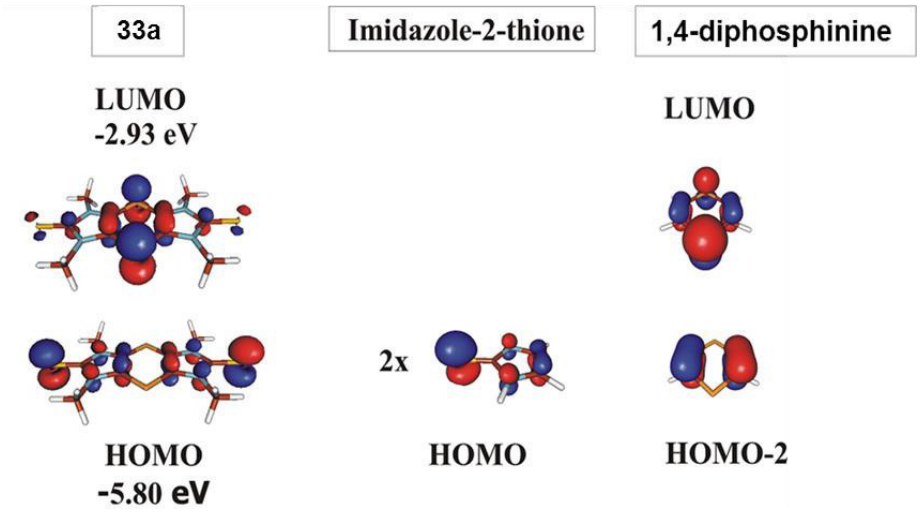

Figure 60: The Kohn-Sham HOMO (bottom) and LUMO (top) of 33a as combination of the orbitals of imidazole-2-thione and 1,4-diphosphinine.

The LUMO of compound **33a** was rather low lying (-2.93 eV) and largely stabilized due to the involvement of the $\pi^*_{P=C}$ orbitals.[90] This orbital encompassed with the lowest π^* orbital of the diphosphinine unit (at -2.54 eV). The LUMO of compound **33a** was even more stabilized compared to the LUMO of parent unsubstituted 1,4-diphosphinines, due to the greater delocalization in the former. Altogether, this high lying HOMO and low lying LUMO resulted in small HOMO-LUMO gap which makes the excitation energy to be small that in turn is also in complete agreement with the observed red color of compound **33a**.

To understand the electronic structure of compound **33a** in more detail, M06-2X/6-311+G** calculations considering also dispersion interactions at the bulky substituents were carried out. The theoretically optimized structural parameters were revealed to be similar to those experimentally obtained, where the closed-shell wave function turned out to be stable with a 44.7 kcal/mol singlet-triplet gap. The structurally indicated aromaticity of the six-membered 1,4-diphosphinine ring in **33a** was further evidenced by the –9.5 ppm NICS(1)[91] value which was in good agreement with the value of the parent 1,4-diphosphinine (-9.4 ppm). The NICS(1) value in the imidazole-2-thione unit for compound 34a was calculated to be -6.8 ppm, in good agreement with the value of -7.5 ppm obtained for imidazole-2-thione itself (at the B3LYP/6-311+G* level -6.0 ppm was reported[92]). The 22.2 kcal/mol ISE (isomeric stabilization energy – Scheme 41) of the parent 1,4-diphosphinine was 75% of the benzene value[93] in agreement with previous conclusions based on ASE studies.[94]

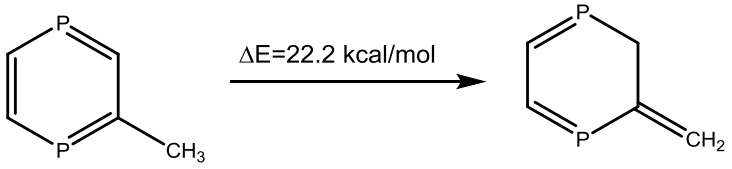

Scheme 41: M06-2X/6-311+G** Isomeric Stabilization Energy (ISE) for the parent 1,4-diphosphinine.[93, 95]

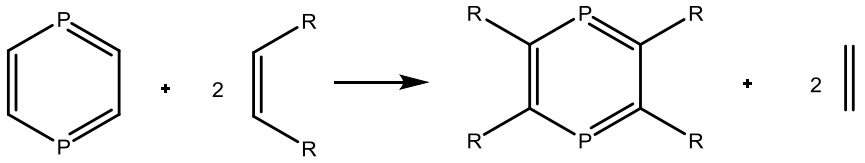

Table 14: M06-2X/6-311+G** isodesmic reaction energies ΔE (kcal/mol) to investigate the effect of the substituents on parent unsubstituted 1,4-diphosphinine, and NICS(1).[95]

	ΔE	NICS(1)
R,R: -N-C(=S)-N-	-2.2	- 8.7
R: -F	8.1	- 9.4
R: $-CF_3$	17.8	-10.5
R: $-CH_3$	2.3	- 9.4
R: $-NH_2$	-1.2	- 8.6
R: $-SiH_3$	0.1	- 8.8

It is noteworthy that compound **33a** appeared to be highly aromatic despite the low HOMO-LUMO gap. Further studies on the effect of the substituents by isodesmic reactions (see Table 14) concluded that the stabilizing effect of the substitution at the ring carbon atoms to be only minor, including the thiourea substitution in **33a**, with the noteworthy exception of the CF_3 substituted compound **L**, which is significantly destabilized by comparison.

7.4.2 UV/vis spectroscopy

The intense red color of these tricyclic 1,4-diphosphinines **33a,b** prompted the necessity of UV/vis spectroscopic investigations to examine the type and strengths of transitions responsible for the color of these compounds; this was then combined with results from TD-DFT studies. The UV/vis spectra for both compounds were taken in dichloromethane solutions at room temperature by taking dilute solutions (concentration ~ 10^{-5} molar) into air-tight and sealed quartz cells.

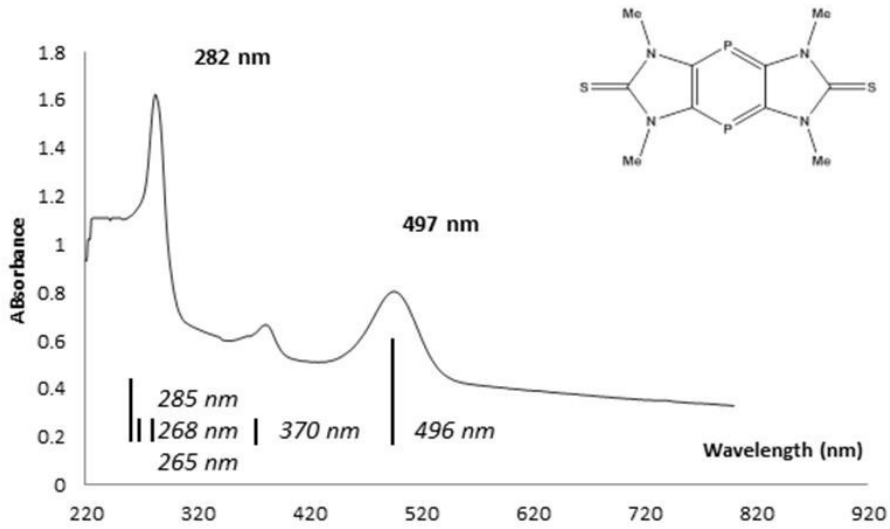

Figure 61: The UV/vis spectrum of **33a** in dichloromethane with the TD-DFT B3LYP/6-311+G**(PCM = dichloromethane)//M06-2X/6-311+G** calculated vertical excitation energies (numbers given in italics) as vertical lines (the length of the vertical lines indicates the calculated oscillatory strength).

The UV/vis-spectra of 1,4-diphosphinines **33a,b** showed a strong absorption (λ_{max} = 497 nm for **33a**, 498 nm for **33b**), which has an excellent numerical agreement with the B3LYP/6-311+G**(PCM:DCM) TD-DFT results for **33a** (Figure 61). [19] While the numerical agreement is somewhat worse at the M06-2X/6-311+G** level (accordingly, for the discussion of the orbital energies we use the B3LYP/6-311+G**(PCM:DCM) values), the intense band corresponds at each investigated level to the HOMO(π)-LUMO(π^*) excitation.

7.4.3 Cyclic voltammetric measurements

The redox behavior of the 1,4-diphosphinines **33a,b** is of great interest due to their rigid, π-electron conjugated tricyclic ring system.[96] To get insight electrochemical studies on these tricyclic 1,4-diphosphinines were carried out in collaboration with Sasamori. Due to the limited solubility of compound **33a** in all common solvents we focused on the *N*-^{n}Bu derivative **33b** in all electrochemical studies.

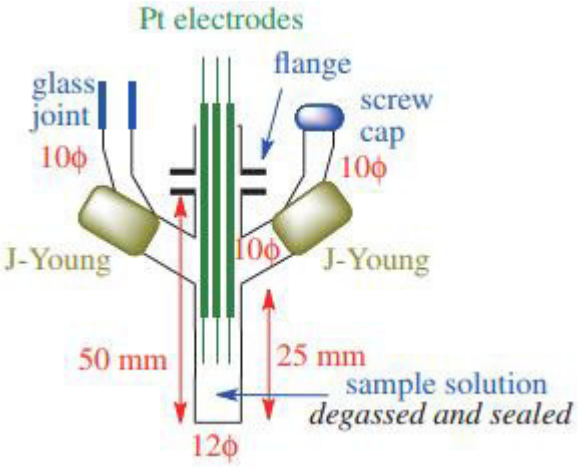

Figure 62: Custom-tailored glassware for electrochemical measurements of reactive species.[97]

The custom-tailored glassware for the electrochemical measurements for 1,4-diphosphinine **33b** was prepared using THF solutions of **33b** in a glass bottle equipped with three Pt electrodes, *i.e.*, the working, reference and counter electrodes (Figure 62).[97] The electrochemical experiments used scan rates of 10–500 mVs^{-1} at r.t. under Ar atmosphere, using ferrocene/ferrocenium hexafluorophosphate as internal/external reference to determine the potentials. Sample solutions (THF) were 3 mM in analyte and 0.1 M in [*n*-Bu_4N]PF_6 as the supporting electrolyte. The redox behavior of **33b** was studied using cyclic and differential potential voltammetry experiments (CV and DPV). In the oxidation region (Figure 64), **33b** showed two irreversible oxidation steps at E_{pa} = –0.61, –0.34 V as determined by DPV measurements. This easy oxidation could be attributed to the high energy of the HOMO of **33a**. The M06-2X/6-31+G* calculations predicted accordingly a rather low (7.24 eV) first ionization energy for **33a**.

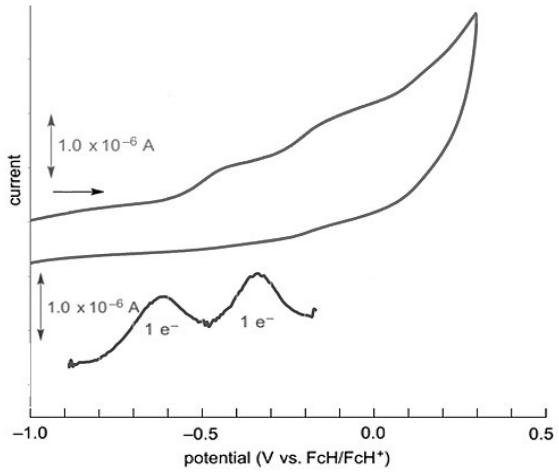

Figure 63: Oxidation region: E1/21 = –0.61 V, E1/22 = –0.34 V (vs. FcH/FcH+) (determined on the basis of DPV measurements).

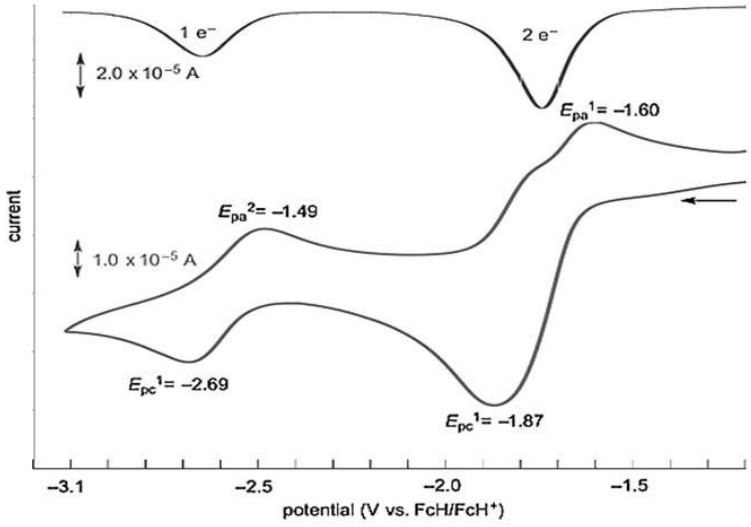

Figure 64: Reduction region: E1/21 = –1.74 V, E1/22 = –2.59 V (vs. FcH/FcH+) (determined on the basis of DPV measurements

The formation of the **33a** dication needs, however, significantly higher energy (18.50 eV),[98] accordingly the observed second oxidation wave should be attributed to a different process: **33a**$^{+\cdot}$ $[C_{10}H_{12}N_4P_2S_2]^{+\cdot}$ forms an adduct (formed as a dimer due to π-stacking interaction) with **33a** itself (and also with THF). Due to this stabilizing interaction the ionization energy is reduced to 6.92 eV, the 0.3 eV difference matching favorably with the 0.27 V difference between the two oxidation waves.

Conversely, **33b** showed two-steps of pseudo-reversible redox waves (Figure 63) in the reduction region. The first step of reduction was found to be a 2e-reduction (!) at $E_{1/2}$ = –1.74 V and a 1e reduction at $E_{1/2}$ = –2.59 V (vs. FcH/FcH$^+$) in the second step. The M06-2X/6-31+G* calculated relative energies showed the stability of the first radical anionic state having[99] an electron affinity 1.9 eV! This is a consequence of the involvement of the low lying π*(P=C) orbitals.[100] Even the calculated Gibbs free energy of the dianion of **5a** is only 0.1 eV, showing the exceptional stability of this species, despite the anti-aromaticity of the central dihosphinine ring (NICS(1): + 8.6 ppm), in full accordance with the Hückel rule![101] Clearly, the mono anionic state cannot be accessed, since the dianion is formed preferentially. It is noteworthy that for 2,4,6-^{t}Bu-1,3,5-triphosphinine a -1.94 V (in DME),[102] and -3.245 V (in THF)[103] reduction wave was reported, indicating that **33a** has a comparable electron affinity to the former one.

Chapter 8

8. Reactivity studies on tricyclic 1,4-diphosphinines

Although phosphinines[47] and 1,4-diphosphinines[61] were first synthesized within one decade, the development of their chemistry showed significant divergences. While the chemistry of phosphinines[104] are richly developed,[105] only a handful of reactions have been reported for the 1,4-diphosphinine derivative **L** as mentioned in the introduction (see Scheme 13). The main reason behind this poorly developed chemistry might be the low stability of **L** and the absence of a facile synthetic protocol.

As reactivity studies are sparse, the newly synthesized tricyclic 1,4-diphosphinines **33a,b** were tested in various reactions: [4+2]-cycloaddition, 1,4-addition reactions, oxidative hydrolysis and others.

8.1 [4+2]-cycloaddition reactions: access to tricyclic 1,4-diphosphabarrelenes

The use of (mono-)phosphinines in [4+2]-cycloaddition reactions are well known since 1968, when Märkl and co-workers synthesized the first example of phosphabarrelene by reacting a phosphinine with alkyne derivatives.[106] They showed that phosphinines, specially the 2,4,6-tri-substituted derivative, are rather weak dienes, and the first example **LXV** were obtained only with a highly reactive, electron-poor dienophiles such as hexafluoro-2-butyne and DMAD (Figure 65). Later on more examples of such phosphabarrelenes were garnered from [4+2]-cycloaddition of phosphinines and arynes.[107] Since the first discovery of phosphabarrelenes, their chemistry has become highly rich and nowadays it is important as a ligand in Rh-catalyzed hydroformylation[108,

109] and hydrogenation[110] of alkenes. Bidentate phosphabarrelenes based P,S ligands[111] were also found to be highly effective in Pd-catalyzed Suzuki-Miyaura cross coupling by Le Floch and co-workers.[112] Recently, a Rh-catalyzed one-pot tandem reaction sequence under hydroformylation conditions was developed using phosphabarrelene as the ligand system by Müller and co-workers.[113]

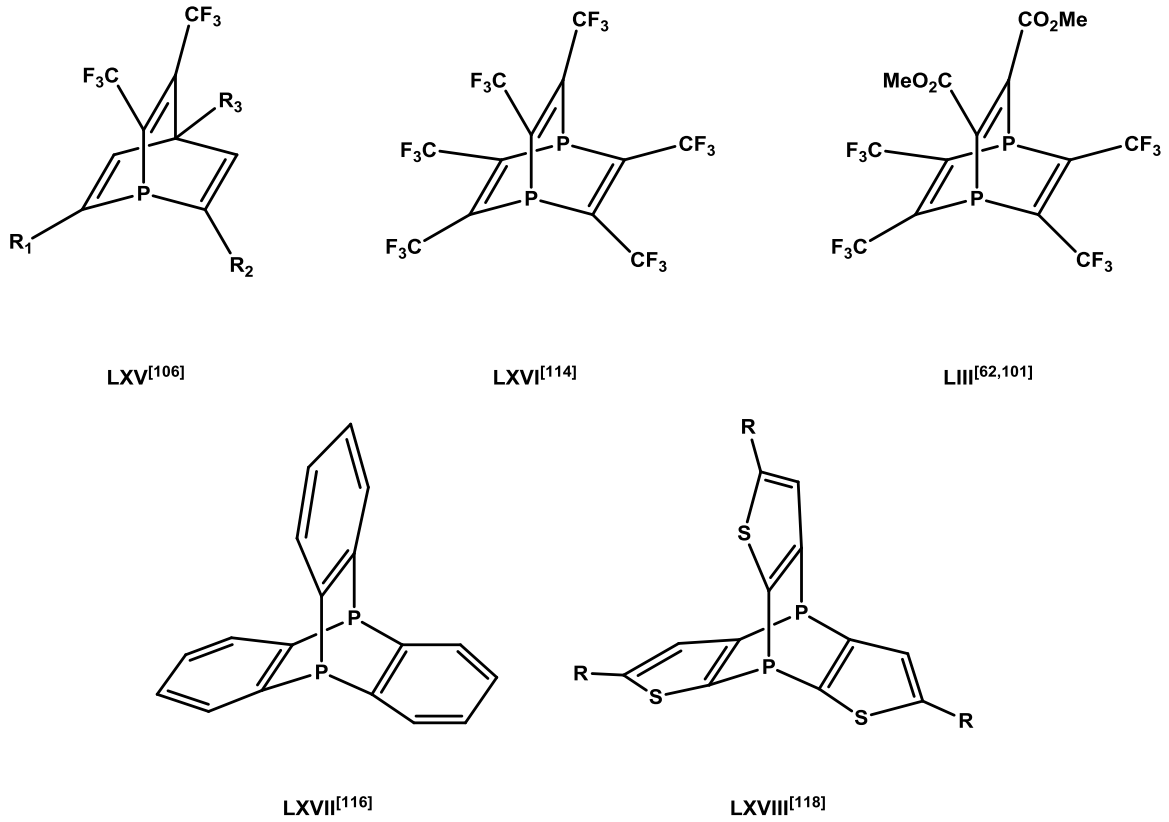

LXV[106] **LXVI**[114] **LIII**[62,101]

LXVII[116] **LXVIII**[118]

Figure 65: Selected examples of phosphabarrelene **LXV**, 1,4-diphosphabarrelenes **LXVI-LXI** and 1,4-diphosphatriptycenes **LXVII-LXIX**.

On the other hand, the first ever example of diphosphabarrelenes was reported back in 1961 by Krespan,[114] where perfluorinated 1,4-diphosphabarrelene **LXVI** was synthesized by iodine catalysed thermolysis of hexafluoro-2-butyne in the presence of red phosphorus. Synthesis of compound **LXVI** requires extreme reaction conditions (heating at 200 °C for 8h under autogenous pressure) and yet the yield is quite moderate (43 %).[114] Though the mechanism of formation of compound **LXVI** was not clear, Märkl suggested the probable intermediacy of tetrakis(trifluoro-methyl)-1,4-diphosphabenzene which would give the final product by [4+2]-cycloaddition with another molecule of hexafluoro-2-butyne. Later on, Kobayashi and co-workers provided firm evidence by synthesizing tetrakis(trifluoromethyl)-1,4-diphosphabenzene **L** from compound

LXVI[61, 115] and reacting it with hexafluoro-2-butyne to get back compound **LXVI**.[61, 64, 115] They also synthesized a variety of 1,4-diphosphabarrelenes from compound **L** as shown beforehand (see Scheme 13).

Apart from these, other derivatives such as diphosphatriptycenes are also known in literature. Although all these are 1,4-diphosphabarrelenes, they were prepared via completely different pathways. Compound **LXVII** was first reported by Weinberg and co-workers in 1971,[116] using thermolysis of *ortho*-dichlorobenzene and white phosphorus in the presence of catalytic amount of $FeCl_3$. This synthetic protocol suffers from the drawback of low yield (20 %) and harsh reaction condition (heating at 280 °C for 4 h). Later on, there have been attempts to synthesize other derivatives of this very 1,4-diphosphatriptycenes by Mazaki and co-workers, but again the yield of these reactions were significantly low (only 9 %).[117] Nakayama and co-workers reported the synthesis of the 4,8-diphosphathiophenetriptycene **LXVIII**,[118] via reaction of tris(thiophene-2-yl)phosphane oxide with trisphenoxyphosphane in the presence of ^{n}BuLi as base. The cyclization in this case requires oxidation of the phosphorus and therefore needs to be reduced back to P^{III} to get access to compound **LXVIII**. The main downside here also is the yield of the reaction, which is only 11% in the cyclization step and gets further low for the necessity of the extra reduction step. Therefore, an easy access to 1,4-diphosphabarrelenes was desirable and, hence, decided to study the reactivity of compound **33** with a series of dienophiles.

8.1.1 Reaction of tricyclic 1,4-diphosphinine 33b with alkynes

Because of the encouraging background, reactivity studies on compound **33b** were started, and the latter chosen due to its high(er) solubility. When compound **33b** was heated at 110 °C with a rather electron-rich alkyne like diphenyl acetylene, no reaction could be observed even after one week. The reaction mixture showed no visible color change (from the red color of the starting material) and no new resonance signal was found in the $^{31}P\{^{1}H\}$ NMR spectrum of the reaction mixture. But when an electron-deficient alkyne such as dimethyl acetylene dicarboxylate (DMAD) was employed at 35-40 °C in toluene (Scheme 42), an immediate reaction was observed, and the color changed from dark red to dark brown and the $^{31}P\{^{1}H\}$ NMR spectrum of the reaction mixture showed a new resonance signal at -87.3 ppm, apart from a complete consumption of **33b**.

A brick red powder could be isolated easily from the reaction mixture in 95 % yield by removing the volatiles under vacuo (8 × 10^{-3} mbar) and washing with *n*-pentane (3 × 3 ml). The chemical shift value (-87.3 ppm) fell well into the range of compound **LXVIII** (-87.1 and -93.4 ppm)[118] indicating the presence of a tricoordinate P-center with three P-C single bonds. Therefore, it was tentatively assigned to the 1,4-diphosphabarrelene derivative **34a**. The ^{1}H and ^{13}C{^{1}H} NMR spectra of this compound also supported this assignment with a spectral splitting pattern that corresponds to a molecule with C_{2v} symmetry. The ^{13}C{^{1}H} NMR spectra showed an extra doublet resonance signal (apart from the peaks of compound **33b**) at 128.6 ppm ($^{1}J_{P,C}$ = 61.2 Hz) which was assigned to the sp^{2}-carbon atoms of the bridging unit, carrying the –CO_2Me groups (166.1 ppm (dd, $^{2}J_{P,C}$ = 16.8 Hz)) and thus showing further evidence for the 1,4-diphosphabarrelene unit. The structural assignment was further supported by mass spectrometry and EA data, e.g., the HRMS spectrum showed the exact mass value of the molecular ion of **34a** (m/z 624.2123).

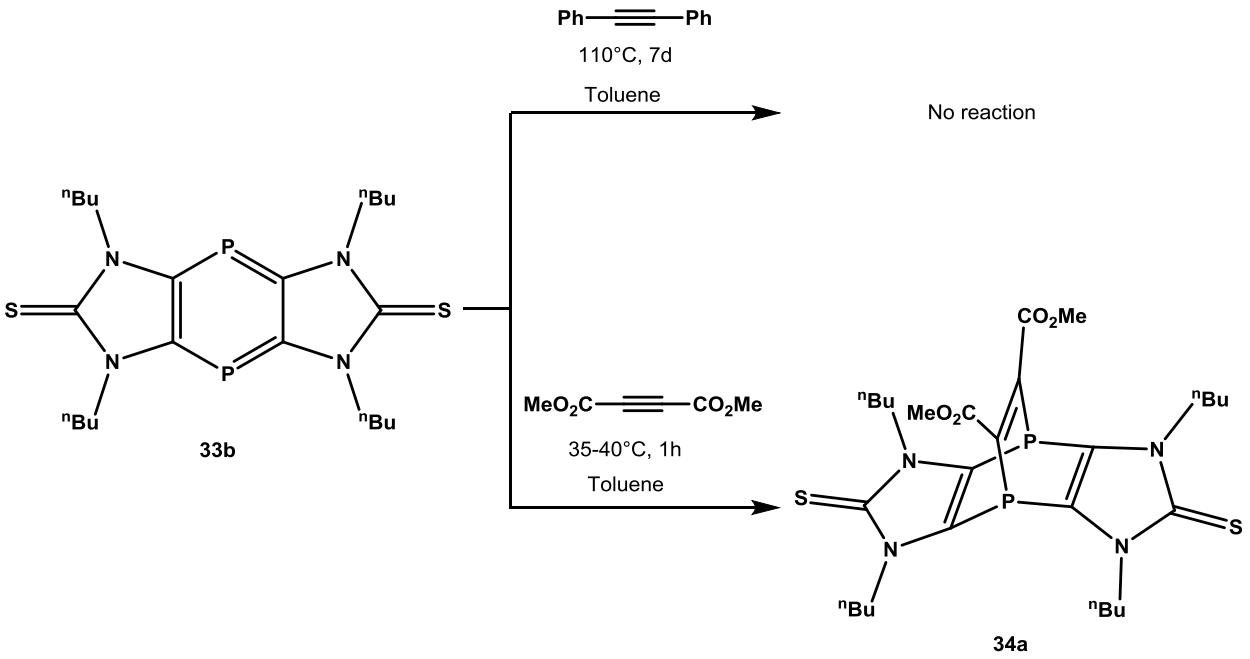

Scheme 42: Reaction of tricyclic 1,4-diphosphinine **33b** with DMAD to give **34a**.

8.1.2 Reaction of tricyclic 1,4-diphosphinine 33b with C=C and N=N double bond systems

After the successful reaction of tricyclic 1,4-diphosphinine **33b** with DMAD, it was decided to try reactions with a C=C bond and N=N double bond systems. For this purpose, *N*-phenylmaleimide (C=C) and 4-phenyl-1,2,4-triazoline-3,5-dione (N=N) were chosen as dienophiles. Monitoring the

reaction of compound **33b** and N-phenylmaleimide in toluene at ambient temperature (Scheme 43), no reaction was observed in the $^{31}P\{^{1}H\}$ NMR spectrum. But at temperatures beyond 60 °C, a new resonance signal at -86.3 ppm grew in, besides that of **33b** at 78.1 ppm. For a complete and fast consumption the temperature was raised to 110 °C, and after 3h a clean conversion was observed. In case of 4-phenyl-1,2,4-triazoline-3,5-dione, the reaction was found to be too fast and uncontrolled at room temperature resulting in a poor selectivity. To improve the selectivity, the reaction was carried out at low temperature (-40 °C) in THF as a rather poor solubility of compound **33b** had prevented the use of toluene at low temperature. Under these new reaction conditions, the reaction was rather selective, and a singlet resonance signal at -49.4 ppm (90 %) was observed in the $^{31}P\{^{1}H\}$ NMR spectrum.

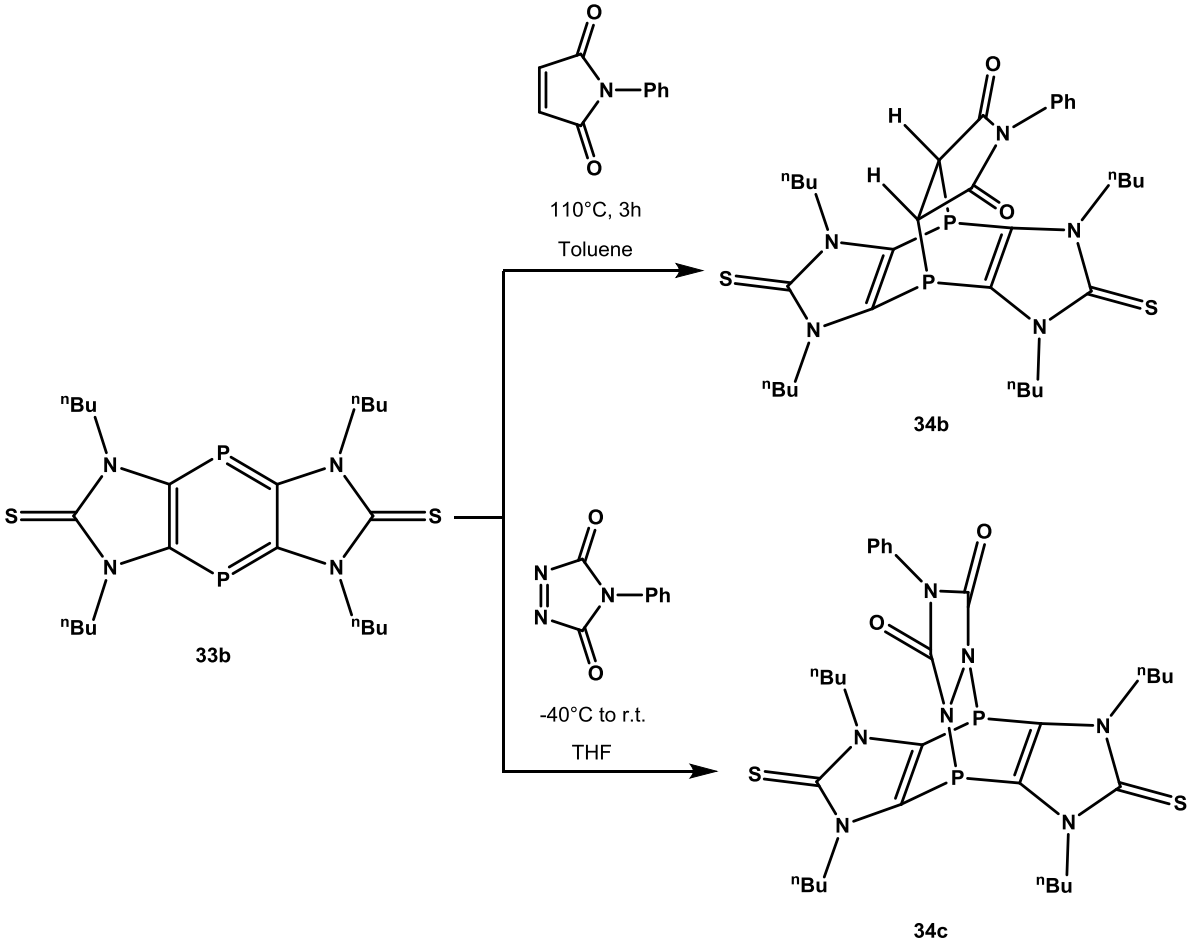

Scheme 43: Reaction of tricyclic 1,4-diphosphinine **33b** with *N*-phenylmaleimide and 4-phenyl-1,2,4-triazoline-3,5-dione.

In case of N-phenylmaleimide, an orange solid was isolated in 90 % yield after evaporation of the solvent under reduced pressure (8×10^{-3} mbar) and washing with *n*-pentane (3 × 3 ml). This orange

solid showed a resonance at -86.3 ppm (in $CDCl_3$), being very similar to that of compound **34a**. The ^1H NMR spectrum also showed a triplet resonance signal at 3.72 ppm ($^3J_{H,H}$ = 4.9 Hz) for the protons of the bridging *P-CH-* fragments referring to the formation of bicycle derivative. Finally, further support came from HRMS and EA data of this orange solid as to be the 7,8-dihydro-1,4-diphosphabarrelene derivative **34b**. In case of 4-phenyl-1,2,4-triazoline-3,5-dione, the reaction mixture was, again, first evaporated to get a yellow residue which upon washing with diethyl ether (3 × 3 ml) furnished pure **34c** in 65 % yield. Compound **34c**, the diazo analogue of **34b**, showed a resonance value of -49.4 ppm in the $^{31}P\{^1H\}$ NMR spectrum ($CDCl_3$) which was significantly lowfield-shifted compared to both **34a,b**. This (relative) low field resonance of compound **34c** is obviously due to the nature of the bridging atoms, thus resulting in an electron-withdrawing effect due to the higher electronegativity of the nitrogen N-atoms. Firm evidence for the formation of these [4+2]-cycloaddition products were obtained from the X-ray crystallographic measurement, for which the single crystals were grown from a saturated dichloromethane solution at -20 °C. The X-ray measurement revealed that compound **34b** crystallizes in the monoclinic crystal system with the C2/c space group (Figure 66).

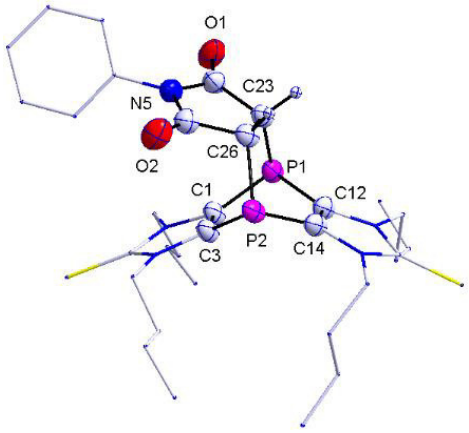

Figure 66: Diamond plot of the molecular structure of compound **34b**. (atomic displacement para-meters set at 50% probability level); hydrogen atoms are omitted for clarity (except those in the bridging carbons). Selected bond distances (Å) and angles (°): P(1)-C(23) = 1.8973(1), P(1)-C(1) = 1.8263(1), C(1)-C(3) 1.3627(1); C(1)-P(1)-C(23) 94.874(2), P(1)-C(1)-C(3) 123.233(3).

The P(1)-C(23) bond length appeared to be significantly longer [1.8973(1) Å] compared to P(1)-C(1) [1.8263(1) Å], which perfectly reflect the different hybridization of C(1) as sp^2 and C(23) as sp^3. Furthermore the P(1)-C(1) bond length fell well into the range of P-C bonds of the 1,4-diphospha-triptycene derivative **LXVII** [1.8399(6) Å].[116] The bond angles revealed a strong pyramidalization at the both P-centers [(Σ∢ P = 284°) compared to that of PPh_3 (Σ∢ P = 308°)]. The extent of this pyramidalization was in good agreement with the amount of pyramidalization for 2,4,6-

triphenyl[7,8]benzo-phospha-bicyclo[2.2.2]octa-2,5,7-triene (283°), reported by Breit and co-workers.[108] This higher extent of pyramidalization should result in higher s-character of the P-lone pairs, which in turn should make **34b** a weaker σ-donor compared to a strain-free phosphane,[119] The latter is of interest for the P-donating ability of these new diphosphabarrelenes.

8.1.3 Theoretical insight into [4+2]-cycloaddition reactions

Theoretical investigations were carried out by Nyulaszi and Kelemen[120] to get informations on the relative ease of reactions and relative stability of the [4+2]-cycloaddition adducts, following M06-2X/6-311+G** level of theory. Apart from **34a-c,** the hypothetical products with acetylene and diphenyl acetylene were investigated. The ΔG values of the corresponding final compounds (Table 15) clearly agrees with experimental results and, accordingly, compound **33b** should react with 4-phenyl-1,2,4-triazoline-3,5-dione (-40 °C), leading preferentially to the final product (**34c**). On the other hand, reaction of **33b** with diphenyl acetylene would result in an endergonic reaction.

Table 15: Relative energetics of the [4+2]-cycloaddition reactions.

	C_2H_2 + **33b**	C_2Ph_2 + **33b**	**34a**	**34b**	**34c**
ΔE (kcal/mol)	-18.6	-13.9	-24.6	-21.6	-31.6
ΔG(kcal/mol)	-2.5	5.4	-4.9	-2.3	-12.3

8.2 Thermal reaction of tricyclic 1,4-diphosphinine 33b with dichalcogenides

As it is known that phosphinines can add oxidatively in a 1,1-fashion, the thermal reactivity of compound **33b** towards diaryl dichalcogenides, *e.g*. Ph_2S_2, Ph_2Se_2, Ph_2Te_2 was examined (Scheme 44). Therefore, the tricyclic 1,4-diphosphinine **33b** and 1 molar eq. of Ph_2E_2 was heated in toluene at 110 °C. The progress of the reaction was monitored by $^{31}P\{^1H\}$ NMR spectroscopy (taken every 30 min). In case of Ph_2S_2 and Ph_2Se_2 the color of the reaction mixture slowly started to change from red to yellow-orange and the $^{31}P\{^1H\}$ NMR spectra of the reaction mixture showed new singlet resonance signals at -34.1 ppm (Ph_2S_2) and -44.6 ppm (Ph_2Se_2), respectively. The reaction mixtures were further heated (2d for Ph_2S_2 and 6h for Ph_2Se_2) until complete consumption of the starting material was achieved.

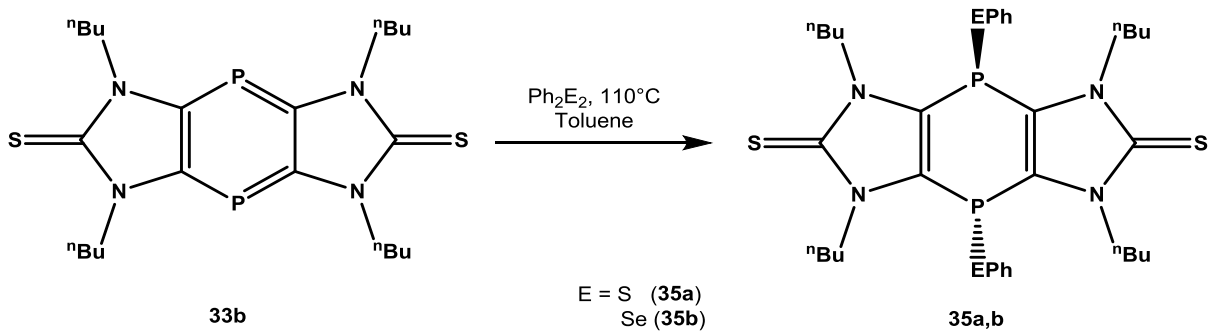

Scheme 44: Thermal 1,4-addition of organic dichalcogenides across the aromatic system of **33b**.

On the contrary, the reaction with Ph_2Te_2 showed no sign of progression even after heating a whole week at 110 °C. The latter might be due to either the lower oxidation potential of Ph_2Te_2 (i) or to the lower stability of the P-Te bond of a transiently formed 1,4-addition product under the given conditions. The major products from the reactions with Ph_2S_2 and Ph_2Se_2, were isolated via removal of the solvents *in vacuo*, and obtained as orange residues. Subsequent washing with diethyl ether and *n*-pentane resulted in yellow powders in 78 % yield (for Ph_2S_2) and 75 % (for Ph_2Se_2) which were used for the full characterization. The $^{31}P\{^1H\}$ NMR spectra showed highfield-shifted singlet resonance signals, as mentioned beforehand, which clearly speak against a 1,1-addition product having a low-coordinate and one a high-coordinate P-center thus resulting in a AB-type spin system (Figure 67). Furthermore, the ^{31}P NMR spectra of these products showed no P-H couplings which indicated that the Ph groups are not directly bound to the P-atom, *i.e.*, eliminating the possibility of a thermal isomerization of the P-EPh into a P(E)Ph fragment. The latter was also supported by the ^1H NMR spectral data supporting the incorporation of two PhE fragment per molecule of **33b**.

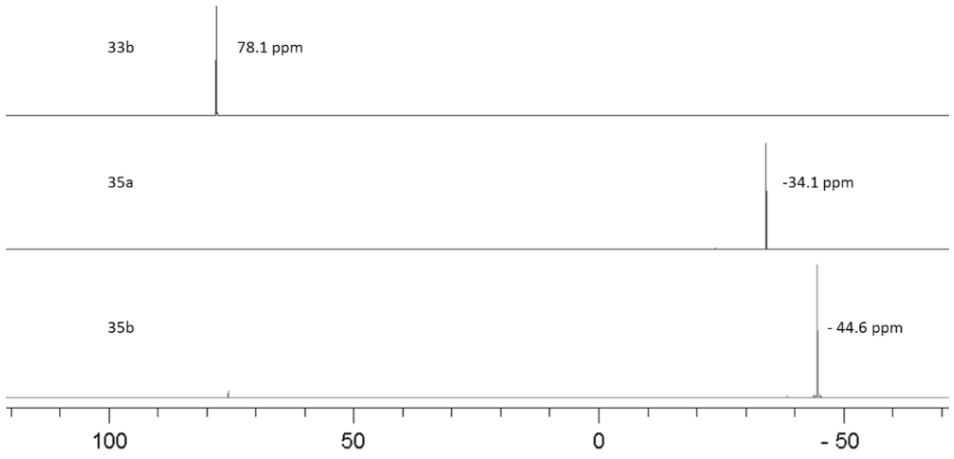

Figure 67: Comparison of $^{31}P\{^{1}H\}$ NMR spectra of compound **33b** with the reaction mixtures for **35a,b**.

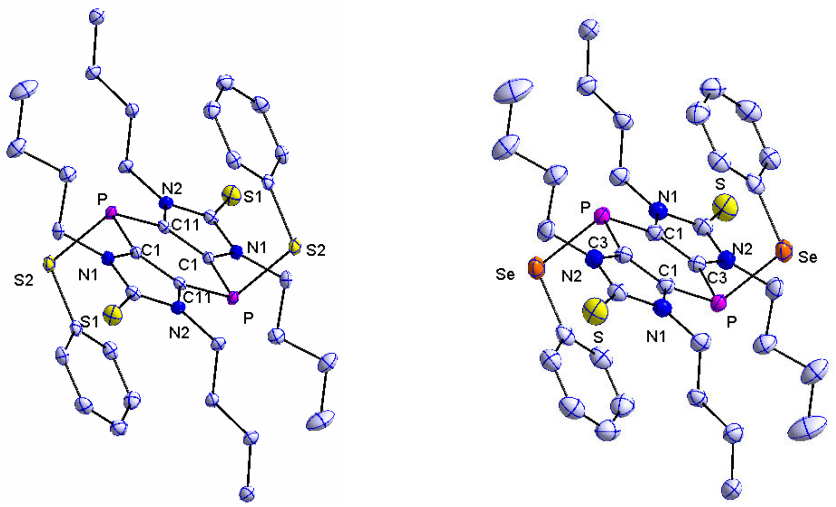

Figure 68: Diamond plot of the molecular structure of compound **35a** (left), **35b** (right); atomic displacement parameters set at 50% probability level and hydrogen atoms are omitted for clarity. Selected bond distances (Å) and angles (°): for **35a**: P-C(1) = 1.8034(1), P-C(11) = 1.7994(2), C(1)-C(11) 1.3691(1), P-S(2) 2.1555(2) ; C(1)-P-C(11) 96.538(7), P-C(1)-C(11) 131.026(9), S(2)-P-C(1) 100.403(7). For **35b**: P-C(1) = 1.7991(1), P-C(3) = 1.7978(2), C(1)-C(3) 1.3632(0), P-Se 2.3003(1) ; C(1)-P-C(3) 96.446(3), P-C(1)-C(3) 132.091(4), Se-P-C(1) 100.993(3).

Finally X-ray crystallographic measurements confirmed these yellow powders as the *P*-thioxy and *P*-selenoxy substituted 1,4-dihydro,1,4-diphosphinines **35a,b**. Single crystals of these compounds could be grown very easily from a saturated solution in dichloromethane at -20 °C. The results of X-ray crystallographic analysis revealed that compound both **35a** and **35b** crystallize in the monoclinic crystal system with the $P2_1/c$ space group (Figure 68). The solid state structures of compound **35a** and **35b** revealed that both compounds prefer to pack in parallel layers. The distance between these layers for **35a** was found to be 1.26 Å whereas that for **35b** was 1.27 Å.

Apart from this parallel packing of the tricyclic heterocyclic part, the phenyl rings and the hydrophobic *n*-butyl chains were also organized in a paired pattern with respect to each other due to dispersive interaction (Figure 69).

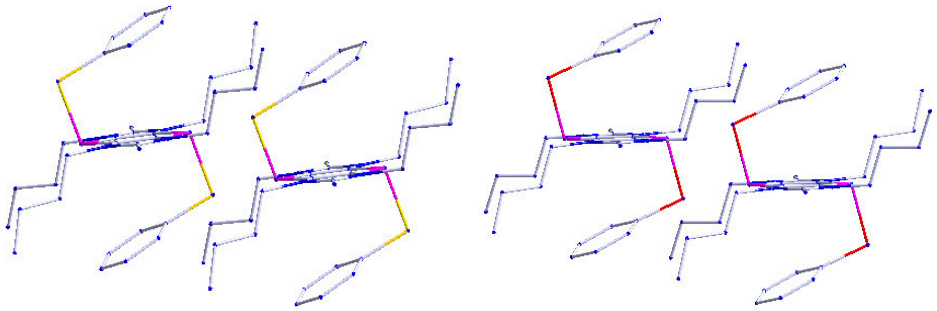

Figure 69: Solid state packing of compound **35a** and **35b**.

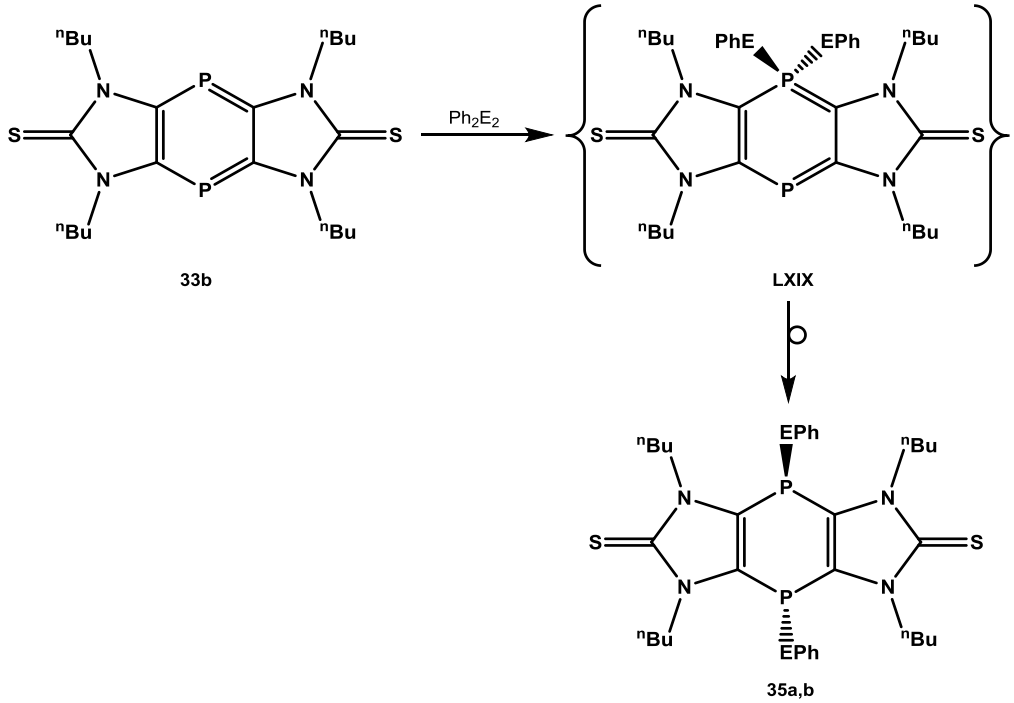

Scheme 45: Plausible pathway for the formation of *trans* **35a,b**.

Another very interesting feature about this reaction was the stereospecificity of the 1,4-addition. In both cases only the *trans* isomer was formed which can be explained by a plausible two step pathway (Scheme 45), but it still remains to be investigated by theoretical calculations. The first possible step would be the 1,1-addition to one P-center – a formal insertion into the E-E bond – to create a transient 1$\sigma^4\lambda^5$,4$\sigma^2\lambda^3$-diphosphinine **LXIX** which then undergoes a 1,4-rearrangement of one EPh group to give the final *trans* products **35a,b** in a stereospecific manner.

8.3 Sequential reactions of 1,4-diphosphinine 33b with nucleophiles and electrophiles

As described in the introductory chapter, phosphinines have their phosphorus lone pair in a less directional and low lying HOMO, and the LUMO has the largest orbital coefficient on the P-center. Therefore, phosphinines are very weak σ-donor and considerably strong π-acceptor ligands, and the P-center significantly electrophilic. The first report came from Märkl and co-workers[121] in 1968

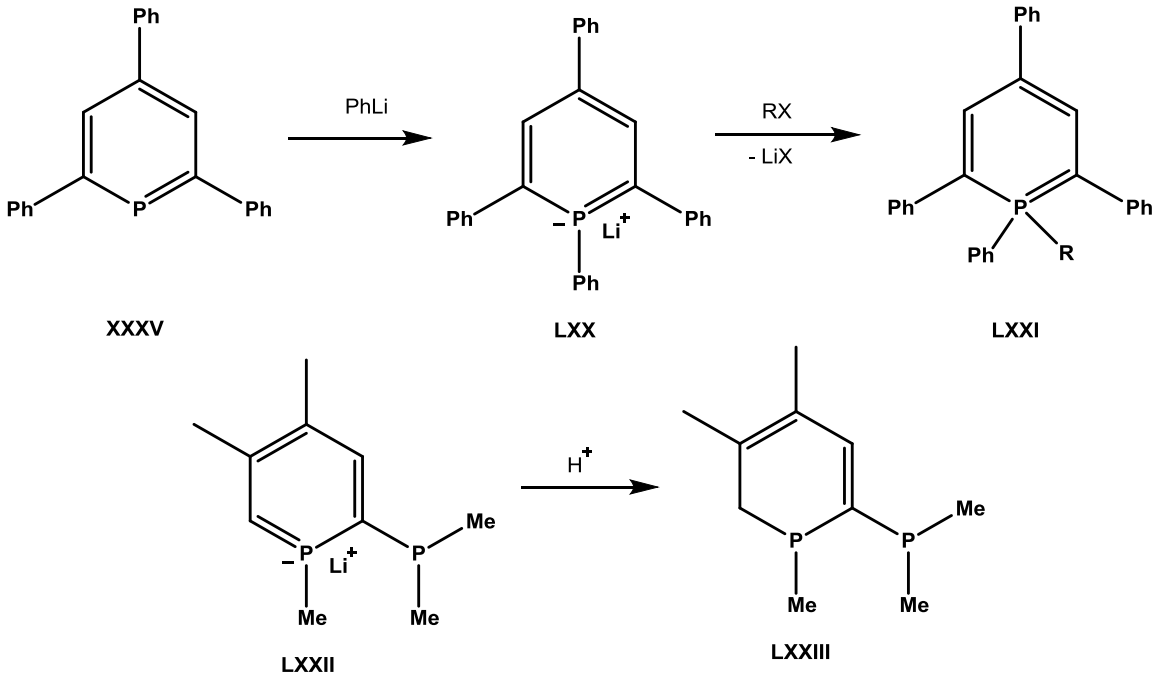

Figure 70: Examples of sequential nucleophilic/electrophilic reactions in phosphinine chemistry.[121, 122]

when 2,4,6-triphenylphosphinine reacted with PhLi to form the 1,2,4,6-tetraphenylphosphinine-ate **LXX** (Figure 70) which could be quenched with electrophiles to access $1\sigma^4\lambda^5$-phosphinines **LXXI**. If the electrophile used for quenching of an intermediate anionic derivative is the proton, then 1,2-substitution can occur as it was observed for the anionic derivative **LXXII** that led to product **LXIII**[122] (Figure 70).

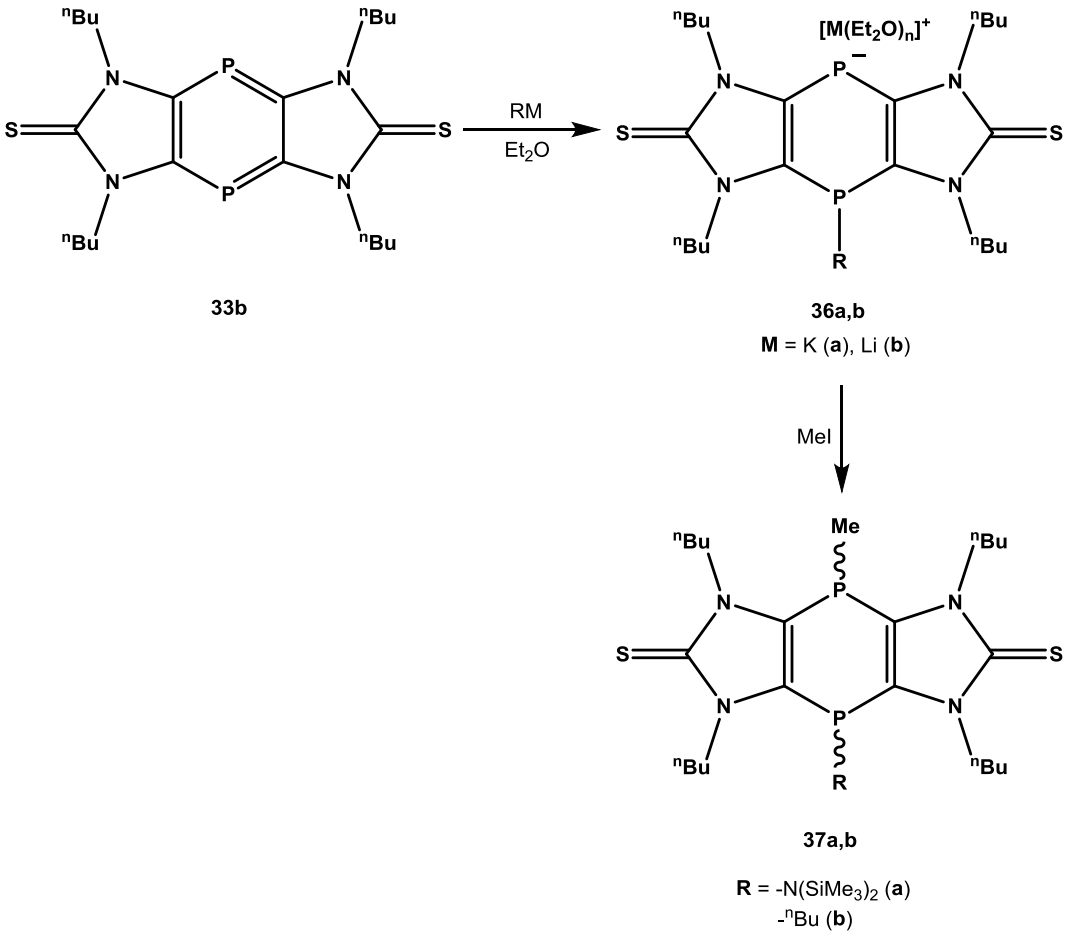

Scheme 46: Reaction of 1,4-diphosphinine **33b** with nucleophiles.

As the Kobayashi 1,4-diphosphinine had not been studied in this regard, the opportunity to investigate this aspect motivated a first study which will be described hereafter. Focusing on the first step, the addition of a nucleophile, compound **33b** was treated with KHMDS or ^{n}BuLi (Scheme 46). When a diethyl ether solution of **33b** was treated with small portions of a KHMDS solution in diethyl ether at room temperature, a drastic color change from dark red to dark purple was observed which then slowly vanished with further addition of the KHMDS solution, to give a bright orange solution, finally. The $^{31}P\{^{1}H\}$ NMR spectrum of the reaction mixture showed two doublets at -12.1 ppm and -76.1 ppm, respectively, with a $^{3}J_{P,P}$ coupling constant magnitude of 5.7 Hz.

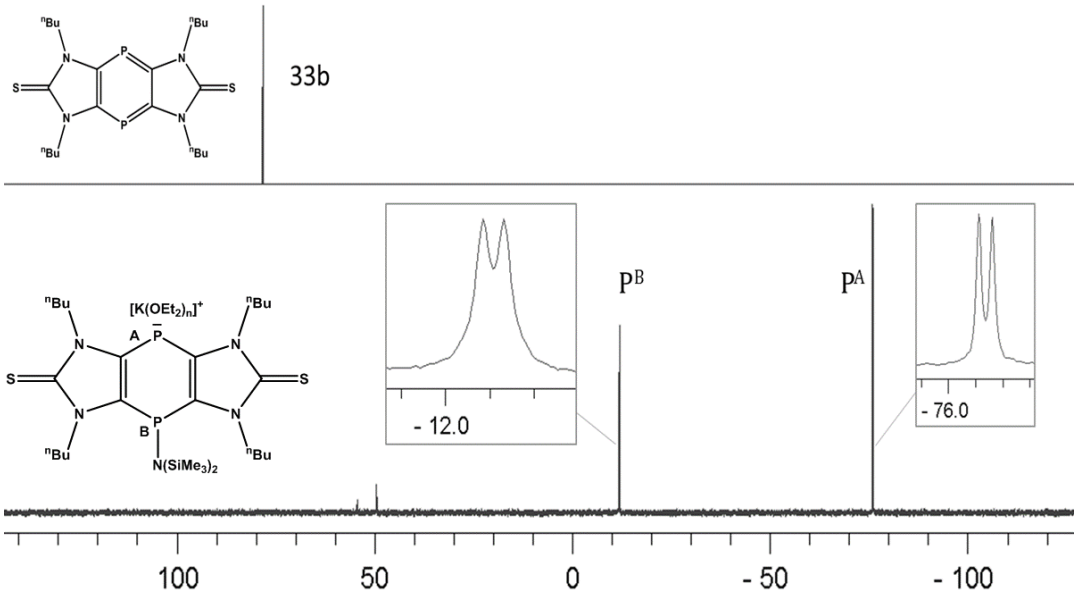

Figure 71: $^{31}P\{^{1}H\}$ NMR spectrum of the reaction mixture of **33b** and KHMDS.

The splitting pattern in the $^{31}P\{^{1}H\}$ NMR spectrum (Figure 71), representing a AB-type spin system, clearly indicated the formation of the anionic adduct **36a** formed via nucleophilic attack of the hexamethyldisilazide anion on the P-center of **33b**. As depicted in Figure 71, the conversion of **33b** into the adduct **36a** was quite selective (up to 90%), but despite this selective reaction, the isolation of **36a** could not be achieved due to a rapid decomposition during workup, *i.e.*, removal of the solvent *in vacuo*, followed by washing with *n*-pentane at room temperature.

In the same manner, when a diethyl ether solution of compound **33b** was treated with 1 molar eq. of ^{n}BuLi at room temperature the color of the solution turned from dark red to bright orange. The $^{31}P\{^{1}H\}$ NMR spectrum of the reaction mixture showed a pair of doublets at -74.3 ppm and -82.5 ppm, respectively, with a $^{3}J_{P,P}$ coupling constant magnitude of 4.1 Hz. The reaction mixture selectivity in this case was lesser compared to the KMHDS reaction and hence no isolation of the anionic intermediate could be achieved. To confirm the nature of the addition products of the anionic derivatives **36a,b** quenching with an electrophile was intended. In a modified protocol, the nucleophile was first added to the diethyl ether solution of compound **33b** at room temperature and then cooled down to -78 °C, before 1 molar eq. of methyl iodide was added. In doing so in both cases (for KHMDS and ^{n}BuLi) the color of the reaction mixture turned from orange to bright yellow. In case of KHMDS, the $^{31}P\{^{1}H\}$ NMR spectrum of the reaction mixture showed a product (**37a**) with

two doublets at -5.1 ppm and -72.4 ppm, respectively, with a $^{3}J_{P,P}$ coupling constant of 16.7 Hz and, hence, the formation of new product.

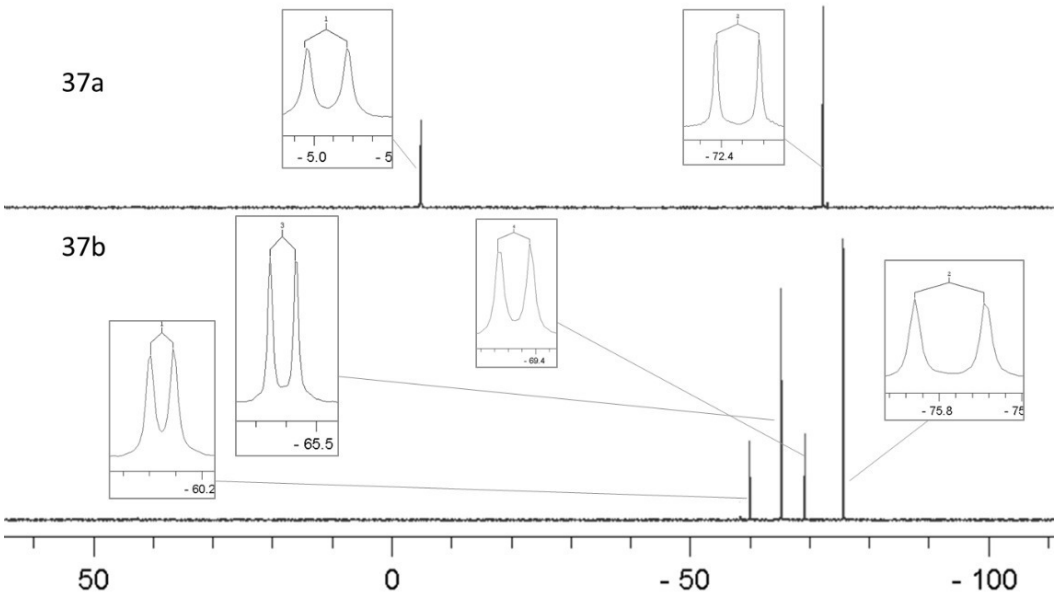

Figure 72: Comparison of the $^{31}P\{^{1}H\}$ NMR spectra of the reaction mixtures for **37a,b**.

Strikingly, the $^{31}P\{^{1}H\}$ NMR spectrum showed the presence of only one stereoisomer for compound **37a**, which might be due to the steric demand of the $N(SiMe_3)_2$ group thus directing stereo chemically the incoming electrophile to the opposite side of the plane resulting in the formation of the *trans* isomer. But when the sterically less demanding nucleophile ^{n}BuLi was employed, the presence of both isomers of **37b,b'** was observed in the $^{31}P\{^{1}H\}$ NMR spectrum of the reaction mixture (Figure 72). It shows two sets of pairs of doublets for the two isomers being present in a ratio of 1:3.5 (by NMR integration). Both **37a** and **37b,b'** were isolated from the reaction mixture in moderate to good yields (80 % for **37a** and 35 % for **37b,b'**) using flash chromatography through silica and pure toluene as the eluent. Further evidence for the constitution of **37a** and **37b,b'** was provided by the ^{1}H, $^{13}C\{^{1}H\}$ NMR spectra and mass spectroscopy. For example, the *P*-Me group in **37a** and **37b,b'** appeared each as doublets in the ^{1}H NMR spectra, *e.g.,* 0.77 ppm ($^{2}J_{P,H}$ = 5.2 Hz) in case of **37a**. The pos-ESI-MS data gave further support for the elementary composition, *e.g.* for **37a** the m/z value 658.3142 was obtained, thus showing a reasonably good agreement with the cation $C_{29}H_{57}N_5P_2Si_2S_2$+H (theor. 658.3154).

8.4 Oxidative hydrolysis of tricyclic 1,4-diphosphinine 33b

Previously, Pfeifer had obtained a structurally characterized bis-phosphinic acid **38a** (-7.8 ppm) which was derived from compound **33a** (without being aware of the real constitution), and which was structurally characterized.[123] To study this serendipitous finding more precisely, a diethyl ether solution of compound **33b** was left stirring under open atmospheric condition for 12 h, which slowly turned colorless. The $^{31}P\{^{1}H\}$ NMR spectrum of the reaction solution showed a complete and clean consumption of the starting material and a new resonance signal appeared at -6.9 ppm. Removal of the solvent in *vacuo*, followed by washing with diethyl ether produced a white powder in excellent yield (92 %). The $^{13}C\{^{1}H\}$ NMR spectrum of this white powder showed a doublet of doublet resonance signal at 125.5 ppm ($^{1}J_{P,C}$ = 167.4 Hz, $^{2}J_{P,C}$ = 21.6 Hz) for the carbons of the six membered ring. The range of coupling constants fell in agreement with the compound **38a** ($^{1}J_{P,C}$ = 162.4 Hz, $^{2}J_{P,C}$ = 20.6 Hz), hence proving the conversion of the P-centers from a low coordinated one to P^{V}-one. The pos-ESI-MS data showed a peak for $C_{22}H_{38}N_4O_4P_2S_2Na$ at 517.1721 (m/z, z=1) (calc. 517.1707) which finally confirmed this white powder as the tricyclic bis-phosphinic acid **38b** Scheme 46).

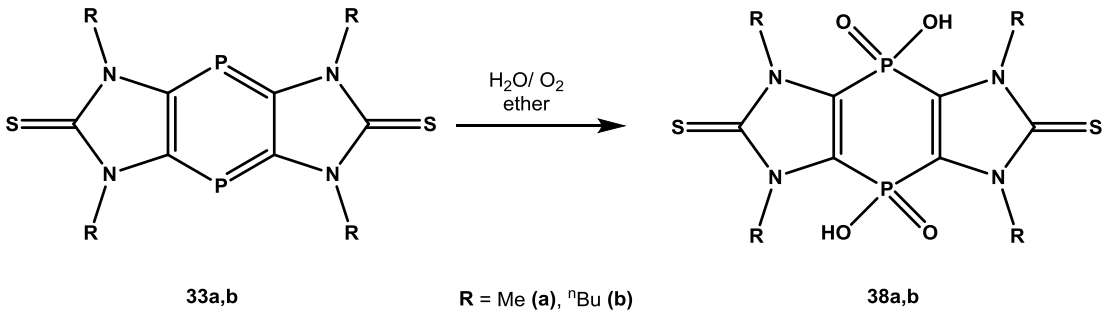

Scheme 47: Oxidative hydrolysis of compound **33b** under atmospheric conditions.

Though the exact pathway for the generation of the bisphosphinic acid **38** remains unknown till date, a plausible route can be proposed following a proposal by Dimroth and coworkers (Figure 73),[124] in which phosphinine oxide **LXXIV** is formed first via reaction with O_2, that reacts with 1 eq. of H_2O due to its electrophilic nature to form the phosphinic acid **LXXV**. Although a similar pathway could be imagined also for the tricyclic diphosphinine **33b**, but the exact reaction pathway still remains to be established, either experimentally and/or theoretically. In particular, the origin of the 4^{th} oxygen atom in the reaction product is unclear.

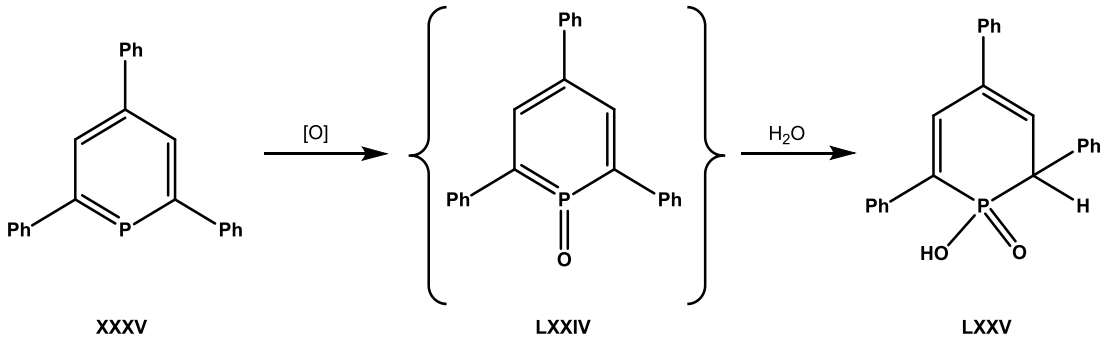

Figure 73: Oxidative hydrolysis of a phosphinine.[124]

Chapter 9

9. Summary

This thesis describes the chemistry of novel tricyclic 1,4-dihydro-1,4-diphosphinines and 1,4-diphosphinines, whereby an early discovery by Sauerbrey on the formation of a tricyclic 1,4-dihydro-1,4-diphosphinine, detected as byproduct (4 % yield), constituted the starting point. Furthermore, a study on synthesis of precursors for backbone phosphaalkenyl substituted imidazole-2-thiones was carried out.

In chapter 3, detailed investigations are described on how the reaction conditions were tuned to achieve improved yields for tricyclic 1,4-dihydro-1,4-diphosphinines. In particular, a comprehensive study was carried out to examine the effect of N- and P-substituents along with the reaction stoichiometry on the reaction outcome, *i.e.* the ratio of acyclic and cyclic products using the following reaction scheme; tricyclic 1,4-dihydro-1,4-diphosphinines **4a,a'-b,b'** were isolated as a mixture of *cis* and *trans* isomers. The isolated compounds (Table 16) were all fully characterized by modern analytical means. One remarkable aspect stands out: a *P*-dialkylamino group and primary alkyl groups at the thione N-atoms are needed for a successful ring closure.

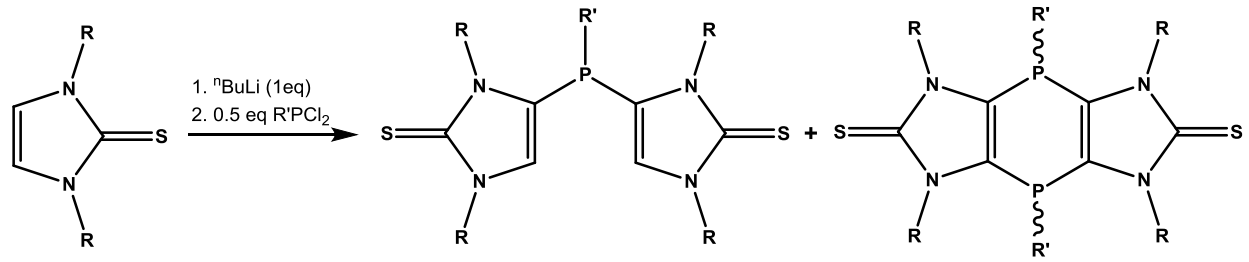

Scheme 48: Studies of the effects of N,P-substituents and reaction stoichiometry on the formation of tricyclic 1,4-dihydro-1,4-diphosphinines.

Table 16: Compounds isolated from the old scheme of backbone phosphanylation (scheme 48).

	3a	**3b**	**3c**	**3d**	**3g**	**3i**	**4a,a'**	**4b,b'**
N-Substituents (R)	Me	Et	Ph	^{i}Pr	^{i}Pr	^{n}Bu	Me	Et
P-substituents (R')	NMe_2	NMe_2	NMe_2	NMe_2	OEt	Ph	NMe_2	NMe_2
Yields (%)	60	32	75	81	75	60	4	16

Albeit better, this protocol did not improve the yields of **4a,a'-b,b'** to more than 16% and also did not provide evidence for the reaction pathway. Therefore, alternative pathways had to be developed, and there mechanism elucidated.

Chapter 4 describes the synthesis of the backbone amino(chloro)phosphanyl substituted imidazole-2-thiones **5a-f** and their use in the synthesis of tricyclic 1,4-dihydro-1,4-diphosphinines **4d,d'-f,f'**. Compounds **5a-f** were obtained from backbone-bis(dialkylamino)phosphanyl substituted phosphanes **7a-f** *via* a PCl_3-mediated P-N bond cleavage (Scheme 49). Compounds **5a-c** were successfully employed to synthesize the tricyclic 1,4-dihydro-1,4-diphosphinines **4d,d'-f,f'** in a selective and high yielding protocol *via* treatment with LDA as a base. The problem of the limited solubility of these 1,4-dihydro-1,4-diphosphinines, which has been a significant hurdle in the exploration of their chemistry could be also solved by introduction of longer N-alkyl chains. Replacing LDA with KHMDS as the base surprisingly resulted in the formation of P-substituted compounds **8a,b** as the major product, in spite of larger steric demand of KHMDS and a very weakly pronounced nucleophilicity.

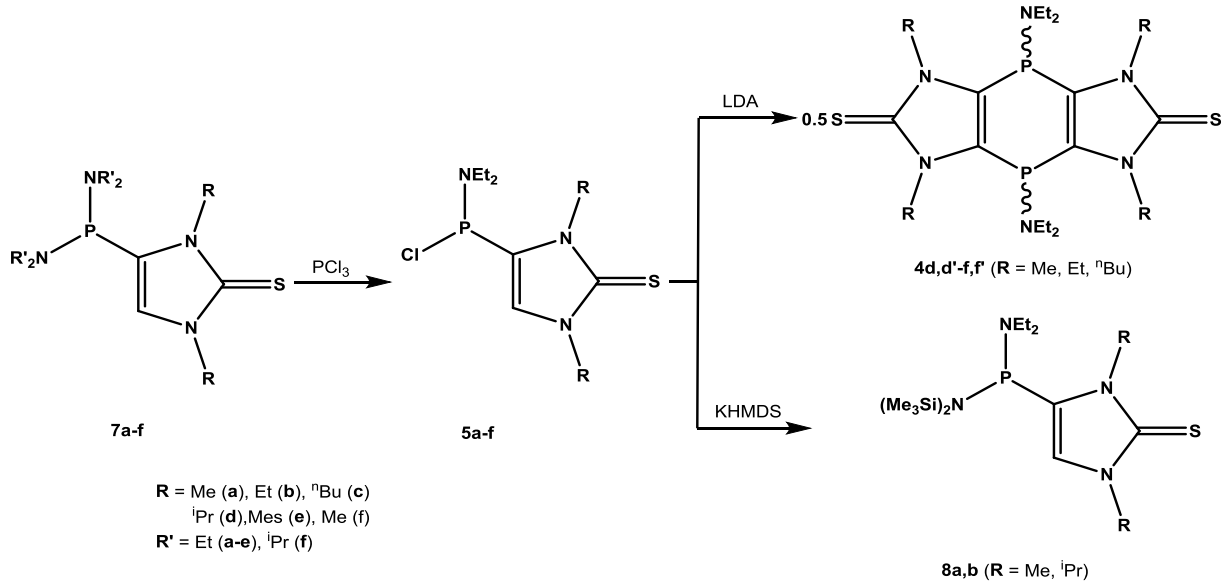

Scheme 49: Reaction of compounds **5** with different amides.

Chapter 4 also describes use of these backbone-amino(chloro)phosphanyl substituted imidazole-2-thiones **5a-f** in the synthesis of precursors of phosphaalkenyl P-substituted imidazole-2-thiones. For this purpose compounds **5d,e** were treated with sterically demanding anionic nucleophiles bearing an acidic α-proton*, e.g.* Ph_2CHLi, FluLi, to get access to compounds **9a-c** (Scheme 50).

Compound **9,** when treated with borane-dimethyl sulfide was transformed selectively into the *P*-borane adduct **10**, whereas with hydrogen peroxide the imidazolium salt **11** was formed (Scheme 50). Compounds **9** was also converted into the P-Cl compounds **12** via reaction with PCl_3.

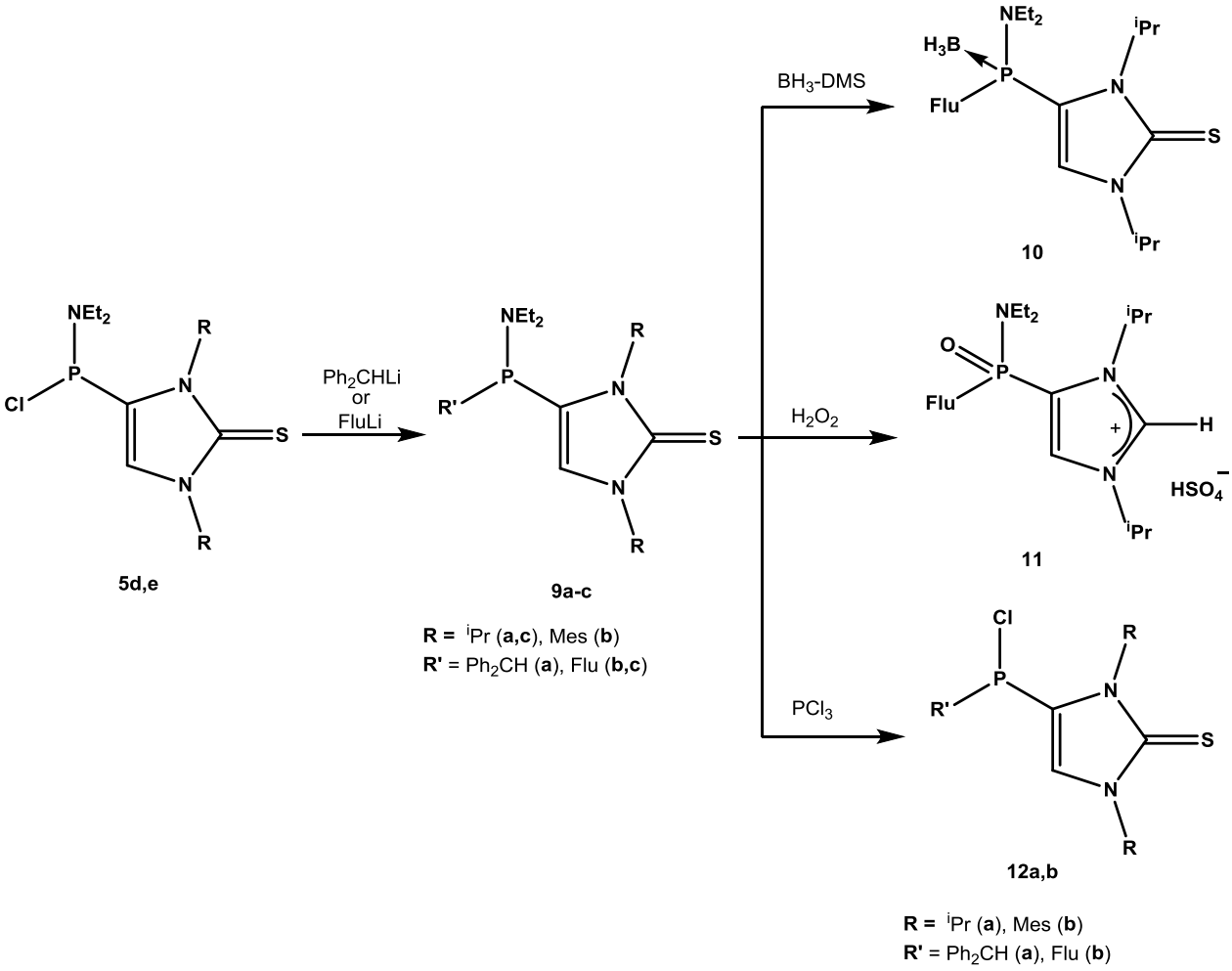

Scheme 50: Reactions of backbone-amino(chloro)phosphanyl substituted imidazole-2-thiones**.**

Compound **12b** could be transformed into NHC-stabilized phosphenium salt **13** when treated with 1,3,4,5-tetramethyl imidazole-2-ylidene (Scheme 51), but it was also used as potential starting point

for the synthesis of phosphaalkenyl P-substituted imidazole-2-thiones using a base-induced dehydrohalogenation reaction.

Compound **12b** reacted with ^{n}BuLi to form the P-substituted product **18**, thus showing a clear preference over the targeted phosphaalkene derivative. But compound **18** also reacted with a second eq. of ^{n}BuLi to generate the carbanion **19** which could be converted back to compound **19** selectively using HCl (Scheme 51).

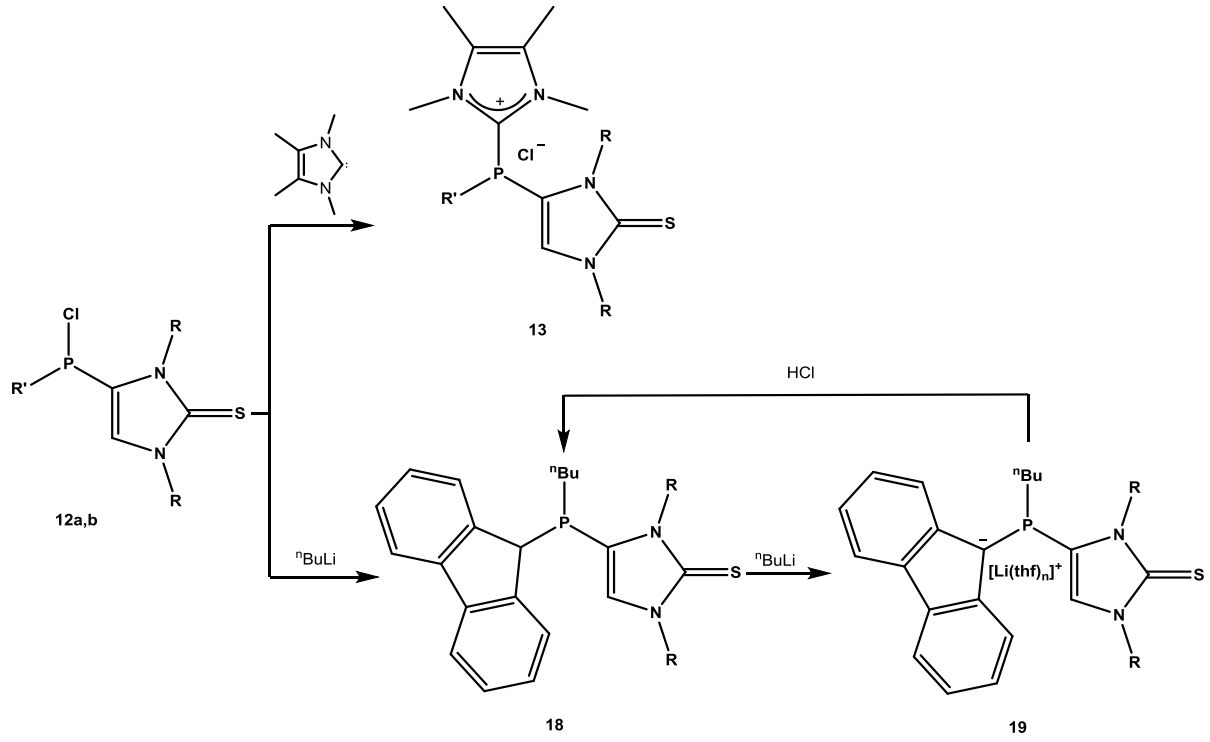

Scheme 51: Reactivity studies of compounds **12**.

Chapter 5 describes the synthesis of new derivatives of tricyclic 1,4-dihydro-1,4-diphosphinines via synthesis and employment of chloro(phenyl)phosphanyl substituted imidazole-2-thiones **21a-c** using the same synthetic protocol.

While compounds **21a-c** could be successful converted into the *P*-Ph derivatives of tricyclic 1,4-dihydro-1,4-diphosphinines **22a,a'-c,c'** using LDA as base, they reacted with KHMDS to furnish P-substituted products **23a,b** (Scheme 52). In order to have an improved starting point for further functionalization of the P-centers, the 1,4-dichloro-1,4-dihydro-1,4-diphosphinines **24a,a'-b,b'** were synthesized from the *P*-NEt_2 derivatives **4d,d';f,f'** via reaction with PCl_3. Compounds **24a,a'-b,b'** opened a new and easy route to access derivatives with different P-substituents using difference

nucleophiles, *e.g.* compounds **25a,a'-c,c'** could be obtained via treatment with two molar eq. of carbon -based nucleophiles (Scheme 52).

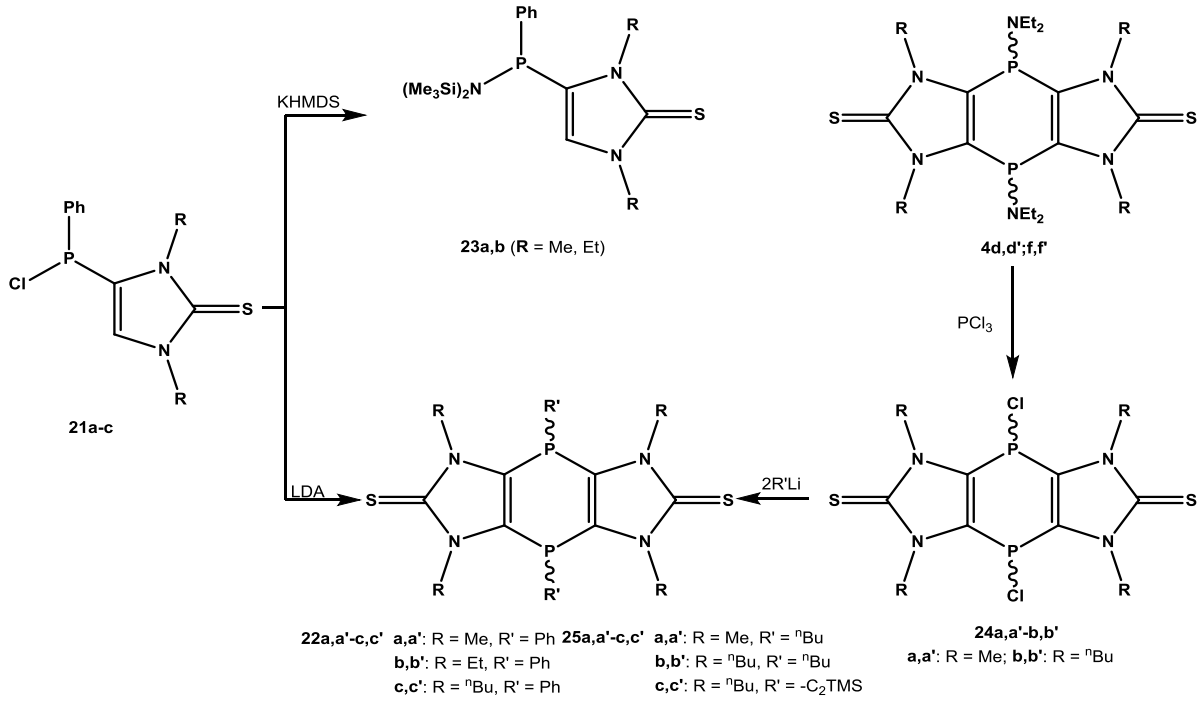

Scheme 52: Extension of the 1,4-dihydro-1,4-diphosphinines chemistry to other P-substituents.

Chapter 6 is focused mainly on redox reaction studies on tricyclic 1,4-dihydro-1,4-diphosphinines. The P-centers of these tricyclic 1,4-dihydro-1,4-diphosphinines could be oxidized (**26a,a'-e,e'**), sulfurized (**27a,a'-e,e'**) and complexed to borane (**30a,a'-c,c'**) upon treatment with hydrogen peroxide, elemental sulfur and borane-dimethyl sulfide complex, respectively (Scheme 53). Furthermore, treatment with 2 eq. of *o*-chloranil resulted in the formation of the corresponding spirocyclic derivatives **28a,a'-c,c'** in excellent yields (Scheme 53).

The tricyclic 1,4-dihydro-1,4-diphosphinines were also tested for the competing reactivity of the P and S-centers towards electrophiles. While the hard electrophile methyl triflate attacked the S-centers (**29a,a'-d,d'**), in agreement with favorable molecular electrostatic potential values, the borane adduct formation to give **30a-c** occurred at the P-centers due to favorable thermodynamics.

The *P*-Ph derivative **23c,c'** showed reductive P-C^{Ph} bond cleavage, when treated with 4 molar eq. of metallic potassium at room temperature, to produce the dianionic species **31**. The latter could not be isolated but used as reactive intermediate in reactions with an electrophile such as ^{n}BuI to yield **25b,b'**. A first study revealed that compound **22b,b'** could be converted to the corresponding bis-

imidazolium salt **32,32'** via an oxidative desulfurization reaction via treatment with 10 molar eq. of hydrogen peroxide (Scheme 53).

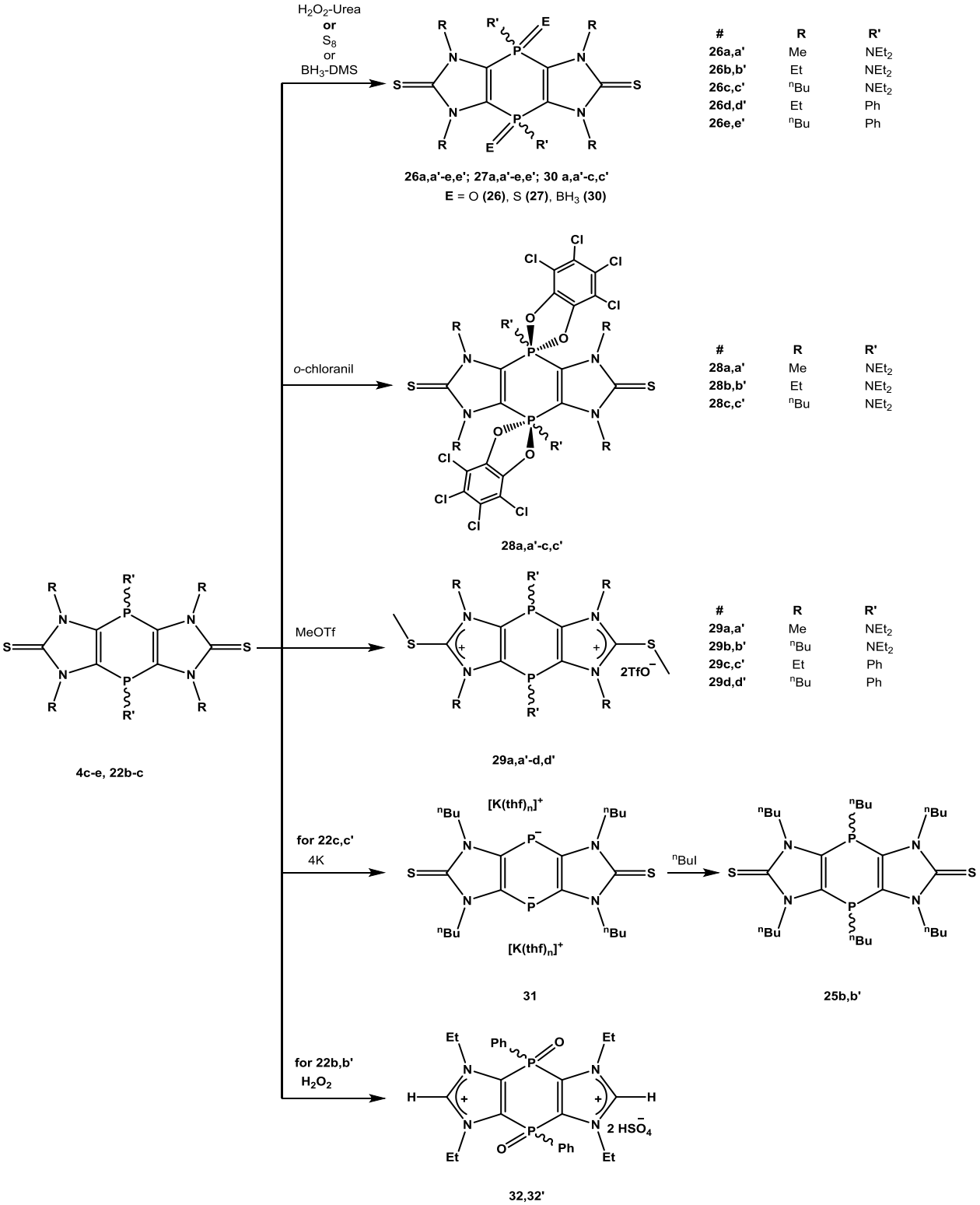

Scheme 53: Some reactivity studies of the tricyclic 1,4-dihydro-1,4-diphosphinines.

Chapter 7 describes first synthesis of the tricyclic 1,4-diphosphinines **33a,b**. The dark red colored tricyclic 1,4-diphosphinines were synthesized *via* a high yielding reduction of the 1,4-dichloro-1,4-dihydro-1,4-diphosphinines **24a,a'-b,b'** using the mild reducing agent $^{n}Bu_3P$. The tricyclic 1,4-diphosphinines **33a,b** were completely characterized by all analytical methods along with X-ray crystallographic measurements of single crystals. Preliminary studies on their electrochemical behavior were performed using cyclic voltammetry which revealed that compound **33b** can undergo two reduction processes (firstly, a 2e-reduction and, secondly, a 1e-reduction) leading to an uptake of 3 electrons. UV/vis spectra were recorded to get first insight into the origin of the red color which was explained as the result of low energy HOMO(π)-LUMO(π^*) excitation on the basis of TD-DFT calculations.

Chapter 8 is focused on chemical reactivity studies focusing on addition and cycloaddition reactions of **33**. In case of [4+2]-cycloaddition reactions, diphenyl acetylene no reaction was observed, even under harsh reaction conditions. When the electron-deficient dimethyl acetylene dicarboxylate (DMAD) was employed, a clean [4+2]-cycloaddition yielded product **34a**. Also electron-deficient C=C or N=N double bond systems such as N-phenylmaleimide or 4-phenyl-1,2,4-triazoline-3,5-dione reacted as dienophiles to yield **34b,c**. The tricyclic 1,4-diphosphinine **33b**, when treated with organic dichalcogenides (Ph_2E_2; E = S, Se) at elevated temperature, gave rise to a stereospecific *trans* 1,4-addition of two EPh fragments to furnish the products **35a,b** (Scheme 54), which were isolated in high yields. The electrophilic nature of the P-centers in the 1,4-diphosphinines was used in reactions with ^{n}BuLi or LDA that led to a nucleophilic attack at the P-center to produce the phosphides **36a,b**, which subsequently reacted with methyl iodide to form the asymmetrically substituted tricyclic 1,4-dihydro-1,4-diphosphinines **37a,b**. Finally these 1,4-diphosphinines were found to be prone to oxidative hydrolysis, thus producing bis-phosphinic acid derivatives **38a,b**, when a solution of **33** was stirred under atmospheric conditions.

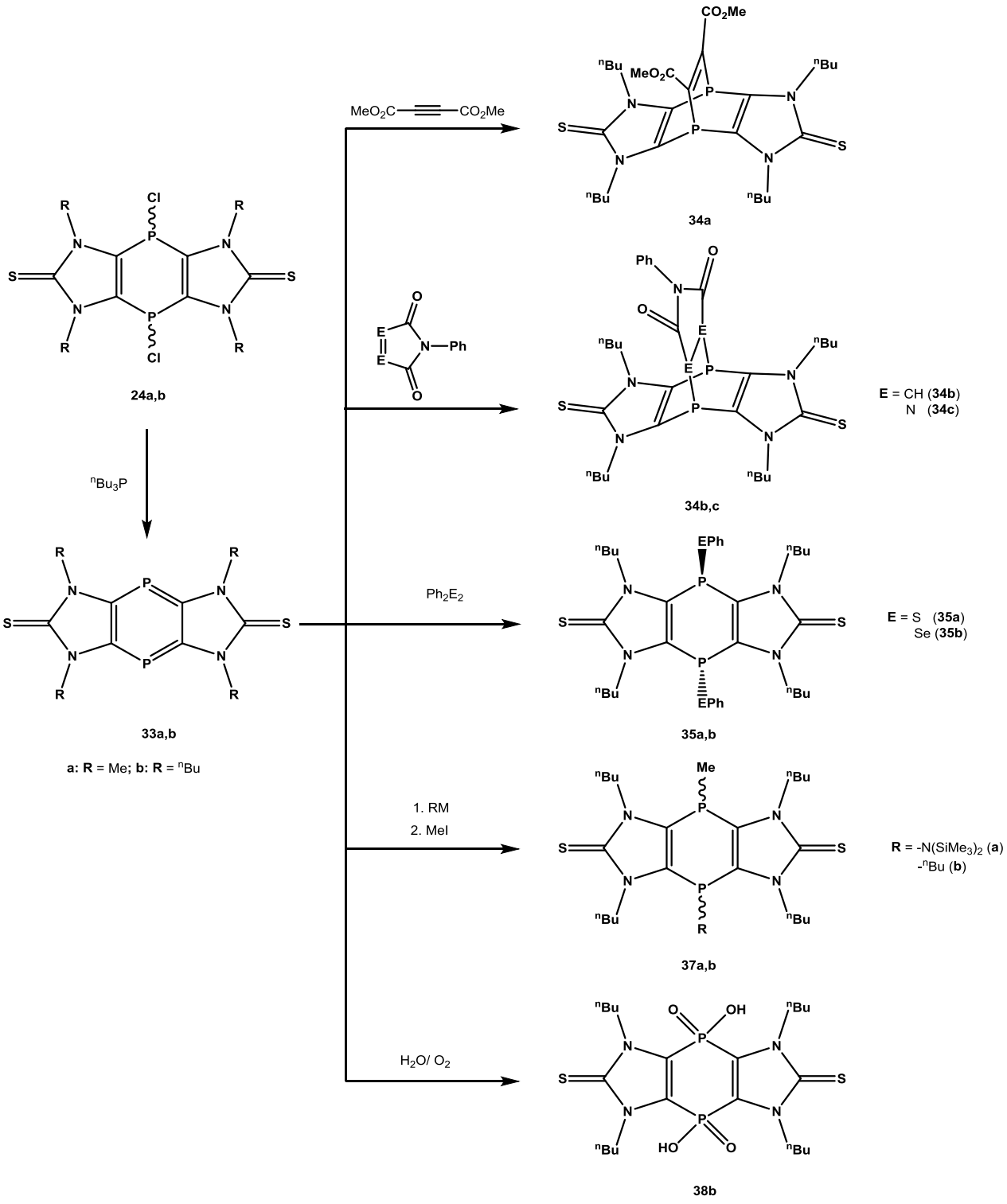

Scheme 54: Examples of [4+2]-cycloaddition, 1,4-addition and other addition reactions of tricyclic 1,4-diphosphinines **33**.

Chapter 10

10. Experimental Section

10.1 General Techniques

All reactions were performed under a stream of deoxygenated (using preheated BTS catalyst at 100-130 °C) and dried (using molecular sieve and phosphorus pentoxide) Argon gas, using standard Schlenk techniques. All sensitive chemicals were stored in either Schlenk flasks or handled in the glovebox. All the solvents used in reactions were dried and distilled over sodium wires or calcium hydride (for methylene dichloride) and stored in brown glass bottles having Schlenk connections. All glass wares used were preheated and dried in the oven prior to use. In case air sensitive reactive the Schlenk flasks or tubes were prepared by heating under high vacuo and subsequently refilling with Argon gas. All the glass joints were lubricated with OKS grease type 1112. The high temperature reactions were done with an oil bath whereas the low temperature ones were performed using a liquid nitrogen/ethanol bath. For the purpose of removing salts formed in the reaction mixture common G3 frits having two Schlenk joints were used, along with either silica gel (Merck 60-200) or Celite. For transferring solvents or filtering, stainless steel double needle or filter cannula were used, which were preheated and dried in the oven at 75 °C. Whatman filter papers or glass microfiber filter papers were used for filtration purposes. All the used glass wares were soaked overnight in a KOH-isopropanol bath having some NaOCl (for oxidizing the metal impurities) and then dipped into a HCl-water bath for the sake of neutralization prior to washing with soap water. Then the cleaned glass wares were rinsed with deionized water and acetone simultaneously before drying at 120 °C in the oven overnight.

10.1.1 Melting point determination

Melting points were determined using a Büchi 535 Type S melting point apparatus, where the sample were placed inside a both sided closed glass capillary tubes; the values are not corrected.

10.1.2 Elemental analysis

All the elemental analyses were performed with an Elementar Vario Micro elemental analyser by the micro analysis section of the Chemical Institute of the University of Bonn. The mean value of at least three measurements is given.

10.1.3 NMR spectroscopy

NMR spectra of all the compounds were recorded on Bruker Avance DMX-300, DPX-300, DPX-400 or DMX-500 spectrometers. Deuterated solvents ($CDCl_3$, THF-d_8 or C_6D_6) were dried using literature procedures and used for the multinuclear NMR characterizations and the chemical resonances are given relative to Tetramethylsilane (^1H, ^{13}C, ^{29}Si NMR), 1 M LiCl in D_2O (^7Li NMR), 15 % $BF_3{\cdot}OEt_2$ in $CDCl_3$ (^{11}B NMR), $CFCl_3$ (^{19}F NMR) or 85% H_3PO_4 (^{31}P NMR), respectively. The chemical shifts are expressed in parts per million, ppm. Coupling constants are abbreviated as $^nJ_{X,Y}$, where X and Y denote the coupling nuclei (ordered by decreasing atomic number, n is the number of bonds that separate X and Y). The following abbreviations were used for expression of the multiplicities of the resonance signals: s = singlet, d = doublet, t = triplet, q = quartet, quin = quintet, sept = septet, m = multiplet and br = broad signal. All the measurements were recorded at 298K unless some specific temperature is given. HMQC, HMBC and DEPT experiments were used in purpose of assigning the ^1H NMR and ^{13}C NMR signals of all compounds.

10.1.4 UV/vis spectroscopy

UV/vis spectra were obtained from a Shimadzu UV-1650PC spectrometer (λ = 190-900 nm) using dichloromethane as the solvent and quartz glass cells (Hellma) of optical path 1cm at room temperature.

10.1.5 Mass spectrometry

Mass spectrometric data were acquired from a Bruker Daltonik micrOTOF-Q using ESI (+/-), a Thermo Finnigan MAT 90 sector instrument equipped with a LIFDI ion source (Linden CMS) or MAT 95 XL Finnigan using EI (70 eV). Only selected data are given for the detected ions (mass to charge ratio, relative intensity in percent).

10.1.6 Infrared spectroscopy

IR-spectra were recorded from the pure solids on a Thermo IR spectrometer with an attenuated total reflection (ATR) attachment or on a Bruker Alpha Diamond ATR FTIR spectrometer at room temperature. The following abbreviations were used for expression of the intensities of the absorption bands: vs = very strong, s = strong, m = medium, w = weak.

10.1.7 Cyclic voltammetry

The custom-tailored glassware for the electrochemical measurements, equipped with three Pt electrodes (working, reference and counter electrodes), has been prepared (see also figure x on page y). Electrochemical experiments were carried out on an ALS 1140A potentiostat/galvanostat. Electrochemical samples were recorded with scan rates of 10–500 mVs^{-1} at r.t. under Ar atmosphere. Ferrocene was used as internal/external reference to determine the potentials. Sample solutions (THF) were 3 mM in analyte and 0.1 M in *n*-Bu_4NPF_6 as the supporting electrolyte.

10.1.8 Single crystal X-ray diffraction studies

Single crystal were grown by evaporation of saturated solutions of the compounds at -20°C or by diffusion technique. After crystal growing the single crystals were separated from the supernatant solution and were covered with Fomblin for the purpose of protection from further decomposition. A suitable single crystal was selected under the microscope and loaded onto the diffractometer. The crystallographic data was collected on Brucker D8-Venture diffractometer, Bruker X8-KappaApexII, Bruker APEX-II CCD, Nonius KappaCCD or STOE IPDS 2T diffractometer equipped with a low-temperature device at 100.0 K using graphite monochromated Cu-Kα radiation (λ = 1.54178 Å) or Cu-K_α radiation (λ = 1.54178). The absorption correction, structure solution and structure refinement was performed by Patterson methods or by full-matrix least squares on F^2 using the SHELXL-97 programs. All non-hydrogen atoms were refined anisotropically, the hydrogen atoms were included isotropically using the riding model on the bound carbon atoms. Data analyses and the picture preparation of the molecular structure for all the compounds were done using Diamond 3.0 program.

10.1.9 Chemicals used

All the chemicals used during the experiments are listed below with supplier name in the brackets. All the chlorophosphane, commercially purchased, were subjected to further purification by means of fractional distillation.

Chemicals	*Supplier*	*Chemicals*	*Supplier*
• Acetonitrile	Fisher Scientific	• Glyoxal	Acros
• Ammonia solution	Grüssing	• Hydrogen peroxide	Acros
• Borane dimethylsulfidecomplex	Alfa Aesar	• Hydrogen peroxide-urea adduct	Acros
• 1-Bromobutane	Acros	• Imidazole	ChemPure
• 1-Bromoethane	Acros	• Iodomethane	Acros
• *n*-Butylamine	Acros	• Isopropanol	Biesterfeld

• *n*-Butyllithium	Acros	• Methanol	Aldrich
• Chloroform	Fisher Scientific	• Potassium metal	Riedel de Haen
• Chloroform-d	Eurisotop	• Potassium *tert*-butoxide	Acros
• Diethylether	VWR	• Potassium bis(trimethylsilyl)amide	Sigma-aldrich
• Dichloromethane	Biesterfeld	• *n*-Pentane	Grüssing
• Diisopropylamine	Acros	• Petrol ether 40/60	Biesterfeld
• Dimethylamino Dichlorophosphane	Sigma-aldrich	• Phenyldichlorophosphane	Acros
• Dimethylsulfoxide	Acros	• Phosphorustrichloride	Acros
• Dimethylacetylenedicarboxylate	Acros	• Sodium Metal	Riedel de Haen
• Diphenyldisulfide	Sigma-aldrich	• Sodium Hydride	Sigma-aldrich
• Diphenyldiselenide	Sigma-aldrich	• Sulfur	Acros
• Diphenylmethane	Acros	• Tetrahydrofuran	Fisher Scientific
• Ethanol	Hofmann	• THF-d8	Eurisotop
• Formaldehyde	Acros	• Triflicacid methyl ester	Sigma-aldrich
• Fluorene	Sigma-aldrich	• Toluene	Fisher Scientific
		• Tributyltin hydride	Sigma-aldrich
		• Tributylphosphane	Acros

The following compound were synthesized following published protocols:

bis(diethylamino)chlorophosphane[125]

Lithium diisopropylamide[126]

1,3-diethylimidazole-2-thione[9]

1,3,4,5-tetramethylimidazole-2-ylidene[11]

1,3-dimethylimidazole-2-thione[9]

1,3-dibutylimidazole-2-thione[9]

10.1.10 Waste disposal

The chemical waste disposal was performed on basis of the "Gefahrstoffverordnung". Organic and inorganic waste were separated from each other and collected in designed container before disposing. Other dry chemical wastes along with column waste were collected together and disposed of. All the dangerous and reactive reagent left overs were destroyed according to the literature reported protocols[127] and taken care of. All the waste were submitted to the department 4.2 "Arbeits und Umweltschutz" of the University of Bonn for further caring.

10.2 Synthesis of bis(imidazole-2-thione-4-yl)phosphanes 3

To a solution of 1,3-dialkyl-imidazole-2-thione **1** (13.2 mmol) in 30 mL of THF, 8.9 ml of ^{n}BuLi (1.6 M in hexane) was added dropwise at –78 °C. Then the reaction mixture was slowly warmed up to –40 °C and stirred for about 3h at this temperature. Then the reaction mixture was again cooled to –78 °C, and 6.6 mmol of dichlorophosphanes **2** were added dropwise into the reaction mixtures. Then the reaction mixtures were allowed to warm up to ambient temperature overnight. For **3a** a white precipitate formed, which was filtered off and washed twice with THF (2 × 2 ml) and finally with *n*-pentane (2 × 5 ml) to get pure *trans* isomer of **4a** as a white powder, finally. The remaining reaction mixture was dried in *vacuo* (8×10^{-3} mbar) to get a brown oily residue which was again taken up in methylene dichloride (60 ml) and filtered through a bed of silica to remove LiCl. The residue after drying this filtrate was subjected to column chromatography over silica gel using a methylene dichloride/diethylether mixture (1:3) as eluent, in order to separate **3a** from other impurities.

For **3b** the reaction mixture was removed in *vacuo* (8×10^{-3} mbar) and then the residue was directly subjected to column chromatography at room temperature using diethylether/petroleum ether (x/y) mixtures (1:4) as the eluent. Finally, both **3b** and **4b** were obtained as white powders after evaporation of all volatiles of the corresponding fractions.

For **3d**,**g,i** reaction mixtures were concentrated under reduced pressure to get dark yellow to brown residues. These residues were then taken up in methylene dichloride and filtered through a silica bed to remove the LiCl and some of the coloring impurities. The filtrates were dried in *vacuo* to light yellow solids as the crude products which were in the next step washed with *n*-pentane (3 × 5 ml) to remove some of the coloring impurities. Finally the remaining solids were dried *in vacuo* (8×10^{-3} mbar) to get the products as slightly off white powders.

10.2.1 Bis(1,3-diethylimidazole-2-thione-4-yl)(dimethylamino)phosphane (3b)

Yield: 0.82 g (2.1 mmol, 31.8 %) **Appearance:** white powder **melting point:** 153 °C

^{1}H NMR (300 MHz, $CDCl_3$): δ = 1.25(t, 6H, $^{3}J_{H,H}$ = 7.1 Hz, $\underline{Me}CH_2N^3$), 1.31 (t, 6H, $^{3}J_{H,H}$ = 7.3 Hz $\underline{Me}CH_2N^1$), 2.63 (d, 6H, $^{3}J_{P,H}$ = 9.9 Hz, P-N$\underline{Me_2}$), 3.96-4.11 (m, 4H, $^{3}J_{H,H}$ = 7.3Hz Me$\underline{CH_2}N^3$), 4.16 (q, 2H, $^{3}J_{HH}$ = 7.1Hz Me$\underline{CH_2}N^1$), 4.19 (q, 2H, $^{3}J_{H,H}$ = 7.1 Hz Me$\underline{CH_2}N^{1'}$), 6.55 (br, 2H, $\underline{C^5H}$).

^{13}C NMR (75.0 MHz, $CDCl_3$): δ = 13.8 & 13.9 (s $\underline{Me}CH_2N^3$), 14.2(s, $\underline{Me}CH_2N^1$), 40.9 (d, $^{2}J_{P,C}$ = 16.5 Hz, P-N$\underline{Me_2}$), 41.7 & 41.8 (s, Me$\underline{CH_2}N^3$), 42.9 (s, Me$\underline{CH_2}N^1$), 121.4(s, $\underline{C^5}$), 125.2 (d, $^{1}J_{P,C}$ = 8.2 Hz, $\underline{C^4}$), 164.2 (s, $\underline{C{=}S}$).

^{31}P NMR (121.5 MHz, $CDCl_3$): δ = 12.6 (sept, $^3J_{P,H}$ = 9.9 Hz).

IR [cm^{-1}]: $\tilde{\nu}$ = 3117 (w), 2973 (w), 2941 (w), 1543 (w), 1434 (m), 1410 (s), 1271 (s), 1147 (s), 978 (s).

MS (EI, 70 eV): m/z (%) = 385.2 (100) $[M]^{\cdot+}$, 341.2 (100) $[M\text{-}NMe_2]^+$, 156.1 (30) $[C_7H_{12}N_2S]^{\cdot+}$.

HRMS: theor./exp. for $[C_{16}H_{28}N_5PS_2]$: 385.1524/385.1520.

EA [%]: theor./exp. C 49.85/49.51, H 7.32/7.03, N 18.17/17.99, S 16.63/17.11.

10.2.2 Bis(1,3-diisopropylimidazole-2-thione-4-yl)(dimethylamino)phosphane (3d)

Yield: 2.36 g (5.4 mmol, 81.1 %) **Appearance:** white powder **melting point:** 184 °C

^{1}H NMR (300 MHz, $CDCl_3$): δ = 1.29(d, 6H, $^3J_{H,H}$ = 5.03 Hz, $N^1CH\underline{Me_2}$), 1.32 (d,6H, $^3J_{H,H}$ = 5.03 Hz, $N^1CH\underline{Me_2}$), 1.47 (d,6H, $^3J_{H,H}$ = 6.9 Hz, $N^3CH\underline{Me_2}$), 1.52 (d,6H, $^3J_{H,H}$ = 6.9 Hz, $N^3CH\underline{Me_2}$), 2.65 (d, 6H, $^3J_{H,H}$ = 9.45 Hz, $\underline{Me_2N}$-P), 5.13 (sept,2H, $^3J_{H,H}$ = 6.9 Hz, $N^3\underline{CH}Me_2$), 5.23 (bs,2H, $N^1\underline{CH}Me_2$), 6.50 (s, 2H, $\underline{C^4H}$).

^{13}C NMR (75.0 MHz, $CDCl_3$): δ = 20.4 & 20.5 (s, $N^3CH\underline{Me_2}$), 20.9 & 21.1 (s, $N^{3'}CH\underline{Me_2}$), 21.7 & 21.9 (s, $N^1CH\underline{Me_2}$), 40.8 (d,$^2J_{P,C}$=16.6 Hz, $\underline{Me_2N}$-P), 48.7 (s, $N^1\underline{CH}Me_2$), 51.9 (s, $N^3\underline{CH}Me_2$), 119.4(s, $\underline{C^5}$), 126.7 (d, $^1J_{P,C}$ = 17.7 Hz, $\underline{C^4}$), 163.7 (s, $\underline{C{=}S}$).

^{31}P NMR (121.5 MHz, $CDCl_3$): δ = 15.5 (sept, $^3J_{P,H}$= 9.5 Hz).

IR [cm^{-1}]: $\tilde{\nu}$ = 2967 (s), 2930 (w), 2874 (w), 1539 (w), 1434 (w), 1412 (s), 1366 (s), 1330 (s), 1288 (s), 1186 (s), 1132 (s), 1062 (s), 982 (vs)

MS (EI, 70 eV): m/z (%) = 441.2 (10) $[M]^{\cdot+}$, 397.1(10) $[M\text{-}NMe_2]^+$, 184.1 (80) $[C_9H_{16}N_2S]^{\cdot+}$.

HRMS: theor./exp. for $[C_{16}H_{28}N_5PS_2]$: 441.2150/441.2150.

EA [%]: theor./exp. C 54.39/53.12, H 8.22/7.99, N 15.86/15.49, S 14.52/13.90.

10.2.3 Bis(1,3-diisopropylimidazole-2-thione-4-yl)(ethoxy)phosphane (3g)

Yield: 2.11 g (4.8 mmol, 72.0 %) **Appearance:** white powder **melting point:** 146 °C

^{1}H NMR (300 MHz, $CDCl_3$): δ = 1.26 (t, 3H, $^3J_{H,H}$= 7.1 Hz, $POCH_2\underline{Me}$), 1.29 (d, 6H, $^3J_{H,H}$= 6.5 Hz, N^3-$CH\underline{Me_2}$), 1.32 (d, 6H, $^3J_{H,H}$ = 6.5 Hz, $N^{3'}$-$CH\underline{Me_2}$), 1.40 (d, 6H, $^3J_{H,H}$= 7.1 Hz, N^1-$CH\underline{Me_2}$), 1.55 (d, 6H, $^3J_{H,H}$=

7 Hz, $N^{1'}$-CH*Me*$_2$), 3.85 (dq, 2H, $^3J_{P,H}$= 10.0 Hz, $^3J_{H,H}$= 7.1 Hz, PO*CH*$_2$Me), 5.12 (sept, 2H, $^3J_{H,H}$= 7 Hz, N^1-*CH*Me$_2$), 5.38 (br sept, 2H, $^3J_{H,H}$ = 6.5 Hz, N^3-*CH*Me$_2$), 6.68 (s, 2H, C^5-*H*).

^{13}C NMR (75.0 MHz, $CDCl_3$): δ = 17.0 (d,$^2J_{P,C}$ = 8.8 Hz, POCH$_2$*Me*), 21.0 and 21.2 (s, N^3-CH *Me*$_2$), 21.5 and 21.6 (s, $N^{3'}$-CH *Me*$_2$), 21.7 (s, N^1-CH*Me*$_2$), 21.9 (s, $N^{1'}$-CH *Me*$_2$), 49.0 (s, N^1-*C*H *Me*$_2$), 50.8 (s, N^3-*C*H *Me*$_2$), 66.3 (d,$^1J_{P,C}$ = 22.3 Hz, PO*CH*$_2$Me), 120.6 (d, $^2J_{P,C}$ = 5.6 Hz, C^5), 127.2 (d, $^1J_{P,C}$ = 22.3 Hz, C^4), 164.4 (s, *C*=*S*).

^{31}P NMR (121.5 MHz, $CDCl_3$): δ = 70.1 (t, $^3J_{P,H}$= 10.0 Hz).

IR [cm^{-1}]: ṽ = 3114 (w), 2974 (s), 2931 (w), 2874 (w), 1540 (s), 1458 (m), 1411 (vs), 1381 (s), 1295 (vs), 1188 (vs), 1034 (vs), 924 (vs), 750 (s), 712 (s).

MS (EI, 70 eV): m/z (%) = 442 (10) $[M]^{\cdot+}$, 184 (75) $[C_9H_{16}N_2S]^+$, 142 (18) $[C_6H_{10}N_2S]$.

HRMS: theor./exp. for $[C_{20}H_{35}N_4OPS_2]$: 442.1990/442.1992.

EA [%]: theor./exp. C 54.27/54.44, H 7.97/7.81, N 12.66/12.57, S 14.49/14.48.

10.2.4 Bis(1,3-di-*n*-butylimidazole-2-thione-4-yl)(Phenyl)phosphane (3d)

Yield: 2.10 g (3.96 mmol, 60.1 %) **Appearance:** white powder **melting point:** 87 °C

^{1}H NMR (300 MHz, $CDCl_3$): δ = 0.85(t, 6H, $^3J_{H,H}$ = 7.4 Hz, *CH*$_3$CH$_2$CH$_2$CH$_2$N^3), 0.91(t, 6H, $^3J_{H,H}$ = 7.4 Hz, *CH*$_3$CH$_2$CH$_2$CH$_2$N^1), 1.23-1.38 (m, 8H, CH$_3$*CH*$_2$CH$_2$CH$_2$N), 1.55-1.73 (m, 8H, CH$_3$CH$_2$*CH*$_2$CH$_2$N), 3.91-4.06 (m, 8H, CH$_3$CH$_2$CH$_2$*CH*$_2$N), 6.29 (s, 2H, C^{5}H), 7.34-7.51 (m, 5H, Ph protons).

^{13}C NMR (75.0 MHz, $CDCl_3$): δ = 13.61 (s, *CH*$_3$CH$_2$CH$_2$CH$_2$N^3), 13.62 (s, *CH*$_3$CH$_2$CH$_2$CH$_2$N^1), 19.8(s, CH$_3$*CH*$_2$CH$_2$CH$_2$N^3), 19.9 (s, CH$_3$*CH*$_2$CH$_2$CH$_2$N^1), 30.7(d, $^3J_{P,C}$=2.9Hz, CH$_3$CH$_2$*CH*$_2$CH$_2$N^3), 30.8 (s, CH$_3$CH$_2$*CH*$_2$CH$_2$N^1), 46.8 (d, $^3J_{P,C}$ = 8.3 Hz, CH$_3$CH$_2$CH$_2$*CH*$_2$N^3), 47.9 (s, CH$_3$CH$_2$CH$_2$*CH*$_2$N^1), 122.4 (d, $^1J_{P,C}$ = 2.9 Hz, C^4), 124.0 (s, *m*-**C** ph ring), 129.3(d, $^2J_{P,C}$ = 8.3 Hz, *o*-**C** ph ring), 130.1(d, $^1J_{P,C}$ = 2.4 Hz, *ipso*-**C** ph ring), 130.8 (s, *p*-**C** ph ring), 133.2 (d, $^2J_{PC}$ = 21.9, Hz, C^5), 165.3 (d, $^3J_{P,C}$ = 1.1 Hz, **C**=S).

^{31}P NMR (121.5 MHz, $CDCl_3$): δ = -59.2 (t, $^3J_{P,H}$= 8.3 Hz).

IR [cm^{-1}]: ṽ = 3114 (w), 3062 (w), 2955 (m), 2930 (w), 2870 (w), 1549 (w), 1440 (m), 1410 (s), 1328 (m), 1220 (m), 1104 (m), 753(m).

MS (EI, 70 eV): m/z (%) = 530.2 (90) $[M]^{\cdot+}$, 453.2 (10) $[M- Ph]^+$, 319.1 (100) $[M- Thione]^+$, 211.1 (20) $[Thione]^{\cdot+}$

HRMS: theor./exp. for [$C_{28}H_{43}N_4PS_2$]: 530.2667/530.2671.

EA [%]: theor./exp. C 63.36/63.31, H 8.17/7.98, N 10.56/10.43, S 12.08/12.00.

10.3 Synthesis of 1,4-dihydro-1,4-diphosphinines 4a,b

Compounds **4a,b** were isolated from the reaction mixtures for the synthesis of compounds **3a,b**. For **3a,4a** there was a white precipitate formed, which was filtered off and washed twice with THF (2 × 2 ml) and finally with *n*-pentane (2 × 5 ml) to get pure *trans* isomer of **4a** as a white powder, finally.

For **3b,4b** the reaction mixture was removed in *vacuo* (8×10^{-3} mbar) and then the residue was directly subjected to column chromatography using diethylether/petroleum ether mixtures (1:4) as the eluent. Finally, both **3b** and **4b** were obtained as white powders after evaporation of all volatiles (8×10^{-3} mbar) of the corresponding fractions.

10.3.1 4,8-Bis(dimethylamino)-1,3,5,7-tetramethyl-4,8-dihydro[1,4]diphosphinine[2,3-d:5,6-d']bisimidazole-2,6-dithione (4a)

Yield: 0.11 g (0.3 mmol, 4.5 %) **Appearance:** white powder **melting point:** 358 °C

^{1}H NMR (300 MHz, $CDCl_3$): δ = 2.52 (br, 12H, P-N$\underline{Me_2}$), 3.76 (s, 12H, N-$\underline{Me}$).

^{13}C NMR (75.0 MHz, $CDCl_3$): δ = 34.5 (t, $^3J_{P,C}$ = 4.8 Hz, N-$\underline{Me}$), 40.0 (br, P-N$\underline{Me_2}$), 129.3 (s, $C^{4,5}$), 167.9 (s, $\underline{C{=}S}$).

^{31}P NMR (121.5 MHz, $CDCl_3$): δ = 9.4 (hept. $^3J_{P,H}$ = 3.6 Hz).

IR [cm^{-1}]: $\tilde{\nu}$ = 3376 (m), 2889 (w), 2800 (w), 1639 (w), 1427 (m), 1366 (s), 1334 (m), 1277 (m), 1161 (s), 1066 (w), 979 (s), 851 (s).

MS (EI, 70 eV): m/z (%) = 402.0 (70) $[M]^{\cdot+}$, 358.0 (15) $[M\text{-}NMe_2]^+$, 315.0 (100) $[M\text{-}NMe_2\text{-}C_2H_5N]^+$.

HRMS: theor./exp. for [$C_{14}H_{24}N_6P_2S_2$]: 402.0974/402.0978.

EA [%]: theor./exp. C 41.78/41.28 , H 6.01/6.08, N 20.88/19.29, S 15.93/14.46.

10.3.2 4,8-Bis(dimethylamino)-1,3,5,7-tetraethyl-4,8-dihydro[1,4]diphosphinine[2,3-d:5,6-d']bisimidazole-2,6-dithione (4b)

Yield: 0.23 g (0.5 mmol, 15.9 %) **Appearance:** white powder **melting point:** decom. at 165 °C

^{1}H NMR (300 MHz, $CDCl_3$): δ = 1.41 & 1.42(t, 12H, $^{3}J_{H,H}$ = 7.1 Hz, *Me*CH_2N) ratio 1:3, 2.52 (br, 6H, P-N*Me*$_2$), 2.70 (d, 6H, $^{3}J_{P,H}$ = 8.1 Hz, P- N*Me*$_2$ *2nd isomer*), 4.10-4.22 (m, 4H, Me*CH*$_2$N), 4.32-4.49 (m, 4H, Me*CH*$_2$N *2nd isomer*).

^{13}C NMR (75.0 MHz, $CDCl_3$): δ = 12.4 (s, *Me*CH_2N), 38.6 (br, P- N*Me*$_2$), 41.6 (two d merged as t, Me*CH*$_2$N), 127.3 (s, *C*^{4,5}), 165.2 (s, ***C***=*S*).

^{31}P NMR (121.5 MHz, $CDCl_3$): δ = 8.61 & 8.71 (br ,3:1) two isomers.

IR [cm^{-1}]: $\tilde{\nu}$ = 2976 (w), 2752 (s), 2485 (s), 1732 (w), 1637 (w), 1443 (w), 1410 (m), 1191 (s), 1041 (s), 797 (s).

MS (EI, 70 eV): m/z (%) = 458.2 (50) $[M]^{\cdot+}$, 341.2 (100) $[M- 2NMe_2 +H]^{+}$, 156.1 (10) $[C_7H_{12}N_2S]^{\cdot+}$.

HRMS: theor./exp. for $[C_{18}H_{32}N_6P_2S_2]$: 458.1605/458.1607.

EA [%]: theor./exp. C 47.15/46.65, H 7.02/6.87, N 18.33/17.76, S 13.98/14.28.

10.4 Synthesis of the backbone amino(chloro)substituted imidazole-2-thiones 5a-f

A solution of **7a-f** (5.6 mmol) in 35 ml diethyl ether was treated with PCl_3 (6.1 mmol, 1.1 equiv) at –40 °C. The reaction mixture was then allowed to warm up slowly till ambient temperature (2h) (for **7d** it was stirred at r.t. for overnight, and for **7e** it was slightly warmed for 1h), after which the solvent was removed under reduced pressure (8×10^{-3} mbar) to get a yellow oily residue. Then 20 ml of *n*-pentane was added to the residue and stirred for few minutes, which results in removal of all the by-products and resulted in the formation of a fine white powder. The powder was then separated by cannula filtration and dried *in vacuo* (8×10^{-3} mbar) to get the pure compounds.

10.4.1 1,3-Dimethyl-4-diethylaminochlorophosphanyl-imidazole-2-thione (5a)

Yield: 1.29 g (4.9 mmol, 87.5 %) **Appearance:** white powder **melting point:** 51 °C

^{1}H NMR (300 MHz, $CDCl_3$): δ = 1.07 (t, 6H, $^{3}J_{H,H}$ = 7.2 Hz, *CH*$_3$$CH_2N$), 3.08 (q, 2H, $^{3}J_{H,H}$ = 7.2 Hz, CH_3*CH*$_2$N), 3.12 (q, 2H, $^{3}J_{H,H}$ = 7.3 Hz, CH_3*CH*$_2$N), 3.56 (s, 3H, N^1-*CH*$_3$), 3.61 (s, 3H, N^3- *CH*$_3$), 7.09 (d, 1H, $^{3}J_{P,H}$ = 2.4Hz, C^{5}H).

^{13}C NMR (75.0 MHz, $CDCl_3$): δ = 13.9 (d, $^{3}J_{P,C}$ = 6.8 Hz, *CH*$_3$$CH_2$N-P), 33.5 (d, $^{3}J_{P,C}$ = 6.6 Hz, N^3-*CH*$_3$), 35.4 (s, N^1- *CH*$_3$), 43.5(d, $^{2}J_{PC}$ = 14.2 Hz, CH_3 *CH*$_3$N), 125.2(d, $^{2}J_{P,C}$ = 8.1 Hz, **C^5**), 126.2 (d, $^{1}J_{P,C}$ = 29.1 Hz, **C^4**), 166.3 (s, **C**=S).

^{31}P NMR (121.5 MHz, $CDCl_3$): δ = 106.06 (quint, $^3J_{P,H}$ = 12.2 Hz).

IR [cm^{-1}]: ṽ = 3152 (w), 2964 (s), 2822 (m), 2481 (m), 1561 (w), 1375 (s), 1152 (s), 1021 (s), 939 (s), 793 (s).

MS (EI, 70 eV): m/z (%) = 265.0 (30) $[M]^{\cdot+}$, 230.0 (10) $[M- Cl]^+$, 192.9 (15) $[M- NEt_2]^+$, 128.0 (100) $[C_5H_8N_2S]^+$

HRMS: theor./exp. for $[C_9H_{17}N_3PClS]$: 265.0569/265.0568.

EA [%]: theor./exp. C 40.65/40.68, H 6.47/6.45, N 15.71/15.81, S 12.11/12.07.

10.4.2 1,3-Diethyl-4-diethylaminochlorophosphanyl-imidazole-2-thione (5b)

Yield: 1.30 g (4.4 mmol, 78.5 %) **Appearance:** white powder **melting point:** 59 °C

^{1}H NMR (300 MHz, $CDCl_3$): δ = 1.10 (t, 6H, $^3J_{H,H}$ = 7.1 Hz, $\underline{CH_3}CH_2N$-P), 1.32 (t, 3H, $^3J_{H,H}$ = 7.1 Hz, $\underline{CH_3}CH_2N^1$), 1.39 (t, 3H, $^3J_{H,H}$ = 7.1 Hz, $\underline{CH_3}CH_2N^3$), 3.14 (dq, 4H, $^3J_{P,H}$ = 13.1 Hz, $^3J_{H,H}$ = 7.1 Hz, $CH_3\underline{CH_2}N$-P), 3.93-4.24 (m, 3H, $CH_3\underline{CH_2}N$), 4.27-4.41 (m, 1H, $CH_3\underline{CH_2}N$), 7.15 (d, 1H, $^3J_{P,H}$ = 2.0Hz, $\underline{C^5H}$).

^{13}C NMR (75.0 MHz, $CDCl_3$): δ = 13.8 (s, $\underline{CH_3}CH_2N^1$), 13.9 (s, $\underline{CH_3}CH_2N^3$), 14.2 (s, $\underline{CH_3}CH_2N$-P), 41.3(d, $^3J_{P,C}$ = 6.1 Hz, $CH_3\underline{CH_2}N^3$), 42.9(s, $CH_3\underline{CH_2}N^1$), 43.5(d, $^2J_{P,C}$ = 14.4 Hz, $CH_3\underline{CH_2}N$-P), 123.8(d, $^2J_{P,C}$ = 6.9 Hz, $\underline{C^5}$), 125.8 (d, $^1J_{P,C}$ = 30.8 Hz, $\underline{C^4}$), 164.8 (s, **C**=S).

^{31}P NMR (121.5 MHz, $CDCl_3$): δ = 106.5 (quint, $^3J_{P,H}$ = 11.9 Hz).

IR [cm^{-1}]: ṽ = 3130 (w), 3173 (w), 2969 (m), 2869 (w), 1549 (w), 1414 (s), 1374 (m), 1271 (s),1150 (s), 1022 (s), 941 (s), 791 (s), 667 (s).

MS (EI, 70 eV): m/z (%) = 293.1 (20) $[M]^{\cdot+}$, 221.0 (40) $[M- NEt_2]^+$, 156.0 (100) $[C_7H_{12}N_2S]^+$.

HRMS: theor./exp. for $[C_{11}H_{21}N_3PClS]$: 293.0882/293.0881.

EA [%]: theor./exp. C 44.78/44.79, H 7.29/7.20, N 14.21/14.30, S 10.09/10.91.

10.4.3 1,3-Di-*n*-butyl-4-diethylaminochlorophosphanyl-imidazole-2-thione (5c)

Yield: 1.63 g (4.6 mmol, 82.1 %) **Appearance:** white powder **melting point:** liquid at r.t.

^{1}H NMR (300 MHz, $CDCl_3$): δ = 0.81 and 0.83 (t, 6H, $^{3}J_{H,H}$ = 7.5 Hz, $\underline{CH_3}CH_2CH_2CH_2N$), 0.98 (t, 3H, $^{3}J_{H,H}$ = 7.2 Hz, $\underline{CH_3}CH_2N$-P), 1.19-1.31 (m, 4H, $CH_3\underline{CH_2}CH_2CH_2N$), 1.56-1.71 (m, 4H, $CH_3CH_2\underline{CH_2}CH_2N$), 2.95-3.06 (m, 4H, $CH_3\underline{CH_2}N$-P), 3.69-4.23 (m, 4H, $CH_3CH_2CH_2\underline{CH_2}N$), 7.04 (d, 1H, $^{3}J_{P,H}$ = 2.0 Hz, $\underline{C^5H}$).

^{13}C NMR (75.0 MHz, $CDCl_3$): δ = 13.60 and 13.64 (s, $\underline{CH_3}CH_2CH_2CH_2N$), 13.76 and 13.85 (s, $\underline{CH_3}CH_2N$-P), 19.70 (s, $CH_3\underline{CH_2}CH_2CH_2N^1$), 19.92 (d, $^{5}J_{P,C}$ = 0.9 Hz, $CH_3\underline{CH_2}CH_2CH_2N^3$), 30.45 (d, $^{4}J_{P,C}$ = 4.5 Hz, $CH_3CH_2\underline{CH_2}CH_2N^3$), 30.78 (s, $CH_3CH_2\underline{CH_2}CH_2N^1$), 43.46 (d, $^{2}J_{P,C}$ = 14.2 Hz, $CH_3\underline{CH_2}N$-P), 46.04 (d, $^{2}J_{P,C}$ = 14.2 Hz, $CH_3CH_2CH_2\underline{CH_2}N^3$), 47.73 (s, $CH_3CH_2CH_2\underline{CH_2}N^1$), 124.4(d, $^{2}J_{P,C}$ = 6.8 Hz, $\underline{C^5}$), 125.7 (d, $^{1}J_{P,C}$ = 31.5 Hz, $\underline{C^4}$), 165.2 (s, **C**=S).

^{31}P NMR (121.5 MHz, $CDCl_3$): δ = 106.4 (quint, $^{3}J_{P,H}$ = 12.4 Hz).

IR [cm^{-1}]: $\tilde{\nu}$ = 2958 (m), 2930 (m), 2871 (w), 1551 (w), 1439 (m), 1411 (s), 1378 (m), 1219 (m), 1199 (m), 1167 (m), 1021 (s), 939 (s), 782 (s).

MS (EI, 70 eV): m/z (%) = 349.1 (40) $[M]^{\cdot+}$, 277.0 (100) $[M- NEt_2]^+$.

HRMS: theor./exp. for $[C_{15}H_{29}N_3PClS]$: 349.1508/349.1508.

EA [%]: theor./exp. C 51.49/51.30, H 8.35/8.61, N 12.01/11.53, S 9.16/8.92.

10.4.4 1,3-Diisopropyl-4-diethylaminochlorophosphanyl-imidazole-2-thione (5d)

Yield: 1.67 g (5.2 mmol, 92.8 %) **Appearance:** white powder **melting point:** 68 °C.

^{1}H NMR (300 MHz, $CDCl_3$): δ = 1.08 (t, 6H, $^{3}J_{H,H}$ = 7.2 Hz, $\underline{CH_3}CH_2N$-P), 1.37 (d, 3H, $^{3}J_{H,H}$ = 6.0 Hz N-$CHCH_3\underline{CH_3}$), 1.39 (d, 3H, $^{3}J_{H,H}$ = 6.0 Hz N-$CH\underline{CH_3}CH_3$), 1.51 (d, 3H, $^{3}J_{H,H}$ = 6.8 Hz, N-$CHCH_3\underline{CH_3}$), 1.61 (d, 3H, $^{3}J_{HH}$ = 6.8 Hz N-$CH\underline{CH_3}CH_3$), 3.15-2.95 (m, 4H, $^{3}J_{H,H}$ = 7.2Hz, $^{3}J_{P,H}$ = 2.8 Hz, $CH_3\underline{CH_2}N$-P), 5.17 (sept, 1H, $^{3}J_{H,H}$ = 6.8 Hz, N-$\underline{CH}CH_3CH_3$), 5.27 (bs, 1H, N-$\underline{CH}CH_3CH_3$), 7.29 (d, 1H, $^{3}J_{P,H}$ = 1.4 Hz, $\underline{C^5\text{-}H}$).

^{13}C NMR (75.0 MHz, $CDCl_3$): δ = 12.78 (d, $^{3}J_{P,C}$ = 7.0 Hz, $\underline{CH_3}CH_2N$-P), 19.7 (s, $N^3CHCH_3\underline{CH_3}$), 20.0 (s, $N^3CH\underline{CH_3}CH_3$), 20.8 (s, $N^1CHCH_3\underline{CH_3}$), 20.9 (s, $N^1CH\underline{CH_3}CH_3$), 42.4 (d, $^{2}J_{P,C}$ = 14.8 Hz, $CH_3\underline{CH_2}N$-P), 47.9 (s, $N^1\underline{CH}CH_3CH_3$), 50.3 (s, $N^3\underline{CH}CH_3CH_3$), 120.8 (d, $^{2}J_{P,C}$ = 5.1 Hz, $\underline{C^5}$), 125.5 (d, $^{1}J_{P,C}$ = 39.3 Hz, $\underline{C^4}$), 163.0 (s, $\underline{C{=}S}$).

^{31}P NMR (121.5 MHz, $CDCl_3$): δ = 108.4 (br, s).

IR [cm^{-1}]: $\tilde{\nu}$ = 3129 (w), 2972 (m), 2871 (w), 2823 (w), 2481 (w), 1541 (m), 1413 (s), 1361 (s), 1336 (s), 1286 (s), 1187 (s), 1168 (s), 1019 (s).

MS (EI, 70 eV): m/z (%) = 321.1 (40) $[M]^{\cdot+}$, 286.1 (10) $[M\text{-}Cl]^+$, 249.0 (55) $[M\text{-}NEt_2]^+$, 184.1 (75) $[Thione]^+$.

HRMS: theor./exp. for $[C_{13}H_{25}N_3PClS]$: 321.1195/321.1200.

EA [%]: theor./exp. C 48.51/47.47, H 7.84/7.56, N 13.06/12.43, S 9.96/9.89.

10.4.5 1,3-Dimesityl-4-diethylaminochlorophosphanyl-imidazole-2-thione (5e)

Yield: 2.32 g (4.9 mmol, 87.5 %) **Appearance:** white powder **melting point:** 153 °C.

^{1}H NMR (300 MHz, $CDCl_3$): δ = 0.96 (t, 6H, $^3J_{H,H}$ = 7.1 Hz, *Me*$_2$CHN-P), 2.12 & 2.13 (s, 3H each, *o*-*CH*$_3$ of N^3-Mes), 2.17 (s, 6H, *p*-*CH*$_3$ of Mes), 2.32 & 2.34 (s, 3H, *o*-*CH*$_3$ of N^1-Mes), 2.91-3.24 (m, 4H, Me$_2$*CH*N-P), 6.97 & 6.99 (s, 1H each, *m*-*CH*$_3$ of N^3-Mes), 7.01 (s, 2H, *m*-*CH*$_3$ of N^1-Mes), 7.28 (d, 1H, $^3J_{P,H}$ = 1.7 Hz, *C*^{5}*H*).

^{13}C NMR (75.0 MHz, $CDCl_3$): δ = 13.8 (d, $^3J_{P,C}$ = 7.8 Hz, P-NCH*Me*$_2$), 18.07 (s, *p*-*CH*$_3$ of Mes), 17.95 & 18.00 (s, *o*-*CH*$_3$ of N^3-Mes), 18.23 & 18.35 (s, *o*-*CH*$_3$ of N^3-Mes), 21.20 & 21.24 (s, *o*-*CH*$_3$ of N^1-Mes), 43.4 (d, $^2J_{P,C}$ = 15.9 Hz, P-N*CH*Me$_2$), 125.4(d, $^2J_{P,C}$ = 3.4 Hz, *C*^{5}), 128.4 (d, $^1J_{P,C}$ = 30.4 Hz, *C*^{4}), 129.27, 129.29, 129.44 & 129.46 (s, *m*-*CH* of Mes), 131.7 (d, $^4J_{P,C}$ = 1.3 Hz, *o*-*C* of Mes), 133.4 (s, *o*-*C* of Mes), 135.2 & 135.7 (*ipso*-*C* of Mes),135.8 (d, $^4J_{P,C}$ = 1.6 Hz, *o*-*C* of Mes), 136.9 (s, *o*-*C* of Mes), 139.4 & 139.6 (s, *p*-*C* of Mes), 166.2 (s, *C*=*S*).

^{31}P NMR (121.5 MHz, $CDCl_3$): δ = 102.9 (quint, $^3J_{P,H}$ = 10.8 Hz).

IR [cm^{-1}]: $\tilde{\nu}$ = 3159 (w), 2973 (m), 2916 (w), 1553 (m), 1481 (m), 1370 (m), 1344 (s), 1296 (w), 1026 (s), 946 (s).

MS (EI, 70 eV): m/z (%) = 473.1 (60) $[M]^{\cdot+}$, 438.1 (25) $[M\text{-}Cl]^+$, 401.1 (100) $[M\text{-}NEt_2]^+$.

HRMS: theor./exp. for $[C_{25}H_{33}N_3PClS]$: 473.1821/473.1824.

EA [%]: theor./exp. C 63.34/62.90, H 7.02/7.22, N 8.86/8.74, S 6.76/6.78.

10.4.6 1,3-Dimethyl-4-diisopropylaminochlorophosphanyl-imidazole-2-thione (5f)

Yield: 1.38 g (4.7 mmol, 83.9 %) **Appearance:** white powder **melting point:** 144 °C.

^{1}H NMR (300 MHz, $CDCl_3$): δ = 1.13 (bs, 6H, $\underline{Me_2}$CHN-P), 1.29 (bs, 6H, $\underline{Me_2}$CHN-P), 3.57 (s, 3H, N^1-$\underline{CH_3}$), 3.63 (s, 3H, N^3-$\underline{CH_3}$), 7.13 (d, 1H, $^3J_{P,H}$ = 2.6 Hz, $\underline{C^5H}$).

^{13}C NMR (75.0 MHz, $CDCl_3$): δ = 23.1 (bs, $\underline{Me_2}$CHN-P), 33.4 (d, $^3J_{P,C}$ = 7.2 Hz, N^3-$\underline{CH_3}$), 35.4 (s, N^1-$\underline{CH_3}$), 47.5(s, $Me_2\underline{CH}$N-P), 125.4(d, $^1J_{P,C}$ = 26.9 Hz, $\underline{C^4}$), 126.1 (d, $^2J_{P,C}$ = 8.1 Hz, $\underline{C^5}$), 166.3 (s, $\underline{C{=}S}$).

^{31}P NMR (121.5 MHz, $CDCl_3$): δ = 98.93 (t, $^3J_{P,H}$ = 10.5 Hz).

IR [cm^{-1}]: $\tilde{\nu}$ = 3134 (w), 3084 (w), 2966 (m), 2927 (w), 2720 (w), 2488 (w), 1556 (m), 1458 (m), 1378 (s), 1150 (s), 1015 (m), 971 (s), 796 (s).

MS (EI, 70 eV): m/z (%) = 321.1 (40) $[M]^{\cdot+}$, 286.1 (10) $[M\text{-}Cl]^+$, 249.0 (55) $[M\text{-}NEt_2]^+$, 128.1 (100) $[C_5H_8N_2S]^+$.

HRMS: theor./exp. for $[C_{11}H_{21}N_3PClS]$: 293.0882/293.0884.

EA [%]: theor./exp. C 44.97/45.02, H 7.20/7.43, N 14.30/14.15, S 10.91/10.50.

10.5 Reaction of compound 5 with KHMDS

To a solution of **5** (4.1 mmol) in 25 mL of THF, a solution of KHMDS (0.826 g, 4.1 mmol, 1equiv) in THF (30 mL) was added at –78 °C. Then the reaction mixture was slowly warmed to room temperature (2h). Afterwards the solvent was removed in *vacuo* (8×10^{-3} mbar) to get a yellow oil, which was again dissolved in 30 ml of toluene. This solution was filtered through a small celite® bed to remove KCl. Then the filtrate was concentrated in *vacuo* (8×10^{-3} mbar) until a yellow oil was obtained as crude product. This was then triturated with 10 ml of *n*-pentane at room temperature to get a white powder, which was dried *in vacuo* (8×10^{-3} mbar) after removal of the *n*-pentane.

10.5.1 1,3-Dimethyl-4-{bis(trimethylsilyl)amino}diethylaminophosphanyl-imidazole-2-thione (8a)

Yield: 1.1g (2.8 mmol, 68.9 %) **Appearance:** white powder **melting point:** 108 °C.

^{1}H NMR (300 MHz, $CDCl_3$): δ = 0.166 & 0.169 (s, 18H, Si$\underline{Me_3}$), 1.05(t, 6H, $^3J_{H,H}$ = 7.2 Hz, $\underline{CH_3}CH_2$N-P), 3.05-3.19 (m, 4H, $CH_3\underline{CH_2}$N-P), 3.54 (s, N^3-$\underline{CH_3}$), 3.57 (s, N^1-$\underline{CH_3}$), 6.45 (d, 1H, $^3J_{P,H}$ = 2.8 Hz, $\underline{C^5H}$).

^{13}C NMR (75.0 MHz, $CDCl_3$): δ = 4.29 (d, $^2J_{Si,P}$= 7.4 Hz, N-Si$\underline{Me_3}$), 14.5 (d, $^3J_{P,C}$ = 2.9 Hz, $\underline{CH_3}CH_2$N-P), 33.6 (d, $^2J_{P,C}$ = 7.1 Hz, N^3-$\underline{CH_3}$), 35.1 (s, N^1-$\underline{CH_3}$), 42.3 (d, $^2J_{P,C}$ = 19.9 Hz, $CH_3\underline{CH_2}$N-P), 120.8 (d, $^2J_{P,C}$ = 7.4 Hz, $\underline{C^5}$), 133.0 (d, $^1J_{P,C}$ = 29.5 Hz, $\underline{C^4}$), 164.3 (s, $\underline{C{=}S}$).

^{31}P NMR (121.5 MHz, $CDCl_3$): δ = 74.92 (bs).

^{29}Si NMR (59.5 MHz, $CDCl_3$, 25 °C): δ = 7.62 (d, $^2J_{Si,P}$ = 7.0 Hz).

IR [cm^{-1}]: $\tilde{\nu}$ = 3139 (w), 2966 (m), 1552 (w), 1381 (m), 1251 (m), 1178 (m), 1016 (m), 917 (s).

MS (EI, 70 eV): m/z (%) = 390.1 (20) $[M]^{\cdot+}$, 318.1 (100) $[M\text{-}NEt_2]^+$, 317.1 (20) $[M\text{-}TMS]^+$, 128.0 (100) $[C_5H_8N_2S]^+$.

HRMS: theor./exp. for $[C_{15}H_{35}N_4PSSi_2]$: 390.1859/390.1858.

EA [%]: theor./exp. C 46.12/45.84, H 9.03/8.66; N 14.34/14.41, S 8.21/8.16.

10.5.1 1,3-Diisopropyl-4-{bis(trimethylsilyl)amino}diethylaminophosphanyl-imidazole-2-thione (8b)

Yield: 1.47 g (3.3 mmol, 80.5 %) **Appearance:** white powder **melting point:** 55 °C.

^{1}H NMR (300 MHz, $CDCl_3$): δ = 0.18 (s, 18H, Si*Me*$_3$), 1.04 (t, 6H, $^3J_{H,H}$ = 7.2 Hz, *Me*CH_2N-P), 1.27 (d, 3H, $^3J_{H,H}$ = 6.8 Hz N^3-CHMe*Me*), 1.30 (d, 3H, $^3J_{H,H}$ = 6.8 Hz N^3-CH*Me*Me), 1.69 (d, 3H, $^3J_{H,H}$ = 6.8 Hz N^1-CHMe*Me*), 1.78 (d, 3H, $^3J_{H,H}$ = 6.8 Hz N^1-CH*Me*Me), 3.11 (br quintet, 4H, $^3J_{H,H}$ = 7.2Hz, Me*CH*$_2$N-P), 4.61 (br, 1H, N^3-*CH*MeMe), 5.17 (sept, 1H, $^3J_{HH}$ = 6.8 Hz, N^1-*CH*MeMe), 6.59 (d, 1H, $^3J_{P,H}$ = 2.0 Hz, *C^{5}H*).

^{13}C NMR (75.0 MHz, $CDCl_3$): δ = 4.2 & 4.3 (s, N-Si*Me*$_3$), 14.3 (d, $^4J_{P,C}$ = 2.8 Hz, *Me*CH_2N-P), 19.8(s, N^3-CHMe*Me*), 19.9(s, N^3 CH*Me*Me), 21.6(s, N^1 CHMe*Me*), 22.3(s, N^1 CH*Me*Me), 42.3 (d, $^2J_{P,C}$ =19.9 Hz, Me*CH*$_2$N-P), 47.2(s, N^1 *CH*MeMe), 51.3(d, $^4J_{PC}$ = 10.9 Hz, N^3*CH*MeMe), 117.2(d, $^2J_{P,C}$ = 5.9 Hz, *C^5*), 133.6 (d, $^1J_{P,C}$ = 36.1 Hz, *C^4*), 160.9 (s, *C=S*).

^{31}P NMR (121.5 MHz, $CDCl_3$): δ = 74.9 (br).

^{29}Si NMR (59.5 MHz, $CDCl_3$, 25 °C): δ = 6.90 (d, $^2J_{Si,P}$ = 7.2 Hz).

IR [cm^{-1}]: $\tilde{\nu}$ = 3142 (w), 2972 (s), 1550 (w), 1432 (m), 1313 (m), 1190 (m), 1020 (m), 927 (s).

MS (EI, 70 eV): m/z (%) = 446.3 (80) $[M]^{\cdot+}$, 374.2 (25) $[M\text{-}NEt_2]^+$, 373.2 (20) $[M\text{-}TMS]^+$,263.2 (100) $[C_{10}H_{28}N_2PSi_2]^+$.

HRMS: theor./exp. for $[C_{19}H_{43}N_4PSSi_2]$: 446.2485/446.2484.

EA [%]: theor./exp. C 51.08/50.43, H 9.70/9.50; N 12.54/12.26, S 7.18/7.26.

10.6 Synthesis of 1,4-dihydro-1,4-diphosphinines 4d-f

A solution of LDA (50.58 mmol) in 50 ml of THF was added dropwise to a solution of **5a-c** (45.16 mmol) in 120 mL of THF with continuous stirring through a double-ended needle over 30 minutes at -80 ˚C. The reaction mixture was then allowed to warm up to ambient temperature overnight. The solvent was then removed to get a dark brown residue which was taken up in 120 ml of methylene dichloride and filtered through a celite® bed to remove LiCl formed during the course of the reaction. The filtrate was concentrated under reduced pressure (8×10^{-3} mbar) to obtain a light brown solid which was then washed again with *n*-pentane (3×10 ml) to get a white powder and, finally, dried under reduced pressure (8×10^{-3} mbar) for 2 h to get the pure compounds as *cis/trans* mixtures (ratio 1:1.7 for **4d**, 1:1.4 for **4e**, 1:9 for **4f**).

10.6.1 4,8-Bis(diethylamino)-1,3,5,7-tetramethyl-4,8-dihydro[1,4]diphosphinine[2,3-d:5,6-d']bisimidazole-2,6-dithione (4d)

Yield: 8.7g (18.9 mmol, 84.4 %) **Appearance:** white powder **melting point:** 160 °C

^{1}H NMR (300 MHz, $CDCl_3$): δ = 0.88 (br s, 12H, P-NCH$_2$*Me*), 0.97 (t, 12H, $^{3}J_{H,H}$ = 7.0 Hz, P-NCH$_2$*Me*) (2nd isomer), 2.86 (bs, 8H, P-N*CH$_2$*Me), 3.06 (quint, 8H, $^{3}J_{H,H}$ = 7.0 Hz, P-N*CH$_2$*Me) (2nd isomer), 3.73 (s, 12H, N-*CH$_3$*), 3.78 (s, 12H, N-*CH$_3$*)(2nd isomer).

^{13}C NMR (75.0 MHz, $CDCl_3$): δ = 14.0 (bs, *CH$_3$*CH$_2$N-P), 14.1 (d, $^{3}J_{P,C}$ =4.6 Hz , *CH$_3$*CH$_2$N-P) (2nd isomer), 32.9 (d, $^{2}J_{P,C}$ =9.8 Hz, N-*CH$_3$*), 34.6 (t, $^{2}J_{P,C}$ = 5.0 Hz , N-*CH$_3$*) (2nd isomer), 43.3 (bs, P-N*CH$_2$*Me), 44.1 (d, $^{2}J_{P,C}$ = 16.9 Hz, P-N*CH$_2$*Me) (2nd isomer), 125.5 (t, $^{1}J_{P,C}$ = 3.5Hz, *P-C* of middle ring), 129.9 (t, $^{1}J_{P,C}$ = 0.99 Hz, *P-C* of middle ring) (2nd isomer), 167.6 (t, $^{3}J_{P,C}$ = 1.5 Hz, *C=S*), 167.7 (t, $^{3}J_{P,C}$ = 1.4 Hz, *C=S*) (2nd isomer).

^{31}P NMR (121.5 MHz, $CDCl_3$): δ = 3.30 (quint, $^{3}J_{P,H}$ = 7.1 Hz), 3.79 (m) two isomers (ratio 1:1.7).

IR [cm^{-1}]: ṽ = 2970 (m), 2363 (w), 1732 (w), 1460 (m), 1426 (m), 1377 (s), 1161 (s), 1018 (s), 931 (s), 852 (s).

MS (EI, 70 eV): m/z (%) = 458.2 (90) $[M]^{\cdot+}$, 386.1 (10) $[M\text{-}NEt_2]^{+}$, 315.0 (100) $[M\text{-}2NEt_2\text{+}H]^{+}$, 128.0 (50) $[C_5H_8N_2S]^{+}$, 72.1 (100) $[NEt_2]^{+}$.

HRMS: theor./exp. for $[C_{18}H_{32}N_6P_2S_2]$: 458.1605/ 458.1605.

EA [%]:theor./exp. C 47.15/46.86, H 7.03/7.14; N 18.33/17.74, S 13.98/13.56.

10.6.2 4,8-Bis(diethylamino)-1,3,5,7-tetraethyl-4,8-dihydro[1,4]diphosphinine[2,3 -d:5,6-d']bisimidazole-2,6-dithione (4e)

Yield: 7.21 g (14.1 mmol, 61.9 %) **Appearance:** white powder **melting point:** decom. at 165°C

^{1}H NMR (300 MHz, $CDCl_3$): δ = 0.84 (br, 12H, P-NCH_2*Me*), 0.99 (t, 12H, $^3J_{H,H}$ = 6.7 Hz, P-NCH_2*Me*) (2nd isomer), 1.39(t, 12H, $^3J_{H,H}$ = 5.9 Hz, NCH_2*Me*), 1.42 (t, 12H, $^3J_{H,H}$ = 6.8 Hz, NCH_2*Me*) (2nd isomer), 2.83 (br, 8H, P-N*CH_2*Me), 3.09 (quintet, 8H, $^3J_{H,H}$ = 7.0 Hz, P-N*CH_2*Me) (2nd isomer), 4.05 (m, 4H, N*CH_2*Me), 4.40-4.66 (m, 4H, N*CH_2*Me).

^{13}C NMR (75.0 MHz, $CDCl_3$): δ = 13.6 (br, NCH_2*Me*), 13.8 (br, NCH_2*Me*) (2nd isomer), 14.0 (br, P-NCH_2*Me*), 14.1 (d, $^2J_{P,C}$ = 5.1 Hz , P-NCH_2*Me*) (2nd isomer), 40.9 (m, N*CH_2*Me), 42.1 (t, $^2J_{P,C}$= 4.1 Hz, N*CH_2*Me) (2nd isomer), 43.3 (br, P- N*CH_2*Me), 43.5 (br, P- N*CH_2*Me) (2nd isomer), 125.3 (t, $^1J_{P,C}$ = 2.4 Hz, *P-C*), 129.2 (t, $^1J_{P,C}$ = 2.0 Hz, *P-C*) (2nd isomer), 166.1 (br, *C=S*).

^{31}P NMR (121.5 MHz, $CDCl_3$): δ = 0.4 & 2.9 (br, two isomers, ratio 1:1.4).

IR [cm^{-1}]: $\tilde{\nu}$ = 2969 (m), 2932 (m), 2829 (w), 1437 (m), 1400 (s), 1267 (s), 1150 (s), 1016 (s), 977 (s), 926 (s), 791 (s).

MS (EI, 70 eV): m/z (%) = 514.1 (50) $[M]^{\cdot+}$, 371.0 (100) $[M-2NEt_2+H]^+$, 72.0 (40) $[NEt_2]^+$.

HRMS: theor./exp. for $[C_{22}H_{40}N_6P_2S_2]$: 514.2231/514.2231.

EA [%]: theor./exp. C 51.34/51.27, H 7.83/7.69; N 16.33/16.16, S 12.46/12.42.

10.6.3 4,8-Bis(diethylamino)-1,3,5,7-tetra-*n*-butyl-4,8-dihydro[1,4]diphosphinine [2,3 -d:5,6-d']bisimidazole-2,6-dithione (4f)

Yield: 7.7 g (11.3 mmol, 50.3 %) **Appearance:** white powder **melting point:** 155 °C

^{1}H NMR (300 MHz, $CDCl_3$): δ = 0.89 (bs, 12H, P-NCH_2*Me*), 0.99 (t, 12H, $^3J_{H,H}$ = 7.4 Hz, $NCH_2CH_2CH_2$*Me*), 1.38-1.50 (m, 8H, NCH_2CH_2*CH_2*Me), 1.76-2.00 (m, 8H, NCH_2*CH_2*CH_2Me), 2.85 (bs, 8H, P-N*CH_2*Me), 3.89-4.02 (m, 4H, N*CH_2*CH_2CH_2Me), 4.49-4.60 (m, 4H, N*CH_2*CH_2CH_2Me) (2^{nd} isomer).

^{13}C NMR (75.0 MHz, $CDCl_3$): δ = 13.8 (s, $NCH_2CH_2CH_2$*Me*), 14.0 (bs, P-NCH_2*CH_3*), 20.1 (s, NCH_2CH_2*CH_2*Me), 20.2 (s, NCH_2CH_2*CH_2*Me) (2^{nd} isomer), 30.2 (bs, NCH_2*CH_2*CH_2Me), 30.4 (t, $^3J_{P,C}$ = 1.4 Hz, NCH_2*CH_2*CH_2Me) (2^{nd} isomer), 44.3 (d, $^2J_{P,C}$ = 17.9 Hz, P-N*CH_2*CH_3), 45.8 (bs, N*CH_2*CH_2CH_2Me),

46.9 (t, $^{2}J_{P,C}$ = 3.4 Hz, N*CH*$_2$CH$_2$CH$_2$Me) (2nd isomer), 125.7 (bs, *P-C* of the middle ring), 129.3 (t, $^{1}J_{P,C}$ = 2.3 Hz, *P-C* of the middle ring) (2nd isomer), 166.5 (t, $^{3}J_{P,C}$ = 1.5 Hz, *C=S*).

^{31}P NMR (121.5 MHz, $CDCl_3$): δ = 0.19 (bs) and 3.62 (bs) two isomers. ratio 1:9.

IR [cm^{-1}]: $\tilde{\nu}$ = 2956 (m), 2930 (m), 2870 (w), 1464 (w), 1434 (w), 1398 (s), 1217 (m), 1176 (m), 1146 (m), 1016 (S), 926 (s).

MS (EI, 70 eV): m/z (%) = 626.3 (40) $[M]^{\cdot+}$, 483.1 (100) $[M\text{-}2NEt_2+H]^+$.

HRMS: theor./exp. for $[C_{30}H_{56}N_6P_2S_2]$: 626.3483/626.3483.

EA [%]:theor./exp. C 57.48/57.53, H 9.00/9.05; N 13.41/13.31, S 10.23/10.15.

10.7 Substitution reaction at the P-center of amino(chloro)compounds/ synthesis of 9a-c

In a Schlenk flask, diphenylmethane (12.4 mmol, for **9a**) or fluorene (12.4 mmol, for **9b,c**) was dissolved in 80 ml of THF and 7.94 ml of ^{n}BuLi (1.6 M in hexane) was added dropwise at -78 °C. The reaction mixture was stirred at this temperature for 1h to complete the lithiation. In the meantime, in a separate Schlenk flask 4g of **5** was dissolved in 60 ml of THF and cooled down to -78 °C. Then the solution of lithiated salt was transferred into the solution of **5**, through a double-ended needle over 15 minutes. After that the reaction mixture was warmed up to ambient temperature and the solvent was removed under reduced pressure to get a yellow solid residue, which was then taken up in 60 ml of methylene dichloride. The solution of the residue was filtered through a layer of Celite® using a G3 frit, to remove the LiCl. The filtrate was concentrated *in vacuo* to get the crude product as a yellow solid, which was then washed with minimum amounts of toluene (~5 mL) followed by washing with *n*-pentane (2 × 15 ml) to remove the coloring impurities. Finally the compound was dried under reduced pressure (8×10^{-3} mbar) to get **9a-c** as white powder.

10.7.1 1,3-Diisopropyl-4-diethylamino(diphenylmethyl)phosphanyl-imidazole-2-thione (9a)

Yield: 2.8 g (7.5 mmol, 60.4 %), **Appearance:** white powder **melting point:** 185 °C

^{1}H NMR (300 MHz, $CDCl_3$): δ = 0.56 (t, 6H, $^{3}J_{H,H}$ = 7.0 Hz, P-NCH$_2$*CH*$_3$), 1.11 (d, 3H, $^{3}J_{H,H}$ = 6.8 Hz, N^{1}CH*CH*$_3$CH$_3$), 1.34 (d, 3H, $^{3}J_{H,H}$ = 6.8 Hz, N^{1}CHCH$_3$*CH*$_3$), 1.61 (d, 3H, $^{3}J_{H,H}$ = 6.9 Hz, N^{3}CHCH$_3$*CH*$_3$), 1.66 (d, 3H, $^{3}J_{H,H}$ = 6.9 Hz, N^{3}CH*CH*$_3$CH$_3$), 2.78-3.03 (m, 4H, P-N*CH*$_2$CH$_3$), 4.67 (d, 1H, $^{3}J_{H,H}$ = 3.4 Hz, P-*CH*),

5.08 (sept, 1H, $^{3}J_{H,H}$ = 6.8 Hz, $N^{1}\underline{CH}CH_3CH_3$), 5.47 (bs, 1H, $N^{3}\underline{CH}CH_3CH_3$), 6.76 (s, 1H, $\underline{C^{5}H}$), 7.10 – 7.49 (m, 10H, *Ph ring protons*).

^{13}C NMR (75.0 MHz, $CDCl_3$): δ = 13.6 (bs, $\underline{CH_3}CH_2$N-P), 21.4 (s, $N^{1}CH\underline{Me_2}$), 22.2 (s, $N^{3}CH\underline{Me_2}$), 43.3 (d, $^{2}J_{P,C}$ = 15.7 Hz, $CH_3\underline{CH_2}$N-P), 48.4 (s, $N^{1}\underline{CH}Me_2$), 50.5 (s, $N^{3}\underline{CH}Me_2$), 51.52 (d, $^{2}J_{P,C}$ = 11 Hz, P-$\underline{CH}$) 126.6 (d, $^{2}J_{P,C}$ = 8.1 Hz, $\underline{C^{5}}$), 128.2 (d, $^{1}J_{P,C}$ = 34.5 Hz, $\underline{C^{4}}$), 128.3 (d, $^{1}J_{P,C}$ = 34.4 Hz, P-$\underline{CH}$), 128.7 (s, o-$\underline{C}$ of Ph), 128.8 (s, m-$\underline{C}$ of Ph), 128.9 (s, p-$\underline{C}$ of Ph), 141.3 (d, $^{2}J_{P,C}$ = 14.6 Hz, quart-$\underline{C}$ Ph ring), 141.8 (d, $^{2}J_{P,C}$ = 14.6 Hz, quart-$\underline{C}$ Ph ring), 161.3 (s, $\underline{C{=}S}$).

^{31}P NMR (121.5 MHz, $CDCl_3$): δ = 34.9 (br. s).

MS (EI, 70 eV): m/z (%) = 453 (50) $[M]^{\cdot+}$, 286 (100) $[M\text{-}Ph_2CH]^{+}$, 184.1 (10) $[C_9H_{16}N_2S]^{+}$, 167 (30) $[Ph_2CH]^{+}$

HRMS: theor./exp. for $[C_{26}H_{36}N_3PS]$: 453.2365/453.2366.

EA [%]:theor./exp. C 68.84/67.94, H 8.00/8.15; N 9.26/8.95, S 7.07/6.85.

10.7.2 1,3-Dimesityl-4-diethylamino(fluorenyl)phosphanyl-imidazole-2-thione (9b)

Yield: 4.47 g, (7.4 mmol, 59.6 %) **Appearance:** white powder **melting point:** 207 °C

^{1}H NMR (300 MHz, $CDCl_3$): δ = 0.82 (t, 6H, $^{3}J_{HH}$ = 7.2 Hz, P-$NCH_2\underline{CH_3}$), 1.62 & 2.12 (s, 3H each, *o*-$\underline{CH_3}$ of N^{3}-Mes), 2.18 & 2.19 (s, 3H each, *p*-$\underline{CH_3}$ of Mes), 2.33 & 2.41 (s, 3H, *o*-$\underline{CH_3}$ of N^{1}-Mes), 2.78-2.92 (m, 4H, $Me_2\underline{CH}$N-P), 4.46 (s, $\underline{C^{9}\text{-}H}$ of Flu), 6.71 & 6.86 (s, 1H each, *m*-$\underline{CH}$ of N^{3}-Mes), 6.76 (d, 1H, $^{3}J_{P,H}$ = 0.5 Hz, $\underline{C^{5}H}$), 7.01-7.67 (m, 10H, *Flu ring protons* and *m*-$\underline{CH}$ of N^{1}-Mes).

^{13}C NMR (75.0 MHz, $CDCl_3$): δ = 14.8 (d, $^{3}J_{PC}$ = 3.9 Hz, $\underline{CH_3}CH_2$N-P), 18.3 (s, *p*-$\underline{CH_3}$ of Mes), 18.5 (d, $^{4}J_{PC}$ = 0.6 Hz, *o*-$\underline{CH_3}$ of N^{3}-Mes), 18.7 (d, $^{4}J_{PC}$ = 4.4 Hz, *o*-$\underline{CH_3}$ of N^{3}-Mes), 21.1 & 21.3 (s, *o*-$\underline{CH_3}$ of N^{1}-Mes), 45.2 (d, $^{2}J_{P,C}$ = 15.7 Hz, P-$N\underline{CH}Me_2$), 46.5 (d, $^{1}J_{P,C}$ = 21.7 Hz, P-$\underline{CH}$ of Flu), 122.2 (d, $^{2}J_{P,C}$ = 4.4 Hz, $\underline{C^{5}}$),120.1 & 120.2 (s, $\underline{CH}$ of Flu), 126.1 (d, $J_{P,C}$ = 2.2 Hz, $\underline{CH}$ of Flu), 126.2 (d, $J_{P,C}$ = 5.2 Hz, $\underline{CH}$ of Flu), 126.3 (d, $J_{P,C}$ = 3.5 Hz, $\underline{CH}$ of Flu), 126.6 (d, $J_{P,C}$ = 4.0 Hz, $\underline{CH}$ of Flu), 127.2 (d, $J_{P,C}$ = 3.9 Hz, $\underline{CH}$ of Flu), 127.3 (d, $J_{P,C}$ = 3.4 Hz, $\underline{CH}$ of Flu), 128.9, 129.2, 129.5 & 129.6 (s, *m*-$\underline{CH}$ of Mes), 131.5 (d, $^{1}J_{P,C}$ = 25.7 Hz, **C^{4}**), 132.5 (d, $^{4}J_{P,C}$ = 1.5 Hz, *o*-$\underline{C}$ of Mes), 133.7 (s, *o*-$\underline{C}$ of Mes), 135.74 (s, *o*-$\underline{C}$ of Mes), 135.5 & 135.7 (*ipso*-$\underline{C}$ of Mes), 136.1 (d, $^{4}J_{P,C}$ = 1.3 Hz, *o*-$\underline{C}$ of Mes), 139.1 & 139.6 (s, *p*-$\underline{C}$ of Mes), 141.1 (d, $J_{P,C}$ = 8.8 Hz, quart-$\underline{C}$ Flu), 141.2 (d, $J_{P,C}$ = 1.5 Hz, quart-$\underline{C}$ Flu), 141.8 (d, $J_{P,C}$ = 3.1 Hz, quart-$\underline{C}$ Flu), 143.1 (d, $J_{P,C}$ = 7.8 Hz, quart-$\underline{C}$ Flu), 165.1 (s, $\underline{C{=}S}$).

^{31}P NMR (121.5 MHz, $CDCl_3$): δ = 30.6 (quint, $^{3}J_{P,H}$ = 8.6 Hz).

MS (EI, 70 eV): m/z (%) = 603.3 (30) $[M]^{\cdot+}$, 531.2 (70) $[M\text{-}NEt_2]^+$, 438.2 (100) $[M\text{-}Flu]^+$.

HRMS: theor./exp. for $[C_{38}H_{42}N_3PS]$: 603.2833/603.2833.

EA [%]:theor./exp. C 75.59/75.23, H 7.01/7.05; N 6.96/6.90, S 5.31/5.54.

10.7.3 1,3-Diisopropyl-4-diethylamino(fluorenyl)phosphanyl-imidazole-2-thione (9c)

Yield: 4.15 g, (9.2 mmol, 74.2 %) **Appearance:** white powder **melting point:** 182 °C

^{1}H NMR (300 MHz, $CDCl_3$): δ = 0.89 (t, 6H, $^3J_{HH,}$ = 7.1 Hz, P-$NCH_2\underline{CH_3}$), 1.36 (bs, 3H, $N^3CH\underline{CH_3}CH_3$), 1.42(d, 3H, $^3J_{H,H}$ = 6.8 Hz, $N^1CH\underline{CH_3}CH_3$), 1.47 (d, 3H, $^3J_{H,H}$ = 6.8 Hz, $N^1CHCH_3\underline{CH_3}$), 1.51 (d, 3H, $^3J_{H,H}$ = 6.9 Hz, $N^3CHCH_3\underline{CH_3}$), 3.02-3.29 (m, 4H, P-N-$\underline{CH_2}CH_3$), 4.81 (s, $\underline{C^9\text{-}H}$ of fluorene), 5.32 (sept, 1H, $^3J_{H,H}$ = 6.8 Hz, $N^1\underline{CH}CH_3CH_3$), 5.57 (bs, 1H, $N^3\underline{CH}CH_3CH_3$), 6.86 & 7.11 (t, $^3J_{H,H}$ = 7.3 Hz; & d, $^3J_{H,H}$ = 7.7 Hz, $\underline{C^1\ \&\ C^8\text{-}H}$ of fluorene), 7.20 (s, 1H, $\underline{C^5H}$), 7.33 (m, 2H, $\underline{C^2\ \&\ C^7\text{-}H}$ of fluorene), 7.40 (m, 2H, $\underline{C^3\ \&\ C^6\text{-}H}$ of fluorene), 7.82 & 7.84 (d, 1H, $^3J_{H,H}$ = 3.9 Hz; & d, 1H, $^3J_{HH}$ = 4.9 Hz, $\underline{C^4\ \&\ C^5\text{-}H}$ of fluorene).

^{13}C NMR (75.0 MHz, $CDCl_3$): δ = 14.2 (bs, $\underline{CH_3}CH_2$N-P), 22.0 (s, $N^1CH\underline{Me_2}$), 22.2 (s, $N^3CH\underline{Me_2}$), 45.1 (d,$^2J_{P,C}$ = 16.5 Hz, $CH_3\underline{CH_2}$N-P), 48.3 (d, $^1J_{P,C}$ = 85.2 Hz, $\underline{P\text{-}CH}$), 50.5 (s, $N^1\underline{CH}Me_2$), 50.6 (s, $N^3\underline{CH}Me_2$), 120.2 (d, $^2J_{P,C}$ = 14.3 Hz, $\underline{C^5}$), 125.2 & 126.3 (d, $^3J_{PC}$ = 4.1 Hz; & d, $^3J_{PC}$ = 4.4 Hz, $\underline{C^1\ \&\ C^8}$ of fluorene), 126.5 & 127.3 (d, $^5J_{P,C}$ = 1.8 Hz; & d, $^5J_{P,C}$ = 1.9 Hz, **C^3** & **C^6** fluorene), 126.6 & 127.2 (d, $^4J_{P,C}$ = 2.3 Hz; & d, $^4J_{P,C}$ = 2.3 Hz, $\underline{C^2\ \&\ C^7}$ fluorene), 129.5 (d, $^1J_{P,C}$ = 34.1 Hz, $\underline{C^4}$), 141.1 (d, $^3J_{P,C}$ = 2.5 Hz, *quart-C* fluorene), 141.7 (d, $^2J_{P,C}$ = 12.7 Hz, *quart-C* fluorene), 141.8 (d, $^3J_{P,C}$ = 3.1 Hz, *quart-C* fluorene), 142.8 (d, $^2J_{P,C}$ = 8.1 Hz, *quart-C* fluorene), 162.4 (s, *C=S*).

^{31}P NMR (121.5 MHz, $CDCl_3$): δ = 28.9 (br. s).

IR (Diamond ATR): υ (cm-1) = 3395 (s), 3114 (w), 2971 (w), 1543 (w), 1431 (s), 1410 (s), 1372 (s), 1330 (s), 1176 (s), 1019 (s), 730 (s).

MS (EI, 70 eV): m/z (%) = 451.1 (20) $[M]^{\cdot+}$, 286.1 (10) $[M\text{-}Flu]^+$, 184.1 (10) $[C_9H_{16}N_2S]^+$, 165.0 (70) $[Fluorene]^+$, 152.0 (40) $[C_{12}H_8]^+$.

HRMS: theor./exp. for $[C_{26}H_{34}N_3PS]$: 451.2211/451.2210.

EA [%]:theor./exp. C 69.15/67.97, H 7.59/7.20; N 9.30/8.80, S 7.10/6.75.

10.8 Synthesis of borane complex of the substitution product/ synthesis for 10

In a Schlenk flask, a solution of 1.42g of **9c** (3.2 mmol) in 15 mL of THF, was treated with 0.4 ml of borane-dimethyl sulfide adduct (3.9 mmol, 1.2 equiv) at r.t. The reaction mixture it was stirred at r.t. for about 2h and then the solvent was removed under vacuum to get a light yellow solid, which upon washing with *n*-pentane (2 × 5 ml) gave a white solid. Finally the com-pound was dried *in vacuo* (8×10^{-3} mbar) to obtain pure **10** as a white powder.

10.8.1 1,3-Diisopropyl-4-diethylamino(fluorenyl)borophosphinoyl-imidazole-2-thione (10)

Yield: 1.3 g (2.8 mmol, 87.5 %) **Appearance:** white powder **melting point:** decom. at 220°C

^{1}H NMR (300 MHz, $CDCl_3$): δ = 0.67 (br, BH_3), 0.79 (t, 6H, $^{3}J_{H,H}$ = 7.2 Hz, $\underline{CH_3}CH_2$N-P), 1.38 (d, 3H, $^{3}J_{H,H}$ = 6.7 Hz, N^{1}CH$\underline{CH_3}CH_3$), 1.40 (d, 3H, $^{3}J_{H,H}$ = 6.7 Hz, N^{1}CHCH$_3\underline{CH_3}$), 1.85 (d, 3H, $^{3}J_{H,H}$ = 11 Hz N^{3}CHCH$_3\underline{CH_3}$), 1.89 (d, 3H, $^{3}J_{H,H}$ = 11 Hz N^{3}CH$\underline{CH_3}CH_3$), 2.79-3.10 (m,8H, $CH_3\underline{CH_2}$N-P), 4.79 (d, 1H, $^{3}J_{P,H}$ = 11.5 Hz, *P-CH* of Flu), 5.06 (sept, 1H, $^{3}J_{H,H}$ = 6.5 Hz, N$^{1}\underline{CH}CH_3CH_3$), 5.31 (sept, 1H, $^{3}J_{H,H}$ = 6.8 Hz, N$^{3}\underline{CH}CH_3CH_3$), 7.01 (d, 1H, $^{3}J_{P,H}$ = 1.5 Hz, $\underline{C^5H}$), 7.08-7.88 (m, 8H, *Flu protons*).

^{13}C NMR (75.0 MHz, $CDCl_3$): δ = 14.5 (s, $\underline{CH_3}CH_2$N-P), 18.9 & 19.1 (two s, N^{1}CH$\underline{Me_2}$), 21.9 & 22.1 (two s, N^{3}CH$\underline{Me_2}$), 42.8 (d, $^{2}J_{P,C}$ = 3.2 Hz, $CH_3\underline{CH_2}$N-P), 47.9 (s, N$^{1}\underline{CH}CH_3CH_3$), 48.2 (d, $^{3}J_{P,C}$ = 32.5 Hz, N$^{3}\underline{CH}CH_3CH_3$), 20.3 (d, $^{2}J_{P,C}$ = 18.8 Hz, $\underline{C^5}$), 121.1 (d, $^{2}J_{P,C}$ = 9.8 Hz, *quart-C* Flu), 122.5 (d, $^{1}J_{P,C}$ = 68.6 Hz, $\underline{C^4}$), 125.4 & 126.6 (d, $^{3}J_{P,C}$ = 2.7 Hz, $\underline{C^1 \text{ \& } C^8}$ of Flu), 126.9 & 128.3 (s , $\underline{C^3 \text{ \& } C^6}$ of Flu), 127.2 & 128.2 (d, $^{4}J_{P,C}$ = 2.4 Hz, & d, $^{4}J_{P,C}$ = 2.4 Hz, $\underline{C^2 \text{ \& } C^7}$ of Flu, 139.0 (s, $\underline{C^4 \text{ \& } C^5}$ of Flu), 139.2 & 142.0 (d, $^{2}J_{P,C}$ = 4.9 Hz, *quart-C* Flu), 142.0 (d, $^{2}J_{P,C}$ = 4.7 Hz, *quart-C* Flu, 142.4 (d, $^{3}J_{P,C}$ = 3.4 Hz, *quart-C* Flu), 163.6 (s, *C=S*).

^{31}P NMR (121.5 MHz, $CDCl_3$): δ = 58.9 (br).

^{11}B NMR (96.25 MHz, $CDCl_3$): δ = - 37.6 (br. s).

MS (EI, 70 eV): m/z (%) = 465.2 (20) $[M]^{\cdot+}$, 451.2 (90) $[M\text{-}BH_3]^{+}$.

HRMS: theor./exp. for $[C_{26}H_{37}N_3PSB]$: 451.2211/451.2211.

EA [%]:theor./exp. C 67.09/66.66, H 8.01/8.12; N 9.03/8.92, S 6.89/6.80.

10.9 Oxidative desulfurization of compound 9c

To a suspension of **9c** (0.18 g, 0.4 mmol) in 10 ml of methanol, 0.2 ml of H_2O_2 (30% in water) (2.4 mmol, 5.5 equiv) was added at 0 °C. As the reaction mixture was stirred, it turned into a clear solution within 30 minutes. It was then stirred at r.t. for 15 more min, and the solvent removed under reduced pressure (8×10^{-3} mbar) to get a yellow oil. This was then dissolved in 20 ml of methylene dichloride and dried over $MgSO_4$ for 15 minutes, and filtered. The filtrate was concentrated *in vacuo* (8×10^{-3} mbar) to get a yellow gel, to which was added 20 ml of *n*-pentane and triturated to a fine powder. Finally the solvent was removed by cannula filtration and the light yellow powder was finally dried under vacuum (8×10^{-3} mbar) to remove traces of solvent.

10.9.1 1,3-Diisopropyl-4-diethylamino(fluorenyl)phosphinoyl-imidazolium hydrogensulfate (11)

Yield: 0.19 g (0.3 mmol, 80.1 %) **Appearance:** yellow powder (extremely hygroscopic) **Melting point:** 81 °C.

^{1}H NMR (300 MHz, $CDCl_3$): δ = 1.05 (d, 3H, $^3J_{H,H}$ = 6.6 Hz, N^{1}CH*CH$_3$*CH$_3$), 1.11 (d, 3H, $^3J_{H,H}$ = 6.6 Hz, N^{1}CHCH$_3$*CH$_3$*), 1.21 (d, 3H, $^3J_{H,H}$ = 6.6 Hz, N^{3}CHCH$_3$*CH$_3$*), 1.26 (t, 6H, $^3J_{H,H}$ = 7.1 Hz, *CH$_3$*CH$_2$N-P), 1.42 (d, 3H, $^3J_{H,H}$ = 6.6 Hz, N^{3}CH*CH$_3$*CH$_3$), 3.27-3.41 (m, 8H, CH$_3$*CH$_2$*N-P), 4.86 (sept, 1H, $^3J_{H,H}$ = 6.6 Hz, N^1*CH*CH$_3$CH$_3$), 5.05 (sept, 1H, $^3J_{H,H}$ = 6.6 Hz, N^3*CH*CH$_3$CH$_3$), 5.90 (s, 1H, P-*CH* of Flu), 7.31 – 7.97 (m, 9H, *C^{5}H* & *Flu ring protons*), 9.89 (s, *C^2-H*).

^{13}C{1H} NMR (75.0 MHz, $CDCl_3$): δ = 13.6 (d, $^3J_{P,C}$ = 4.4 Hz, *CH$_3$*CH$_2$N-P), 22.2 (s, N^{1}CH*CH$_3$*CH$_3$), 22.5 (s, N^{1}CH*CH$_3$*CH$_3$), 23.1 (s, N^{3}CH*CH$_3$*CH$_3$), 24.3 (s, N^{3}CHCH$_3$*CH$_3$*), 40.04 (br, s, CH$_3$*CH$_2$*N-P), 48.6 (d, $^1J_{P,C}$ = 91.1 Hz, *P-CH*), 52.7 (s, N^{1}CH*Me$_2$*), 53.4 (s, N^{3}CH*Me$_2$*), 120.1 & 120.6 (d, $^4J_{P,C}$ = 1.1 Hz, & d, $^4J_{P,C}$ = 1.2 Hz; *C^4 & C^5* of Flu), 124.2 (d, $^2J_{P,C}$ = 14.7 Hz, *C^5*), 125.6 & 127.7 (d, $^4J_{P,C}$ = 2.9 Hz, & d, $^4J_{P,C}$ = 2.6 Hz*; C^2 & C^7* of Flu), 127.5 (two d merged, *C^3 & C^6* of Flu), 128.7 & 128.8 (d, $^3J_{P,C}$ = 2.3 Hz, & d, $^3J_{P,C}$ = 2.3 Hz; *C^1 & C^8* of Flu), 137.7 & 138.3 (d, $^3J_{P,C}$ = 3.9 Hz, & d, $^3J_{P,C}$ = 5.0 Hz; *quart-C* of Flu), 138.5 (d, $^2J_{P,C}$ = 6.4 Hz, *quart-C* of Flu), 140.8 (d, $^1J_{P,C}$ = 5.5 Hz, *C^4*), 142.5 (d, $^3J_{P,C}$ = 5.4 Hz, *C^2*).

^{31}P NMR (121.5 MHz, $CDCl_3$): δ = 29.5 (nonet, $^3J_{P,H}$ = 12.4 Hz).

Pos. ESI-MS: for $C_{29}H_{36}N_4OP^+$ theor. 436.25, exp. 436.30.

EA[%]: not measured due to an extreme hygroscopicity.

10.10 PCl_3 induced P-N bond cleavage in compound 9

To a solution of **9a,b** (2.3 mmol) in 15 ml of dichloromethane, 0.2 mL of PCl_3 (2.4 mmol, 1.1 equiv) was added at –20 °C and slowly warmed till room temperature within 2 hours. Afterwards the solvent was removed in vacuo (8×10^{-3} mbar) to get a yellow oil, to which 10 ml of *n*-pentane was added and stirred for a few minutes, which resulted in the formation of a white solid. The solid was separated by cannula filtration and was dried in vacuo (8×10^{-3} mbar) to get pure **12a,b**.

10.10.1 1,3-Diisopropyl-4-chloro(diphenylmethyl)phosphanyl-imidazole-2-thione (12a)

Yield: 0.71 g (1.7 mmol, 73.9 %) **Appearance:** white powder **Melting Point:** 169 °C

^{1}H NMR (300 MHz, $CDCl_3$): δ = 1.26 (d, 3H, $^3J_{H,H}$ = 6.6 Hz N^1-CHCH$_3$*CH$_3$*), 1.34 (d, 3H, $^3J_{H,H}$ = 6.6 Hz N^1-CH*CH$_3$*CH$_3$), 1.42 (bs, 3H, N^3-CHCH$_3$*CH$_3$*), 1.58 (d, 3H, $^3J_{H,H}$ = 6.6 Hz, N^3-CH*CH$_3$*CH$_3$), 4.84 (s, 1H, P-*CH*), 5.11 (sept, 1H, $^3J_{H,H}$ = 6.6 Hz N^1-*CH*CH$_3$CH$_3$), 5.44 (bs, 1H, N^3-*CH*CH$_3$CH$_3$), 7.13 (bs, 1H, *C^{5}H*), 7.08-7.58 (m, 10H, *Ph ring protons*).

^{13}C{1H} NMR (75.0 MHz, CDCl3): δ = 21.4 (bs, N^{3}CH*Me$_2$*), 21.9 (s, N^{1}CH*Me$_2$*), 49.2 (s, N^1*CH*Me$_2$), 51.0 (s, N^3*CH*Me$_2$), 58.1 (d, $^1J_{P,C}$ = 26.4 Hz, P-*CH*), 122.7 (d, $^2J_{P,C}$ = 3.6 Hz, *C^5*), 125.7 (d, $^1J_{P,C}$ = 51.7 Hz, *C^4*), 127.6 (s, Ph ring *CH*), 128.5 (d, $^3J_{PC}$ = 9.9 Hz, Ph ring *CH*), 128.9 (d, $^3J_{PC}$ = 9.6 Hz, Ph ring *CH*), 128.9 (s, Ph ring *CH*), 129.2 (s, Ph ring *CH*), 138.5 (d, $^2J_{PC}$ = 5.7 Hz, *quart-C* Ph ring), 138.7 (d, $^2J_{PC}$ = 5.2 Hz, *quart-C* Ph ring), 162.9 (s, *C=S*).

^{31}P NMR (121.5 MHz, $CDCl_3$): δ = 53.4 (br).

MS (EI, 70 eV): m/z (%) = 416 (40) $[M]^{\cdot+}$.

HRMS: theor./exp. for [$C_{22}H_{26}N_2PClS$]: 416.1239/416.1239.

EA[%]:theor./exp. C 63.37/61.97, H 6.29/6.53; N 6.72/6.65, S 7.69/6.69.

10.10.2 1,3-Dimesityl-4-chloro(diphenylmethyl)phosphanyl-imidazole-2-thione (12b)

Yield: 1.03 g (1.8 mmol, 78.3 %) **Appearance:** white powder **Melting Point:** 197 °C

^{1}H NMR (300 MHz, $CDCl_3$): δ = 1.39 & 1.84 (s, 3H each, *o*-*CH$_3$* of N^3-Mes), 2.04 & 2.14 (s, 3H, *o*-*CH$_3$* of N^1-Mes), 2.33 & 2.36 (s, 3H each, *p*-*CH$_3$* of Mes), 4.67 (d, $^2J_{P,H}$ = 7.8 Hz, *C^9-H* of Flu),5.86 (s, *C^5-H*), 6.88 & 7.02 (s, 1H each, *m*-*CH* of N^3-Mes), 6.95 (s, *m*-*CH* of N^1-Mes), 7.30-7.94 (m, 8H, *Flu ring protons*).

^{13}C{1H} NMR (75.0 MHz, CDCl3): δ = 17.4 & 17.8 (s, *o*-*CH*$_3$ of N^1-Mes), 17.5 (d, $^4J_{PC}$ = 0.9 Hz, *o*-*CH*$_3$ of N^3-Mes), 18.1 (d, $^4J_{PC}$ = 3.5 Hz, *o*-*CH*$_3$ of N^3-Mes), 21.2 & 21.3 (s, *p*-*CH*$_3$ of Mes), 50.2 (d, $^1J_{P,C}$ = 34.9 Hz, P-*CH* of Flu), 120.3 & 120.4 (s, *CH* of Flu), 125.5 (d, $^1J_{P,C}$ = 46.3 Hz, *C*^{4}), 125.51 (d, $^2J_{P,C}$ = 7.3 Hz, *C*^{5}), 125.6 (s, *CH* of Flu), 125.7 (d, $J_{P,C}$ = 3.2 Hz, *CH* of Flu), 127.1 (s, *CH* of Flu), 127.4 (d, $J_{P,C}$ = 1.8 Hz, *CH* of Flu), 128.4 (s, *CH* of Flu), 128.5 (d, $J_{P,C}$ = 2.7 Hz, *CH* of Flu), 129.1, 129.2, 129.3 & 129.4 (s, *m*-*CH* of Mes), 125.5 (d, $^1J_{P,C}$ = 46.3 Hz, *C*^{4}), 131.6 (d, $^4J_{P,C}$ = 2.1 Hz, *o*-*C* of Mes), 133.1 (s, *o*-*C* of Mes), 134.9 & 135.4 (s, *ipso-C* of Mes), 136.1 (d, $^4J_{P,C}$ = 2.3 Hz, *o*-*C* of Mes), 136.6 (d, $^4J_{P,C}$ = 1.5 Hz, *o*-*C* of Mes), 139.3 & 139.7 (s, *p*-*C* of Mes), 139.5 (s, *quart*-*C* Flu), 141.2 (d, $J_{P,C}$ = 3.5 Hz, *quart-C* Flu), 141.6 (s, *quart-C* Flu), 141.8 (d, $J_{P,C}$ = 2.1 Hz, *quart-C* Flu), 165.0 (s, *C=S*).

^{31}P NMR (121.5 MHz, $CDCl_3$): δ = 64.7 (d, $^2J_{P,H}$ = 7.5 Hz).

MS (EI, 70 eV): m/z (%) = 566.2 (10) $[M]^{\cdot+}$, 532.2 (20) $[M\text{-}Cl+H]^{\cdot+}$, 401.1 (100) $[M\text{-}Flu]^{\cdot+}$.

HRMS: theor./exp. for $[C_{34}H_{32}N_2PClS]$: 566.1708/566.1708.

EA[%]:theor./exp. C 72.01/71.20, H 5.69/5.86; N 4.94/4.94, S 5.65/5.36.

10.11 Synthesis of imidazole-2-ylidene stabilized phosphenium salt 13

To a solution of **12a** (0.77 g, 1.9 mmol) in 8 ml of THF, the 1,3,4,5-tetramethylimidazol-2-ylidene (0.23 g, 1.8 mmol) in THF (3 mL) was added slowly at –40 °C. The reaction mixture was stirred for overnight upon which a white precipitate was observed which was isolated via cannulation and washed multiple times with tetrahydrofuran, followed by washing with *n*-pentane and then dried *in vacuum* (8×10^{-3} mbar) to obtain a white powder.

10.11.1 1,3,4,5-Tetramethyl-2-((1,3-diisopropyl-imidazole-2-thione)-4-yldiphenyl-methylphosphino)-imidazolium chloride

Yield: 0.6 g (1.2 mmol, 60.6 %) **Appearance:** white powder. **Melting Point:** 163 °C

^{1}H NMR (300 MHz, $CDCl_3$): δ = 1.09 (d, 3H, $^3J_{H,H}$ = 7.1Hz, N^1-CHCH$_3$**CH$_3$**), 1.20 (d, 3H, $^3J_{H,H}$ = 7.1Hz, N^1-CH**CH$_3$**CH$_3$), 1.50 (m, 6H, N^3-CH**Me$_2$**), 2.17 (s, 6H, C-**CH$_3$**), 3.78 (s, 6H, N-**CH$_3$**), 4.93 (sept, 1H, $^3J_{H,H}$ = 7.1Hz, N^1-**CH**Me$_2$), 5.42 (bs, 1H, N^3-**CH**Me$_2$), 6.92 (d, 1H, $^3J_{H,H}$ = 8.2 Hz, C^5-**H**), 6.99-8.01 (10H, Ph protons), 8.79 (s, P-**CH**).

^{13}C{1H} NMR (75.0 MHz, $CDCl_3$): δ = 9.5 (s, C-(***C*H$_3$**)$_2$), 20.9 (d, $^4J_{P,C}$ = 8.7 Hz, N^3-CHCH$_3$**CH$_3$**), 21.3 (s, N^1-CHCH$_3$**CH$_3$**), 22.2 (d, $^4J_{P,C}$ = 8.2 Hz, N^3-CH**CH$_3$**CH$_3$), 22.4 (s, N^1-CH**CH$_3$**CH$_3$), 34.5 (d, $^3J_{P,C}$ = 10 Hz, N-**CH$_3$**), 50.1 (s, N^1-**CH**Me$_2$), 50.3 (s N^3-**CH**Me$_2$), 68.1 (s, P-**CH**), 111.2 (d, $^1J_{P,C}$ = 8.4 Hz, **C^4**), 127.7 (s, C^5),

128.6 (d, $^{3}J_{P,C}$= 6.5 Hz, Ph ring C), 128.9 (s, Ph ring CH), 129.1(s, Ph ring CH), 130.3 (s, p-CH of Ph), 130.9 (s, C=C), 138.2 (d, $^{2}J_{P,C}$ = 16.6 Hz, quart-C of Ph ring), 139.0 (d,$^{2}J_{P,C}$ = 11.8 Hz, quart-C of Ph ring), 140.6 (d, $^{1}J_{P,C}$ = 58.6 Hz, N-C-N), 164.0 (s, C=S).

^{31}P NMR (121.5 MHz, $CDCl_3$): δ = - 47.4 (br).

Pos. ESI-MS: for $C_{29}H_{36}N_4PS^+$ theor. 505.25, exp. 505.30.

10.12 Synthesis of compound 18

To a solution of **12b** (0.15 g, 0.3 mmol) in THF, 0.55 mmol of ^{n}BuLi (2.1 equiv) was added at –78 °C. The color of the solution changed from colorless to bright yellow. Under these conditions the reaction mixture was stirred for 30 min and then cooled to –78 °C. Then 0.3 mmol of HCl (1M solution in diethyl ether) was added to the reaction mixture, upon which the bright yellow color disappeared and the solution became colorless. The solvent was removed in the next step to get a light yellow residue, which was taken up in toluene (30 ml) and filtered through a silica bed to separate from the lithium chloride formed in the reaction mixture. The filtrate was concentrated under reduced pressure (8 × 10^{-3} mbar) to get a light yellow solid, which was washed with pentane (2 × 2 ml) and then dried *in vacuo* (8 × 10^{-3} mbar) to get the pure compound.

10.12.1 1,3-Dimesityl-4-butyl(fluorenyl)phosphanyl-imidazole-2-thione (18)

Yield: 0.09 g (0.2 mmol, 66.7 %) **Appearance:** white powder. **Melting Point:** 188 °C.

^{1}H NMR (300 MHz, $CDCl_3$): δ = 0.62 (t, 3H, $^{3}J_{HH,}$ = 6.9 Hz, $PCH_2CH_2CH_2\underline{CH_3}$), 0.87- 1.35 (m, 6H, $P\underline{CH_2CH_2CH_2}CH_3$), 2.14 (s, 3H, *p*-$\underline{CH_3}$ of N^3-Mes), 2.18 & 2.24 (s, 3H each, *o*-$\underline{CH_3}$ of N^3-Mes), 2.33 (s, 3H, *p*-$\underline{CH_3}$ of N^1-Mes), 2.37 & 2.41 (s, 3H each, *o*-$\underline{CH_3}$ of N^1-Mes), 4.03 (s, $\underline{C^9\text{-}H}$ of Flu), 6.49 (s, 1H, $\underline{C^5H}$), 7.01 & 7.03 (s, 1H each, *m*-$\underline{CH}$ of N^3-Mes), 7.08 & 7.14 (*m*-$\underline{CH}$ of N^1-Mes), 7.23-7.82 (m, 10H, *Flu ring protons*).

^{13}C{^{1}H} NMR (75.0 MHz, $CDCl_3$): δ = 13.4 (s, $PCH_2CH_2CH_2\underline{CH_3}$), 17.9 & 18.1 (s, *p*-$\underline{CH_3}$ of Mes), 18.3 (s, *o*-$\underline{CH_3}$ of N^1-Mes), 18.6 (d, $^{4}J_{PC}$ = 8.1 Hz, *o*-$\underline{CH_3}$ of N^3-Mes), 18.8 (d, $^{3}J_{PC}$ = 11.7 Hz, $PCH_2CH_2\underline{CH_2}CH_3$), 21.2 & 21.3 (s, *o*-$\underline{CH_3}$ of N^1-Mes) 23.9 (d, $^{2}J_{PC}$ = 13.4 Hz, $PCH_2\underline{CH_2}CH_2CH_3$), 27.6 (d, $^{1}J_{PC}$ = 17.8 Hz, $P\underline{CH_2}CH_2CH_2CH_3$) 44.7 (d, $^{1}J_{P,C}$ = 25.1 Hz, P-$\underline{C^9H}$ of Flu), 119.9 & 120.3 (s, $\underline{CH}$ of Flu), 122.6 (d, $^{2}J_{P,C}$ = 3.1 Hz, $\underline{C^5}$), 124.4 (d, $J_{P,C}$ = 2.6 Hz, $\underline{CH}$ of Flu), 124.9 (d, $J_{P,C}$ = 9.4 Hz, $\underline{CH}$ of Flu), 126.3 (s, $\underline{CH}$ of Flu), 126.9 (d, $J_{P,C}$ = 0.9 Hz, $\underline{CH}$ of Flu), 127.1 (s, $\underline{CH}$ of Flu), 127.2 (d, $J_{P,C}$ = 2.1 Hz, $\underline{CH}$ of Flu), 129.3, 129.4, 129.5 & 129.6 (s, *m*-$\underline{CH}$ of Mes), 132.5 (d, $^{4}J_{P,C}$ = 0.6 Hz, *o*-$\underline{C}$ of Mes), 133.6 (s, *o*-$\underline{C}$ of Mes), 135.3 & 135.7 (*ipso*-$\underline{C}$ of Mes), 136.1 (d, $^{4}J_{P,C}$ = 1.3 Hz, *o*-$\underline{C}$ of Mes), 136.2 (s, *o*-$\underline{C}$ of Mes), 139.4 & 139.5 (s, *p*-$\underline{C}$

of Mes), 140.1 (d, $J_{P,C}$ = 3.6 Hz, *quart-C* Flu), 141.1 (s, *quart-C* Flu), 142.5 (d, $J_{P,C}$ = 2.9 Hz, *quart-C* Flu), 143.1 (d, $J_{P,C}$ = 10.4 Hz, *quart-C* Flu, 165.6 (s, *C=S*).

^{31}P NMR (121.5 MHz, $CDCl_3$): δ = -31.3 (t, $^3J_{P,H}$ = 7.9 Hz).

MS (EI, 70 eV): m/z (%) = 588.3 (10) $[M]^{\cdot+}$, 423.2 (30) $[M\text{-}Flu]^+$,180.0 (100) $[C_{14}H_{12}]^+$,

Pos. ESI-MS: for $[C_{38}H_{41}N_2PS + H]^+$ calc. 589.2801 found 589.2823.

EA: theor./exp. C 77.52/76.95, H 7.02/6.96; N 4.76/4.56, S 5.45/5.32.

10.13 Synthesis of backbone phenyl(chloro)phosphanyl substituted imidazole-2-thiones 21a-c

A solution of **20a-c** (5.6 mmol) in 35 mL of diethyl ether was treated with PCl_3 (6.1 mmol, 1.1 equiv) at –40°C. The reaction mixture was then allowed to warm up slowly till ambient temperature (2h), after which the solvent was removed under reduced pressure (8 × 10^{-3} mbar) to get a yellow oily residue. Then 20 ml of *n*-pentane was added to the residue and stirred for few minutes. The solvent was removed by cannula filtration and the white solid was isolated. This resulted in removal of all the by-products and formation of a fine white powder. The powder was then separated by cannula filtration and dried *in vacuo* (8 × 10^{-3} mbar) to get the pure compounds **21a-c**.

10.13.1 1,3-Dimethyl-4-phenyl(chloro)phosphanyl-imidazole-2-thione (21a)

Yield: 1.29 g (4.7 mmol, 83.9 %) **Appearance:** white powder **Melting point:** 110 °C.

^{1}H NMR (300 MHz, $CDCl_3$): δ = 3.52 (s, 3H, N^3-*Me*), 3.57 (s, 3H, N^1-*Me*), 6.67 (s, 1H, C^5H), 7.45- 7.65 (m, 5H, *Ph ring protons*).

^{13}C{^{1}H} NMR (75.0 MHz, $CDCl_3$): δ = 33.8 (d, $^3J_{P,C}$ = 5.6 Hz, N^3-*Me*), 35.4 (s, N^1-*Me*), 126.0 (d, $^1J_{P,C}$ = 48.0 Hz, C^4), 127.4 (d, $^2J_{P,C}$ = 31.2 Hz, C^5), 129.0 & 129.1 (s, *Ph ring C*), 130.7 (s, *Ph ring C*), 130.9 & 131.1 (s, *Ph ring C*), 133.6 (d, $^1J_{P,C}$ = 25.2 Hz, *ipso-C of Ph*), 167.4 (s, *C=S*).

^{31}P NMR (121.5 MHz, $CDCl_3$): δ = 50.5 (t, $^3J_{P,H}$ = 8.5 Hz).

IR [cm^{-1}]: $\tilde{\nu}$ = 3128 (w), 3051 (w), 2931 (w), 1543 (m), 1468 (m), 1392 (m), 1373 (m), 1341 (m), 1161 (m), 794 (s).

MS (EI, 70 eV): *m/z* (%) = 270.0 (25) $[M]^{\cdot+}$, 252.0 (100) $[M\text{-}Cl+ OH]^+$, 236.0 (40) $[M\text{-}Cl+H]^+$.

HRMS m/z: theor./exp. for $[C_{11}H_{12}N_2PClS]$: 423.0147/270.0143.

EA [%]: theor./exp. C 48.80/48.41, H 4.47/4.68; N 10.35/10.22, S 11.84/11.90.

10.13.2 1,3-Diethyl-4-phenyl(chloro)phosphanyl-imidazole-2-thione (21b)

Yield: 1.24 g (4.1 mmol, 73.2 %) **Appearance:** white powder **Melting Point:** 68 °C

^{1}H NMR (300 MHz, $CDCl_3$): δ = 1.26 (s, 3H, $^{3}J_{P,H}$ = 7.1 Hz, N^3-CH_2*Me*), 1.29 (s, 3H, $^{3}J_{P,H}$ = 7.1 Hz, N^1-CH_2*Me*), 4.01 (q, 2H, $^{3}J_{P,H}$ = 7.1 Hz, N^3-*CH_2*Me), 4.17 (br, 2H, N^1-*CH_2*Me), 6.50 (s, 1H, *C^5H*), 7.46- 7.72 (m, 5H, *Ph ring protons*).

^{13}C{^{1}H} NMR (75.0 MHz, $CDCl_3$): δ = 13.3 (d, $^{4}J_{P,C}$ = 1.9 Hz, N^3- CH_2*Me*), 14.1 (s, N^1- CH_2*Me*), 41.9 (d, $^{3}J_{P,C}$ = 6.2 Hz, N^3-*CH_2*Me), 42.9 (d, $^{3}J_{P,C}$ = 6.2 Hz, N^1-*CH_2*Me), 125.2 (d, $^{2}J_{P,C}$ = 20.9 Hz, *C^5*), 126.7 (d, $^{1}J_{P,C}$ = 45.7 Hz, *C^4*), 128.9 & 129.1 (s, *Ph ring C*) 131.2 & 131.3 (s, *Ph ring C*) 131.4 (s, *Ph ring C*), 133.6 (d, $^{1}J_{P,C}$ = 24.9 Hz, *ipso-C of Ph*), 165.6 (s, *C=S*).

^{31}P NMR (121.5 MHz, $CDCl_3$): δ = 50.2 (t, $^{3}J_{P,H}$ = 8.9 Hz).

IR [cm^{-1}]: $\tilde{\nu}$ = 3112 (w), 2977 (w), 1538 (m), 1414 (vs), 1320 (s), 1296 (vs), 1180 (s), 1153 (vs), 1090 (s).

MS (EI, 70 eV): *m/z* (%) 298.0 (40) $[M]^{\cdot+}$, 282.0 (100) $[M\text{-}Cl+OH]^+$, 264.0 (50) $[M\text{-}Cl+H]^+$.

HRMS m/z: theor./exp. for $[C_{13}H_{16}N_2PClS]$: 298.0460/298.0462.

EA [%]: theor./exp. C 52.26/51.56, H 5.40/5.78; N 9.38/9.28, S 10.73/10.96.

10.13.3 1,3-Di-*n*-butyl-4-phenyl(chloro)phosphanyl-imidazole-2-thione (21c)

Yield: 1.59 g (4.5 mmol, 80.4 %) **Appearance:** orange oil **Melting Point:** liq. at r.t.

^{1}H NMR (300 MHz, $CDCl_3$): δ = 0.91 (s, 3H, $^{3}J_{H,H}$ = 7.4 Hz, N^3-$CH_2CH_2CH_2$*Me*), 0.93 (s, 3H, $^{3}J_{H,H}$ = 7.4 Hz, N^1-$CH_2CH_2CH_2$*Me*), 1.27-1.39 (m, 4H, N-CH_2CH_2*CH_2*Me), 1.65-1.75 (m, 4H, N-CH_2*CH_2*CH_2Me), 3.97 (t, 2H, $^{3}J_{H,H}$ = 7.4 Hz, N^1-*CH_2*CH_2CH_2Me), 4.09 (br, 2H, $^{3}J_{H,H}$ = 7.4 Hz, N^3-*CH_2*CH_2CH_2Me), 6.50 (s, 1H, *C^5H*), 7.49- 7.75 (m, 5H, *Ph ring protons*).

^{13}C{^{1}H} NMR (75.0 MHz, $CDCl_3$): δ = 13.61 & 13.62 (s, N-$CH_2CH_2CH_2$*Me*), 19.8 & 20.1 (s, N-CH_2CH_2*CH_2*Me), 30.1 (d, $^{4}J_{P,C}$ = 2.0 Hz, N^3-CH_2*CH_2*CH_2Me), 30.8 (s, N^1-CH_2*CH_2*CH_2Me), 46.8 (d, $^{3}J_{P,C}$ = 6.0 Hz, N^3-*CH_2*CH_2CH_2Me), 47.8 (s,N^1*CH_2*CH_2CH_2Me), 125.7 (d, $^{2}J_{P,C}$ = 19.9 Hz, *C^5*), 126.8 (d, $^{1}J_{P,C}$ = 45.6

Hz, *C*^{4}), 128.9 & 129.0 (s, *Ph ring C*) 131.2 & 131.3 (s, *Ph ring C*), 133.8 (d, $^{1}J_{P,C}$ = 25.1 Hz, *ipso-C of Ph*), 165.9 (s, *C=S*).

^{31}P NMR (121.5 MHz, $CDCl_3$): δ = 49.9 (t, $^{3}J_{P,H}$ = 8.9 Hz).

IR [cm^{-1}]: ṽ = 3112 (w), 3054 (w), 2956 (m), 2930 (m), 2871 (m), 1536 (m), 1414 (s), 1218 (m), 1156 (s), 1103 (s), 749 (s).

MS (EI, 70 eV): *m/z* (%) 354.1 (40) $[M]^{\cdot+}$, 336.1 (60) $[M\text{-}Cl+OH]^{+}$.

HRMS m/z: theor./exp. for $[C_{17}H_{24}N_2PClS]$: 354.1086/354.1085.

EA [%]: theor./exp. C 57.54/57.66, H 6.82/6.87; N 7.89/7.89, S 9.03/9.37.

10.14 Synthesis of 1,4-dihydro-1,4-diphosphinines 22a-c

The synthetic protocol for **22a-c** is the same as that for **4c-e**, and the reactions were also done in the same scale. Only difference in these cases is that the product obtained after the filtration over the silica gel is not completely pure. Compound **22a,b** were washed with diethyl ether (3×10 ml) to remove these impurities and finally after drying in *vacuo* (8×10^{-3} mbar) pure **9a,b** were obtained as white powders. In case of **22c**, due to its high solubility it could not be washed with ether. That's why this crude product was again subjected to a flash chromatography over silica gel using toluene as the eluting solvent. And finally after concentrating the filtrate the residue was washed with *n*-pentane (2×10ml) to get pure **22c** as a white powder.

10.14.1 4,8-Diphenyl-1,3,5,7-tetramethyl-4,8-dihydro[1,4]diphosphinine[2,3-d:5,6-d'] bisimidazole-2,6-dithione (22a)

Yield: 8.58 g (18.3 mmol, 80.2 %) **Appearance:** white powder. **Melting Point:** decom. at 350 °C.

^{1}H NMR (300 MHz, CD_2Cl_2): δ = 3.51 & 3.57 (s, 12H, N-*Me*), 7.44-7.68 (m, 10H, *Ph ring protons*).

^{13}C{^{1}H} NMR (75.0 MHz, CD_2Cl_2): δ = 33.4 (t, $^{3}J_{P,C}$ = 5.3 Hz, N-*Me*), 124.0 (dd, $^{1}J_{P,C}$ = 5.1 Hz, $^{2}J_{P,C}$ = 3.9 Hz *C*^{4,5}), 129.6 (t, $J_{P,C}$ = 4.2 Hz, *Ph ring C*), 131.1 (d, $^{1}J_{P,C}$ = 13.7 Hz, *ipso-C of Ph*), 131.4 (s, *Ph ring C*), 133.9 (t, $J_{P,C}$ = 6.5 Hz, *Ph ring C*), 134.2 (t, (t, $J_{P,C}$ = 6.8 Hz, *Ph ring C*) 168.1 (t, $^{3}J_{P,C}$ = 1.3 Hz, *C=S*).

^{31}P NMR (121.5 MHz, CD_2Cl_2): δ = -55.6 & -57.4 (s, two isomers).

IR [cm^{-1}]: ṽ = 2931 (w), 1975 (w), 1458 (w), 1432 (s), 1369 (s), 1330 (m), 1159 (s), 854 (s), 744 (s).

MS (EI, 70 eV): *m/z* (%) = 468.1 (40) $[M+H_2O]^{\cdot+}$, 372.9 (100) $C_{15}H_{11}N_4P_2S_2$.

HRMS m/z: theor./exp. for [$C_{11}H_{12}N_2PClS$]: 468.0761/468.0762.

EA [%]: theor./exp. C 56.40/56.35, H 4.73/5.04; N 11.96/11.80, S 13.69/13.79.

10.14.2 4,8-Diphenyl-1,3,5,7-tetraethyl-4,8-dihydro[1,4]diphosphinine[2,3-d:5,6-d'] bisimidazole-2,6-dithione (22b)

Yield: 6.13 g (11.7 mmol, 51.3 %) **Appearance:** white powder. **Melting Point:** decom. at 330 °C.

^{1}H NMR (300 MHz, $CDCl_3$): δ = 0.95 (t, 12H, $^3J_{H,H}$ = 6.9 Hz, N-CH_2*Me*), 1.11 (m, 12H, $^3J_{H,H}$ = 6.9 Hz N-CH_2*Me*) 2nd isomer, 3.81-4.35 (m, 8H, N-*CH_2*Me), 7.33-7.64 (m, 10H, *Ph ring protons*).

^{13}C{^{1}H} NMR (75.0 MHz, $CDCl_3$): δ = 12.7 (s, N-CH_2*Me*), 13.1 (s, N-CH_2*Me*) 2nd isomer, 42.0 (t, $^3J_{P,C}$ = 4.8 Hz, N-*CH_2*Me), 42.7 (t, $^3J_{P,C}$ = 4.8 Hz, N-*CH_2*Me) 2nd isomer, 124.0 (dd, $^1J_{P,C}$ = 4.5 Hz, $^2J_{P,C}$ = 3.2 Hz *C^{4,5}*), 125.1 (br, *C^{4,5}*) *2nd isomer*, 129.6 (d, *Ph ring C*), 131.7 (d, *Ph ring C*), 132.2 (m, *ipso*-C) 134.2 (m, *Ph ring C*) 166.2 (s, *C=S*), 166.4 (s, *C=S*) 2nd isomer.

^{31}P NMR (121.5 MHz, $CDCl_3$): δ = -55.4 & -56.8 (s, two isomers, ratio 1.2:1).

IR [cm^{-1}]: $\tilde{\nu}$ = 2979 (w), 2933 (w), 1437 (s), 1401 (vs), 1336 (m), 1155 (s), 1024 (w), 998 (s).

MS (EI, 70 eV): *m/z* (%) = 524.1(100) $[M]^+$, 447.0 (30) $[C_{20}H_{25}N_4P_2S_2]^+$, 156.1 (5) $[C_7H_{12}N_2S]^{2+}$.

HRMS m/z: theor./exp. for [$C_{26}H_{30}N_4P_2S_2$]: 524.1387/524.1387.

EA [%]: theor./exp. C 59.53/58.87, H 5.76/6.01; N 10.68/10.25, S 12.22/11.43.

10.14.3 4,8-Diphenyl-1,3,5,7-tetra-*n*-butyl-4,8-dihydro[1,4]diphosphinine[2,3-d:5,6-d'] bisimidazole-2,6-dithione (22c)

Yield: 7.01 g (10.9 mmol, 48.7 %) **Appearance:** white powder **Melting Point:** decom. at 250 °C

^{1}H NMR (300 MHz, $CDCl_3$): δ = 0.83 & 0.85 (t, 12H, $^3J_{H,H}$ = 7.2 Hz, N-$CH_2CH_2CH_2$*Me*), 1.09-1.36 (m, 8H, N-CH_2CH_2*CH_2*Me), 1.83 (br, 8H, N-CH_2*CH_2*CH_2Me), 3.78-4.21 (m, 8H, N-*CH_2*CH_2CH_2Me), 7.39-7.64 (m, 10H, *Ph ring protons*).

^{13}C{^{1}H} NMR (75.0 MHz, $CDCl_3$): δ = 13.5 & 13.6 (s, N-$CH_2CH_2CH_2$*Me*), 19.9 (s, N-CH_2CH_2*CH_2*Me), 29.4 & 29.8 (br N-CH_2*CH_2*CH_2Me), 46.2 (t, $^3J_{P,C}$ = 4.4 Hz, N-*CH_2*CH_2CH_2Me), 47.7 (t, $^3J_{P,C}$ = 4.4 Hz, N-*CH_2*CH_2CH_2Me) 2nd isomer, 125.1 (dd, $^1J_{P,C}$ = 4.5 Hz, $^2J_{P,C}$ = 3.1 Hz, *C^{4,5}*), 125.3 (br, *C^{4,5}*) 2nd isomer,

129.5-129.7 (m, *Ph ring C*), 131.5 & 131.7 (s, *Ph ring C*), 133.9-134.5 (m, *Ph ring C*) 132.3-132.4 (m, *ipso-C of Ph*), 166.6 (t, $^{3}J_{P,C}$ = 1.4 Hz, *C=S*), 166.7 (t, $^{3}J_{P,C}$ = 1.4 Hz, *C=S*) 2nd isomer.

^{31}P NMR (121.5 MHz, $CDCl_3$): δ = -55.3 & -57.2 (s, two isomers, ratio 1:1.3).

IR [cm^{-1}]: ṽ = 3049 (w), 2956 (m), 2929 (w), 2867 (w), 1435 (m), 1404 (s), 1288 (w), 1216 (m).

MS (EI, 70 eV): *m/z* (%) = 636.2(50) $[M]^+$, 559.2 (10) $[M\text{-}Ph]^{+\cdot}$, 319.1 (60) $[M+2H]^{2+}$.

HRMS m/z: theor./exp. for $[C_{34}H_{46}N_4P_2S_2]$: 636.2639/636.2641.

EA [%]: theor./exp. C 64.13/63.97, H 7.28/7.30; N 8.80/8.65, S 10.07/10.15.

10.15 Reaction of compound 21 with KHMDS

To a solution of **21a,b** (4.1 mmol) in 25 mL THF, a solution of KHMDS (0.826 g, 4.1 mmol, 1eq) in THF (30 mL) was added at –78°C. Then the reaction mixture was slowly warmed to room temperature (2 hours). Afterwards the solvent was removed in *vacuo* (8×10^{-3} mbar) to get a yellow oil, which was again dissolved in 30 ml of toluene. This solution was filtered through a small celite® bed to remove KCl. Then the filtrate was concentrated in *vacuo* (8×10^{-3} mbar) till yellow oil was obtained as crude product. This was then triturated with 10 ml of *n*-pentane at room temperature to get a white powder, which was dried *in vacuo* (8×10^{-3} mbar) after removal of the *n*-Pentane.

10.15.1 1,3-Dimethyl-4-{bis(trimethylsilyl)amino}phenylphosphanyl-imidazole-2-thione (23a)

Yield: (1.38 g, 3.5 mmol, 85.4 %) **Appearance:** White solid **Melting point:** 157 °C

^{1}H NMR (300.1 MHz, $CDCl_3$, 25 °C): δ = 0.18 (s, 18H, Si*Me*$_3$), 3.61 (S, N^3-*Me*), 3.70 (s, N^1-*Me*), 6.49 (d, 1H, $^{3}J_{P,H}$ = 1.7 Hz, *C*^{5}*H*), 7.32-7.41 (m, 5H, *Ph protons*).

^{13}C{^{1}H} NMR (75.5 MHz, $CDCl_3$, 25 °C): δ = 4.2 & 4.3 (s, N-Si*Me*$_3$), 33.8 (d, $^{3}J_{P,C}$ = 11.1 Hz, N^3-*Me*), 35.3 (s, N^1-*Me*), 122.6 (br, *C*^{5}), 128.2 & 128.3 (s, *Ph ring C*), 128.4 (d, $J_{P,C}$ = 1.1 Hz, *Ph ring C*), 129.9 (d, $^{1}J_{P,C}$ = 26.8 Hz, *C*^{4}), 130.1 & 130.4 (s, *Ph ring C*), 138.5 (d, $^{1}J_{P,C}$ = 17.2 Hz, *ipso C of Ph*), 164.9 (s, *C=S*).

^{31}P NMR (121.5 MHz, $CDCl_3$, 25 °C): δ = 27.1 (br).

IR [cm^{-1}]: ṽ = 3162 (w), 2949 (w), 1520 (w), 1432 (w), 1378 (m), 1247 (s), 1152 (m), 1089 (w).

MS (EI, 70 eV): m/z (%) = 395.1 (100) $[M]^{+\cdot}$, 380.1 (20) $[M\text{- }Me]^+$, 323.1 (20) $[M\text{-TMS}]^+$.

HRMS m/z: theor./exp. for $[C_{17}H_{30}N_3PSSi_2]$: 395.1436/395.1437.

EA [%]: theor./exp. C 51.61/51.23, H 7.64/7.18; N 10.62/9.81, S 8.10/8.05.

10.15.2 1,3-Diethyl-4-{bis(trimethylsilyl)amino}phenylphosphanyl-imidazole-2-thione (23b)

Yield: (1.18 g, 2.8 mmol, 68.3 %) **Appearance:** White solid **Melting Point:** 105 °C

^{1}H NMR (300.1 MHz, Toluene-d$_8$, 25 °C): δ = 0.17 (s, 9H, Si*Me$_3$*), 0.18 (s, 9H, Si*Me$_3$*), 0.96 (t, 3H, $^{3}J_{H,H}$ = 7.19 Hz, N^{3}-CH$_2$*Me*), 1.51 (t, 1H, $^{3}J_{H,H}$ = 7.07, N^{1}- CH$_2$*Me*), 3.42-3.55 (m, 1H, N-*CH$_2$*Me), 3.87-3.99 (m, 1H, N-CH$_2$CH$_3$), 4.18-4.29 (m, 1H, N-*CH$_2$*Me), 4.49-4.61 (m, 1H, N-*CH$_2$*Me), 6.27 (d, 1H, $^{3}J_{P,H}$ = 1.3 Hz, C^{5}-H), 7.05-7.45 (m, 5H, *Ph protons*).

^{13}C{^{1}H} NMR (75.5 MHz, Toluene-d$_8$, 25 °C): δ = 3.8 & 3.9 (s, N-Si*Me$_3$*), 13.7 (d, $^{4}J_{P,C}$ = 3.9 Hz, N^{3}-CH$_2$*Me*), 13.9 (s, N^{1}- CH$_2$*Me*), 41.4 (d, $^{3}J_{P,C}$ = 8.4 Hz, N^{3}-*CH$_2$*Me), 42.1 (s, N^{1}-*CH$_2$*Me), 121.4 (br, *C^{5}*), 127.9 & 128.0 (s, *Ph ring C*), 127.5 (d, $^{1}J_{P,C}$ = 25.6 Hz, *C^{4}*), 129.9 & 130.2 (s, *Ph ring C*), 137.1 (s, *Ph ring C*) 139.5 (d, $^{1}J_{P,C}$ = 17.5 Hz, *ipso C of Ph*), 165.8 (s, *C=S*).

^{31}P NMR (121.5 MHz, Toluene-d$_8$, 25 °C): δ = 24.5 (br).

IR [cm^{-1}]: ṽ = 2973 (w), 1540 (w), 1440 (vs), 1348 (m), 1252 (vs), 1148 (s), 1091 (m), 1024 (w).

MS (EI, 70 eV): m/z (%) = 423.1 (100) [M]$^{+}$, 254.1 (35) [C$_{11}$H$_{21}$NPSi$_2$]$^{+}$.

HRMS m/z: theor. /exp. for [C$_{19}$H$_{34}$N$_3$PSSi$_2$]: 423.1750/423.1750.

EA [%]: theor./exp. C 53.86/53.86, H 8.09/7.94; N 9.92/9.90, S 7.31/7.80.

10.16 Synthesis of 1,4-dihydro-1,4-dichloro-1,4-diphosphinines 24a,b

PCl$_3$ (0.35 mL, 4 mmol) was added to a solution of **4d,f** (0.92 g of **4d**, 1.25 g of **4f**, 2 mmol each) in 30 mL of methylene dichloride at room temperature, and the color of the solution turned orange in both cases, though **24a** started to precipitate from the reaction mixture. The reaction for **24a** was completed within 3h, but for **24b** it took around 24h to complete conversion. Thereafter, the solvent was removed under reduced pressure (8 × 10^{-3} mbar) and the residue was washed with *n*-pentane (3 × 5 ml). After washing, the yellow products were dried under reduced pressure (8 × 10^{-3} mbar) for 1h to remove any volatiles left, thus affording compounds **24a** and **24b** as light yellow-orange solids.

10.16.1 4,8-Dichloro-1,3,5,7-tetramethyl-4,8-dihydro[1,4]diphosphinine[2,3-d:5,6-d'] bisimidazole-2,6-dithione (24a)

Yield: (0.69 g, 1.8 mmol, 90.0 %). **Appearance:** Orange solid. **Melting Point:** decomp. at 160 °C

^{1}H NMR (300.1 MHz, CD_2Cl_2, 25 °C): δ = 3.89 & 4.01 (s, N-$\underline{CH_3}$).

^{13}C{^{1}H} NMR (75.5 MHz, $CDCl_3$, 25 °C): δ = 34.1(t, $^{3}J_{P,C}$ = 4.5Hz, N$\underline{CH_3}$), 170.1 (s, $\underline{C{=}S}$).

^{31}P NMR (121.5 MHz, CD_2Cl_2, 25 °C): δ = 9.2 (br).

IR [cm^{-1}]: $\tilde{\nu}$ = 2933 (w), 1428 (s), 1367 (s), 1329 (s), 1299 (m), 1165 (s), 1061 (w), 858 (s).

MS(EI, 70 eV): m/z (%) = 383.9 (10) $[M]^{\cdot+}$, 313.9 (100) $[M\text{-}2Cl]^{+}$.

HRMS: theor./exp. for $[C_{10}H_{12}N_4Cl_2P_2S_2]$: 383.9355/ 383.9357.

EA [%]: theor./exp. C 31.18/31.54 , H 3.18/2.99 ; N 14.55/14.61 , S 16.65/17.55.

10.16.2 4,8-Dichloro-1,3,5,7-tetra-*n*-butyl-4,8-dihydro[1,4]diphosphinine[2,3-d:5,6-d'] bisimidazole-2,6-dithione (24b)

Yield: (0.91 g, 1.6 mmol, 82.1 %) **Appearance:** Orange solid **Melting Point:** decomp. at 150 °C

^{1}H NMR (300.1 MHz, $CDCl_3$, 25 °C): δ = 1.02 (t, 12H, $^{3}J_{H,H}$ = 7.3 Hz, $NCH_2CH_2CH_2\underline{Me}$), 1.43-1.56 (m, 8H, $NCH_2CH_2\underline{CH_2}Me$), 1.93 (bs, 8H, $NCH_2\underline{CH_2}CH_2Me$), 4.23 (bs, 4H, $N\underline{CH_2}CH_2CH_2Me$), 4.41 (bs, 4H, $N\underline{CH_2}CH_2CH_2Me$) (2nd isomer).

^{13}C{^{1}H} NMR (75.5 MHz, $CDCl_3$, 25 °C): δ = 13.6 (s, $NCH_2CH_2CH_2\underline{Me}$), 20.1 (s, $NCH_2CH_2\underline{CH_2}Me$), 30.4 (bs, $NCH_2\underline{CH_2}CH_2Me$), 47.2 (bs, $N\underline{CH_2}CH_2CH_2Me$), 127.0 (bs, $\underline{P\text{-}C}$ of the middle ring), 168.5 (bs, $\underline{C{=}S}$).

^{31}P NMR (121.5 MHz, $CDCl_3$, 25 °C): δ = 2.58 (br) & 10.88 (br) ratio of two isomers 1.85:1.

IR [cm^{-1}]: $\tilde{\nu}$ = 2956 (m), 2930 (w), 2870 (w), 1398 (s), 1337 (m), 1217 (s), 1176 (s), 1146 (s), 1016 (s), 926 (s).

MS (EI, 70 eV): m/z (%) = 552.1 (40) $[M]^{\cdot+}$, 482.1 (100) $[M\text{-}2Cl]^{+}$.

HRMS (m/z): theor./exp. for $[C_{22}H_{36}N_4Cl_2P_2S_2]$: 552.1233/552.1234.

EA [%]: theor./exp. C 47.74/47.31 , H 6.56/6.71, N 10.12/9.92, S 11.58/10.97.

10.17 Substitution reaction on the P-centers of 24a,b

A solution of **24a,b** (2.2 mmol) in 30 ml of THF was treated with 4.4 mmol of ^{n}BuLi (for **25a,b**) or 4.4 mmol of lithiumtrimethylsilyl acetylide (for **25c**) at –78 °C. The reaction mixture was then slowly warmed up to r.t. over a span of 3 h. Afterwards the reaction mixture was concentrated to a dark yellow residue in *vacuo* (8×10^{-3} mbar). This residue was then taken up in toluene (30 ml) and filtered through a silica bed to remove salts and coloring impurities. The filtrate was then concentrated in vacuo (8×10^{-3} mbar) to get a solid which was then triturated with *n*-pentane (2×2 ml) to get yellow to beige powders that were then dried in *vacuo* (8×10^{-3} mbar) for prolonged time.

10.17.1 4,8-Di-*n*-butyl-1,3,5,7-tetramethyl-4,8-dihydro[1,4]diphosphinine[2,3-d:5,6-d']bisimidazole-2,6-dithione (25a)

Yield: 0.36 g (0.85 mmol, 38.6 %) **Appearance:** beige powder. **Melting Point:** m.p. 185 °C

^{1}H NMR (300 MHz, $CDCl_3$): δ = 0.77 (t, 12H, $^{3}J_{H,H}$ = 7.3 Hz, P-$CH_2CH_2CH_2$*Me*), 0.88 (t, 6H, $^{3}J_{H,H}$ = 6.9 Hz, P-$CH_2CH_2CH_2$*Me*), 1.13-1.79 (m, 12H, *methylene protons of* P-*CH₂CH₂CH₂*Me) 3.73 & 3.75 (s, 12H, N-*Me*) *two isomers*.

^{13}C{^{1}H} NMR (75.0 MHz, $CDCl_3$): δ = 13.5 (s, P-$CH_2CH_2CH_2$*Me*), 23.6 & 24.1 (m, P-CH_2CH_2*CH₂*Me, *two isomers*), 27.3 & 28.3 (m, P-CH_2*CH₂*CH_2Me, *two isomers*), 31.9 (t, $^{1}J_{P,C}$ = 7.5 Hz, P-*CH₂*CH_2CH_2Me), 32.1 (t, $^{1}J_{P,C}$ = 7.5 Hz, P-*CH₂*CH_2CH_2Me) 2nd isomer, 33.8 (m, N-*Me*), 34.8 (m, N-*Me*) 2nd isomer, 125.2 (t, $J_{P,C}$ = 1.6 Hz, *C*^{4,5}), 127.1 (d, $J_{P,C}$ = 2.4 Hz, *C*^{4,5}) 2nd isomer, 167.3 & 167.9 (s, *C=S for two isomers*).

^{31}P NMR (121.5 MHz, $CDCl_3$): δ = -56.5& -63.5 (br, two isomers, ratio 1:2.3).

IR [cm^{-1}]: ṽ = 3371 (s), 2925 (m), 2855 (w), 1430 (s), 1332 (m), 1160 (s), 1042 (w), 853 (s).

MS (EI, 70 eV): *m/z* (%) = 428.1(30) $[M]^+$, 371.0(50) $[M\text{-}C_4H_9]^+$, 313.9 (100) $[M\text{-}C_8H_{18}]^+$.

HRMS m/z: theor./exp. for $[C_{18}H_{30}N_4P_2S_2]$: 428.1387/428.1388.

EA [%]: theor./exp. C 50.45/49.85, H 7.06/6.95; N 13.07/12.91, S 14.96/14.88.

10.17.2 4,8-Di-*n*-butyl-1,3,5,7-tetra-*n*-butyl-4,8-tetrahydro[1,4]diphosphinine[2,3-d:5,6-d']bisimidazole-2,6-dithione (25b)

Yield: 1.12 g (1.9 mmol, 86.4 %) **Appearance:** white powder **Melting Point:** 108 °C.

^{1}H NMR (300 MHz, $CDCl_3$): δ = 0.74 (t, 6H, $^{3}J_{H,H}$ = 7.3 Hz, P-$CH_2CH_2CH_2$*Me*), 0.99 (t, 12H, $^{3}J_{H,H}$ = 7.3 Hz, N-$CH_2CH_2CH_2$*Me*), 1.08-1.21 (m, 4H, P-CH_2CH_2*CH*$_2$Me), 1.38-1.51 (m, 12H, P-CH_2CH_2*CH*$_2$Me & P-CH_2*CH*$_2$$CH_2$Me), 1.61 (q, 4H, $^{3}J_{H,H}$ = 8.6 Hz, P-*CH*$_2$$CH_2CH_2$Me), 1.67-1.81 (m, 4H, N-CH_2*CH*$_2$$CH_2$Me), 1.96-2.10 (m, 4H, N-CH_2*CH*$_2$$CH_2$Me), 3.81-3.91 (m, 4H, N-*CH*$_2$$CH_2CH_2$Me), 4.42-4.52 (m, 4H, N-*CH*$_2$$CH_2CH_2$Me).

^{13}C{^{1}H} NMR (75.0 MHz, $CDCl_3$): δ = 13.6 (s, P-$CH_2CH_2CH_2$*Me*), 13.7 (s, N-$CH_2CH_2CH_2$*Me*), 19.9 (s, N-CH_2CH_2*CH*$_2$Me), 23.4 (t, $^{3}J_{P,C}$ = 2.7 Hz, P-CH_2CH_2*CH*$_2$Me), 25.7 (br, P-CH_2*CH*$_2$$CH_2$Me) 28.4 (d, $^{1}J_{P,C}$ = 5.5 Hz, P-*CH*$_2$$CH_2CH_2$Me), 28.7 (d, $^{1}J_{P,C}$ = 5.5 Hz, P-*CH*$_2$$CH_2CH_2$Me), 30.3 (s, N-$CH_2$*CH*$_2$$CH_2$Me), 47.5 (t, $^{3}J_{P,C}$ = 7.5 Hz, N-*CH*$_2$$CH_2CH_2$Me),124.7 (t, $J_{P,C}$ = 2.7 Hz, *C*^{4,5}), 166.8(s, *C=S*).

^{31}P NMR (121.5 MHz, $CDCl_3$): δ = -58.5 & -66.3 (s, two isomers, ratio 12:1).

IR [cm^{-1}]: ṽ = 2956(m), 2929 (m), 2871 (w), 1435 (m), 1400 (s), 1217 (m), 1150 (m), 859 (m). MS (EI, 70 eV): *m/z* (%) = 596.4(40) $[M]^+$, 539.3 (100) $[M\text{-}C_4H_9]^+$.

HRMS m/z: theor./exp. for $[C_{30}H_{54}N_4P_2S_2]$: 596.3265/596.3259.

EA [%]: theor./exp. C 60.37/60.10, H 9.12/8.76; N 9.39/9.29, S 10.74/10.44.

10.17.3 4,8-Bis(trimethylsilylethinyl)-1,3,5,7-tetra-*n*-butyl-4,8-tetrahydro[1,4]diphosphinine[2,3-d:5,6-d']bisimidazole-2,6-dithione (25c)

Yield: 0.61 g (0.9 mmol, 40.9 %) **Appearance:** beige powder. **Melting Point:** 158 °C.

^{1}H NMR (300 MHz, $CDCl_3$): δ = 0.18 & 0.19 (s, 18H, Si*Me*$_3$ *for two isomers*), 1.02 (t, 6H, $^{3}J_{H,H}$ = 7.4 Hz, N-$CH_2CH_2CH_2$*Me*), 1.04 (t, 6H, $^{3}J_{H,H}$ = 7.4 Hz, N-$CH_2CH_2CH_2$*Me*) *2nd isomer*, 1.44-1.56 (m, 8H, N-CH_2CH_2*CH*$_2$Me), 1.82-2.08 (m, 8H, N-CH_2*CH*$_2$$CH_2$Me), 4.11-4.44 (m, 8H, N-*CH*$_2$$CH_2CH_2$Me).

^{13}C{^{1}H} NMR (75.0 MHz, $CDCl_3$): δ = -0.7 & -0.6 (s, Si*Me*$_3$), 13.6 & 13.7 (s, N-$CH_2CH_2CH_2$*Me*), 20.0 & 20.1 (s, N-CH_2CH_2*CH*$_2$Me), 29.9 & 30.5 (s, N-CH_2*CH*$_2$$CH_2$Me), 47.1 (t, $^{3}J_{P,C}$ = 4.7 Hz, N-*CH*$_2$$CH_2CH_2$Me), 47.9 (t, $^{3}J_{P,C}$ = 3.5 Hz, N-*CH*$_2$$CH_2CH_2$Me) 2nd isomer, 117.1 (t, $^{2}J_{P,C}$ = 1.9 Hz, P-***C***-C-TMS), 117.3 (t, $^{2}J_{P,C}$ = 2.1 Hz, P-***C***-C-TMS) *2nd isomer*, 120.7 (t, $^{2}J_{P,C}$ = 3.9 Hz, P-C-***C***-TMS), 121.6 (t, $^{1}J_{P,C}$ = 15.7 Hz, *C*^{4,5}), 166.8 (t, $^{3}J_{P,C}$ = 1.9 Hz, *C=S*), 167.6 (t, $^{3}J_{P,C}$ = 1.6 Hz, *C=S*) *2nd isomer*.

^{31}P NMR (121.5 MHz, $CDCl_3$): δ = -79.9 & -88.1 (br, two isomers, ratio 1:2).

IR [cm^{-1}]: ṽ = 2958 (m), 2931 (m), 2871 (w), 1437 (m), 1401 (s), 1216 (m), 1159 (m), 840 (s).

MS (EI, 70 eV): *m/z* (%) = 676.1(100) $[M]^+$.

HRMS m/z: theor./exp. for $[C_{32}H_{54}N_4P_2S_2Si_2]$: 676.2804/676.2806.

EA [%]: theor./exp. C 56.77/56.57, H 8.04/7.93; N 8.28/8.21, S 9.47/9.52.

10.18 Oxidation of the tricyclic 1,4-dihydro-1,4-diphosphinines / Synthesis of the P-dioxides 26a-e

A solution of **4d-f;22b,c** (5.5 mmol) in methylene dichloride (50 ml) at r.t. was treated with 27.5 mmol (5 equiv) of hydrogen peroxide-urea adduct. The reaction mixture was then stirred at for 2days to complete the oxidation. Afterwards the reaction mixture was filtered through a filter paper to remove the urea. $MgSO_4$ was then added to the filtrate in order to remove traces of water. In the next step the solution was again filtered to remove the $MgSO_4$. This filtrate was then concentrated in vacuo (8×10^{-3} mbar) to get a yellow solid which was then triturated with 20 ml of *n*-pentane. After filtering of the *n*-pentane, a white solid was left which was finally dried under reduced pressure (8×10^{-3} mbar).

10.18.1 4,8-bis(diethylamino)-1,3,5,7-tetramethyl-4,8-dihydro[1,4]diphosphinine[2,3 -d:5,6-d']bisimidazole-2,6-dithione-4,8-dioxide (26a)

Yield: (1.51 g, 3.1 mmol, 56.4 %) **Appearance:** White powder **Melting Point:** 280 °C.

^{1}H NMR (300.1 MHz, $CDCl_3$, 25 °C): δ = 1.00(t, 12H, $^3J_{H,H}$ = 7.2 Hz, P-NCH_2*Me*), 1.05(t, 12H, $^3J_{H,H}$ = 7.2 Hz, P-NCH_2*Me*) (2nd isomer), 3.11- 3.24 (m, 8H, P-N*CH_2*Me), 3.77 (s, 12H, N-*Me*).

^{13}C{^{1}H} NMR (75.5 MHz, $CDCl_3$, 25 °C): δ = 13.2 & 13.3 (s, P-NCH_2*Me*), 34.5 (br, N-*Me*), 37.8 (d, $^2J_{P,C}$ = 5.8 Hz, P-N*CH_2*Me), 126.7(dd, $^1J_{P,C}$ = 155.1 Hz, , $^2J_{P,C}$ = 19.6 Hz *C*^{5}), 126.9(dd, $^1J_{P,C}$ = 155.1 Hz, , $^2J_{P,C}$ = 19.6 Hz, *C*^{5}) (2nd isomer), 169.8 (t, $^3J_{P,C}$ = 6.9 Hz, *C=S*).

^{31}P NMR (121.5 MHz, $CDCl_3$, 25 °C): δ = -4.3 (quin, $^3J_{P,H}$ = 12.2 Hz), -5.1(quin, $^3J_{P,H}$ = 12.2 Hz) *2nd isomer*, ratio = 1.9 :1.

IR [cm^{-1}]: ṽ = 2971 (s), 1699 (w), 1436 (m), 1333 (m), 1230 (s), 1169 (s), 1018 (s), 951 (s), 853 (s), 735 (s).

MS (EI, 70 eV): m/z (%) = 490.2 (100) $[M]^{\cdot+}$, 72 (60) $[NEt_2]^+$.

HRMS m/z: theor./exp. for $[C_{18}H_{32}N_6P_2S_2O_2]$: 490.1503/490.1508.

EA [%]: theor./exp. C 44.07/43.55, H 6.57/6.53; N 17.13/16.89, S 13.07/12.58.

10.18.2 4,8-Bis(diethylamino)-1,3,5,7-tetraethyl-4,8-dihydro[1,4]diphosphinine[2,3-d:5,6-d']bisimidazole-2,6-dithione-4,8-dioxide (26b)

Yield: (1.95 g, 3.6 mmol, 65.5 %) **Appearance:** White powder **Melting Point:** 268 °C.

^{1}H NMR (300.1 MHz, $CDCl_3$, 25 °C): δ = 1.02 (t, 12H, $^3J_{H,H}$ = 7.1 Hz, $NCH_2\underline{Me}$), 1.10 (t, 12H, $^3J_{H,H}$ = 7.1 Hz, $NCH_2\underline{Me}$) (2nd isomer), 1.44-1.49 (m, 12H, P-$NCH_2\underline{Me}$), 3.14-3.31 (m, 8H, P-N$\underline{CH_2}$Me), 4.01-4.15 (m, 4H, N$\underline{CH_2}$Me), 4.48-4.63 (m, 4H, N$\underline{CH_2}$Me).

^{13}C{^{1}H} NMR (75.5 MHz, $CDCl_3$, 25 °C): δ = 13.1 (d, $^3J_{P,C}$ = 2.2 Hz, P-$NCH_2\underline{Me}$), 13.3 (d, $^3J_{P,C}$ = 1.9 Hz, P-$NCH_2\underline{Me}$) *2nd isomer*, 13.4 & 13.7 (s, $NCH_2\underline{Me}$, *two isomers*), 37.9 (d, $^2J_{P,C}$ = 4.8 Hz, P-N$\underline{CH_2}$Me), 38.0 (d, $^2J_{P,C}$ = 5.4 Hz, P-N$\underline{CH_2}$Me) *2nd isomer*,43.2 & 43.3 (s, N$\underline{CH_2}$Me), 126.6(dd, $^1J_{P,C}$ = 154.9 Hz, $^2J_{P,C}$ = 19.7 Hz $\underline{C^5}$), 126.8(dd, $^1J_{P,C}$ = 155.1 Hz, $^2J_{P,C}$ = 19.9 Hz, $\underline{C^5}$) (2nd isomer), 168.2 (t, $^3J_{P,C}$ = 7.1 Hz, $\underline{C{=}S}$), 168.3 (t, $^3J_{P,C}$ = 7.1 Hz, $\underline{C{=}S}$) *2nd isomer*.

^{31}P NMR (121.5 MHz, $CDCl_3$, 25 °C): δ = -4.6 (quin, $^3J_{P,H}$ = 11.8 Hz), -5.2 (quin, $^3J_{P,H}$ = 12.2 Hz) *2nd isomer*, ratio = 1.5 :1.

IR [cm^{-1}]: ṽ = 2974 (m), 2938 (w), 1673 (w), 1440 (m), 1410 (s), 1315 (m), 1266 (s), 1163 (s), 1066 (s), 945 (s), 794 (s), 712 (s).

Pos-ESI-MS: for $C_{22}H_{40}N_6P_2S_2O_2Na$ theor./exp. 569.2027/ 569.2029.

EA [%]: theor./exp. C 48.34/47.99, H 7.38/7.28; N 15.37/15.56, S 11.73/12.66.

10.18.3 4,8-Diphenyl-1,3,5,7-tetraethyl-4,8-dihydro[1,4]diphosphinine[2,3-d:5,6-d']bisimidazole-2,6-dithione-4,8-dioxide (26d)

Yield: 2.08 g (3.7 mmol, 67.3 %) **Appearance:** white powder **Melting Point:** 245 °C.

^{1}H NMR (300 MHz, $CDCl_3$): δ = 0.96 (t, 12H, $^3J_{H,H}$ = 7.1 Hz, N-$CH_2\underline{Me}$), 1.07 (m, 12H, $^3J_{H,H}$ = 7.1 Hz N-$CH_2\underline{Me}$) 2nd isomer, 3.92-4.08 (m, 8H, N-$\underline{CH_2}$Me), 4.26-4.39 (m, 8H, N-$\underline{CH_2}$Me) 2nd isomer, 7.62-7.96 (m, 10H, *Ph ring protons*).

^{13}C{^{1}H} NMR (75.0 MHz, $CDCl_3$): δ = 12.6 (s, N-$CH_2\underline{Me}$), 12.8 (s, N-$CH_2\underline{Me}$) 2nd isomer, 43.5 (br, N-$\underline{CH_2}$Me), 125.5 (dd, $^1J_{P,C}$ = 132.4 Hz, $^2J_{P,C}$ = 16.6 Hz, $\underline{C^5}$), 125.9 (dd, $^1J_{P,C}$ = 131.9 Hz, $^2J_{P,C}$ = 16.1 Hz, $\underline{C^5}$) 2nd isomer, 126.6 (d, $^1J_{P,C}$ = 54.1 Hz, *ipso*-C), 128.2 (d, $^1J_{P,C}$ = 54.6 Hz, *ipso*-C) 2nd isomer, 130.12, 130.13, 130.32 & 130.33 (s, *o-C of Ph ring*), 131.6, 131.8, 131.9 & 132.1 (s, *m-C of Ph ring*), 134.3,

134.4, 134.5 & 134.6 (s, *p-C of Ph ring*), 168.8 (t, $^{3}J_{P,C}$ = 6.1 Hz, *C=S*), 168.9 (t, $^{3}J_{P,C}$ = 6.1 Hz, *C=S*) 2nd isomer.

^{31}P NMR (121.5 MHz, $CDCl_3$): δ = -5.9 (t, $^{3}J_{P,H}$ = 14.4 Hz) & -7.4 (t, $^{3}J_{P,H}$ = 13.5 Hz) ratio 1:1.3.

IR [cm^{-1}]: ṽ = 2988 (w), 1723 (w), 1439 (m), 1216 (s), 1151 (s), 1059 (s), 997 (s).

MS (EI, 70 eV): *m/z* (%) = 556.1(100) $[M]^+$.

HRMS m/z: theor./exp. for $[C_{26}H_{30}N_4O_2P_2S_2]$: 556.1285/556.1281.

EA [%]: theor./exp. C 56.10/56.19, H 5.43/5.53; N 10.07/10.18, S 11.52/10.58.

10.18.4 4,8-Diphenyl-1,3,5,7-tetra-*n*-butyl-4,8-dihydro[1,4]diphosphinine[2,3-d:5,6-d']bisimidazole-2,6-dithione-4,8-dioxide (26e)

Yield: 2.76 g (4.1 mmol, 74.5 %) **Appearance:** white powder **Melting Point:** 182 °C

^{1}H NMR (300 MHz, $CDCl_3$): δ = 0.56-0.91 (m, 4H, N-CH_2*CH_2*CH_2Me), 0.76 & 0.78 (t, 12H, $^{3}J_{H,H}$ = 6.6 Hz, N-$CH_2CH_2CH_2$*Me*), 1.05-1.32 (m, 8H, N-CH_2CH_2*CH_2*Me), 1.74-1.90 (br, 4H, N-CH_2*CH_2*CH_2Me), 3.82-4.23 (m, 8H, N-*CH_2*CH_2CH_2Me), 7.61-7.97 (m, 10H, *Ph ring protons*).

^{13}C{^{1}H} NMR (75.0 MHz, $CDCl_3$): δ = 13.4 (s, N-$CH_2CH_2CH_2$*Me*), 19.8 & 19.9 (s, N-CH_2CH_2*CH_2*Me), 29.3 & 29.4 (s, N-CH_2*CH_2*CH_2Me), 48.1 & 48.3 (s, N-*CH_2*CH_2CH_2Me), 125.5 (dd, $^{1}J_{P,C}$ = 132.4 Hz, $^{2}J_{P,C}$ = 16.4 Hz, *C^{4,5}*), 125.9 (dd, $^{1}J_{P,C}$ = 131.9 Hz, $^{2}J_{P,C}$ = 16.3 Hz, *C^{4,5}*) 2nd isomer, 126.8 (d, $^{1}J_{P,C}$ = 50.6 Hz, *ipso*-C), 128.4 (d, $^{1}J_{P,C}$ = 51.2 Hz, *ipso*-C) 2nd isomer, 129.9, 130.1, 130.2 & 130.3 (s, *o-C of Ph ring*), 131.7, 131.8, 131.9 & 132.0 (s, *m-C of Ph ring*), 134.2, 134.3, 134.3 & 134.4 (s, *p-C of Ph ring*), 169.1 (t, $^{3}J_{P,C}$ = 6.6 Hz, *C=S*), 169.2 (t, $^{3}J_{P,C}$ = 6.9 Hz, *C=S*) 2nd isomer.

^{31}P NMR (121.5 MHz, $CDCl_3$): δ = -6.7 (t, $^{3}J_{P,H}$ = 16.5 Hz) & -8.4 (t, $^{3}J_{P,H}$ = 14.0 Hz) ratio 1.3:1.

IR [cm^{-1}]: ṽ = 2957 (m), 2872 (w), 1435 (m), 1412 (s), 1212 (s), 1108 (w), 856 (s), 724 (s), 694(s).

Pos-ESI-MS: for $C_{22}H_{40}N_6P_2S_2O_2Na$ theor./exp. 691.2435/ 691.2433.

EA [%]: theor./exp. C 61.06/60.18, H 6.93/7.05; N 8.38/8.65, S 9.59/9.06.

10.19 Oxidation of the tricyclic 1,4-dihydro-1,4-diphosphinines with elemental sulfur / synthesis of the P-dioxides 27a-e

To a solution of **4d-f; 22b,c** (5.5 mmol) in toluene (50 ml), 12.1 mmol (2.2 equiv) of elemental sulfur was added. This mixture was then heated at 105°C for a week to complete the reactions. After the completion of the reaction the solvent was removed under reduced pressure (8×10^{-3} mbar) and the residue was washed with *n*-pentane (3 × 5 ml) to get a light yellow solid as the pure compound.

10.19.1 4,8-Bis(diethylamino)-1,3,5,7-tetramethyl-4,8-dihydro[1,4]diphosphinine[2,3-d:5,6-d']bisimidazole-2,6-dithione-4,8-disulfide (27a)

Yield: (1.87 g, 3.6 mmol, 65.4 %). **Appearance:** light yellow solid **Melting Point:** 275 °C

^{1}H NMR (300.1 MHz, $CDCl_3$, 25 °C): δ = 1.07 (t, 12H, $^3J_{H,H}$ = 6.7 Hz, P-NCH_2*Me*), 1.09 (t, 12H, $^3J_{H,H}$ = 6.7 Hz, P-NCH_2*Me*) (2nd isomer), 3.27- 3.42 (m, 8H, P-N*CH_2*Me), 3.89 & 3.91 (s, 12H, N-*Me*).

^{13}C{^{1}H} NMR (75.5 MHz, $CDCl_3$, 25 °C): δ = 13.2 (d, $^3J_{P,C}$ = 2.3 Hz, P-NCH_2*Me*), 13.3 (d, $^3J_{P,C}$ = 2.7 Hz, P-NCH_2*Me*) *2nd isomer*, 34.2 (br, N-*Me*), 39.1 (d, $^2J_{P,C}$ = 5.2 Hz, P-N*CH_2*Me), 39.2 (d, $^2J_{P,C}$ = 5.8 Hz, P-N*CH_2*Me) 2nd isomer, 125.1 (dd, $^1J_{P,C}$ = 134.7 Hz, , $^2J_{P,C}$ = 16.5 Hz *C^5*), 125.2 (dd, $^1J_{P,C}$ = 133.1 Hz, , $^2J_{P,C}$ = 16.5 Hz, *C^5*) (2nd isomer), 169.8 (t, $^3J_{P,C}$ = 6.4 Hz, *C=S*), 170.0(t, $^3J_{P,C}$ = 5.8 Hz, *C=S*) *2nd isomer*.

^{31}P NMR (121.5 MHz, $CDCl_3$, 25 °C): δ = 19.7 (quin, $^3J_{P,H}$ = 13.6 Hz), 20.3 (quin, $^3J_{P,H}$ = 13.6 Hz) *2nd isomer*, ratio = 1 :1.5.

IR [cm^{-1}]: ṽ = 3387 (s), 2971 (w), 2939 (w), 1431 (m), 1382 (s), 1324 (s), 1160 (s), 1011 (s), 945 (s), 852 (s), 793 (m).

MS (EI, 70 eV): m/z (%) = 522.1 (70) $[M]^{\cdot+}$, 315.0 (100) $[C_{10}H_{13}N_4P_2S_2]^{\cdot+}$.

HRMS m/z: theor./exp. for $[C_{18}H_{32}N_6P_2S_4]$: 522.1046/522.1044.

EA [%]: theor./exp. C 41.36/41.25, H 6.17/5.83; N 16.08/16.19, S 24.53/23.98.

10.19.2 4,8-Bis(diethylamino)-1,3,5,7-tetraethyl-4,8-dihydro[1,4]diphosphinine[2,3-d:5,6-d']bisimidazole-2,6-dithione-4,8-disulfide (27b)

Yield: (2.29 g, 3.9 mmol, 70.9 %). **Appearance:** light yellow solid **Melting Point:** 245 °C

^{1}H NMR (300.1 MHz, $CDCl_3$, 25 °C): δ = 1.03 (t, 12H, $^3J_{H,H}$ = 7.2 Hz, NCH_2*Me*), 1.08 (t, 12H, $^3J_{H,H}$ = 7.2 Hz, NCH_2*Me*) (2nd isomer), 1.51 (t, 12H, $^3J_{H,H}$ = 7.0 Hz, P-NCH_2*Me*), 1.54 (t, 12H, $^3J_{H,H}$ = 7.0 Hz, P-

$NCH_2\underline{Me}$) 2nd isomer, 3.27-3.44 (m, 8H, P-N$\underline{CH_2}$Me), 4.14-4.32 (m, 4H, N$\underline{CH_2}$Me), 4.47-4.64 (m, 4H, N$\underline{CH_2}$Me).

$^{13}C\{^1H\}$ NMR (75.5 MHz, $CDCl_3$, 25 °C): δ = 13.1 (br, P-$NCH_2\underline{Me}$), 13.3 (br, P-$NCH_2\underline{Me}$) *2nd isomer*, 13.2 (br, $NCH_2\underline{Me}$), 39.3 (d, $^2J_{P,C}$ = 2.8 Hz, P-N$\underline{CH_2}$Me), 39.4 (d, $^2J_{P,C}$ = 2.9 Hz, P-N$\underline{CH_2}$Me) *2nd isomer*, 42.7 & 42.8 (s, N$\underline{CH_2}$Me), 125.3 (dd, $^1J_{P,C}$ = 133.8 Hz, $^2J_{P,C}$ = 8.4 Hz $\underline{C^5}$), 125.5 (dd, $^1J_{P,C}$ = 133.8 Hz, $^2J_{P,C}$ = 8.7 Hz, $\underline{C^5}$) (2nd isomer), 168.5 (t, $^3J_{P,C}$ = 6.5 Hz, $\underline{C{=}S}$).

^{31}P NMR (121.5 MHz, $CDCl_3$, 25 °C): δ = 20.1 (quin, $^3J_{P,H}$ = 13.8 Hz), 20.5 (quin, $^3J_{P,H}$ = 13.9 Hz) *2nd isomer*, ratio = 1 :1.2.

IR [cm^{-1}]: ṽ = 2974 (m), 2934 (w), 1440 (m), 1407 (s), 1309 (m), 1232 (s), 1162 (s), 1014 (s), 978 (s), 805 (s), 709 (s).

Pos-ESI-MS: for $C_{22}H_{40}N_6P_2S_4H$ theor./exp. 579.1751/ 579.1745.

EA [%]: theor./exp. C 45.65/45.29, H 6.97/6.75; N 14.52/14.56, S 22.16/22.57.

10.19.3 4,8-Bis(diethylamino)-1,3,5,7-tetra-*n*-butyl-4,8-dihydro[1,4]diphosphinine[2,3 -d:5,6-d']bisimidazole-2,6-dithione-4,8-disulfide (27c)

Yield: (2.14 g, 3.1 mmol, 56.4 %) **Appearance:** light yellow solid **Melting Point:** 167 °C

^1H NMR (300.1 MHz, $CDCl_3$, 25 °C): δ = 1.01 (t, 12H, $^3J_{H,H}$ = 6.9 Hz, $NCH_2CH_2CH_2\underline{Me}$) ,1.07 (t, 12H, $^3J_{H,H}$ = 6.7 Hz, P-$NCH_2\underline{Me}$), 1.38-1.51 (m, 8H, $NCH_2CH_2\underline{CH_2}$Me), 1.88-2.07 (m, 8H, $NCH_2\underline{CH_2}CH_2$Me), 3.25-3.37 (m, 8H, P-N$\underline{CH_2}$Me), 4.06-4.19 (m, 4H, N$\underline{CH_2}CH_2CH_2$Me), 4.35-4.49 (m, 4H, N$\underline{CH_2}CH_2CH_2$Me).

$^{13}C\{^1H\}$ NMR (75.5 MHz, $CDCl_3$, 25 °C): δ = 13.3 (d, $^3J_{P,C}$ = 2.7 Hz, P-$NCH_2\underline{Me}$), 13.7 (br, $NCH_2CH_2CH_2\underline{Me}$), 19.9 (s,$NCH_2CH_2\underline{CH_2}$Me), 29.2 (s, $NCH_2\underline{CH_2}CH_2$ Me), 39.3 (d, $^2J_{P,C}$ = 5.7 Hz, P-N$\underline{CH_2}$Me), 47.6 (s, N$\underline{CH_2}CH_2CH_2$Me), 125.2 (dd, $^1J_{P,C}$ = 134.1 Hz, $^2J_{P,C}$ = 16.3 Hz $\underline{C^{4,5}}$), 168.7 (t, $^3J_{P,C}$ = 6.6 Hz, $\underline{C{=}S}$).

^{31}P NMR (121.5 MHz, $CDCl_3$, 25 °C): δ = 19.9 (quin, $^3J_{P,H}$ = 13.5 Hz), 20.2 (quin, $^3J_{P,H}$ = 13.5 Hz) *2nd isomer*, ratio = 15 :1.

IR [cm^{-1}]: ṽ = 2959 (m), 2933 (w), 2870 (w), 1440 (m), 1407 (s), 1309 (m), 1216 (m), 1160 (s), 1016 (s), 947 (m), 707 (s).

Pos-ESI-MS: for $C_{30}H_{56}N_6P_2S_4H$ theor./exp. 691.3003/ 691.2997.

EA [%]: theor./exp. C 52.15/52.18, H 8.17/8.28; N 12.16/11.83, S 18.56/18.26.

10.19.4 4,8-Diphenyl-1,3,5,7-tetraethyl-4,8-dihydro[1,4]diphosphinine[2,3-d:5,6-d']bisimidazole-2,6-dithione-4,8-disulfide (27d)

Yield: 2.59 g (4.4 mmol, 80.0 %) **Appearance:** white powder **Melting Point:** 236 °C

^{1}H NMR (300 MHz, $CDCl_3$): δ = 0.74 (t, 12H, $^3J_{H,H}$ = 7.1 Hz, N-CH_2*Me*), 0.86 (m, 12H, $^3J_{H,H}$ = 7.1 Hz N-CH_2*Me*) 2nd isomer, 3.94-4.46 (m, 8H, N-*CH_2*Me), 7.17-8.13 (m, 10H, *Ph ring protons*).

^{13}C{^{1}H} NMR (75.0 MHz, $CDCl_3$): δ = 11.9 (s, N-CH_2*Me*), 12.0 (s, N-CH_2*Me*) 2nd isomer, 43.0 (br, N-*CH_2*Me), 123.7 (dd, $^1J_{P,C}$ = 115.9 Hz, $^2J_{P,C}$ = 13.6 Hz, *C^5*), 124.1 (dd, $^1J_{P,C}$ = 115.0 Hz, $^2J_{P,C}$ = 13.3 Hz, *C^5*) 2nd isomer, 127.2 (d, $^1J_{P,C}$ = 48.5 Hz, *ipso*-C), 128.4 (d, $^1J_{P,C}$ = 48.9 Hz, *ipso*-C) 2nd isomer, 130.0, 130.1, 130.2 & 130.3 (s, *o-C of Ph ring*), 132.2, 132.3, & 132.5 (s, *m-C of Ph ring*), 134.1 (br, *p-C of Ph ring*), 169.0 (t, $^3J_{P,C}$ = 6.3 Hz, *C=S*), 169.1 (t, $^3J_{P,C}$ = 6.3 Hz, *C=S*) 2nd isomer.

^{31}P NMR (121.5 MHz, $CDCl_3$): δ = 1.5 (t, $^3J_{P,H}$ = 15.9 Hz) & 3.0 (t, $^3J_{P,H}$ = 16.1 Hz) ratio 1.3:1.

IR [cm^{-1}]: $\tilde{\nu}$ = 2976 (w), 1436 (vs), 1372 (s), 1339 (m), 1263 (s), 1094 (s), 996 (m).

MS (EI, 70 eV): *m/z* (%) = 588.1 $[M]^+$ (10), 255.8 $[C_{10}H_{12}N_2PS_2]^+$ (100), 159.9 (50) $[C_8H_5N_2P]^+$.

HRMS m/z: theor./exp. for $[C_{26}H_{30}N_4P_2S_4]$: 588.0828/588.0827.

EA [%]: theor./exp. C 53.04/52.56, H 5.14/4.87; N 9.52/9.02, S 21.78/21.58.

10.19.5 4,8-Diphenyl-1,3,5,7-tetra-*n*-butyl-4,8-dihydro[1,4]diphosphinine[2,3-d:5,6-d']bisimidazole-2,6-dithione-4,8-disulfide (27e)

Yield: 2.89 g (4.1 mmol, 74.5 %) **Appearance:** white powder **Melting Point:** 162 °C

^{1}H NMR (300 MHz, $CDCl_3$): δ = 0.19-0.35 (m, 4H, N-CH_2CH_2*CH_2*Me), 0.68 (t, 12H, $^3J_{H,H}$ = 7.4 Hz, N-$CH_2CH_2CH_2$*Me*), 0.91-1.03 (m, 4H, N-CH_2CH_2*CH_2*Me), 1.09-1.22 (m, 4H, N-CH_2*CH_2*CH_2Me), 1.67-1.82 (m, 4H, N-CH_2*CH_2*CH_2Me), 3.97-4.31 (m, 8H, N-*CH_2*CH_2CH_2Me), 7.61-8.15 (m, 10H, *Ph ring protons*).

^{13}C{^{1}H} NMR (75.0 MHz, $CDCl_3$): δ = 13.4 (s, N-$CH_2CH_2CH_2$*Me*), 19.8 (s, N-CH_2CH_2*CH_2*Me), 28.7 (s, N-CH_2*CH_2*CH_2Me) , 47.7 (s, N-*CH_2*CH_2CH_2Me), 123.6 (dd, $^1J_{P,C}$ = 115.9 Hz, $^2J_{P,C}$ = 13.6 Hz, *C^5*), 127.7 (d,

$^{1}J_{P,C}$ = 93.4 Hz, *ipso*-C), 129.9 & 130.1 (s, *o-C of Ph ring*), 132.3 & 132.5 (s, *m-C of Ph ring*), 133.9 & 134.0 (s, *p-C of Ph ring*), 169.4 (t, $^{3}J_{P,C}$ = 5.9 Hz, *C=S*).

^{31}P NMR (121.5 MHz, $CDCl_3$): δ = 1.4 (t, $^{3}J_{P,H}$ = 15.3 Hz) & 3.1 (t, $^{3}J_{P,H}$ = 16.1 Hz) ratio 10:1.

IR [cm^{-1}]: ṽ = 2958 (w), 2930 (w), 2872 (w), 1407 (s), 1383 (s), 1357 (m), 1217 (s), 1158 (m), 1094 (s), 856 (s).

Pos-ESI-MS: for $C_{34}H_{46}N_4P_2S_4H$ theor./exp. 701.2158/ 701.2156.

EA [%]: theor./exp. C 58.26/57.98, H 6.61/6.56; N 7.99/7.86, S 18.29/17.92.

10.20 Oxidation of tricyclic 1,4-dihydro-1,4-diphosphinines with *o*-chloranil

A solution of **4d-f** (1.1 mmol) in methylene dichloride (15 ml) was treated with 2.2 mmol (2 equiv) of *o*-chloranil at room temperature. The reaction mixture was then allowed to stir for overnight to reach completion. Afterwards the reaction mixture was dried in *vacuo* (8×10^{-3} mbar) to get a dark brown residue. This crude product was later on washed once with diethyl ether (5 ml) to remove the coloring impurity, to get a light brown solid. This solid was then washed with *n*-pentane (2 × 5 ml) and dried in *vacuo* (8×10^{-3} mbar) to get a light brown powder.

10.20.1 4,8-Bis(diethylamino)-1,3,5,7-tetramethyl-4,8-dihydro[1,4]diphosphinine[2,3-d:5,6-d']bisimidazole-2,6-dithione-4,8-bis(tetrachlorobenzodioxaphosphole) (28a)

Yield: (0.85g, 0.9 mmol, 82.1 %) **Appearance:** light brown powder **Melting Point:** decomp. at 350 °C

^{1}H NMR (300.1 MHz, CD_2Cl_2, 25 °C): δ = 1.19 (t, 12H, $^{3}J_{H,H}$ = 6.9 Hz, P-NCH_2*Me*), 1.21 (br, 12H, P-NCH_2*Me*) (2nd isomer), 3.16 (br, 8H, P-N*CH_2*Me), 3.85 & 3.91 (s, 12H, N-*Me*).

^{13}C{^{1}H} NMR (75.5 MHz, CD_2Cl_2, 25 °C): δ = 14.1 (br, P-NCH_2*Me*), 37.1 (br, N-*Me*), 44.4 (br, P-N*CH_2*Me), 114.4 (s, *o-chloranil ring C*), 124.8 (s, *o-chloranil ring C*), 135.9 (dd, $^{1}J_{P,C}$ = 164.9 Hz, , $^{2}J_{P,C}$ = 24.9 Hz *C^5*), 140.1 (s, *o-chloranil ring C*), 170.1 (t, $^{3}J_{P,C}$ = 7.3 Hz, *C=S*).

^{31}P NMR (121.5 MHz, CD_2Cl_2, 25 °C): δ = -53.2 (quin, $^{3}J_{P,H}$ = 13.8 Hz), -54.9 (br) *2nd isomer*, ratio = 12:1.

IR [cm^{-1}]: ṽ = 2968 (w), 1454 (s), 1383 (m), 1321 (m), 1156 (s), 1009 (s), 994 (s), 825 (s), 814 (s).

Pos-ESI-MS: for $C_{30}H_{32}N_6Cl_8P_2O_4S_2H$ theor./exp. 950.8929/950.8928.

EA [%]: theor./exp. C 37.92/36.91, H 3.39/3.72; N 8.84/8.23, S 7.75/7.72.

10.20.2 4,8-Bis(diethylamino)-1,3,5,7-tetraethyl-4,8-tetrahydro[1,4]diphosphinine[2,3-d:5,6-d']bisimidazole-2,6-dithione-4,8-bis(tetrachlorobenzodioxaphosphole) (28b)

Yield: (0.89 g, 0.88 mmol, 80.2 %) **Appearance:** beige powder **Melting Point:** decom. at 300 °C

^{1}H NMR (300.1 MHz, $CDCl_3$, 25 °C): δ = 1.03 (t, 12H, $^3J_{H,H}$ = 7.0 Hz, $NCH_2\underline{\mathit{Me}}$), 1.19 (t, 12H, $^3J_{H,H}$ = 7.0 Hz, $NCH_2\underline{\mathit{Me}}$) (2nd isomer), 1.44 (t, 12H, $^3J_{H,H}$ = 6.3 Hz, P-$NCH_2\underline{\mathit{Me}}$), 1.47 (t, 12H, $^3J_{H,H}$ = 6.3 Hz, P-$NCH_2\underline{\mathit{Me}}$) 2nd isomer, 2.94-3.24 (m, 8H, P-N$\underline{\mathit{CH_2}}$Me), 4.31-4.68 (m, 4H, N$\underline{\mathit{CH_2}}$Me).

^{13}C{^{1}H} NMR (75.5 MHz, $CDCl_3$, 25 °C): δ = 13.4 (s, $NCH_2\underline{\mathit{Me}}$), 13.8 (s, $NCH_2\underline{\mathit{Me}}$) *2nd isomer*, 13.8 (br, P-$NCH_2\underline{\mathit{Me}}$), 14.4 (br, P-$NCH_2\underline{\mathit{Me}}$) *2nd isomer*, 43.4 (s, N$\underline{\mathit{CH_2}}$Me), 44.2 (s, N$\underline{\mathit{CH_2}}$Me), 44.5 (br, P-N$\underline{\mathit{CH_2}}$Me), 114.6 & 114.9 (s, *o-chloranil ring C*), 125.4 & 125.8 (s, *o-chloranil ring C*), 134.6 (dd, $^1J_{P,C}$ = 167.1 Hz, $^2J_{P,C}$ = 22.9 Hz, $\underline{\mathit{C^5}}$), 135.9 (dd, $^1J_{P,C}$ = 175.5 Hz, $^2J_{P,C}$ = 24.6 Hz $\underline{\mathit{C^5}}$), (2nd isomer), 139.9 & 140.4 (s, *o-chloranil ring C*), 166.5 (t, $^3J_{P,C}$ = 8.1 Hz, $\underline{\mathit{C{=}S}}$), 168.1 (t, $^3J_{P,C}$ = 7.5 Hz, $\underline{\mathit{C{=}S}}$).

^{31}P NMR (121.5 MHz, $CDCl_3$, 25 °C): δ = -46.7 (quin, $^3J_{P,H}$ = 15.1 Hz), -52.2 (quin, $^3J_{P,H}$ = 13.9 Hz) *2nd isomer*, ratio = 1 :2.5.

IR [cm^{-1}]: $\tilde{\nu}$ = 2974 (w), 2936 (w), 1452 (s), 1405 (s), 1263 (m), 1154 (s), 1008 (s), 914 (s), 825 (s), 817 (s).

Pos-ESI-MS: for $C_{34}H_{40}N_6Cl_8O_4P_2S_2H$ theor./exp. 1006.9555/ 1006.9556.

EA [%]: theor./exp. C 40.58/39.67, H 4.01/3.93; N 8.35/7.98, S 6.37/6.41.

10.20.2 4,8-Bis(diethylamino)-1,3,5,7-tetra-*n*-butyl-4,8-dihydro[1,4]diphosphinine[2,3-d:5,6-d']bisimidazole-2,6-dithione-4,8-bis(tetrachlorobenzodioxaphosphole) (28c)

Yield: 1.08 g (0.97 mmol, 88.1 %) **Appearance:** white powder **Melting Point:** decom. at 260 °C

^{1}H NMR (300 MHz, $CDCl_3$): δ = 0.89 & 0.92 (t, 12H, $^3J_{H,H}$ = 7.6 Hz, N-$CH_2CH_2CH_2\underline{\mathit{Me}}$), 1.01 (t, 12H, $^3J_{H,H}$ = 6.3 Hz, P-$NCH_2\underline{\mathit{Me}}$), 1.20 (t, 12H, $^3J_{H,H}$ = 6.3 Hz, P-$NCH_2\underline{\mathit{Me}}$) *2nd isomer*, 1.25-1.52 (m, 8H, N-$CH_2CH_2\underline{\mathit{CH_2}}$Me), 1.72-2.11 (m, 8H, N-$CH_2\underline{\mathit{CH_2}}CH_2$Me), 2.88-3.18 (m, 8H, P-$NCH_2\underline{\mathit{Me}}$), 4.11-4.55 (m, 8H, N-$\underline{\mathit{CH_2}}CH_2CH_2$Me).

$^{13}C\{^1H\}$ NMR (75.0 MHz, $CDCl_3$): δ = 13.6 & 13.7 (s, N-$CH_2CH_2CH_2$*Me*), 13.9 & 14.2 (br, P-NCH_2*Me*), 20.3 & 20.4 (s, N-CH_2CH_2*CH_2*Me), 29.5 & 29.9 (s, N-CH_2*CH_2*CH_2Me), 43.9 & 44.4 (br, P-N*CH_2*Me), 48.6 & 49.0 (s, N-*CH_2*CH_2CH_2Me), 114.7 (m, *o-chloranil ring C*), 125.4 & 125.7 (s, *o-chloranil ring C*), 136.0 (dd, $^1J_{P,C}$ = 179.2 Hz, $^2J_{P,C}$ = 23.8 Hz, *C*^{4,5}), 139.8 & 140.5 (s, *o-chloranil ring C*), 166.6 (t, $^3J_{P,C}$ = 8.1 Hz, *C=S*), 168.7 (t, $^3J_{P,C}$ = 7.5 Hz, *C=S*) 2nd isomer.

^{31}P NMR (121.5 MHz, $CDCl_3$): δ = -43.6 (quin, $^3J_{P,H}$ = 14.8 Hz), -52.2 (quin, $^3J_{P,H}$ = 14.1 Hz) *2nd isomer*, ratio = 1 :1.

IR [cm^{-1}]: ṽ = 2959 (m), 2871 (w), 1457 (s), 1403 (s), 1258 (s), 1217 (m), 1155 (m), 1009(s), 996 (s), 816 (s).

Pos-ESI-MS: for $C_{42}H_{56}N_6Cl_8O_4P_2S_2H$ theor./exp. 1119.0810/ 1119.0808.

EA [%]: theor./exp. C 45.10/44.70, H 5.05/4.93; N 7.51/7.32, S 5.73/6.12.

10.21 S-methylation of 1,4-dihydro-1,4-diphosphinines with methyl triflate

4d,f; 22b,c (1.1 mmol) in 20 mL of methylene dichloride were treated with 2.2 mmol of methyl triflate at room temperature. In the case of **4d** a white precipitate slowly formed with time. This precipitate was separated by means of cannula filtration and washed with diethyl ether (2 × 2 ml) to get **29a**. In other three cases the reaction mixtures were concentrated in vacuo to get the **29b-d**. The products were finally washed with *n*-pentane (2 × 5 ml) and then dried under reduced pressure to remove traces of methylene dichloride.

10.21.1 4,8-Bis(diethylamino)-1,3,5,7-tetramethyl-4,8-dihydro[1,4]diphosphinine[2,3-d:5,6-d']bisimidazole-2,6-bis(imidazolium)trifluoromethanesulfonate (29a)

Yield: (0.39 g, 0.5 mmol, 45.4 %) **Appearance:** White powder **Melting Point:** 223 °C

^1H NMR (300.1 MHz, DMSO-d_6, 25 °C): δ = 0.91 (br, 12H, P-NCH_2*Me*), 2.50 & 2.60 (br, S-*Me*) two isomers, 2.95 (br, 12H, P-N*CH_2*Me), 4.02 & 4.08 (s, N-*Me*).

$^{13}C\{^1H\}$ NMR (75.5 MHz, DMSO-d_6, 25 °C): δ = 14.1 (br, P-NCH_2*Me*), 17.6 & 17.7 (s, S-*Me*), 36.8(t, $^3J_{P,C}$ = 5.4 Hz, N-*Me*), P-N*CH_2*Me signal was hidden under the solvent signal, 121.1 (q, $^1J_{P,F}$ = 332.1 Hz, $CF_3SO_3^-$), 135.9 & 136.0 (d, $^1J_{P,C}$ = 5.9 Hz, *C*^{4,5}), 149.7 (br, ***C*-*SMe***).

^{31}P NMR (121.5 MHz, DMSO-d_6, 25 °C): δ = 3.7 (quin, $^3J_{P,H}$ = 8.3 Hz) & 5.9 (br) *2nd isomer,* ratio = 1:11.

IR [cm^{-1}]: $\tilde{\nu}$ = 2982 (w), 2944 (w), 1444 (w), 1385 (w), 1257 (s), 1150 (s), 1058 (s), 941 (m), 838(s).

Pos-ESI-MS: for $[C_{20}H_{38}N_6P_2S_2]^{2+}$ theor./exp. 244.103/ 244.103,

Neg-ESI-MS: for $[CF_3SO_3]^-$ theor./exp. 148.9/148.9.

EA [%]: theor./exp. C 33.59/33.70, H 4.87/4.80; N 10.68/10.67, S 16.30/16.30.

10.21.2 4,8-Bis(diethylamino)-1,3,5,7-tetra-*n*-butyl-4,8-dihydro[1,4]diphosphinine[2,3-d:5,6-d']bisimidazole-2,6-bis(imidazolium)trifluoromethanesulfonate (29b)

Yield: (0.96 g, 0.97 mmol, 88.1 %) **Appearance:** orange oil **Melting Point:** liq. at r.t.

^{1}H NMR (300.1 MHz, $CDCl_3$, 25 °C): δ = 0.98 (br, 12H, P-$NCH_2\underline{\textit{Me}}$), 1.06 (t, 12H, $^3J_{H,H}$ = 7.5 Hz, $NCH_2CH_2CH_2\underline{\textit{Me}}$), 1.43-1.61 (m, 8H, $NCH_2CH_2\underline{\textit{CH}_2}Me$), 1.81-1.99 (m, 4H, $NCH_2\underline{\textit{CH}_2}CH_2Me$), 2.04-2.19 (m, 4H, $NCH_2\underline{\textit{CH}_2}CH_2Me$), 2.69 & 2.71 (br, S-$\underline{\textit{Me}}$) *two isomers*, 2.91-3.32 (m, 8H, P-$N\underline{\textit{CH}_2}Me$), 4.31-4.147 (m, 4H, $N\underline{\textit{CH}_2}CH_2CH_2Me$), 4.56-4.78 (m, 4H, $N\underline{\textit{CH}_2}CH_2CH_2Me$).

^{13}C{^{1}H} NMR (75.5 MHz, $CDCl_3$, 25 °C): δ = 13.2 & 13.8 (br, $NCH_2CH_2CH_2\underline{\textit{Me}}$), 13.5 (br, P-$NCH_2\underline{\textit{Me}}$), 19.2 & 19.3 (S-$\underline{\textit{Me}}$), 19.9 & 20.0 (s, $NCH_2CH_2\underline{\textit{CH}_2}Me$), 31.9 & 32.2 (br, $NCH_2\underline{\textit{CH}_2}CH_2Me$), 45.0 (br, P-$N\underline{\textit{CH}_2}Me$), 45.7 (d, $^2J_{P,C}$ = 18.3 Hz, P-$N\underline{\textit{CH}_2}Me$) *2nd isomer*, 48.6 & 49.7 (br, $N\underline{\textit{CH}_2}CH_2CH_2Me$), 120.8 (q, $^1J_{P,F}$ = 321.2 Hz, $CF_3SO_3^-$), 136.4 (dt, $^1J_{P,C}$ = 16.5 Hz, $^2J_{P,C}$ = 6.8 Hz $\underline{\textit{C}^{4,5}}$), 147.5 (br, ***C***=SMe), 147.8 (br, ***C***=SMe) *2nd isomer*.

^{31}P NMR (121.5 MHz, $CDCl_3$, 25 °C): δ = 2.2 (br) & 3.2 (br) *two isomers*, ratio = 2.4:1.

IR [cm^{-1}]: $\tilde{\nu}$ = 2966 (m), 2935 (w), 2876 (w), 1468 (m), 1382 (w), 1262 (s), 1146 (s), 1030 (s), 937 (m), 794 (m).

Pos-ESI-MS: for $[C_{32}H_{62}N_6P_2S_2]^{2+}$ theor./exp. 328.198/ 328.198

Neg-ESI-MS: for $[CF_3SO_3]^-$ theor./exp. 148.9/148.9.

EA [%]: theor./exp. C 42.76/41.65, H 6.54/6.35; N 8.80/8.22, S 13.43/13.39.

10.21.3 4,8-Diphenyl-1,3,5,7-tetraethyl-4,8-dihydro[1,4]diphosphinine[2,3-d:5,6-d']bisimidazole-2,6-bis(imidazolium) trifluoromethanesulfonate (29c)

Yield: 0.76 g (0.94 mmol, 85.6 %) **Appearance:** white powder **Melting Point:** 249 °C

^{1}H NMR (300 MHz, $CDCl_3$): δ = 0.88 (t, 12H, $^{3}J_{H,H}$ = 7.2 Hz, N-CH_2*Me*), 1.47 (m, 12H, $^{3}J_{H,H}$ = 7.3 Hz N-CH_2*Me*) 2nd isomer, 2.63 & 2.69 (s, 6H, S-*Me*), 4.22-4.79 (m, 8H, N*CH*$_2$Me), 7.17-7.89 (m, 10H, *Ph ring protons*).

^{13}C{^{1}H} NMR (75.0 MHz, $CDCl_3$): δ = 14.2 (s, N-CH_2*Me*), 15.5 (s, N-CH_2*Me*) 2nd isomer, 18.9 & 19.1 (s, S-*Me*) *two isomers*, 45.4 (m, N-*CH*$_2$Me), 45.9 (m, N-*CH*$_2$Me) 2nd isomer, 120.6 (q, $^{1}J_{P,F}$ = 320.6 Hz, $CF_3SO_3^-$), 128.1 (m, *C*^{4,5}), 130.0 (t, $J_{P,C}$ = 3.8 Hz, *Ph ring-C*), 130.6 (m, *Ph ring-C*), 130.9 (s, *Ph ring-C*), 132.3 (m, *Ph ring-C*), 133.2 (s, *Ph ring-C*), 133.4 (d, $^{1}J_{P,C}$ = 8.1 Hz, *ipso-C Ph ring*), 136.1, 136.2 & 136.5 (s, *Ph ring-C*), 147.5 (br, ***C***=SMe), 147.8 (br, ***C***=SMe) *2nd isomer*.

^{31}P NMR (121.5 MHz, $CDCl_3$): δ = -49.54 (br) & -55.84 (br), two isomers, ratio 1:1.3.

IR [cm^{-1}]: ṽ = 2992 (w), 1472 (m), 1259 (vs), 1140 (s), 1087 (m), 1000 (m).

Pos-ESI-MS: theor./exp. for $[C_{28}H_{36}N_4P_2S_2]^{2+}$: 277.093/277.093

Neg-ESI-MS: for $[CF_3SO_3]^-$ theor./exp. 148.9/148.9.

EA [%]: theor./exp. C 42.25/41.94, H 4.26/4.26; N 6.57/6.30, S 15.04/14.89.

10.21.4 4,8-Diphenyl-1,3,5,7-tetra-*n*-butyl-4,8-dihydro[1,4]diphosphinine[2,3-d:5,6-d']bisimidazole-2,6-bis(imidazolium) trifluoromethanesulfonate (29d)

Yield: 1.01 g (1.06 mmol, 95.2 %) **Appearance:** white powder **Melting Point:** 187 °C

^{1}H NMR (300 MHz, CD_2Cl_2): δ = 0.62-0.72 (m, 2H, N-CH_2CH_2*CH_2*Me), 0.81 & 0.91 (t, 12H, $^{3}J_{H,H}$ = 7.5 Hz, N-$CH_2CH_2CH_2$*Me*) *two isomers*, 1.14-1.23 (m, 2H, N-CH_2CH_2*CH_2*Me), 1.25-1.35 (m, 4H, N-CH_2CH_2*CH_2*Me), 1.35-1.45 (m, 4H, N-CH_2*CH_2*CH_2Me), 1.62-1.73 (m, 2H, N-CH_2*CH_2*CH_2Me), 1.85-1.95 (m, 2H, N-CH_2*CH_2*CH_2Me), 2.61 & 2.68 (s, S-*Me*, *two isomers*), 4.16-4.55 (m, 8H, N-*CH_2*CH_2CH_2Me), 7.43-7.89 (m, 10H, *Ph ring protons*).

^{13}C{^{1}H} NMR (75.0 MHz, CD_2Cl_2): δ = 13.0 & 13.1 (s, N-$CH_2CH_2CH_2$*Me*), 18.9 & 19.1 (s, S-*Me*) *two isomers*, 19.8 & 19.9 (s, N-CH_2CH_2*CH_2*Me), 31.1 & 31.9 (br N-CH_2*CH_2*CH_2Me), 49.8 (m, N-*CH_2*CH_2 CH_2Me), 50.4 (m, N-*CH_2*CH_2CH_2Me) 2nd isomer, 120.8 (q, $^{1}J_{P,F}$ = 321.1 Hz, $CF_3SO_3^-$), 128.3 (m, *C*^{4,5}), 130.3 (t, $J_{P,C}$ = 4.4 Hz, *Ph ring-C*), 130.5 (m, *Ph ring-C*), 132.1 (s, *Ph ring-C*), 132.2 (s, *Ph ring-C*), 133.8 (m, *Ph ring-C*), 133.3 (d, $^{1}J_{P,C}$ = 8.1 Hz, *ipso-C Ph ring*), 136.0, & 136.3 (s, *Ph ring-C*), 146.7 (br, ***C***=SMe), 147.1(br, ***C***=SMe) *2nd isomer*.

^{31}P NMR (121.5 MHz, CD_2Cl_2): δ = -50.1 & -53.7 (br, two isomers, ratio 1.1:1).

IR [cm^{-1}]: ṽ = 2960 (m), 2872 (w), 1469 (w), 1344(w), 1255 (s), 1151 (s), 1027 (s), 846 (m).

Pos-ESI-MS: theor./exp. for $[C_{28}H_{36}N_4P_2S_2]^{2+}$: 333.155/333.155

Neg-ESI-MS: for $[CF_3SO_3]^-$ theor./exp. 148.9/148.9.

EA [%]: theor./exp. C 47.30/46.91, H 5.43/5.40; N 5.81/5.65, S 13.29/13.91.

10.22 Synthesis of P-borane complexes of 1,4-dihydro-1,4-diphosphinines

A solution of **4d-f** (1.1 mmol) in methylene dichloride (10 ml) was treated with 2.4 mmol of borane-dimethyl sulfide adduct at room temperature. The reaction mixture was stirred for 2h and concentrated in *vacuo* (8×10^{-3} mbar) to get a yellow residue. This yellow residue was washed with *n*-pentane (3 × 5 ml) to remove the yellow coloring impurities and obtain a white powder. Finally, these white powders were dried in *vacuo* (8×10^{-3} mbar) to obtain pure **30a-c**.

10.22.1 4,8-Bis(diethylamino)-1,3,5,7-tetramethyl-4,8-dihydro[1,4]diphosphinine[2,3-d:5,6-d']bisimidazole-2,6-dithione-4,8-diborane (30a)

Yield: 0.45 g (0.94 mmol, 85.4 %) **Appearance:** white powder **Melting Point:** decomp. at 210 °C

^{1}H NMR (300.1 MHz, $CDCl_3$, 25 °C): δ = 1.08 (br, 12H, P-NCH_2*Me*), 3.86 & 3.88 (s, 12H, N-*Me*).

^{13}C{^{1}H} NMR (75.5 MHz, $CDCl_3$, 25 °C): δ = 13.1 (br, P-NCH_2*Me*), 34.8 & 35.1 (s, N-*Me*), 41.3 & 41.4 (br, P-N*CH_2*Me), 123.2 (dd, $^1J_{P,C}$ = 87.6 Hz, $^2J_{P,C}$ = 9.4 Hz *C*^{5}), 124.6 (dd, $^1J_{P,C}$ = 87.6 Hz, , $^2J_{P,C}$ = 7.9 Hz, *C*^{5}) (2nd isomer), 170.6 (t, $^3J_{P,C}$ = 5.0 Hz, *C=S*), 170.7 (t, $^3J_{P,C}$ = 4.7 Hz, *C=S*) *2nd isomer*.

^{31}P NMR (121.5 MHz, $CDCl_3$, 25 °C): δ = 34.4 (br).

IR [cm^{-1}]: ṽ = 2974 (m), 2937 (w), 2410 (s), 2355 (w), 1424 (w), 1383 (s), 1328 (s), 1166 (s), 1057 (s), 1020 (s), 854(s).

MS (EI, 70 eV): m/z (%) = 472.2 (40) $[M - BH_3]^+$, 458.1 (70) $[M - 2BH_3]^+$, 315 (100) $[C_{10}H_{14}N_4P_2S_2]$.

EA [%]: theor./exp. C 44.46/43.81, H 7.88/7.76; N 17.28/16.53, S 13.19/13.45.

10.22.2 4,8-Bis(diethylamino)-1,3,5,7-tetraethyl-4,8-dihydro[1,4]diphosphinine[2,3-d:5,6-d']bisimidazole-2,6-dithione-4,8-diborane (30b)

Yield: 0.49 g (0.91 mmol, 82.3 %) **Appearance:** White powder **Melting Point:** decom. at 180 °C

^{1}H NMR (300.1 MHz, $CDCl_3$, 25 °C): δ = 1.07 (br, 12H, P-$NCH_2\underline{Me}$), 1.51 (t, 12H, $3J_{H,H}$ = 6.9 Hz, $NCH_2\underline{Me}$), 1.54 (t, 12H, $3J_{H,H}$ = 6.9 Hz, $NCH_2\underline{Me}$) 2nd isomer, 3.25 (br, 8H, P-$N\underline{CH_2}Me$), 4.17-4.32 (m, 8H, $N\underline{CH_2}Me$), 4.42-4.53 (m, 8H, $N\underline{CH_2}Me$) *2nd isomer*.

^{13}C{^{1}H} NMR (75.5 MHz, $CDCl_3$, 25 °C): δ = 13.3 & 13.4 (s, $NCH_2\underline{Me}$), 13.3 (br, P-$NCH_2\underline{Me}$), 41.5 & 41.6 (br, P-$N\underline{CH_2}Me$), 43.2 & 43.4 (s, $N\underline{CH_2}Me$), 122.9 (dd, $^{1}J_{P,C}$ = 87.7 Hz, $^{2}J_{P,C}$ = 9.0 Hz $\underline{C^5}$), 124.4 (dd, $^{1}J_{P,C}$ = 85.9 Hz, $^{2}J_{P,C}$ = 7.6 Hz, $\underline{C^5}$) (2nd isomer), 169.0 (t, $^{3}J_{P,C}$ = 4.8 Hz, $\underline{C{=}S}$), 169.1 (t, $^{3}J_{P,C}$ = 4.5 Hz, $\underline{C{=}S}$) *2nd isomer*.

^{31}P NMR (121.5 MHz, $CDCl_3$, 25 °C): δ = 33.7 (br), 34.3 (br) *2nd isomer*, ratio = 1.3:1.

IR [cm^{-1}]: $\tilde{\nu}$ = 2975 (m), 2936 (w), 2873 (w), 2414 (w), 1444 (w), 1404 (s), 1307 (m), 1264 (s), 1202 (s), 1162 (s), 1059 (m), 1020 (s), 978 (m), 950 (m).

Pos-ESI-MS: for $C_{22}H_{43}BN_6P_2S_2H$ theor./exp. 529.2632/ 529.2635.

EA [%]: theor./exp. C 48.72/47.93, H 8.55/8.20; N 15.50/14.77, S 11.82/11.94.

10.22.3 4,8-Bis(diethylamino)-1,3,5,7-tetra-*n*-butyl-4,8-dihydro[1,4]diphosphinine[2,3-d:5,6-d']bisimidazole-2,6-dithione-4,8-diborane (30c)

Yield: 0.43 g,(0.7 mmol, 63.6 %) **Appearance:** white powder **Melting point:** decomp. at 140 °C

^{1}H NMR (300.1 MHz, $CDCl_3$, 25 °C): δ = 1.01 (t, 24H, $^{3}J_{H,H}$ = 7.1 Hz, $NCH_2CH_2CH_2\underline{Me}$ & P-$NCH_2\underline{Me}$), 1.46 (br, 8H, $NCH_2CH_2\underline{CH_2}Me$), 1.95 (br, 8H, $NCH_2\underline{CH_2}CH_2Me$), 3.14 (br, 8H, P-$N\underline{CH_2}Me$), 4.03-4.15 (m, 4H, $N\underline{CH_2}CH_2CH_2Me$), 4.28-4.39 (m, 4H, $N\underline{CH_2}CH_2CH_2Me$).

^{13}C{^{1}H} NMR (75.5 MHz, $CDCl_3$, 25 °C): δ = 13.2 (br, P-$NCH_2\underline{Me}$), 13.6 (s, $NCH_2CH_2CH_2\underline{Me}$), 19.9 (s,$NCH_2CH_2\underline{CH_2}Me$), 29.3 (s, $NCH_2\underline{CH_2}CH_2Me$), 41.5 & 41.6 (s, P-$N\underline{CH_2}Me$), 48.3 (br, $N\underline{CH_2}CH_2CH_2Me$), 124.3 (dd, $^{1}J_{P,C}$ = 85.8 Hz, $^{2}J_{P,C}$ = 7.5 Hz $\underline{C^{4,5}}$), 169.3 (t, $^{3}J_{P,C}$ = 4.9 Hz, $\underline{C{=}S}$).

^{31}P NMR (121.5 MHz, $CDCl_3$, 25 °C): δ = 33.3 (br).

IR [cm^{-1}]: $\tilde{\nu}$ = 2967 (m), 2935 (w), 2872 (w), 2442 (w), 2410 (m), 2347 (w), 1441 (m), 1406 (s), 1200 (s), 1122 (s), 950 (s), 857 (s).

Pos-ESI-MS: for $C_{22}H_{59}BN_6P_2S_2H$ theor./exp. 641.3889/641.3890.

EA [%]: theor./exp. C 55.05/54.85, H 9.55/8.87; N 12.84/12.39, S 9.80/9.39.

10.23 Reductive cleavage of the *P*-Ph bonds in compound 22

To a THF (50 ml) solution of **22c** (1.1 mmol, 0.71 g), 4.4 mmol (0.16 g) of potassium metal was added at r.t. and left stirring overnight. Upon adding the metal, the color of the solution slowly changed to orange and gradually an orange precipitate started to form. After ~12h the reaction mixture was cooled to –78 °C and 4.4 mmol of *n*-butyl iodide were added to quench the dianion **31**, formed by reduction of **22c**. The reaction mixture turned clear and light yellow after adding the electrophile. The reaction mixture was then concentrated under reduced pressure (8×10^{-3} mbar) and the residue taken up in 30 ml of toluene. This toluene solution was then filtered through a silica bed to filter off the KCl. This filtrate was then dried in *vacuo* and finally the residue was washed with *n*-pentane. After wards the washed solid was dried in vacuo (8×10^{-3} mbar) to get a beige powder. The product was finally confirmed as **25b** by all analytical data.

10.24 Oxidative desulfurization of compound 22b

A solution of 0.98 g (1.9 mmol) of **22b** in 50 ml of chloroform was treated with 1,76ml of H_2O_2/H_2O at room temperature and left stirring for overnight. After 12h the solvent was removed under reduced pressure and the remaining solid was washed with diethyl ether for three times (5 ml) and afterwards dried for 3 hours.

10.24.1 4,8-Diiphenyl-1,3,5,7-tetraethyl-4,8-dihydro[1,4]diphosphinine[2,3-d:5,6-d'] bisimidazole-4,8-dioxide-2,6-bis(imidazolium) hydrogensulfate (32)

Yield: 1.18 g (1.7 mmol, 92.4 %) **Appearance:** white powder **Melting point:** 245 °C

^{1}H NMR (300.1 MHz, $CDCl_3$, 25 °C): δ = 1.20 (t, 12H, $^3J_{H,H}$ = 7.25 Hz, N-CH_2*CH_3*) 1.26 (t, 12H, $^3J_{H,H}$ = 7.23 Hz, N-CH_2*CH_3*) (2nd isomer), 4.05-4.30 (m, 12H, N-*CH_2*CH_3), 7.75-8.05 (m, 10H, P-Ph), 9.96 (s, 2H, C^2-H), 10.00 (s, 2H, C^2-H) (2nd isomer).

^{13}C{^{1}H} NMR (75.5 MHz, $CDCl_3$, 25 °C): δ = 14.8 (s, N-CH_2*CH_3*), 14.9 (s, N-CH_2*CH_3*) (2nd isomer), 46.1 (s, N-*CH_2*CH_3), 46.3 (s, N-*CH_2*CH_3) (2nd isomer), 123.9 and 124.1 (d, $^1J_{P,C}$ = 122.7 Hz, *ipso*-C), 133.5-136.1 (m, *Ph ring carbons*) , 146.8 (s, C^2-H, both-isomers)

^{31}P NMR (121.5 MHz, $CDCl_3$, 25 °C): δ = -5.4 (t, $^3J_{P,H}$ = 16.1 Hz) , -5.1 (t, $^3J_{P,H}$ = 15.6 Hz) ratio 1.2:1.

IR [cm^{-1}]: $\tilde{\nu}$ = 2988 (w), 1723 (w), 1439 (m), 1216 (vs), 1151 (vs), 1059 (vs), 997 (s).

Pos-ESI-MS: for $C_{26}H_{34}N_4P_2S_2O_{10}$ theor./exp. 247.10/247.099.

Neg-ESI-MS: for $[HSO_4]^-$ theor./exp. 96.96 /96.96

EA [%]: theor./exp. C 45.35/45.15, H 4.98/5.27; N 8.14/7.42, S 9.31/8.40.

10.25 Synthesis of tricyclic 1,4-diphosphinines

Tris(*n*-butyl)phosphane (0.12 mL, 0.5 mmol) was added to a suspension of **24a** (0.19 g, 0.5 mmol) in 5 mL of dichloromethane at room temperature. Then the reaction mixture was left stirring for 24h, until the whole orange suspension is converted into a red one. Then the solid was filtered and washed few times with DCM, followed by drying under reduced pressure to get the pure compound. In case of **24b,** tris(*n*-butyl)phosphane (0.12 mL, 0.5mmol) was added to **24b** (0.28 g, 0.5 mmol) in 5 mL of DCM at room temperature. After stirring for 1h the solvent was removed and the residue was filtered through a silica® bed with diethyl ether as the eluent to get the pure compound.

10.25.1 1,3,5,7-Tetramethyl-[2,3-d:5,6-d']diimidazole-2,6-dithione-4,8-[1,4]diphosphinine (33a)

Yield: 0.1 g (0.33 mmol, 65.1 %) **Appearance:** Red solid **Melting Point:** 220 °C

^{1}H NMR (300.1 MHz, $CDCl_3$, 25 °C): δ = 4.00 (s, 12H).

^{13}C{^{1}H} NMR (75.5 MHz, $CDCl_3$, 25 °C): δ = 33.7 (t, $^{3}J_{PC}$= 6.2 Hz, N-$\underline{CH_3}$), all ring carbon atom resonances could not be observed.

^{31}P NMR (121.5 MHz, $CDCl_3$, 25 °C): δ = 76.2 (s).

IR [cm^{-1}]: $\tilde{\nu}$ = 1428 (m), 1369 (s), 1352 (s), 1258 (s), 886 (s).

UV-Vis. (CH_2Cl_2): λ_{max} [nm]/ (abs.) 282 (1.623), 497 (0.805).

MS (EI, 70 eV): m/z (%) = 313.9 (100) $[M]^{\cdot+}$, 128.0 (60) $[C_5H_8N_2S]^+$

HRMS: theor./exp. for $[C_{10}H_{12}N_4P_2S_2]$: 313.9979/313.9976.

EA [%]: theor./exp. C 38.21/37.96 , H 3.85/3.89; N 17.83/17.56, S 20.40/20.02.

10.25.2 1,3,5,7-Tetra-*n*-butyl-[2,3-d:5,6-d']diimidazole-2,6-dithione-4,8-[1,4]diphosphinine (33b)

Yield: 0.09 g (0.29 mmol, 58.3 %) **Appearance:** Red solid **Melting Point:** 165 °C

^{1}H NMR (300.1 MHz, $CDCl_3$, 25 °C): δ = 1.02 (t, 12H, $^{3}J_{H,H}$ = 7.4 Hz, $NCH_2CH_2CH_2\underline{Me}$), 1.48-1.60 (m, 8H, $NCH_2CH_2\underline{CH_2}Me$), 1.88-1.98 (m, 8H, $NCH_2\underline{CH_2}CH_2Me$), 4.53 (t, 8H, $^{3}J_{H,H}$ = 7.4 Hz $N\underline{CH_2}CH_2CH_2Me$).

$^{13}C\{^{1}H\}$ NMR (75.5 MHz, $CDCl_3$, 25 °C): δ = 13.8 (s, $NCH_2CH_2CH_2\underline{Me}$), 20.1 (s, $NCH_2CH_2\underline{CH_2}Me$), 28.8 (s, $NCH_2\underline{CH_2}CH_2Me$), 46.8 (t, $^{3}J_{P,C}$ = 4.6 Hz, $N\underline{CH_2}CH_2CH_2Me$), 151.7 (t, $^{1}J_{P,C}$ = 22.5 Hz, $\underline{P\text{-}C}$ of the middle ring), 169.6 (t, $^{3}J_{P,C}$ = 2.3 Hz, $\underline{C{=}S}$).

^{31}P NMR (121.5 MHz, $CDCl_3$, 25 °C): δ = 78.1 (s).

UV-Vis. (CH_2Cl_2) λ_{max} [nm]/ (abs.) 286 (0.334), 498 (0.121).

IR [cm^{-1}]: $\tilde{\nu}$ = 2956 (m), 2930 (m), 2870 (w), 1434 (m), 1398 (s), 1377 (s), 1217 (m), 1176 (m), 1016 (s), 926 (s).

MS (EI, 70 eV): m/z (%) = 482.2 (85) $[M]^{\cdot+}$,

HRMS: theor./exp. for $[C_{22}H_{36}N_4P_2S_2]$: 482.1856/482.1859.

EA [%]: theor./exp. C 54.75/54.78 , H 7.52/7.61, N 11.61/11.40, S 13.29/13.19.

10.26 [4+2]-cycloaddition reactions of 1,4-diphosphinines

A solution of **33b** (0.48 g, 1 mmol) in toluene (20 ml) was heated with 0.12 ml of dimethyl acetylene dicarboxylate (for **34a**; heated for 1 h at 50 °C) or *N*-phenylmaleimide (for **34b**; heated at 110 °C for 3h) in a Schlenk tube. The color of the reaction mixture turned dark reddish brown for **34a** and light red-orange for **34b**. Afterwards the solvent was removed under reduced pressure (8× 10^{-3} mbar) and the residue was washed with *n*-pentane (3×5 ml). Finally it was dried under vacuum (8× 10^{-3} mbar) to get **34a,b** in pure form.

In case of **34c**, a THF (10 ml) solution of compound **33b** (0.48 g, 1mmol) was treated with a THF (5 ml) solution of 4-phenyl-1,2,4-triazoline-3,5-dione (0.18 g, 1 mmol) at -40°C. The color of the reaction mixture changed from dark red to bright yellow immediately upon addition of the triazoline derivative. Afterwards the reaction mixture was warmed up to the room temperature and concentrated under reduced pressure (8× 10^{-3} mbar). The crude product was then washed with diethyl ether (3 × 2 ml) at -30 °C to remove small amount of the impurity and to get compound **34c** in pure form.

10.26.1 7,8-Bis(methyloxocarbonyl)-[2,3-d:5,6-d']bis(1,3-di-*n*-butyl-imidazole-2-thione)-1,4-diphospha-bicyclo[2.2.2]octa-2,5,7-triene (34a)

Yield: 0.59 g (0.95 mmol, 95.0 %) **Appearance:** Red solid **Melting Point:** decomp. at 180 °C

^{1}H NMR (300.1 MHz, $CDCl_3$, 25 °C): δ = 0.99 (t, 12H, $^{3}J_{H,H}$ = 7.3 Hz, $NCH_2CH_2CH_2\underline{Me}$), 1.39(tq, 8H, $^{3}J_{H,H}$ = 7.3 Hz = 14.9 Hz, $^{3}J_{H,H}$ = 7.49 Hz, $NCH_2CH_2\underline{CH_2}Me$), 1.69-1.86 (m, 8H, $NCH_2\underline{CH_2}CH_2Me$), 3.87 (s, 6H, $-CO_2\underline{Me}$), 4.27 (t, 8H, $^{3}J_{H,H}$ = 7.4 Hz $N\underline{CH_2}CH_2CH_2Me$).

^{13}C{^{1}H} NMR (75.5 MHz, $CDCl_3$, 25 °C): δ = 13.8 (s, $NCH_2CH_2CH_2\underline{Me}$), 20.1 (s, $NCH_2CH_2\underline{CH_2}Me$), 31.6 (s, $NCH_2\underline{CH_2}CH_2Me$), 47.8 (dd, $^{3}J_{P,C}$ = 4.6 Hz, $N\underline{CH_2}CH_2CH_2Me$), 53.4 (s, $-CO_2\underline{Me}$), 128.6 (d, $^{1}J_{P,C}$ = 61.2 Hz, P-$\underline{C}O_2Me$), 142.5 (t, $J_{P,C}$ = 4.1 Hz, *P-C* of the middle ring), 160.5 (dd, $^{2}J_{P,C}$ = 14.1 Hz, $^{2}J_{P,C}$ = 11.9 Hz, -$\underline{C}O_2Me$) 164.3 (s, *C=S*), 166.1 (dd, $^{2}J_{P,C}$ = 16.8 Hz, -$\underline{C}O_2Me$).

^{31}P NMR (121.5 MHz, $CDCl_3$, 25 °C): δ = -87.3 (s).

IR [cm^{-1}]: $\tilde{\nu}$ = 2957 (w), 2933 (w), 2873 (w), 1721 (s), 1435 (m), 1404 (s), 1245 (s), 1217 (s).

MS (EI, 70 eV): m/z (%) = 624.1 (10) $[M]^{\cdot+}$, 482.2 (100) $[M-C_6H_6O_4]^{\cdot+}$

HRMS: theor./exp. for $[C_{28}H_{42}N_4O_4P_2S_2]$: 624.2123/624.2123.

EA [%]: theor./exp. C 53.83/53.55 , H 6.78/6.73, N 8.97/8.82, S 10.26/9.84.

10.26.2 7,8-(*N*-Phenylmaleimide)-[2,3-d:5,6-d']bis(1,3-di-*n*-butyl-imidazole-2-thione)-1,4-diphospha-7,8-dihydro-bicyclo[2.2.2]octa-2,5-diene (34b)

Yield: 0.59 g (0.91 mmol, 91.0 %) **Appearance:** orange solid **Melting Point:** decomp. at 160 °C

^{1}H NMR (300.1 MHz, $CDCl_3$, 25 °C): δ = 0.89 (t, 6H, $^{3}J_{H,H}$ = 7.3 Hz, $NCH_2CH_2CH_2\underline{Me}$), 1.01 (t, 6H, $^{3}J_{H,H}$ = 7.3 Hz, $NCH_2CH_2CH_2\underline{Me}$), 1.29-1.49 (m, 8H, $NCH_2CH_2\underline{CH_2}Me$), 1.63-1.84 (m, 8H, $NCH_2\underline{CH_2}CH_2Me$), 3.72 (t, 2H, $^{3}J_{P,H}$ = 4.9 Hz, P-*CH*), 4.09-4.39 (m, 8H, $N\underline{CH_2}CH_2CH_2Me$), 6.75-7.45 (m, 5H, *Ph ring protons*).

^{13}C{^{1}H} NMR (75.5 MHz, $CDCl_3$, 25 °C): δ = 13.5 & 13.8 (s, $NCH_2CH_2CH_2\underline{Me}$), 19.9 & 20.1 (s, $NCH_2CH_2\underline{CH_2}Me$), 31.5 & 31.7 (s, $NCH_2\underline{CH_2}CH_2Me$), 44.5 (dd, $^{3}J_{P,C}$ = 8.4 Hz, P-*CH*), 47.3 (t, $^{3}J_{P,C}$ = 1.9 Hz, $N\underline{CH_2}CH_2CH_2Me$), 47.5 (t, $^{3}J_{P,C}$ = 2.1 Hz, $N\underline{CH_2}CH_2CH_2Me$), 126.3 (s, *Ph ring C*), 129.5 (s, *Ph ring C*), 129.6 (s, *Ph ring C*), 130.5 (s, *Ph ring C*), 133.0 (dd, $J_{P,C}$ = 6.4 Hz, *P-C* of the middle ring), 134.5 (dd, $J_{P,C}$ = 3.5 Hz, *P-C* of the middle ring), 167.4 (s, -*C*(O)-), 172.4 (t, $^{3}J_{P,C}$ = 3.3 Hz, *C=S*).

^{31}P NMR (121.5 MHz, $CDCl_3$, 25 °C): δ = -86.3 (t, $^{2}J_{P,H}$ = 4.9 Hz).

IR [cm^{-1}]: $\tilde{\nu}$ = 2956 (w), 2930 (w), 2870 (w), 1768 (w), 1704 (s), 1404 (s), 1373 (s), 1217 (w), 1162 (s).

Pos-ESI-MS: for $C_{32}H_{43}N_5O_2P_2S_2H$ theor./exp. 656.2417/656.2406.

EA [%]: theor./exp. C 58.61/58.02 , H 6.61/6.76, N 10.68/10.12, S 9.78/9.10.

10.26.3 7,8-(4-Phenyl-1,2,4-triazoline-3,5-dione)-[2,3-d:5,6-d']bis(1,3-di-*n*-butyl-imidazole-2-thione)-1,4-diphospha-7,8-dihydro-bicyclo[2.2.2]octa-2,5-diene (34c)

Yield: 0.39 g (0.6 mmol, 60.0 %) **Appearance:** yellow solid **Melting Point:** decomp. at 160 °C

^{1}H NMR (300.1 MHz, $CDCl_3$, 25 °C): δ = 1.01 (t, 12H, $^{3}J_{H,H}$ = 7.3 Hz, $NCH_2CH_2CH_2\underline{\textit{Me}}$), 1.36-1.48 (m, 8H, $NCH_2CH_2\underline{\textit{CH}_2}Me$), 1.69-1.94 (m, 8H, $NCH_2\underline{\textit{CH}_2}CH_2Me$), 4.14-4.44 (m, 8H, $N\underline{\textit{CH}_2}CH_2CH_2Me$), 7.37-7.51 (m, 5H, *Ph ring protons*).

^{13}C{^{1}H} NMR (75.5 MHz, $CDCl_3$, 25 °C): δ = 13.7 (s, $NCH_2CH_2CH_2\underline{\textit{Me}}$), 20.1 (s, $NCH_2CH_2\underline{\textit{CH}_2}Me$), 31.7 (s, $NCH_2\underline{\textit{CH}_2}CH_2Me$), 47.6 (t, $^{3}J_{P,C}$ = 1.9 Hz, $N\underline{\textit{CH}_2}CH_2CH_2Me$), 125.8 (s, *Ph ring C*), 128.9(s, *Ph ring C*), 129.3 (s, *Ph ring C*), 130.7 (s, *Ph ring C*), 131.8 (dd, $J_{P,C}$ = 2.2 Hz, *P-C* of the middle ring), 150.1 (dd, $^{2}J_{P,C}$ = 7.9 Hz, $^{3}J_{P,C}$ = 7.1 Hz, -*C*(O)-), 166.3 (s, *C=S*).

^{31}P NMR (121.5 MHz, $CDCl_3$, 25 °C): δ = -49.6 (s).

IR [cm^{-1}]: $\tilde{\nu}$ = 2957 (w), 2931 (w), 2872 (w), 1762 (w), 1717 (s), 1402 (s), 1387 (s), 1263 (m), 1217 (m).

MS (EI, 70 eV): m/z (%) = 657.2 (10) $[M]^{\cdot+}$, 482.2 (50) $[M\text{-}C_8H_5N_3O_2]^{\cdot+}$

HRMS: theor./exp. for $[C_{28}H_{42}N_4O_4P_2S_2]$: 657.2238/657.2229.

EA [%]: theor./exp. C 54.78/54.30, H 6.28/6.27, N 14.91/14.72, S 9.75/9.26.

10.27 Reaction of 1,4-diphosphinines with Ph_2E_2

A solution of **33b** (0.48 g, 1 mmol) in toluene (20 ml) was heated with 0.22 g of diphenyl disulfide (for **35a**; heated for 2 days) or 0.31 g of diphenyl diselenide (for **35b**; heated for 6h) at 110°C in a Schlenk tube. The color of the reaction mixture turned yellow in both cases from dark blood red during the course of the reaction. After the complete consumption of the starting materials the solvent was removed under reduced pressure (8× 10^{-3} mbar) and Afterwards the solvent was removed under reduced pressure (8× 10^{-3} mbar) and the residue was washed with *n*-pentane (3×5 ml). Finally it was dried under vacuum (8× 10^{-3} mbar) to get **35a,b** in pure form as yellow powders.

10.27.1 4,8-Bis(thiophenoxy)-1,3,5,7-tetra-*n*-butyl-4,8-dihydro[1,4]diphosphinine [2,3 -d:5,6-d']bisimidazole-2,6-dithione (35a)

Yield: 0.55 g (0.78 mmol, 78.0 %) **Appearance:** yellow solid **Melting Point:** 195 °C

^{1}H NMR (300.1 MHz, $CDCl_3$, 25 °C): δ = 1.06 (t, 12H, $^3J_{H,H}$ = 7.3 Hz, $NCH_2CH_2CH_2\underline{Me}$), 1.42-1.54 (m, 8H, $NCH_2CH_2\underline{CH_2}Me$), 1.58-1.73 (m, 4H, $NCH_2\underline{CH_2}CH_2Me$), 1.82-1.97 (m, 4H, $NCH_2\underline{CH_2}CH_2Me$), 3.98-4.08 (m, 4H, $N\underline{CH_2}CH_2CH_2Me$), 4.47-4.57 (m, 4H, $N\underline{CH_2}CH_2CH_2Me$), 6.33 (d, 4H, $^3J_{H,H}$ = 7.9 Hz, *o-protons of Ph ring*), 7.07 (t, 4H, $^3J_{H,H}$ = 7.5 Hz, *m-protons of Ph ring*), 7.29 (t, 2H, $^3J_{H,H}$ = 7.5 Hz, *p-protons of Ph ring*).

^{13}C{^{1}H} NMR (75.5 MHz, $CDCl_3$, 25 °C): δ = 13.8 (s, $NCH_2CH_2CH_2\underline{Me}$), 20.1 (s, $NCH_2CH_2\underline{CH_2}Me$), 31.1 (s, $NCH_2\underline{CH_2}CH_2Me$), 46.9 (t, $^3J_{P,C}$ = 3.4 Hz, $N\underline{CH_2}CH_2CH_2Me$), 125.4 (dd, , $^3J_{P,C}$ = 7.4 Hz, $^3J_{P,C}$ = 6.5 Hz, *ipso-C of Ph ring*), 126.3 (t, $J_{P,C}$ = 4.1 Hz, *P-C* of the middle ring), 128.9 (s, *Ph ring C*) 129.2 (s, *p-C of Ph ring*), 134.9 (s, *Ph ring C*), 167.5 (t, $^3J_{P,C}$ = 1.6 Hz *C=S*).

^{31}P NMR (121.5 MHz, $CDCl_3$, 25 °C): δ = -34.2 (s).

IR [cm^{-1}]: $\tilde{\nu}$ = 2958 (w), 2931 (w), 2871 (w), 1436 (s), 1398 (s), 1286 (s), 1216 (s), 1159 (s), 861 (s), 745 (s).

Pos-ESI-MS: for $C_{34}H_{46}N_4P_2S_4H$ theor./exp. 701.2165/701.2153.

EA [%]: theor./exp. C 58.26/58.01, H 6.61/6.66, N 7.99/7.83, S 18.29/17.43.

10.27.2 4,8-Bis(selenophenoxy)-1,3,5,7-tetra-*n*-butyl-4,8-dihydro[1,4]diphosphinine [2,3 -d:5,6-d']bisimidazole-2,6-dithione (35b)

Yield: 0.59 g (0.75 mmol, 75.0 %) **Appearance:** yellow solid **Melting Point:** 188 °C

^{1}H NMR (300.1 MHz, C_6D_6, 25 °C): δ = 0.91 (t, 12H, $^3J_{H,H}$ = 7.2 Hz, $NCH_2CH_2CH_2\underline{Me}$), 1.25-1.35 (m, 8H, $NCH_2CH_2\underline{CH_2}Me$), 1.67-1.78 (m, 4H, $NCH_2\underline{CH_2}CH_2Me$), 1.92-2.03(m, 4H, $NCH_2\underline{CH_2}CH_2Me$), 4.01-4.08 (m, 4H, $N\underline{CH_2}CH_2CH_2Me$), 4.60-4.68 (m, 4H, $N\underline{CH_2}CH_2CH_2Me$), 6.42 (d, 4H, $^3J_{H,H}$ = 7.6 Hz, *o-protons of Ph ring*), 6.77 (t, 4H, $^3J_{H,H}$ = 6.8 Hz, *m-protons of Ph ring*), 6.91 (tt, 2H, $^3J_{H,H}$ = 7.5 Hz, $^3J_{H,H}$ = 1.2 Hz *p-protons of Ph ring*).

^{13}C{^{1}H} NMR (75.5 MHz, C_6D_6, 25 °C): δ = 13.6 (s, $NCH_2CH_2CH_2\underline{Me}$), 20.1 (s, $NCH_2CH_2\underline{CH_2}Me$), 30.9 (s, $NCH_2\underline{CH_2}CH_2Me$), 46.7 (t, $^3J_{P,C}$ = 3.8 Hz, $N\underline{CH_2}CH_2CH_2Me$), 124.1 (t, $J_{P,C}$ = 4.1 Hz, *P-C* of the middle

ring), 124.6 (dd, , $^{3}J_{P,C}$ = 9.5 Hz, $^{3}J_{P,C}$ = 7.9 Hz, *ipso-C of Ph ring*), 128.7 (s, *Ph ring C*) 129.0 (s, *p-C of Ph ring*), 136.3 (s, *Ph ring C*), 168.9 (br, *C=S*).

^{31}P NMR (121.5 MHz, C_6D_6, 25 °C): δ = -44.6 (s).

IR [cm^{-1}]: $\tilde{\nu}$ = 2957 (w), 2930 (w), 2871 (w), 1436 (s), 1396 (s), 1285 (s), 1216 (s), 1157 (s), 861 (s), 739 (s).

Pos-ESI-MS: for $C_{34}H_{46}N_4P_2Se_2S_2H$ theor./exp. 797.1052/797.1047.

EA [%]: theor./exp. C 51.38/50.71, H 5.83/5.83, N 7.05/6.92, S 8.07/8.12.

10.28 Nucleophilic 1,4-addition reaction of 1,4-diphosphinines

A solution of compound **33b** (0.48 g, 1mmol) in diethyl ether (20 ml) was treated first with 0.63 ml of ^{n}BuLi solution (for **36a**; for **36b** 0.21 g of KMHDS) at room temperature. During this addition the color of the reaction mixture changed from dark red to dark violet, which eventually turned bright orange. Then this solution was cooled down to –78 °C and 1 mmol of methyl iodide was added as the quenching agent. The color of the reaction mixture changed from orange to light yellow during the methyl iodide addition. The reaction mixture was allowed to slowly warmup to the room temperature. After this the reaction mixture was concentrated under vacuo (8× 10^{-3} mbar) to get a yellow residue which was again taken up into 30 ml toluene. This toluene solution was filtered through a silica bed to remove the salt (LiI) and some minor colored impurities. After concentrating this filtrate under reduced pressure, a white solid was obtained which was further dried (8× 10^{-3} mbar) to get pure **37a,b**.

10.28.1 4-Bis(trimethylsilyl)amino-8-methyl-1,3,5,7-tetra-*n*-butyl-4,8-dihydro[1,4] diphosphinine[2,3-d:5,6-d']bisimidazole-2,6-dithione (37a)

Yield: 0.53 g (0.8 mmol, 80.0 %) **Appearance:** white solid **Melting Point:** 139 °C

^{1}H NMR (300.1 MHz, C_6D_6, 25 °C): δ = -0.26 (s, 9H, *N-SiMe$_3$*), 0.31 (t, 9H, $^{4}J_{P,H}$ = 2.7 Hz, *N-SiMe$_3$*), 0.78 (d, $^{3}J_{H,H}$ = 5.1 Hz, *P-Me*), 0.84 (t, 6H, $^{3}J_{H,H}$ = 7.3 Hz, $NCH_2CH_2CH_2$*Me*), 0.88 (t, 6H, $^{3}J_{H,H}$ = 7.5 Hz, $NCH_2CH_2CH_2$*Me*), 1.24-1.48 (m, 8H, NCH_2CH_2*CH$_2$*Me), 1.85-2.26 (m, 8H, NCH_2*CH$_2$*CH_2Me), 3.55-3.63 (m, 2H, N*CH$_2$*CH_2CH_2Me), 3.98-4.06 (m, 2H, N*CH$_2$*CH_2CH_2Me), 4.61-4.68 (m, 2H, N*CH$_2$*CH_2CH_2Me), 4.91-4.99 (m, 2H, N*CH$_2$*CH_2CH_2Me).

$^{13}C\{^{1}H\}$ NMR (75.5 MHz, C_6D_6, 25 °C): δ = 2.9 (s, <u>*N-SiMe$_3$*</u>), 4.3 (t, $^{2}J_{P,C}$ = 14.7 Hz, <u>*N-SiMe$_3$*</u>), 13.4 & 13.6 (s, $NCH_2CH_2CH_2$<u>*Me*</u>), 16.3 (dd, $J_{P,C}$ = 18.2 Hz, $J_{P,C}$ = 12.2 Hz, <u>*P-Me*</u>), 19.9 & 20.2 (s, NCH_2CH_2<u>*CH$_2$*</u>Me), 30.6 (br, NCH_2<u>*CH$_2$*</u>CH_2Me), 46.9 (d, $^{3}J_{P,C}$ = 5.7 Hz, N<u>*CH$_2$*</u>CH_2CH_2Me), 47.3 (d, $^{3}J_{P,C}$ = 8.6 Hz, N<u>*CH$_2$*</u>CH_2CH_2Me), 126.5 (d, $J_{P,C}$ = 1.5 Hz, <u>*P-C*</u> of the middle ring), 128.6 (dd, $J_{P,C}$ = 16.8 Hz , $J_{P,C}$ = 2.8 Hz, <u>*P-C*</u> of the middle ring), 168.5 (br, <u>*C=S*</u>).

^{31}P NMR (121.5 MHz, C_6D_6, 25 °C): δ = -72.4 (dq, $^{3}J_{P,P}$ = 15.7 Hz, $^{3}J_{P,H}$ = 5.2 Hz, <u>*P-Me*</u>); -5.1 (br. d, $^{3}J_{P,P}$ = 15.7 Hz, <u>*P-N(SiMe$_3$)$_2$*</u>).

IR [cm^{-1}]: $\tilde{\nu}$ = 2956 (w), 2929 (w), 2861 (w), 1437 (m), 1402 (s), 1253 (m), 1217 (m), 887 (s), 871 (s), 842 (s).

Pos-ESI-MS: for $C_{29}H_{57}N_5P_2Si_2S_2H$ theor./exp. 658.3154/658.3142.

EA [%]: theor./exp. C 52.93/52.71, H 8.73/8.70, N 10.64/10.58, S 9.74/9.45.

10.28.2 4-*n*-Butyl-8-methyl-1,3,5,7-tetra-*n*-butyl-4,8-dihydro[1,4]diphosphinine[2,3 -d:5,6-d']bisimidazole-2,6-dithione (37b)

Yield: 0.19 g (0.35 mmol, 35.0 %) **Appearance:** white solid **Melting Point:** 175 °C

^{1}H NMR (300.1 MHz, C_6D_6, 25 °C): δ = 0.73 (t, 3H, $^{3}J_{H,H}$ = 7.4 Hz, $PCH_2CH_2CH_2$<u>*Me*</u>), 0.88 (t, 3H, $^{3}J_{H,H}$ = 6.7 Hz, $PCH_2CH_2CH_2$<u>*Me*</u>) 2nd isomer, 0.98 (t, 3H, $^{3}J_{H,H}$ = 7.1 Hz, $NCH_2CH_2CH_2$<u>*Me*</u>), 0.99 (t, 3H, $^{3}J_{H,H}$ = 7.2 Hz, $NCH_2CH_2CH_2$<u>*Me*</u>) 2nd isomer, 1.11-1.16 (m, 2H, PCH_2CH_2<u>*CH$_2$*</u>Me), 1.34-1.42 (m, 4H, P<u>*CH$_2$CH$_2$*</u>CH_2Me), 1.40 (d, $^{2}J_{P,H}$ = 4.9 Hz, <u>*P-Me*</u>), 1.42-1.48 (m, 8H, NCH_2CH_2<u>*CH$_2$*</u>Me), 1.50 (d, $^{2}J_{P,H}$ = 5.2 Hz, <u>*P-Me*</u>) 2nd isomer, 1.67-1.94(m, 8H, NCH_2<u>*CH$_2$*</u>CH_2Me), 3.79-4.51 (m, 8H, N<u>*CH$_2$*</u>CH_2CH_2Me).

$^{13}C\{^{1}H\}$ NMR (75.5 MHz, C_6D_6, 25 °C): δ = 13.4 & 13.6 (s, $PCH_2CH_2CH_2$<u>*Me*</u> of two isomers), 13.7 & 13.8 (s, $NCH_2CH_2CH_2$<u>*Me*</u> of two isomers), 17.6 (dd, $^{1}J_{P,C}$ = 16.3 Hz, $^{3}J_{P,C}$ = 1.6 Hz, <u>*P-Me*</u>), 18.2 (dd, $^{1}J_{P,C}$ = 19.2 Hz, $^{3}J_{P,C}$ = 3.7 Hz, <u>*P-Me*</u>) 2nd isomer, 19.9 & 20.0 (s, NCH_2CH_2<u>*CH$_2$*</u>Me), 23.3 & 23.4 (s, PCH_2CH_2<u>*CH$_2$*</u>Me), 23.9 & 24.1 (s, PCH_2CH_2<u>*CH$_2$*</u>Me) (2nd isomer), 25.6 (d, $^{3}J_{P,C}$ = 1.9 Hz, PCH_2<u>*CH$_2$*</u>CH_2Me), 28.3 (d, $^{3}J_{P,C}$ = 8.8 Hz, PCH_2<u>*CH$_2$*</u>CH_2Me) (2nd isomer), 28.8 (dd, $^{1}J_{P,C}$ = 20.0 Hz, $^{4}J_{P,C}$ = 5.2 Hz, P<u>*CH$_2$*</u>CH_2CH_2Me), 30.3 (dd, $^{1}J_{P,C}$ = 7.8 Hz, $^{4}J_{P,C}$ = 2.5 Hz, P<u>*CH$_2$*</u>CH_2CH_2Me) (2nd isomer), 30.7 (d, $^{3}J_{P,C}$ = 2.6 Hz, NCH_2<u>*CH$_2$*</u>CH_2Me), 30.9 (d, $^{3}J_{P,C}$ = 2.6 Hz, NCH_2<u>*CH$_2$*</u>CH_2Me), 32.8 (d, $^{3}J_{P,C}$ = 2.1 Hz, NCH_2<u>*CH$_2$*</u>CH_2Me) (2nd isomer), 32.9 (d, $^{3}J_{P,C}$ = 2.1 Hz, NCH_2<u>*CH$_2$*</u>CH_2Me) (2nd isomer), 46.7 (t, $^{3}J_{P,C}$ = 7.2 Hz, N<u>*CH$_2$*</u>CH_2CH_2Me), 46.8 (t, $^{3}J_{P,C}$ = 6.5 Hz, N<u>*CH$_2$*</u>CH_2CH_2Me), 47.5 (t, $^{3}J_{P,C}$ = 2.5 Hz, N<u>*CH$_2$*</u>CH_2CH_2Me)(2nd isomer), 47.6 (t, $^{3}J_{P,C}$ = 3.5 Hz, N<u>*CH$_2$*</u>CH_2CH_2Me)(2nd isomer), 122.7 (t, $J_{P,C}$ = 2.1

Hz, *P-C* of the middle ring), 127.1 (t, $J_{P,C}$ = 4.4 Hz, *P-C* of the middle ring) (2nd isomer), 128.1 (t, $J_{P,C}$ = 2.7 Hz, *P-C* of the middle ring), 128.3 (dd, $J_{P,C}$ = 7.1 Hz, $J_{P,C}$ = 4.3 Hz, *P-C* of the middle ring)(2nd isomer), 165.8 (br, *C=S*), 166.8 (br, *C=S*) 2nd isomer.

^{31}P NMR (121.5 MHz, C_6D_6, 25 °C): δ = -75.8 (dq, $^3J_{P,P}$ = 9.6 Hz, $^3J_{P,H}$ = 4.9 Hz, *P-Me*) & -69.4 (qd, $^3J_{P,H}$ = 5.2 Hz, $^3J_{P,H}$ = 4.8 Hz, *P-Me*); -65.4 (br, *P-^{n}Bu*) & -60.1 (br, *P-^{n}Bu*). Ratio of two isomers 1:3.5.

IR [cm^{-1}]: ṽ = 2955 (w), 2927 (w), 2859 (w), 1464 (w), 1434 (m), 1400 (s), 1361 (m), 1216 (m), 896 (m), 855 (m).

Pos-ESI-MS: for $C_{27}H_{48}N_4P_2S_2H$ theor./exp. 555.2881/555.2868.

EA [%]: theor./exp. C 58.46/57.86, H 8.72/8.75, N 10.10/9.74, S 11.56/12.19.

10.29 Oxidative hydrolysis of tricyclic 1,4-diphosphinine 33b

A solution of compound **33b** (0.48 g, 1 mmol) in 50 mL of diethyl ether was stirred for overnight in open atmospheric conditions. The red color of the compound vanished during this process and a light yellow solution was obtained. This solution was dried in vacuum to get a residue which was again washed with diethylether (2 × 2 ml) and *n*-pentane (2 × 5 ml). Finally it was dried under reduced pressure (8× 10^{-3} mbar) to get hands on pure **38**.

10.29.1 1,3,5,7-Tetra-*n*-butyl-4,8-dihydro[1,4]bisphosphinicacid[2,3-d:5,6-d']bisimidazole-2,6-dithione (38b)

Yield: 0.51 g (0.92 mmol, 92.0 %) **Appearance:** white solid **Melting Point:** 176 °C

^{1}H NMR (300.1 MHz, C_6D_6, 25 °C): δ = 1.01 (t, 12H, $^3J_{H,H}$ = 7.4 Hz, $NCH_2CH_2CH_2$*Me*), 1.39-1.52 (m, 8H, NCH_2CH_2*CH$_2$*Me), 1.87-1.98 (m, 8H, NCH_2*CH$_2$*CH_2Me), 4.31-4.36 (m, 8H, N*CH$_2$*CH_2CH_2Me).

^{13}C{^{1}H} NMR (75.5 MHz, C_6D_6, 25 °C): δ = 13.1 (s, $NCH_2CH_2CH_2$*Me*), 19.8 (s, NCH_2CH_2*CH$_2$*Me), 30.0 (s, NCH_2*CH$_2$*CH_2Me), 47.5 (s, N*CH$_2$*CH_2CH_2Me), 125.4 (dd, $^1J_{P,C}$ = 167.4 Hz, $^1J_{P,C}$ = 21.6 Hz, *P-C* of the middle ring), 168.6 (t, $^3J_{P,C}$ = 7.6 Hz, *C=S*).

^{31}P NMR (121.5 MHz, C_6D_6, 25 °C): δ = -6.9 (s).

IR [cm^{-1}]: ṽ = 2956 (w), 2931 (w), 2872 (w), 2269 (m), 1516 (w), 1450 (m), 1419 (s), 1361 (m), 1213 (s), 1191 (s), 1143 (s), 960 (s).

Pos-ESI-MS: for $C_{22}H_{38}N_4O_4P_2S_2Na$ theor./exp. 571.1702/517.1721.

EA [%]: theor./exp. C 48.16/48.84, H 6.98/7.08, N 10.21/9.89, S 11.69/11.47.

References

[1] W. O. Foye, J. R. Lo, *J. Pharm. Sci.* **1972**, *61*, 1209-1212.

[2] F. J. Welcher, *Organic Analytical Reagents, Vol. 4*, Van Nostrand, New York, **1948**.

[3] B. C. Bera, M. M. Chakrabarty, *Anal. Chem.* **1966**, *38*, 1419-1421; M. J. Stiff, *Analyst* **1972**, *97*, 146-147.

[4] *Martindale: The Extra Pharmacopoeia, Vol. 27th edn*, Pharmaceutical Press, London, **1977**.

[5] H. Kohn, B. A. Kohn, M. L. Steenberg, J. P. Buckley, *J. Med. Chem.* **1977**, *20*, 158-160.

[6] S. M. Belenskii, *Zashch. Met.* **1965**, *1*, 125; T. C. D. B. Donnelly, R. Grzeskowiak, H. R. Hamburg, D. Short, *Corros. Sci.* **1978**, *18*, 109.

[7] J. Kister, G. Assef, G. Mille, J. Metzger, *Can. J. Chem.* **1979**, *57*, 813-821; D. W. Karkhanis, L. Field, *Phosphorus Sulfur Silicon Relat. Elem.* **1985**, *22*, 49-57; U. Zoller, *Tetrahedron* **1988**, *44*, 7413-7426; T. Xiao-Le, L. Ming, W. Yan-Guang, *Synth. Commun.* **2007**, *37*, 399-408.

[8] D. M. Wolfe, P. R. Schreiner, *Eur. J. Org. Chem.* **2007**, *2007*, 2825-2838.

[9] G. Roy, P. N. Jayaram, G. Mugesh, *Chem. Asian J.* **2013**, *8*, 1910-1921.

[10] S. Sauerbrey, P. K. Majhi, G. Schnakenburg, A. J. Arduengo III, R. Streubel, *Dalton Trans.* **2012**, *41*, 5368-5376.

[11] N. Kuhn, T. Kratz, *Synthesis* **1993**, *1993*, 561-562.

[12] A. J. Arduengo III, J. R. Goerlich, R. Krafczyk, W. J. Marshall, *Angew. Chem. Int. Ed.* **1998**, *37*, 1963-1965; Y. M. Loksha, A. A. El-Barbary, M. A. El-Badawi, C. Nielsen, E. B. Pedersen, *Synthesis* **2004**, *2004*, 116-120.

[13] T. Welton, *Chem. Rev.* **1999**, *99*, 2071-2084; N. V. Plechkova, K. R. Seddon, *Chem. Soc. Rev.* **2008**, *37*, 123-150.

[14] J. J. H. Davis, *Chem. Lett.* **2004**, *33*, 1072-1077.

[15] A. E. Visser, R. P. Swatloski, W. M. Reichert, R. Mayton, S. Sheff, A. Wierzbicki, J. J. H. Davis, R. D. Rogers, *Chem. Commun.* **2001**, 135-136.

[16] D. Li, F. Shi, J. Peng, S. Guo, Y. Deng, *J. Org. Chem.* **2004**, *69*, 3582-3585.

[17] Z. Mu, W. Liu, S. Zhang, F. Zhou, *Chem. Lett.* **2004**, *33*, 524-525.

[18] Z. Fei, D. Zhao, D. Pieraccini, W. H. Ang, T. J. Geldbach, R. Scopelliti, C. Chiappe, P. J. Dyson, *Organometallics* **2007**, *26*, 1588-1598; C. Chiappe, D. Pieraccini, D. Zhao, Z. Fei, P. J. Dyson, *Adv. Synth. Catal.* **2006**, *348*, 68-74.

[19] P. K. Majhi, G. Schnakenburg, A. J. Arduengo, R. Streubel, *Aust. J. Chem.* **2015**, *68*, 1282-1292.

[20] P. K. Majhi, S. Sauerbrey, G. Schnakenburg, A. J. Arduengo, R. Streubel, *Inorg. Chem.* **2012**, *51*, 10408-10416.

[21] A. J. Arduengo, F. Davidson, H. V. R. Dias, J. R. Goerlich, D. Khasnis, W. J. Marshall, T. K. Prakasha, *J. Am. Chem. Soc.* **1997**, *119*, 12742-12749.

[22] M. L. Cole, C. Jones, P. C. Junk, *New J. Chem.* **2002**, *26*, 1296-1303.

[23] M. K. Denk, J. M. Rodezno, *J. Organomet. Chem.* **2001**, *617*, 737-740.

[24] H. Cui, Y. Shao, X. Li, L. Kong, C. Cui, *Organometallics* **2009**, *28*, 5191-5195.

[25] R. S. Ghadwal, H. W. Roesky, M. Granitzka, D. Stalke, *J. Am. Chem. Soc.* **2010**, *132*, 10018-10020; R. S. Ghadwal, R. Azhakar, H. W. Roesky, *Acc. Chem. Res.* **2013**, *46*, 444-456.

[26] J. I. Bates, P. Kennepohl, D. P. Gates, *Angew. Chem. Int. Ed.* **2009**, *48*, 9844-9847.

[27] D. Mendoza-Espinosa, B. Donnadieu, G. Bertrand, *J. Am. Chem. Soc.* **2010**, *132*, 7264-7265.

[28] E. Aldeco-Perez, A. J. Rosenthal, B. Donnadieu, P. Parameswaran, G. Frenking, G. Bertrand, *Science* **2009**, *326*, 556-559; G. Ung, G. Bertrand, *Chem. Eur. J.* **2011**, *17*, 8269-8272.

[29] J. Ruiz, A. F. Mesa, *Chem. Eur. J.* **2012**, *18*, 4485-4488.

[30] J. Ruiz, A. F. Mesa, D. Sol, *Organometallics* **2015**, *34*, 5129-5135.

[31] A. Solovyev, E. Lacôte, D. P. Curran, *Org. Lett.* **2011**, *13*, 6042-6045.

[32] P. K. Majhi, S. Sauerbrey, A. Leiendecker, G. Schnakenburg, A. J. Arduengo III, R. Streubel, *Dalton Trans.* **2013**, *42*, 13126-13136.

[33] P. K. Majhi, G. Schnakenburg, Z. Kelemen, L. Nyulaszi, D. P. Gates, R. Streubel, *Angew. Chem. Int. Ed.* **2013**, *52*, 10080-10083.

[34] P. K. Majhi, G. Schnakenburg, R. Streubel, *Dalton Trans.* **2014**, *43*, 16673-16679.

[35] S. Sauerbrey, P. K. Majhi, S. Schwieger, A. J. Arduengo, R. Streubel, *Heteroat. Chem.* **2012**, *23*, 513-519.

[36] P. K. Majhi, A. Koner, G. Schnakenburg, Z. Kelemen, L. Nyulászi, R. Streubel, *Eur. J. Inorg. Chem.* **2016**, 3559-3573.

[37] S. Sauerbrey, *PhD Thesis*, University of Bonn, **2010**.

[38] M. Davis, F. G. Mann, *J. Chem. Soc.* **1964**, 3770-3785.

[39] H. Akutsu, M. Ogasawara, M. Saburi, K. Kozawa, T. Uchida, *Bull. Chem. Soc. Jpn.* **1996**, *69*, 1223-1226.

[40] G. Märkl, W. Weber, W. Weiß, *Chem. Ber.* **1985**, *118*, 2365-2395.

[41] W. R. Cullen, A. W. Wu, *J. Fluorine Chem.* **1976**, *8*, 183-187.

[42] Y. Uchiyama, T. Kawaguchi, K. Kuroda, *Heteroat. Chem* **2014**, *25*, 326-336.

[43] Y. Uchiyama, Y. Mazaki, *Phosphorus, Sulfur, Silicon Relat. Elem.* **2011**, *186*, 822-825.

[44] N. Avarvari, M. Fourmigué, *Chem. Commun.* **2004**, 2794-2795.

[45] D. Fenske, E. Langer, M. Heymann, H. J. Becher, *Chem. Ber.* **1976**, *109*, 359-362.

[46] A. N. Huryeva, A. P. Marchenko, G. N. Koidan, A. A. Yurchenko, E. V. Zarudnitskii, A. M. Pinchuk, A. N. Kostyuk, *Heteroat. Chem* **2010**, *21*, 103-118.

[47] G. Märkl, *Angew. Chem. Int. Ed. Engl.* **1966**, *5*, 846-847.

[48] I. Alkorta, J. Elguero, *Magn. Reson. Chem.* **2010**, *48*, S32-S37.

[49] C. Müller, L. E. E. Broeckx, I. de Krom, J. J. M. Weemers, *Eur. J. Inorg. Chem.* **2013**, *2013*, 187-202.

[50] G. Märkl, F. Lieb, A. Merz, *Angew. Chem. Int. Ed. Engl.* **1967**, *6*, 458-459; G. Märkl, F. Lieb, A. Merz, *Angew. Chem. Int. Ed. Engl.* **1967**, *6*, 944-945.

[51] A. J. Ashe, *J. Am. Chem. Soc.* **1971**, *93*, 3293-3295.

[52] K. Blatter, W. Rösch, U.-J. Vogelbacher, J. Fink, M. Regitz, *Angew. Chem. Int. Ed. Engl.* **1987**, *26*, 85-86; G. Maas, J. Fink, H. Wingert, K. Blatter, M. Regitz, *Chem. Ber.* **1987**, *120*, 819-824.

[53] G. Märkl, K.-H. Heier, *Angew. Chem. Int. Ed. Engl.* **1972**, *11*, 1017-1019.

[54] S. Holand, L. Ricard, F. Mathey, *J. Org. Chem.* **1991**, *56*, 4031-4035.

[55] G. Märkl, C. Dörges, T. Riedl, F. G. Klärner, C. Lodwig, *Tetrahedron Lett.* **1990**, *31*, 4589-4592; G. Märkl, G. Dorfmeister, *Tetrahedron Lett.* **1987**, *28*, 1093-1096.

[56] Y. Van Den Winkel, J. Van Der Laarse, F. J. J. De Kanter, T. Van Der Does, F. Bickelhaupt, W. J. J. Smeets, A. L. Spek, *Heteroat. Chem* **1991**, *2*, 17-28.

[57] D. Böhm, F. Knoch, S. Kummer, U. Schmidt, U. Zenneck, *Angew. Chem. Int. Ed. Engl.* **1995**, *34*, 198-201.

[58] G. Jochem, A. Schmidpeter, in *Z. Naturforsch. B, Vol. 51*, **1996**, p. 773.

[59] E. Fluck, G. Heckmann, E. Gorbunowa, M. Westerhausen, F. Weller, *J. Organomet. Chem.* **1997**, *529*, 223-231.

[60] G. Märkl, in *Z. Naturforsch. B, Vol. 18*, **1963**, p. 1136.

[61] Y. Kobayashi, I. Kumadaki, A. Ohsawa, H. Hamana, *Tetrahedron Lett.* **1976**, *17*, 3715-3716.

[62] Y. Kobayashi, H. Hamana, S. Fujino, A. Ohsawa, I. Kumadaki, *J. Am. Chem. Soc.* **1980**, *102*, 252-255.

[63] I. M. Downie, J. B. Lee, M. F. S. Matough, *Chem. Commun.* **1968**, 1350b-1351.

[64] Y. Kobayashi, S. Fujino, I. Kumadaki, *J. Am. Chem. Soc.* **1981**, *103*, 2465-2466.

[65] K. Bergander, R. He, N. Chandrakumar, O. Eppers, H. Günther, *Tetrahedron* **1994**, *50*, 5861-5868.

[66] Andrei S. Batsanov, Stephanie M. Cornet, Lindsey A. Crowe, Keith B. Dillon, Robin K. Harris, P. Hazendonk, Mark D. Roden, *Eur. J. Inorg. Chem.* **2001**, *2001*, 1729-1737.

[67] M. K. Denk, S. Gupta, A. J. Lough, *Eur. J. Inorg. Chem.* **1999**, *1999*, 41-49.

[68] S. Grimme, J. Antony, S. Ehrlich, H. Krieg, *J. Chem. Phys.* **2010**, *132*, 154104; Y. Shao, L. F. Molnar, Y. Jung, J. Kussmann, C. Ochsenfeld, S. T. Brown, A. T. B. Gilbert, L. V. Slipchenko, S. V. Levchenko, D. P. O'Neill, R. A. DiStasio Jr, R. C. Lochan, T. Wang, G. J. O. Beran, N. A. Besley, J. M. Herbert, C. Yeh Lin, T. Van Voorhis, S. Hung Chien, A. Sodt, R. P. Steele, V. A. Rassolov, P. E. Maslen, P. P. Korambath, R. D. Adamson, B. Austin, J. Baker, E. F. C. Byrd, H. Dachsel, R. J. Doerksen, A. Dreuw, B. D. Dunietz, A. D. Dutoi, T. R. Furlani, S. R. Gwaltney, A. Heyden, S. Hirata, C.-P. Hsu, G. Kedziora, R. Z. Khalliulin, P. Klunzinger, A. M. Lee, M. S. Lee, W. Liang, I. Lotan, N. Nair, B. Peters, E. I. Proynov, P. A. Pieniazek, Y. Min Rhee, J. Ritchie, E. Rosta, C. David Sherrill, A. C. Simmonett, J. E. Subotnik, H. Lee Woodcock Iii, W. Zhang, A. T. Bell, A. K. Chakraborty, D. M. Chipman, F. J. Keil, A. Warshel, W. J. Hehre, H. F. Schaefer Iii, J. Kong, A. I. Krylov, P. M. W. Gill, M. Head-Gordon, *PCCP* **2006**, *8*, 3172-3191; R. Ahlrichs, M. Bär, M. Häser, H. Horn, C. Kölmel, *Chem. Phys. Lett.* **1989**, *162*, 165-169.

[69] L. Baiget, M. Bouslikhane, J. Escudie, G. C. Nemes, I. Silaghi-Dumitrescu, L. Silaghi-Dumitrescu, *Phosphorus Sulfur Silicon Relat. Elem.* **2003**, *178*, 1949-1961.

[70] B. H. Gillon, K. J. T. Noonan, B. Feldscher, J. M. Wissenz, Z. M. Kam, T. Hsieh, J. J. Kingsley, J. I. Bates, D. P. Gates, *Can. J. Chem.* **2007**, *85*, 1045-1052.

[71] Vasily V. Kotov, Evgeni V. Avtomonov, J. Sundermeyer, K. Harms, Dmitry A. Lemenovskii, *Eur. J. Inorg. Chem.* **2002**, *2002*, 678-691.

[72] P. K. Majhi, S. C. Serin, G. Schnakenburg, D. P. Gates, R. Streubel, *Eur. J. Inorg. Chem.* **2014**, *2014*, 4975-4983.

[73] M. Azouri, J. Andrieu, M. Picquet, P. Richard, B. Hanquet, I. Tkatchenko, *Eur. J. Inorg. Chem.* **2007**, *2007*, 4877-4883.

[74] S. Sauerbrey, P. K. Majhi, J. Daniels, G. Schnakenburg, G. M. Brändle, K. Scherer, R. Streubel, *Inorg. Chem.* **2011**, *50*, 793-799.

[75] M. Well, W. Albers, A. Fischer, P. G. Jones, R. Schmutzler, *Chem. Ber.* **1992**, *125*, 801-808; K. C. K. Swamy, R. O. Day, J. M. Holmes, R. R. Holmes, *J. Am. Chem. Soc.* **1990**, *112*, 6095-6103.

[76] J. Emsley, *Chem. Soc. Rev.* **1980**, *9*, 91-124.

[77] E. H. Braye, I. Caplier, R. Saussez, *Tetrahedron* **1971**, *27*, 5523-5537.

[78] K. F. Crespo Andrada, L. E. Peisino, M. Guney, A. Dastan, A. B. Pierini, *Org. Biomol. Chem.* **2013**, *11*, 955-965; W. Kuchen, H. Buchwald, *Chem. Ber.* **1959**, *92*, 227-231; E. R. N. Bornancini, R. A. Alonso, R. A. Rossi, *J. Org. Chem.* **1987**, *52*, 2166-2170.

[79] S. Holand, M. Jeanjean, F. Mathey, *Angew. Chem. Int. Ed. Engl.* **1997**, *36*, 98-100.

[80] F. Dornhaus, M. Bolte, H.-W. Lerner, M. Wagner, *Eur. J. Inorg. Chem.* **2006**, *2006*, 1777-1785.

[81] J. W. Kamplain, C. W. Bielawski, *Chem. Commun.* **2006**, 1727-1729.

[82] D. M. Khramov, A. J. Boydston, C. W. Bielawski, *Angew. Chem. Int. Ed.* **2006**, *45*, 6186-6189.

[83] A pure sample of diethylamine (0.2 ml) was dissolved in pure C_6D_6 (0.3) and the ^1H NMR was recorded at room temperature. This spectral data was used for the comparison.

[84] L. E. E. Broeckx, S. Güven, F. J. L. Heutz, M. Lutz, D. Vogt, C. Müller, *Chem. Eur. J.* **2013**, *19*, 13087-13098.

[85] S. Gundersen, S. Samdal, T. G. Strand, H. V. Volden, *J. Mol. Struct.* **2007**, *832*, 164-171.

[86] S. Grimme, *J. Comput. Chem.* **2004**, *25*, 1463-1473; S. Grimme, *ChemPhysChem* **2012**, *13*, 1407-1409; B. Zou, K. Dreger, C. Mück-Lichtenfeld, S. Grimme, H. J. Schäfer, H. Fuchs, L. Chi, *Langmuir* **2005**, *21*, 1364-1370.

[87] G. A. Wiley, W. R. Stine, *Tetrahedron Lett.* **1967**, *8*, 2321-2324.

[88] M. J. Frisch, G. W. Trucks, H. B. Schlegel, G. E. Scuseria, M. A. Robb, J. R. Cheeseman, G. Scalmani, V. Barone, B. Mennucci, G. A. Petersson, H. Nakatsuji, M. Caricato, X. Li, H. P. Hratchian, A. F. Izmaylov, J. Bloino, G. Zheng, J. L. Sonnenberg, M. Hada, M. Ehara, K. Toyota, R. Fukuda, J. Hasegawa, M. Ishida, T. Nakajima, Y. Honda, O. Kitao, H. Nakai, T. Vreven, J. A. Montgomery, J. E. Peralta, F. Ogliaro, M. Bearpark, J. J. Heyd, E. Brothers, K. N. Kudin, V. N. Staroverov, R. Kobayashi, J. Normand, K. Raghavachari, A. Rendell, J. C. Burant, S. S. Iyengar, J. Tomasi, M. Cossi, N. Rega, J. M. Millam, M. Klene, J. E. Knox, J. B. Cross, V. Bakken, C. Adamo, J. Jaramillo, R. Gomperts, R. E. Stratmann, O. Yazyev, A. J. Austin, R. Cammi, C. Pomelli, J. W. Ochterski, R. L. Martin, K. Morokuma, V. G. Zakrzewski, G. A. Voth, P. Salvador, J. J.

Dannenberg, S. Dapprich, A. D. Daniels, Farkas, J. B. Foresman, J. V. Ortiz, J. Cioslowski, D. J. Fox, Wallingford CT, **2010**.

[89] Y. Zhao, D. G. Truhlar, *Theor. Chem. Acc.* **2008**, *120*, 215-241.

[90] A. Modelli, B. Hajgató, J. F. Nixon, L. Nyulászi, *J. Phys. Chem. A* **2004**, *108*, 7440-7447.

[91] P. v. R. Schleyer, H. Jiao, N. J. R. v. E. Hommes, V. G. Malkin, O. L. Malkina, *J. Am. Chem. Soc.* **1997**, *119*, 12669-12670.

[92] Z. Kelemen, R. Streubel, L. Nyulaszi, *RSC Advances* **2015**, *5*, 41795-41802.

[93] P. v. R. Schleyer, F. Pühlhofer, *Org. Lett.* **2002**, *4*, 2873-2876.

[94] S. M. Bachrach, P. Magdalinos, *J. Mol. Struct.* **1996**, *368*, 1-6; L. Colombet, F. Volatron, P. Maître, P. C. Hiberty, *J. Am. Chem. Soc.* **1999**, *121*, 4215-4221; L. Nyulászi, *J. Organomet. Chem.* **2005**, *690*, 2597-2602; T. R. Galeev, A. I. Boldyrev, *PCCP* **2011**, *13*, 20549-20556; A. Saieswari, U. Deva Priyakumar, G. Narahari Sastry, *J. Mol. Struct.: THEOCHEM* **2003**, *663*, 145-148; G. Sánchez-Sanz, *Tetrahedron* **2015**, *71*, 826-839; L. Nyulászi, T. Veszprémi, *J. Phys. Chem.* **1996**, *100*, 6456-6462.

[95] A. Koner, G. Pfeifer, Z. Kelemen, G. Schnakenburg, L. Nyulászi, T. Sasamori, R. Streubel, *Angew. Chem. Int. Ed.* **2017**, *56*, 9231-9235.

[96] T. Sasamori, N. Tokitoh, R. Streubel, in *π-Electron Redox Systems of Heavier Group-15 Elements, in Organic Redox Systems, Synthesis, Properties and Applications* (Ed.: T. Nishinaga), Wiley, Hoboken, New Jersey, **2016**, pp. 563-578.

[97] S. Michiyasu, S. Takahiro, S. Heisuke, F. Yukio, T. Norihiro, *Bull. Chem. Soc. Jpn.* **2013**, *86*, 1132-1143.

[98] The closed-shell wavefunction of the dication has UHF instability, and the central diphosphinine ring shows antiaromaticity (NICS(1): + 3.7 ppm). Nevertheless, the open-shell singlet is only a few kcalmol@1 more stable than the closed-shell dication; thus the second oxidation wave cannot be attributed to dication formation.

[99] R. L. Falconer, C. A. Russell, *Coord. Chem. Rev.* **2015**, *297–298*, 146-167.

[100] L. Nyulászi, *Chem. Rev.* **2001**, *101*, 1229-1246.

[101] E. Hückel, *Z. Phys.* **1931**, *70*, 204-286; E. Hückel, *Z. Phys.* **1931**, *72*, 310-337.

[102] K. Eggers, F. W. Heinemann, M. Hennemann, T. Clark, P. Binger, U. Zenneck, *C. R. Chim.* **2010**, *13*, 1203-1212.

[103] F. G. N. Cloke, P. B. Hitchcock, J. F. Nixon, D. J. Wilson, *Organometallics* **2000**, *19*, 219-220.

[104] P. L. Floch, in *Phosphorous Heterocycles I* (Ed.: R. K. Bansal), Springer Berlin Heidelberg, Berlin, Heidelberg, **2009**, pp. 147-184.

[105] C. Müller, L. E. E. Broeckx, I. de Krom, J. J. M. Weemers, *Eur. J. Inorg. Chem.* **2013**, *2013*, 187-202; F. Mathey, in *Modern Heterocyclic Chemistry*, Wiley-VCH Verlag GmbH & Co. KGaA, **2011**, pp. 2071-2116; P. L. Floch, *Coord. Chem. Rev.* **2006**, *250*, 627-681.

[106] G. Märkl, F. Lieb, *Angew. Chem. Int. Ed. Engl.* **1968**, *7*, 733-733.

[107] G. Märkl, F. Lieb, C. Martin, *Tetrahedron Lett.* **1971**, *12*, 1249-1252.

[108] B. Breit, E. Fuchs, *Chem. Commun.* **2004**, 694-695.

[109] E. Fuchs, M. Keller, B. Breit, *Chem. Eur. J.* **2006**, *12*, 6930-6939.

[110] B. Breit, E. Fuchs, *Synthesis* **2006**, *2006*, 2121-2128.

[111] O. Piechaczyk, M. Doux, L. Ricard, P. le Floch, *Organometallics* **2005**, *24*, 1204-1213.

[112] M. Blug, C. Guibert, X.-F. Le Goff, N. Mezailles, P. Le Floch, *Chem. Commun.* **2008**, 203.

[113] P. S. Bauerlein, I. A. Gonzalez, J. J. M. Weemers, M. Lutz, A. L. Spek, D. Vogt, C. Muller, *Chem. Commun.* **2009**, 4944-4946.

[114] C. G. Krespan, *J. Am. Chem. Soc.* **1961**, *83*, 3432-3433.

[115] Y. Kobayashi, S. Fujino, H. Hamana, Y. Hanzawa, S. Morita, I. Kumadaki, *J. Org. Chem.* **1980**, *45*, 4683-4685.

[116] K. G. Weinberg, E. B. Whipple, *J. Am. Chem. Soc.* **1971**, *93*, 1801-1802.

[117] U. Yosuke, S. Jun, S. Munenori, Y. Gaku, M. Yasuhiro, *Bull. Chem. Soc. Jpn.* **2009**, *82*, 819-828.

[118] A. Ishii, R. Yoshioka, J. Nakayama, M. Hoshino, *Tetrahedron Lett.* **1993**, *34*, 8259-8262.

[119] A. G. Orpen, N. G. Connelly, *Organometallics* **1990**, *9*, 1206-1210.

[120] A. Koner, Z. Kelemen, G. Schnakenburg, L. Nyulaszi, R. Streubel, *Unpublished Work*.

[121] G. Märkl, A. Merz, *Tetrahedron Lett.* **1968**, *9*, 3611-3614.

[122] K. Waschbüsch, P. Le Floch, F. Mathey, *Organometallics* **1996**, *15*, 1597-1603.

[123] G. Pfeifer, Diploma Thesis, University of Bonn **2012**.

[124] A. Hettche, K. Dimroth, *Chem. Ber.* **1973**, *106*, 1001-1011.

[125] B. Punji, J. T. Mague, M. S. Balakrishna, *Inorg. Chem.* **2007**, *46*, 10268-10275.

[126] M. T. Reetz, W. F. Maier, *Liebigs Ann. Chem.* **1980**, *1980*, 1471-1473.

[127] G. Lunn, E. B. Sansone, in *Destruction of Hazardous Chemicals in the Laboratory*, John Wiley & Sons, Inc., **2012**, pp. 17-465.

Appendix

11.1 Crystal data and structure refinement for compound *cis* 4b

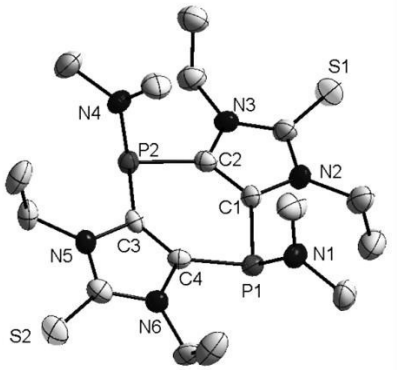

Identification code	GSTR353, 3365	Z	8
Device Type	Nonius KappaCCD	ρ_{calc}g/cm^3	1.281
Empirical formula	$C_{18}H_{32}N_6P_2S_2$	μ/mm^{-1}	0.375
Moiety formula	$C_{18}H_{32}N_6P_2S_2$	F(000)	1952
Formula weight	458.56	Crystal size/mm	0.12 x 0.08 x 0.04
Temperature/K	293(2)	2Θ range for data collection/°	2.70 to 26.00
Wavelength/Å	0.71073	Limiting indices	-28 ≤ h ≤ 23, -12 ≤ k ≤ 15, -20 ≤ l ≤ 18
Crystal system	Orthorhombic	Reflections collected / unique	29973 / 8941 [R(int) = 0.0493]
space group	P n a 21	Completeness to theta	0.998
a/Å	23.4008(7)	Absorption correction	Semi-empirical from eq.s
b/Å	12.3463(2)	Max. and min. transmission	0.9852 and 0.9564
c/Å	16.4552(5)	Refinement method	Full-matrix least-squares on F^2
σ/°	90	Goodness-of-fit on F^2	0.974
β/°	90	Final R indices [I>2sigma(I)]	R1 = 0.0396, wR2 = 0.0903
γ/°	90	R indices (all data)	R1 = 0.0548, wR2 = 0.0958
Volume/ Å^3	4754.1(2)	Largest diff. peak and hole/ e Å^{-3}	0.354 and -0.298

11.2 Crystal data and structure refinement for compound 3g

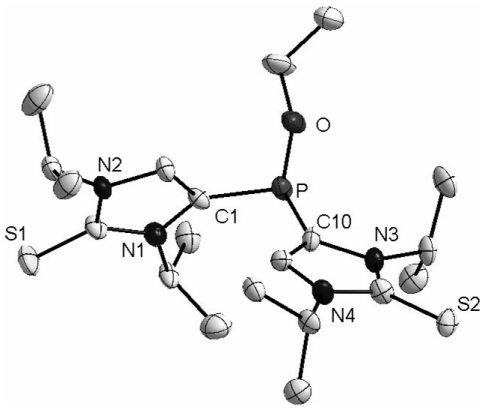

Identification code	GSTR550, ABK-38	Z	4
Device Type	Bruker X8-KappaApexII	ρcalc g/cm3	1.210
Empirical formula	$C_{20}H_{35}N_4OPS_2$	μ/mm-1	2.740
Moiety formula	$C_{20}H_{35}N_4OPS_2$	F(000)	952.0
Formula weight	442.61	Crystal size/mm	0.24 × 0.15 × 0.13
Temperature/K	100(2)	2Θ range for data collection/°	8.402 to 135.464
Wavelength/Å	0.71073	Radiation	CuKα (λ = 1.54178)
Crystal system	monoclinic	Reflections collected / unique	4399 [Rint = 0.3466, Rsigma = 0.0697]
space group	P21/n	Completeness to theta	1.000
a/Å	11.9964(4)	Absorption correction	Semi-empirical from eq.s
b/Å	16.5050(6)	Max. and min. transmission	0.18398; 0.753817
c/Å	13.3543(5)	Refinement method	Full-matrix least-squares on F2
σ/°	90	Goodness-of-fit on F^2	1.196
β/°	113.292(2)	Final R indices [I>2 σ (I)]	R1 = 0.1142, wR2 = 0.2434
γ/°	90	R indices (all data)	R1 = 0.1340, wR2 = 0.2560
Volume/ Å3	2428.66(15)	Largest diff. peak and hole/ e Å-3	0.49/-0.74

11.3 Crystal data and structure refinement for compound 3i

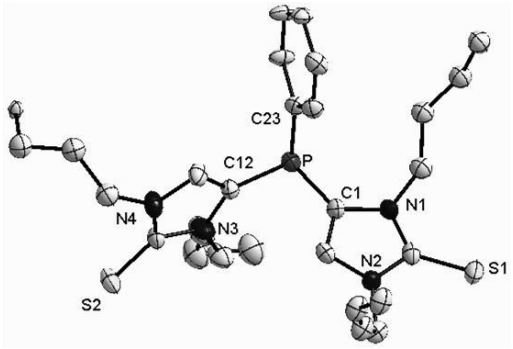

Identification code	GSTR465, ABK-92	ρ_{calc}g/cm^3	1.177
Crystal Habitus	clear colourless block	μ/mm^{-1}	2.278
Device Type	Bruker D8-Venture	F(000)	2288.0
Empirical formula	$C_{28}H_{43}N_4PS_2$	Crystal size/mm^3	0.25 × 0.18 × 0.08
Moiety formula	$C_{28}H_{43}N_4PS_2$	Absorption correction	empirical
Formula weight	530.75	Tmin; Tmax	0.3334; 0.7536
Temperature/K	123.01	Radiation	CuKα (λ = 1.54178)
Crystal system	monoclinic	2Θ range /°	6.986 to 135.496
Space group	C2/c	Completeness to theta	0.991
a/Å	29.1175(16)	Index ranges	-34 ≤ h ≤ 34, -12 ≤ k ≤ 12, -26 ≤ l ≤ 26
b/Å	10.9059(6)	Reflections collected	76097
c/Å	21.7084(11)	Independent reflections	5372 [R_{int} = 0.1435, R_{sigma} = 0.0514]
α/°	90	Data/restraints/parameters	5372/261/407
β/°	119.655(3)	Goodness-of-fit on F^2	1.051
γ/°	90	Final R indexes [I>=2σ (I)]	R_1 = 0.1233, wR_2 = 0.3190
Volume/Å^3	5990.7(6)	Final R indexes [all data]	R_1 = 0.1446, wR_2 = 0.3409
Z	8	Largest diff. peak/hole / e Å^{-3}	2.01/-1.51

11.4 Crystal data and structure refinement for compound 5f

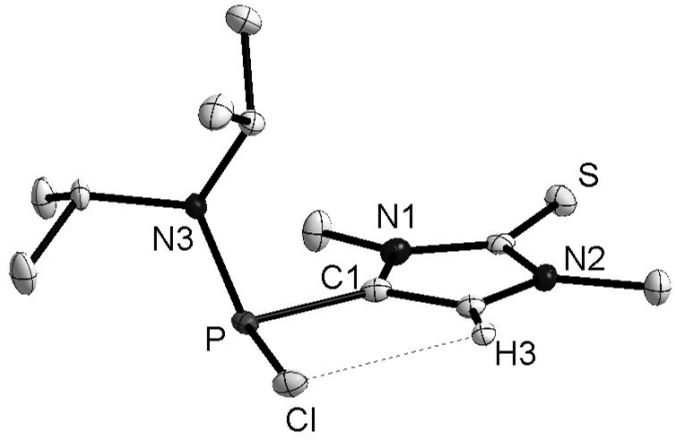

Identification code	GSTR443, ABK-247	ρ_{calc}g/cm^3	1.309
Crystal Habitus	clear colourless block	μ/mm^{-1}	4.456
Device Type	Bruker D8-Venture	F(000)	624.0
Empirical formula	$C_{11}H_{21}N_3PSCl$	Crystal size/mm^3	0.11 × 0.06 × 0.04
Moiety formula	$C_{11}H_{21}ClN_3PS$	Absorption correction	empirical
Formula weight	293.79	Tmin; Tmax	0.3776; 0.7536
Temperature/K	100.0	Radiation	CuKα (λ = 1.54178)
Crystal system	monoclinic	2Θ range for data collection/°	8.104 to 135.488°
Space group	$P2_1/c$	Completeness to theta	0.997
a/Å	11.6794(7)	Index ranges	-14 ≤ h ≤ 14, -11 ≤ k ≤ 11, -17 ≤ l ≤ 17
b/Å	9.3892(6)	Reflections collected	20754
c/Å	14.5557(9)	Independent reflections	2693 [R_{int} = 0.0872, R_{sigma} = 0.0492]
α/°	90	Data/restraints/parameters	2693/0/160
β/°	110.915(3)	Goodness-of-fit on F^2	1.066
γ/°	90	Final R indexes [I>=2σ (I)]	R_1 = 0.0465, wR_2 = 0.1147
Volume/Å^3	1491.01(16)	Final R indexes [all data]	R_1 = 0.0550, wR_2 = 0.1214
Z	4	Largest diff. peak/hole / e Å^{-3}	0.40/-0.81

11.5 Crystal data and structure refinement for compound 4d

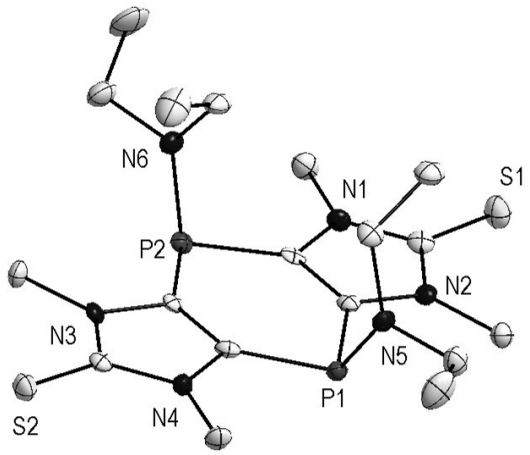

Identification code	GSTR459, ABK-274	ρ_{calc}g/cm^3	1.341
Crystal Habitus	clear colourless block	μ/mm^{-1}	0.392
Device Type	Bruker D8-Venture	F(000)	488.0
Empirical formula	$C_{18}H_{32}N_6P_2S_2$	Crystal size/mm^3	0.3 × 0.27 × 0.26
Moiety formula	$C_{18}H_{32}N_6P_2S_2$	Absorption correction	empirical
Formula weight	458.55	Tmin; Tmax	0.4821; 0.7452
Temperature/K	100	Radiation	MoKα (λ = 0.71073)
Crystal system	triclinic	2Θ range/°	4.86 to 51.034°
Space group	P-1	Completeness to theta	0.992
a/Å	10.5879(15)	Index ranges	-12 ≤ h ≤ 12, -13 ≤ k ≤ 13, -13 ≤ l ≤ 13
b/Å	11.3529(15)	Reflections collected	26099
c/Å	11.5102(15)	Independent reflections	4205 [R_{int} = 0.0972, R_{sigma} = 0.0702]
α/°	101.361(3)	Data/restraints/parameters	4205/12/260
β/°	116.339(3)	Goodness-of-fit on F^2	1.098
γ/°	103.068(3)	Final R indexes [I>=2σ (I)]	R_1 = 0.0773, wR_2 = 0.1581
Volume/Å^3	1135.6(3)	Final R indexes [all data]	R_1 = 0.1174, wR_2 = 0.1778
Z	2	Largest diff. peak/hole / e Å^{-3}	0.69/-0.56

11.6 Crystal data and structure refinement for compound 4f

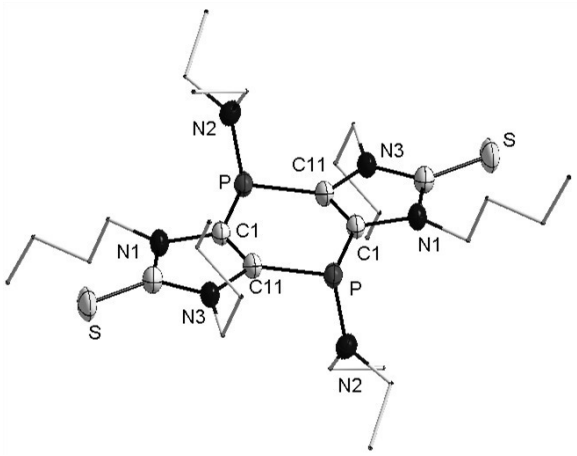

Identification code	GSTR531, ABK-339	ρ_{calc}g/cm^3	1.147
Crystal Habitus	clear colourless plate	μ/mm^{-1}	2.365
Device Type	Bruker D8-Venture	F(000)	2720.0
Empirical formula	$C_{30}H_{56}N_6P_2S_2$	Crystal size/mm^3	0.09 × 0.04 × 0.03
Moiety formula	$C_{30}H_{56}N_6P_2S_2$	Absorption correction	empirical
Formula weight	626.86	Tmin; Tmax	0.5634; 0.7536
Temperature/K	100.0	Radiation	CuKα (λ = 1.54178)
Crystal system	tetragonal	2Θ range /°	6.808 to 134.952°
Space group	$I4_1/a$	Completeness to theta	0.954
a/Å	25.9652(8)	Index ranges	-31 ≤ h ≤ 30, -28 ≤ k ≤ 31, -12 ≤ l ≤ 12
b/Å	25.9652(8)	Reflections collected	51235
c/Å	10.7734(4)	Independent reflections	3121 [R_{int} = 0.1236, R_{sigma} = 0.0457]
α/°	90	Data/restraints/parameters	3121/45/214
β/°	90	Goodness-of-fit on F^2	1.095
γ/°	90	Final R indexes [I>=2σ (I)]	R_1 = 0.0603, wR_2 = 0.1428
Volume/Å^3	7263.3(5)	Final R indexes [all data]	R_1 = 0.0882, wR_2 = 0.1552
Z	8	Largest diff. peak/hole / e Å^{-3}	0.55/-0.31

11.7 Crystal data and structure refinement for compound 9a

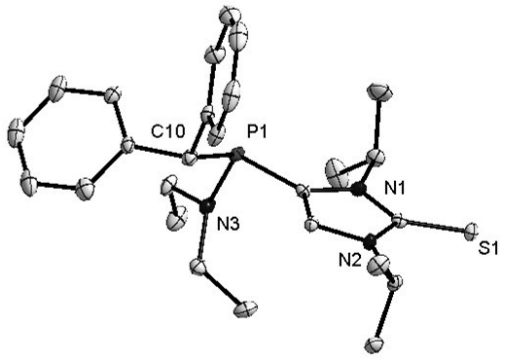

Identification code	dg-232, ABK-UBC-20	γ/°	92.645(4)
Crystal Habitus	clear colourless plate	Volume/Å^3	2546.5(7)
Device Type	Bruker APEX-DUO	Z	4
Empirical formula	$C_{26}H_{36}N_3PS$	ρcalcg/cm^3	1.183
Formula weight	453.61	μ/mm-1	0.208
Temperature/K	90(2)	Crystal size/mm^3	0.06 × 0.1 × 0.19
Crystal system	triclinic	Radiation	MoKα (λ = 0.71073)
Space group	P-1	2Θ rmax /°	60.19
a/Å	9.4412 (16)	Completeness to theta	0.954
b/Å	15.818(3)	Independent reflections	14925
c/Å	17.317(3)	Goodness-of-fit on F^2	1.008
α/°	99.675(4)	Final R indexes [I>=2σ (I)]	R1 = 0.0462, wR2 = 0.1121
β/°	90.025(4)	Largest diff. peak/hole / e Å^{-3}	0.78/−0.42

11.8 Crystal data and structure refinement for compound 9b

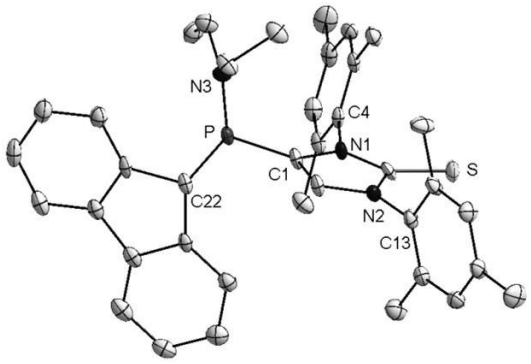

Identification code	GSTR489, ABK-315	ρ_{calc}g/cm^3	1.176
Crystal Habitus	clear colourless needle	μ/mm^{-1}	0.191
Device Type	Bruker D8-Venture	F(000)	1104.0
Empirical formula	$C_{29}H_{43}N_4PS$	Crystal size/mm^3	0.14 × 0.05 × 0.04
Moiety formula	$C_{29}H_{43}N_4PS$	Absorption correction	empirical
Formula weight	510.70	Tmin; Tmax	0.6294; 0.7456
Temperature/K	150	Radiation	MoKα (λ = 0.71073)
Crystal system	monoclinic	2Θ range for data collection/°	4.506 to 55.998°
Space group	$P2_1/c$	Completeness to theta	0.998
a/Å	11.7230(6)	Index ranges	-15 ≤ h ≤ 15, -39 ≤ k ≤ 39, -11 ≤ l ≤ 11
b/Å	29.7836(16)	Reflections collected	118005
c/Å	8.5162(4)	Independent reflections	6940 [R_{int} = 0.0923, R_{sigma} = 0.0307]
α/°	90	Data/restraints/parameters	6940/0/327
β/°	103.9668(17)	Goodness-of-fit on F^2	1.169
γ/°	90	Final R indexes [I>=2σ (I)]	R_1 = 0.0853, wR_2 = 0.2340
Volume/Å^3	2885.5(3)	Final R indexes [all data]	R_1 = 0.0957, wR_2 = 0.2394
Z	4	Largest diff. peak/hole / e Å^{-3}	1.64/-0.46

11.9 Crystal data and structure refinement for compound 10

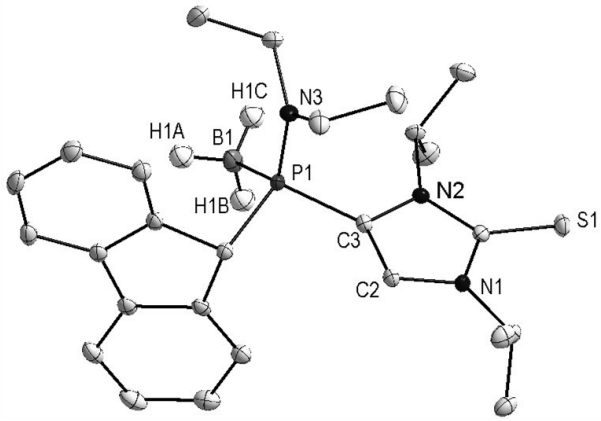

Identification code	dg-311, ABK-UBC-5	γ/°	90
Crystal Habitus	clear colourless plate	Volume/Å^3	2613.18(40)
Device Type	Bruker APEX-DUO	Z	4
Empirical formula	$C_{26}H_{37}BN_3PS$	ρ_{calc}g/cm^3	1.183
Formula weight	465.42	μ/mm-1	0.203
Temperature/K	90(2)	Crystal size/mm^3	0.11 × 0.12 × 0.28
Crystal system	monoclinic	Radiation	MoKα (λ = 0.71073)
Space group	$P2_1/c$	$2\Theta_{max}$/°	60.20
a/Å	11.5715(10)	Completeness to theta	0.954
b/Å	13.5369(12)	Independent reflections	7687
c/Å	16.9067(15)	Goodness-of-fit on F^2	1.020
α/°	90	Final R indexes [I>=2σ (I)]	R1 = 0.0360, wR2 = 0.0940
β/°	99.317(2)	Largest diff. peak/hole / e Å^{-3}	0.43/−0.29

11.10 Crystal data and structure refinement for compound 21a

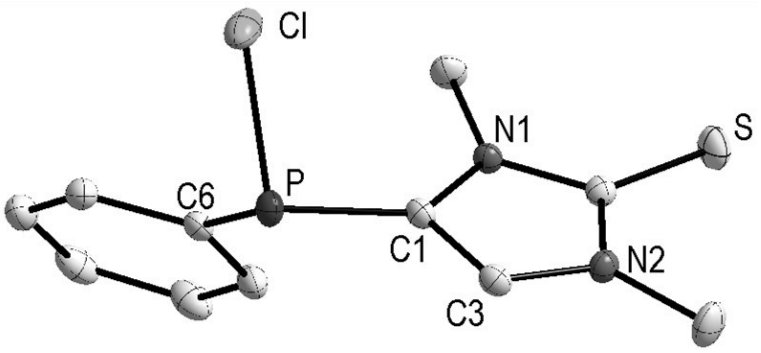

Identification code	GSTR484, ABK-323	$\rho_{calc}g/cm^3$	1.450
Crystal Habitus	clear colourless plate	μ/mm^{-1}	0.579
Device Type	Bruker X8 Kappa Apex	F(000)	280.0
Empirical formula	$C_{11}H_{12}N_2PSCl$	Crystal size/mm^3	0.22 × 0.2 × 0.09
Moiety formula	$C_{11}H_{12}N_2PSCl$	Absorption correction	empirical
Formula weight	270.71	Tmin; Tmax	0.6578; 0.7459
Temperature/K	150.0	Radiation	MoKα (λ = 0.71073)
Crystal system	triclinic	2Θ range for data collection/°	4.574 to 56°
Space group	P-1	Completeness to theta	1.000
a/Å	8.3058(5)	Index ranges	-10 ≤ h ≤ 10, -12 ≤ k ≤ 12, -13 ≤ l ≤ 13
b/Å	9.1140(9)	Reflections collected	29551
c/Å	9.9160(7)	Independent reflections	2990 [R_{int} = 0.0621, R_{sigma} = 0.0280]
α/°	63.984(3)	Data/restraints/parameters	2990/0/147
β/°	78.086(2)	Goodness-of-fit on F^2	1.039
γ/°	66.898(2)	Final R indexes [I>=2σ (I)]	R_1 = 0.0294, wR_2 = 0.0724
Volume/$Å^3$	619.94(9)	Final R indexes [all data]	R_1 = 0.0374, wR_2 = 0.0767
Z	2	Largest diff. peak/hole / e $Å^{-3}$	0.41/-0.39

11.11 Crystal data and structure refinement for compound 22a

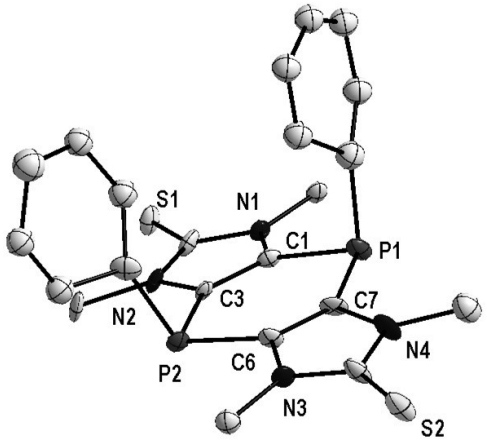

Identification code	GSTR483, ABK-324	ρ_{calc}g/cm^3	1.399
Crystal Habitus	clear colourless block	μ/mm^{-1}	0.401
Device Type	Bruker D8-Venture	F(000)	976.0
Empirical formula	$C_{22}H_{22}N_4P_2S_2$	Crystal size/mm^3	0.24 × 0.12 × 0.08
Moiety formula	C22 H22 N4 P2 S2	Absorption correction	empirical
Formula weight	468.49	Tmin; Tmax	0.4015; 0.7449
Temperature/K	123	Radiation	MoKα (λ = 0.71073)
Crystal system	monoclinic	2Θ range for data collection/°	4.648 to 47.61°
Space group	$P2_1/c$	Completeness to theta	0.746
a/Å	13.390(8)	Index ranges	-15 ≤ h ≤ 15, -17 ≤ k ≤ 17, -11 ≤ l ≤ 10
b/Å	15.743(9)	Reflections collected	29748
c/Å	10.566(6)	Independent reflections	3262 [R_{int} = 0.2943, R_{sigma} = 0.1727]
α/°	90	Data/restraints/parameters	3262/173/340
β/°	93.25(2)	Goodness-of-fit on F^2	1.047
γ/°	90	Final R indexes [I>=2σ (I)]	R_1 = 0.1518, wR_2 = 0.3602
Volume/Å^3	2224(2)	Final R indexes [all data]	R_1 = 0.2285, wR_2 = 0.4184
Z	4	Largest diff. peak/hole / e Å^{-3}	0.88/-0.84

11.12 Crystal data and structure refinement for compound 22c

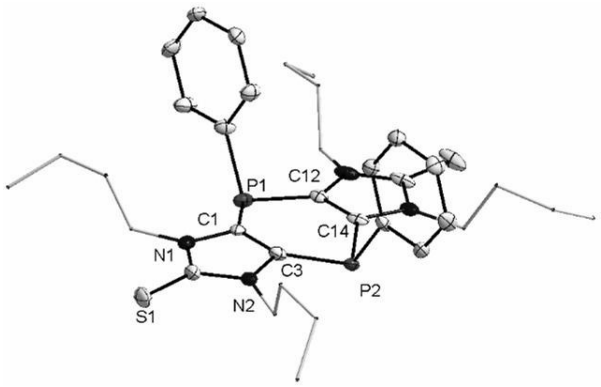

Identification code	GSTR560, ABK-476	ρ_{calc}g/cm^3	1.250
Crystal Habitus	clear colourless block	μ/mm^{-1}	0.282
Device Type	Bruker D8-Venture	F(000)	1360.0
Empirical formula	$C_{34}H_{46}N_4P_2S_2$	Crystal size/mm^3	0.23 × 0.18 × 0.17
Moiety formula	$C_{34}H_{46}N_4P_2S_2$	Absorption correction	empirical
Formula weight	636.81	Tmin; Tmax	0.5234; 0.7459
Temperature/K	99.99	Radiation	MoKα (λ = 0.71073)
Crystal system	triclinic	2Θ range for data collection/°	4.264 to 55.998°
Space group	P-1	Completeness to theta	0.992
a/Å	14.250(2)	Index ranges	-18 ≤ h ≤ 18, -20 ≤ k ≤ 19, -23 ≤ l ≤ 23
b/Å	15.1496(18)	Reflections collected	132335
c/Å	17.733(3)	Independent reflections	16255 [R_{int} = 0.1491, R_{sigma} = 0.0769]
α/°	71.768(6)	Data/restraints/parameters	16255/53/785
β/°	70.775(7)	Goodness-of-fit on F^2	1.098
γ/°	75.242(6)	Final R indexes [I>=2σ (I)]	R_1 = 0.1561, wR_2 = 0.4133
Volume/Å^3	3383.7(8)	Final R indexes [all data]	R_1 = 0.1917, wR_2 = 0.4350
Z	4	Largest diff. peak/hole / e Å^{-3}	2.91/-1.14

11.13 Crystal data and structure refinement for compound 23b

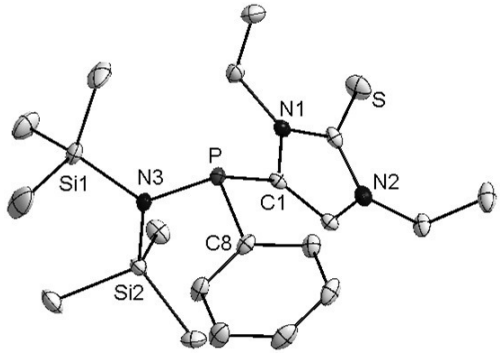

Identification code	GSTR514, ABK-MK-08	ρcalcg/cm3	1.165
Crystal Habitus	clear colourless block	μ/mm^{-1}	0.308
Device Type	Bruker X8-KappaApexII	F(000)	912.0
Empirical formula	C19H34N3Si2PS	Crystal size/mm^3	0.18 × 0.16 × 0.08
Moiety formula	C19H34N3Si2PS	Absorption correction	empirical
Formula weight	423.70	Tmin; Tmax	0.6563; 0.7459
Temperature/K	100	Radiation	MoKα (λ = 0.71073)
Crystal system	orthorhombic	2Θ range for data collection/°	4.676 to 55.998°
Space group	P212121	Completeness to theta	0.995
a/Å	7.9723(5)	Index ranges	-10 ≤ h ≤ 7, -22 ≤ k ≤ 20, -22 ≤ l ≤ 22
b/Å	17.3933(11)	Reflections collected	20496
c/Å	17.4227(9)	Independent reflections	5819 [Rint = 0.0415, Rsigma = 0.0406]
α/°	90	Data/restraints/parameters	5819/0/244
β/°	90	Goodness-of-fit on F^2	1.080
γ/°	90	Final R indexes [I>=2σ (I)]	R1 = 0.0352, wR2 = 0.0765
Volume/Å^3	2415.9(2)	Final R indexes [all data]	R1 = 0.0394, wR2 = 0.0787
Z	4	Largest diff. peak/hole / e Å^{-3}	0.29/-0.22
Flack parameter	0.39(9)		

11.14 Crystal data and structure refinement for compound 25b

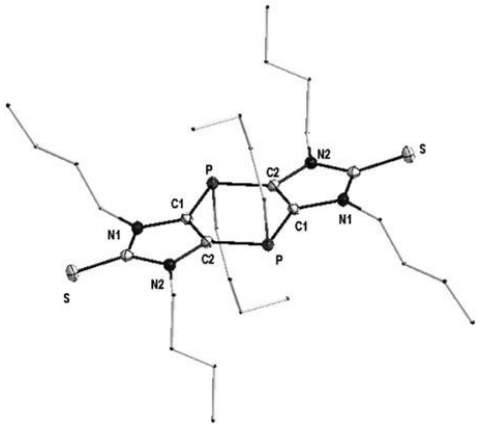

Identification code	GSTR542, ABK-470	ρcalcg/cm3	1.177
Crystal Habitus	clear orange plank	μ/mm-1	0.278
Device Type	Bruker D8-Venture	F(000)	1296.0
Empirical formula	$C_{30}H_{54}N_4P_2S_2$	Crystal size/mm3	0.18 × 0.1 × 0.08
Moiety formula	$2(C_{15}H_{27}N_2PS)$	Absorption correction	empirical
Formula weight	596.83	Tmin; Tmax	0.5517; 0.7459
Temperature/K	100.01	Radiation	MoKα (λ = 0.71073)
Crystal system	monoclinic	2Θ range for data collection/°	4.738 to 56°
Space group	P21/c	Completeness to theta	0.989
a/Å	17.997(2)	Index ranges	-23 ≤ h ≤ 19, -25 ≤ k ≤ 25, -12 ≤ l ≤ 12
b/Å	19.612(2)	Reflections collected	43984
c/Å	9.6079(11)	Independent reflections	8059 [Rint = 0.1400, Rsigma = 0.1106]
α/°	90	Data/restraints/parameters	8059/0/349
β/°	96.652(4)	Goodness-of-fit on F2	1.030
γ/°	90	Final R indexes [I>=2σ (I)]	R1 = 0.0549, wR2 = 0.1071
Volume/Å3	3368.2(7)	Final R indexes [all data]	R1 = 0.1069, wR2 = 0.1261
Z	4	Largest diff. peak/hole / e Å-3	0.74/-0.49

11.15 Crystal data and structure refinement for compound 26a

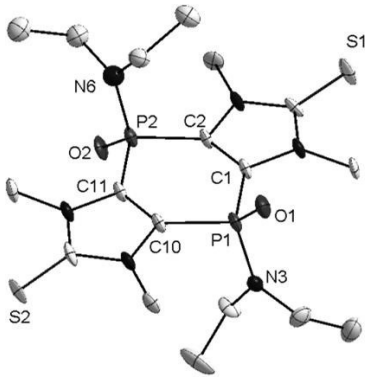

Identification code	GSTR475, ABK-286	ρ_{calc}g/cm^3	1.310
Crystal Habitus	clear colourless plate	μ/mm^{-1}	3.609
Device Type	Bruker D8-Venture	F(000)	1602.0
Empirical formula	$C_{109}H_{194}Cl_2N_{36}O_{12}P_{12}S_{12}$	Crystal size/mm^3	0.16 × 0.14 × 0.08
Moiety formula	CH_2Cl_2, 6($C_{18}H_{32}N_6O_2P_2S_2$)	Absorption correction	empirical
Formula weight	3028.25	Tmin; Tmax	0.2969; 0.7536
Temperature/K	123	Radiation	CuKα (λ = 1.54178)
Crystal system	triclinic	2Θ range for data collection/°	4.368 to 135.498°
Space group	P-1	Completeness to theta	0.998
a/Å	9.2983(3)	Index ranges	-11 ≤ h ≤ 11, -25 ≤ k ≤ 25, -26 ≤ l ≤ 26
b/Å	20.5513(8)	Reflections collected	117863
c/Å	21.2034(8)	Independent reflections	13876 [R_{int} = 0.1808, R_{sigma} = 0.0877]
α/°	100.916(2)	Data/restraints/parameters	13876/312/882
β/°	102.062(2)	Goodness-of-fit on F^2	1.083
γ/°	96.821(2)	Final R indexes [I>=2σ (I)]	R_1 = 0.1245, wR_2 = 0.2866
Volume/Å^3	3837.4(2)	Final R indexes [all data]	R_1 = 0.1538, wR_2 = 0.3012
Z	1	Largest diff. peak/hole / e Å^{-3}	1.47/-0.94

11.16 Crystal data and structure refinement for compound 26d

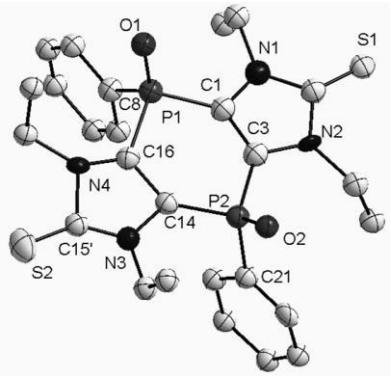

Identification code	GSTR533, ABK-MK-13	$\rho_{calc}g/cm^3$	1.405
Crystal Habitus	clear colourless plate	μ/mm^{-1}	0.490
Device Type	Bruker X8-KappaApexII	F(000)	2672.0
Empirical formula	$C_{27}H_{32}Cl_2N_4O_2P_2S_2$	Crystal size/mm^3	0.09 × 0.08 × 0.03
Moiety formula	$C_{26}H_{30}N_4O_2P_2S_2$, CH_2Cl_2	Absorption correction	empirical
Formula weight	641.52	Tmin; Tmax	0.6666; 0.7459
Temperature/K	100	Radiation	MoKα (λ = 0.71073)
Crystal system	monoclinic	2Θ range for data collection/°	3.036 to 56°
Space group	$P2_1/n$	Completeness to theta	0.998
a/Å	16.7459(15)	Index ranges	-22 ≤ h ≤ 22, 0 ≤ k ≤ 23, 0 ≤ l ≤ 26
b/Å	17.9798(17)	Reflections collected	17853
c/Å	20.1929(19)	Independent reflections	17853 [R_{int} = 0.1970, R_{sigma} = 0.1954]
α/°	90	Data/restraints/parameters	17853/1014/721
β/°	94.071(3)	Goodness-of-fit on F^2	1.149
γ/°	90	Final R indexes [I>=2σ (I)]	R_1 = 0.3242, wR_2 = 0.5993
Volume/$Å^3$	6064.5(10)	Final R indexes [all data]	R_1 = 0.3897, wR_2 = 0.6355
Z	8	Largest diff. peak/hole / e $Å^{-3}$	2.68/-2.67

10.17 Crystal data and structure refinement for compound 27a

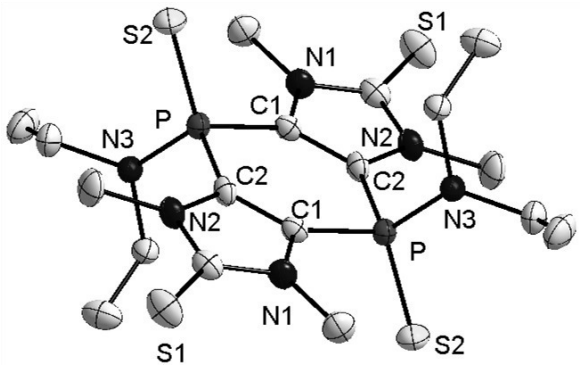

Identification code	GSTR513, ABK-MK-36	ρ_{calc}g/cm^3	1.342
Crystal Habitus	clear colourless plate	μ/mm^{-1}	0.444
Device Type	Nonius KappaCCD	F(000)	326.0
Empirical formula	$C_{25}H_{40}N_6P_2S_4$	Crystal size/mm^3	0.18 × 0.06 × 0.04
Moiety formula	C18 H32 N6 P2 S4, C7 H8	Absorption correction	multi-scan
Formula weight	614.81	Tmin; Tmax	0.8771; 1.0511
Temperature/K	100	Radiation	MoKα (λ = 0.71073)
Crystal system	triclinic	2Θ range for data collection/°	5.898 to 55.988°
Space group	P-1	Completeness to theta	0.999
a/Å	7.5153(4)	Index ranges	-9 ≤ h ≤ 9, -12 ≤ k ≤ 12, -15 ≤ l ≤ 13
b/Å	9.3062(8)	Reflections collected	8843
c/Å	11.8949(9)	Independent reflections	3645 [R_{int} = 0.0814, R_{sigma} = 0.1013]
α/°	95.800(3)	Data/restraints/parameters	3645/31/192
β/°	100.379(4)	Goodness-of-fit on F^2	1.029
γ/°	109.282(4)	Final R indexes [I>=2σ (I)]	R_1 = 0.0579, wR_2 = 0.1097
Volume/Å^3	760.76(10)	Final R indexes [all data]	R_1 = 0.1024, wR_2 = 0.1256
Z	1	Largest diff. peak/hole / e Å^{-3}	0.47/-0.44

10.18 Crystal data and structure refinement for compound 27d

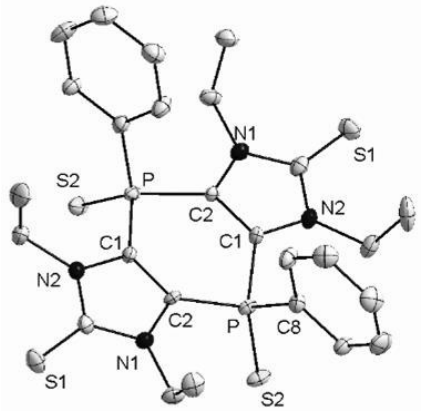

Identification code	GSTR532, ABK-MK-23	ρ_{calc}g/cm^3	1.221
Crystal Habitus	clear colourless block	μ/mm^{-1}	0.418
Device Type	Bruker X8-KappaApexII	F(000)	924.0
Empirical formula	$C_{26}H_{30}N_4P_2S_4$	Crystal size/mm^3	0.11 × 0.1 × 0.06
Formula weight	588.72	Absorption correction	empirical
Temperature/K	100	Tmin; Tmax	0.6086; 0.7459
Crystal system	trigonal	Radiation	MoKα (λ = 0.71073)
Space group	$P3_121$	2Θ range for data collection/°	4.558 to 55.96°
a/Å	15.0072(6)	Completeness to theta	0.990
b/Å	15.0072(6)	Index ranges	-20 ≤ h ≤ 19, -20 ≤ k ≤ 20, -16 ≤ l ≤ 17
c/Å	12.3126(6)	Reflections collected	28461
α/°	90	Independent reflections	3833 [R_{int} = 0.1350, R_{sigma} = 0.1145]
β/°	90	Data/restraints/parameters	3833/0/166
γ/°	120	Goodness-of-fit on F^2	1.028
Volume/Å^3	2401.5(2)	Final R indexes [I>=2σ (I)]	R_1 = 0.0548, wR_2 = 0.1213
Z	3	Final R indexes [all data]	R_1 = 0.0773, wR_2 = 0.1322
Flack parameter	0.02(18)	Largest diff. peak/hole / e Å^{-3}	0.49/-0.49

10.19 Crystal data and structure refinement for compound 29d

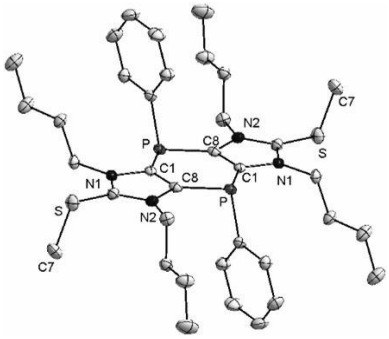

Identification code	GSTR553, ABK-521	ρ_{calc}g/cm^3	1.450
Crystal Habitus	clear colourless block	μ/mm^{-1}	0.519
Device Type	Bruker X8-KappaApexII	F(000)	1176.0
Empirical formula	$C_{40}H_{56}Cl_4F_6N_4O_6P_2S_4$	Crystal size/mm^3	0.24 × 0.16 × 0.14
Moiety formula	2(CH_2Cl_2), 2($C_{18}H_{26}N_2PS$), 2(CF_3O_3S)	Absorption correction	empirical
Formula weight	1134.86	Tmin; Tmax	0.5986; 0.7459
Temperature/K	100	Radiation	MoKα (λ = 0.71073)
Crystal system	triclinic	2Θ range for data collection/°	1.966 to 55.996°
Space group	P-1	Completeness to theta	0.997
a/Å	10.5491(12)	Index ranges	-13 ≤ h ≤ 13, -16 ≤ k ≤ 16, -28 ≤ l ≤ 28
b/Å	12.4821(14)	Reflections collected	72578
c/Å	21.887(3)	Independent reflections	12414 [R_{int} = 0.0615, R_{sigma} = 0.0533]
α/°	73.686(6)	Data/restraints/parameters	12414/109/630
β/°	76.144(8)	Goodness-of-fit on F^2	1.104
γ/°	72.404(6)	Final R indexes [I>=2σ (I)]	R_1 = 0.0720, wR_2 = 0.1384
Volume/Å^3	2598.6(5)	Final R indexes [all data]	R_1 = 0.1029, wR_2 = 0.1521
Z	2	Largest diff. peak/hole / e Å^{-3}	1.21/-0.68

10.20 Crystal data and structure refinement for compound 30a

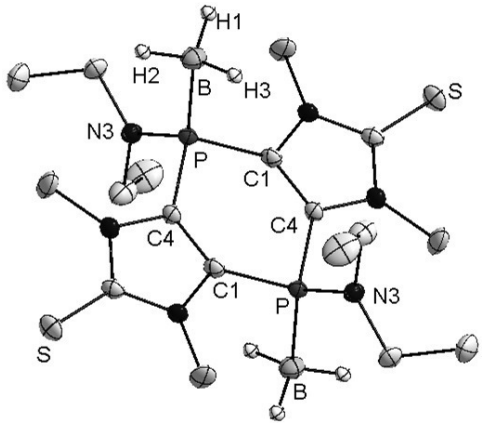

Identification code	GSTR557, ABK-320	ρ_{calc}g/cm^3	1.327
Crystal Habitus	clear colourless block	μ/mm^{-1}	0.607
Device Type	Nonius KappaCCD	F(000)	688.0
Empirical formula	$C_{20}H_{42}B_2Cl_4N_6P_2S_2$	Crystal size/mm^3	0.25 × 0.2 × 0.1
Moiety formula	2(CH_2Cl_2), $C_{18}H_{38}B_2N_6P_2S_2$	Absorption correction	empirical
Formula weight	656.07	Tmin; Tmax	0.6786; 0.7459
Temperature/K	123	Radiation	MoKα (λ = 0.71073)
Crystal system	monoclinic	2Θ range for data collection/°	3.916 to 55.998°
Space group	$P2_1/c$	Completeness to theta	0.995
a/Å	10.0982(8)	Index ranges	-13 ≤ h ≤ 13, -10 ≤ k ≤ 9, -28 ≤ l ≤ 28
b/Å	7.8176(6)	Reflections collected	22733
c/Å	21.2936(18)	Independent reflections	3945 [R_{int} = 0.0648, R_{sigma} = 0.0445]
α/°	90	Data/restraints/parameters	3945/1/195
β/°	102.342(3)	Goodness-of-fit on F^2	1.039
γ/°	90	Final R indexes [I>=2σ (I)]	R_1 = 0.0403, wR_2 = 0.0894
Volume/Å^3	1642.1(2)	Final R indexes [all data]	R_1 = 0.0583, wR_2 = 0.0976
Z	2	Largest diff. peak/hole / e Å^{-3}	0.35/-0.28

10.21 Crystal data and structure refinement for compound 33a

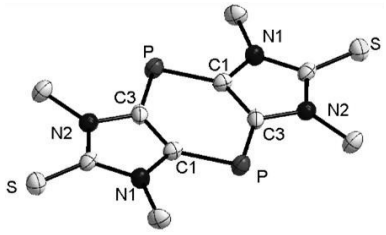

Identification code	GSTR360, 3460f	ρ_{calc}mg/mm^3	1.573
Empirical formula	$C_{10}H_{12}N_4P_2S_2$	m/mm^{-1}	0.628
Formula weight	314.30	F(000)	324.0
Temperature/K	123.15	Crystal size/mm^3	0.18 × 0.16 × 0.02
Crystal system	monoclinic	Radiation	MoKα (λ = 0.71073)
Space group	$P2_1/c$	2Θ range for data collection	6.66 to 55.98°
a/Å	4.3829(8)	Index ranges	-5 ≤ h ≤ 5, -21 ≤ k ≤ 20, -11 ≤ l ≤ 12
b/Å	16.111(3)	Reflections collected	6828
c/Å	9.5606(16)	Independent reflections	1592 [R_{int} = 0.0898, R_{sigma} = 0.1127]
α/°	90.00	Data/restraints/parameters	1592/0/84
β/°	100.562(7)	Goodness-of-fit on F^2	1.150
γ/°	90.00	Final R indexes [I>=2σ (I)]	R_1 = 0.0750, wR_2 = 0.1823
Volume/Å^3	663.7(2)	Final R indexes [all data]	R_1 = 0.1447, wR_2 = 0.2107
Z	2	Largest diff. peak/hole / e Å^{-3}	1.19/-0.70

10.22 Crystal data and structure refinement for compound 33b

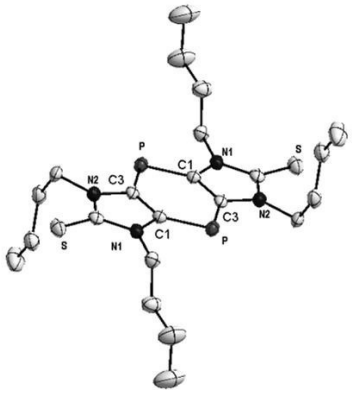

Identification code	GSTR526, ABK-340B	ρ_{calc}g/cm^3	1.225
Crystal Habitus	clear red plate	μ/mm^{-1}	0.323
Device Type	Bruker X8-KappaApexII	F(000)	558.0
Empirical formula	$C_{49}H_{84}N_8P_4S_4$	Crystal size/mm^3	0.09 × 0.05 × 0.02
Moiety formula	2($C_{22}H_{36}N_4P_2S_2$), C_5H_{12}	Absorption correction	empirical
Formula weight	1037.36	Tmin; Tmax	0.6480; 0.7459
Temperature/K	100	Radiation	MoKα (λ = 0.71073)
Crystal system	triclinic	2Θ range for data collection/°	6.01 to 56°
Space group	P-1	Completeness to theta	0.997
a/Å	9.3810(11)	Index ranges	-12 ≤ h ≤ 12, -16 ≤ k ≤ 16, -17 ≤ l ≤ 17
b/Å	12.2140(13)	Reflections collected	48495
c/Å	13.1530(16)	Independent reflections	6764 [R_{int} = 0.1641, R_{sigma} = 0.1376]
α/°	90.957(7)	Data/restraints/parameters	6764/57/322
β/°	109.757(7)	Goodness-of-fit on F^2	1.004
γ/°	96.772(7)	Final R indexes [I>=2σ (I)]	R_1 = 0.0624, wR_2 = 0.1339
Volume/Å^3	1405.9(3)	Final R indexes [all data]	R_1 = 0.1621, wR_2 = 0.1707
Z	1	Largest diff. peak/hole / e Å^{-3}	0.62/-0.44

10.23 Crystal data and structure refinement for compound 34b

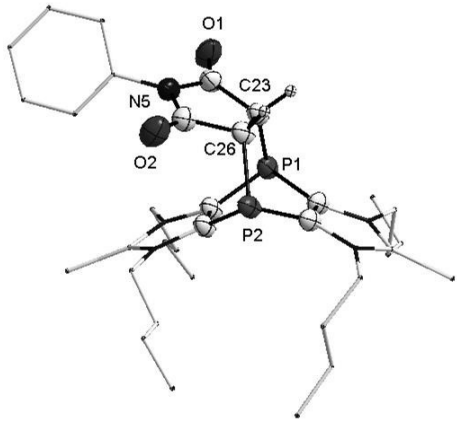

Identification code	GSTR548, ABK-445	ρ_{calc}g/cm^3	1.262
Crystal Habitus	clear colourless block	μ/mm^{-1}	0.313
Device Type	Bruker X8-KappaApexII	F(000)	2868.0
Empirical formula	$C_{129}H_{174}Cl_2N_{20}O_8P_8S_8$	Crystal size/mm^3	0.18 × 0.12 × 0.07
Moiety formula	4($C_{32}H_{43}N_5O_2P_2S_2$), CH_2Cl_2	Absorption correction	empirical
Formula weight	2708.01	Tmin; Tmax	0.6894; 0.7459
Temperature/K	100	Radiation	MoKα (λ = 0.71073)
Crystal system	monoclinic	2Θ range for data collection/°	6.332 to 56°
Space group	C2/c	Completeness to theta	0.996
a/Å	27.7111(12)	Index ranges	-27 ≤ h ≤ 36, -19 ≤ k ≤ 19, -29 ≤ l ≤ 21
b/Å	14.5378(7)	Reflections collected	48634
c/Å	21.9682(16)	Independent reflections	8586 [R_{int} = 0.0533, R_{sigma} = 0.0439]
α/°	90	Data/restraints/parameters	8586/64/439
β/°	126.3663(11)	Goodness-of-fit on F^2	1.062
γ/°	90	Final R indexes [I>=2σ (I)]	R_1 = 0.0729, wR_2 = 0.2022
Volume/Å^3	7126.5(7)	Final R indexes [all data]	R_1 = 0.0981, wR_2 = 0.2277
Z	2	Largest diff. peak/hole / e Å^{-3}	1.26/-0.51

10.24 Crystal data and structure refinement for compound 35a

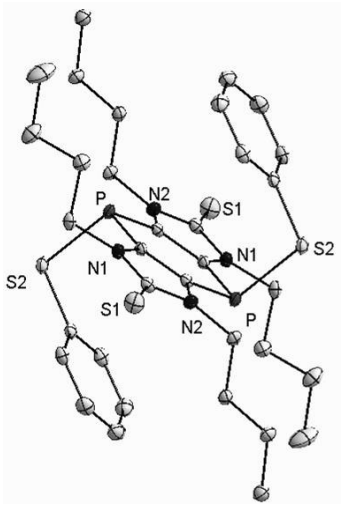

Identification code	GSTR558, ABK-465	ρ_{calc}g/cm^3	1.264
Crystal Habitus	clear yellow plate	μ/mm^{-1}	0.374
Device Type	Bruker X8-KappaApexII	F(000)	1488.0
Empirical formula	$C_{34}H_{46}N_4P_2S_4$	Crystal size/mm^3	0.18 × 0.14 × 0.05
Moiety formula	$C_{34}H_{46}N_4P_2S_4$	Absorption correction	empirical
Formula weight	700.93	Tmin; Tmax	0.4664; 0.7459
Temperature/K	100	Radiation	MoKα (λ = 0.71073)
Crystal system	monoclinic	2Θ range for data collection/°	2.266 to 56°
Space group	$P2_1/c$	Completeness to theta	0.998
a/Å	18.465(3)	Index ranges	-24 ≤ h ≤ 23, -17 ≤ k ≤ 17, -17 ≤ l ≤ 20
b/Å	13.1095(18)	Reflections collected	50325
c/Å	15.633(2)	Independent reflections	8895 [R_{int} = 0.0776, R_{sigma} = 0.0589]
α/°	90	Data/restraints/parameters	8895/0/401
β/°	103.230(5)	Goodness-of-fit on F^2	1.078
γ/°	90	Final R indexes [I>=2σ (I)]	R_1 = 0.0466, wR_2 = 0.0901
Volume/Å^3	3683.8(9)	Final R indexes [all data]	R_1 = 0.0630, wR_2 = 0.0975
Z	4	Largest diff. peak/hole / e Å^{-3}	0.54/-0.40

10.25 Crystal data and structure refinement for compound 35b

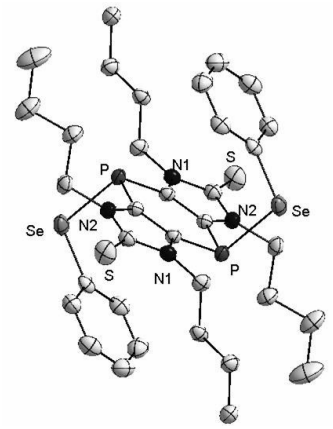

Identification code	GSTR549, ABK-466	ρ_{calc}g/cm^3	1.408
Crystal Habitus	clear yellow block	μ/mm^{-1}	2.197
Device Type	Bruker X8-KappaApexII	F(000)	1632.0
Empirical formula	$C_{34}H_{46}N_4P_2S_2Se_2$	Crystal size/mm^3	0.24 × 0.12 × 0.08
Moiety formula	$C_{34}H_{46}N_4P_2S_2Se_2$	Absorption correction	empirical
Formula weight	794.73	Tmin; Tmax	0.5809; 0.7459
Temperature/K	100	Radiation	MoKα (λ = 0.71073)
Crystal system	monoclinic	2Θ range for data collection/°	4.348 to 55.998°
Space group	$P2_1/c$	Completeness to theta	0.997
a/Å	18.5972(7)	Index ranges	-24 ≤ h ≤ 15, -17 ≤ k ≤ 17, -20 ≤ l ≤ 20
b/Å	13.2665(5)	Reflections collected	61648
c/Å	15.6185(6)	Independent reflections	9047 [R_{int} = 0.0775, R_{sigma} = 0.0563]
α/°	90	Data/restraints/parameters	9047/18/401
β/°	103.2796(13)	Goodness-of-fit on F^2	1.007
γ/°	90	Final R indexes [I>=2σ (I)]	R_1 = 0.0353, wR_2 = 0.0629
Volume/Å^3	3750.4(2)	Final R indexes [all data]	R_1 = 0.0725, wR_2 = 0.0754
Z	4	Largest diff. peak/hole / e Å^{-3}	0.39/-0.40

List of Figures

List of Schemes

List of Tables